APPLICATION OF DYNAMIC AND VIBRO COMPACTION METHODS FOR Ddensification OF GRANULAR FILL IN RECLAIMED LAND IN SRI LANKA

Amil Indumini Samarasinghe

(168980V)

Degree of Master of Engineering in Foundation Engineering and Earth Retaining Systems

Department of Civil Engineering

University of Moratuwa

Sri Lanka

September 2019

APPLICATION OF DYNAMIC AND VIBRO COMPACTION METHODS FOR DENSIFICATION OF GRANULAR FILL IN RECLAIMED LAND IN SRI LANKA

Amil Indumini Samarasinghe

(168980V)

Thesis submitted in partial fulfilment of the requirements for the degree of Master of Engineering in Foundation Engineering and Earth Retaining Systems

Supervised by

Dr. L.I.N. De Silva

Department of Civil Engineering

University of Moratuwa

Sri Lanka

DECLARATION

I hereby declare that, this is my own work and this thesis does not incorporate without acknowledgement of any material previously submitted for a Degree or Diploma in any other university or Institute of higher learning to the best of my knowledge and belief**.** It does not contain any material previously published or written by another person except where the acknowledgement is made in text**.**

Also, I hereby grant to University of Moratuwa the non-exclusive right to reproduce and distribute my thesis, as whole or a part in print, electronic or other medium**.** I retain the right to use this content in whole or part in future works **(**such as articles or books**).**

…… ……..

A.I. Samarasinghe Date

The above candidate has carried out research for the Master**'**s thesis under my supervision

…… ……

Dr. L.I.N. De Silva Date

ACKNOWLEGEMENT

At the outset, I would like to express my sincere and heartfelt gratitude to my research supervisor, Dr. L.I.N. De Silva for the continuous support to my study with guidance, motivation and immense knowledge. Without his dedicated supervision and continual guidance, this thesis would not be successfully completed within the time frame. During this period, he basically allowed this research to be my own work while steering me towards the right direction whenever he thought that I needed it.

It is my duty to pay gratitude to Eng. Nihal Rupasinghe, the Secretary to the Ministry of Megapolis and Western Province Development, Mr. Nihal Fernando, Project Director, Colombo Port City Development, Eng. Bimal Prabath Gonaduwage, Deputy Project Director, Colombo Portcity Development Project for providing me required data without restrictions.

In addition, It is my duty to pay my heart felt gratitude to all teachers served in or visited to Geotechnical Engineering Unit, Department of Civil Engineering including Professor Puswewala, Professor S.A.S. Kulatilake, Professor Saman Thilakasiri, Dr. Udeni Nawagamuwa etc. for not only their contribution to improve my knowledge, but also for their guidance on my carrier success.

Moreover, I would like to pay my gratitude to University of Moratuwa for providing me an opportunity to follow this Master degree and Management of Central Engineering Consultancy Bureau including Eng. K.L.S. Sahabandu, The General Manager, Eng. K.L.S.R. Sahabandu, The Additional General Manager and Dr. J.S.M Fowze, The Deputy General Manager for arranging sponsorship and relieving me from part of my duties and encouraging me for successfully completion of my master degree. Further, I extend my sincere thanks to all my colleagues in Royal Haskoning DHV, CHEC Port City Colombo (Pvt) Ltd. and China Harbour Engineering Company Ltd and Geotechnical Engineering Unit of CECB for their assistance and encouragement for completion of this thesis.

Finally, Especially I must express my very profound gratitude to my loving mother for her dedications, encouragement and blessing for not only this work but also for my whole life. Further, my gratitude goes to my loving kids, Abiru and Theviru and wife, Pramila, for relieving me from part of my house works during this study.

CASE STUDY: APPLICATION OF DYNAMIC AND VIBRO COMPACTION METHODS FOR DENSIFICATION OF GRANULAR FILL IN RECLAIMED LAND IN SRI LANKA

ABSTRACT

In the recent past, Government of Sri Lanka executed a large-scale reclamation project in Sri Lanka to add a brand-new land of 267-hectare to the Capital, Colombo with strategy of converting Colombo as a commercial hub of South Asia. For this project, 72 Million m^3 of sea sand which was dredged by Trailing Suction Hopper Dredgers at 10km off from shore of Colombo was placed mainly by hydraulic methods at lower elevation while applying bulldozers at the top. This reclamation material was noted as clean uniform sand and which was under loose to medium dense condition prior to densification.

This sand fill was densified using two methods, namely dynamic compaction and vibro compaction. Dynamic compaction, which is generally considered as one of the most economical sand improving methods, was applied in all areas except vibration sensitive areas at the city end and the areas where deep ground improvement was required for stability of earth retaining structures.

Since settlement of subsoil in the seabed is not critical, the considered major geotechnical issues were achieving of required bearing capacity, shear strength and avoiding possible liquefaction. To sort out all geotechnical issues, sand densification was the only solution. Though there is a very long history for dynamic and vibro compaction methods, still reclamation projects are not pre-planned to utilize the self-compaction achieves during sand placing very effectively, while designs always follow a very conservative approach. Moreover, designs are carried out using pre-defined energy criterions rather than considering existing fill material properties and its pre-compaction condition. Thus, there was a paramount requirement to assess the dynamic and vibro compaction methods for Sri Lankan fill materials and reclamation methods with the intention of optimization of the above compaction methods. In order to optimize dynamic compaction method, the pre-and post-compaction condition (by CPTs) was evaluated by crater depth, net volume changes, influenced depth and related indices, which assess the degree of improvement based on applied

energy. Similarly, densification by vibro compaction was evaluated with respect to the factor such as point spacing, amperage and compaction holding time. In addition, effect such as age of the compacted fill was considered for both dynamic and vibro compaction in this reclamation fill of clean sand.

Finally, verification of densified ground by selecting CPTs at least compacted points with respect to the compaction grids was assessed for both dynamic and vibro compaction to confirm the optimization has no adverse effect on the final design.

Based on the finding of this research, fill material's index properties of Sri Lankan sea sand were determined while being noted that there is no hesitation for applicability of dynamic and vibro compaction for densification. During the analysis it was suggested to modify some correlations derived based on laboratory test data to achieve more realistic output for actual reclamation condition. In addition, design of dynamic and vibro compaction by performance-based method through trial compaction was discussed.

Key words;

Dredging, Dynamic Compaction, Vibro Compaction, Crater Depth, Influence Depth, Ground Improvement Index, Amperage, Compaction Time, Applicability, Verification, Optimization

CONTENTS

LIST OF FIGURES

LIST OF TABLES

LIST OF ABBREVIATIONS

Abbreviation	Description
TSHD	Trailer Suction Hopper Dredger
(D)DC	(Deep) Dynamic Compaction
VC	Vibro Compaction
CPT	Cone Penetration Test
SPT	Standard Penetration Test
SBT	Soil Behaviour Type
MDD	Maximum Dry Density
CC	Calibration Chamber
NC	Normal Consolidation
CRR	Cyclic Resistant Ratio
CSR	Cyclic Stress Ratio
PPV	Peak Particle Velocity
PGA	Peak Ground Acceleration

1. INTRODUCTION

1.1. General

With the strategy of achieving economic development of Sri Lanka through a large-scale development and expansion of the Capital, Colombo by upgrading it to a world class city and converting to a commercial hub of South Asia, Government of Sri Lanka executed two type of projects. First one is the utilization of existing underutilized land by removing shanty dwellers and resettling them in high rise or middle rise apartments and the second project is adding brand new land to Colombo through reclamation. Accordingly, there was a paramount requirement for a newly reclaimed land associated with the Colombo Port, which is easy to convert to a commercial hub to access south Asian market through Colombo port and airport. To fulfil that requirement, Colombo Port City Development Project was initiated. It is the biggest Foreign Direct Investment; Sri Lanka has ever had.

This brand-new land of 269 hectares basically consists of development lands, road areas, green areas, retaining structure areas, and artificial sand beach areas etc. Development areas in the Port City was again planned as a financial district with high rise buildings, residential areas with middle rise buildings and marina and central park with luxury villas etc.

To reclaim this vast land, off-shore sea sand, dredged by Trailer Suction Hopper Dredgers (TSHD) from a sand deposit, which is 10km away from shore of Negombo was used. Required sand quantity for the reclamation was 72 million m^3.

1.2. Background

Reclamation was achieved by TSHD using methods namely, Bottom dumping, Subaerial rainbow discharge, Pipeline discharge, dumping by trucks or earthmovers. After reclamation, the newly filled land was improved using two techniques namely, dynamic and vibro-compaction methods applying different energies and frequencies required to achieve different degree of compaction demanded by different pre-planned constructions. During reclamation, samples of fill materials i.e. sea sand, were taken from each TSHD in operation as well as from the newly reclaimed land daily and tested for gradation and bulk density etc.

During design stage of this project, following geotechnical problems were identified;

- Stability of edge (retaining) structures.
- Settlement of land area and other structures.
- Liquefaction potential of sand under the predicted earthquake possibilities.
- Adverse effect on foundations including pile foundations by settlement and liquefaction.

As per the available subsoil condition, settlement was not a key issue as maximum settlement was estimated as merely 200mm. At the same time, it was noted that all the other issues could be managed by densification of the reclaimed land. As per the relative density requirement were defined with respect to the depth, ground improvement method was selected accordingly for each area. Relative density requirement varies from 40% to 75% in this study area.

At the outset, dynamic compaction and vibro compaction trials were conducted to select the optimum design. Based on the selected design, permanent ground improvement was conducted in the sub lots. Upon completion of ground improvement, Cone Penetration Test (CPT) was conducted to verify the compaction with respect to the design criteria.

1.3. Objectives of the Research

1. To evaluate self-compaction of sand while being reclaimed by different methods.
2. To evaluate the properties of Sri Lankan sea sand including compactability and liquefiability.
3. Optimization of compaction of the reclaimed sea sand fill by evaluating construction data;
    - To identify the applicability of dynamic and vibro compaction in reclaimed land in Sri Lanka.
    - To identify the optimum number of blows in dynamic compaction by crater depth and net volume changes.
    - To verify the influence depth of Dynamic compaction with applied energy.
    - To identify the optimum number of blows based on ground improvement index.

- To understand the effect of amperage, holding time and depth on the vibro compaction.
- To identify the other critical factors which affect the outcome of dynamic and vibro compaction.

4. To evaluate achievement in ground improvement by selecting CPTs at critical locations in dynamic and vibro compaction.

1.4. Scope of Work

The proposed scope of work to achieve the above objectives are as listed below.

- Undertake dynamic compaction trials using various spacing distances for different energies such as 6.5m for 4000kNm, 5m for 2000kNm and 2m for 1000kNm using square pattern with monitoring related site measurement.
- Undertake vibro compaction trials using various spacing distances such as 3.9m, 4.2m & 4.5m for triangular pattern by applying equal energy condition.
- Conducting CPTs to check the compaction/relative density in the compacted sand.
- Conducting laboratory test to determine achievable density (BS1377: Part-9) for sand with different relative densities.
- Conducting laboratory tests for minimum and maximum dry densities of fill material (BS 1377-part-4 sec-4) to evaluate the relative density.

1.5. Outline of the Thesis

Chapter 2 presents a literature review for the historical background and findings of the following:

- Review of the reclamtion methods and its effects to the self compaction.
- Index properties of the reclamation material (seasand) used for off-shore reclamation in Sri Lanka.
- Potential failure models in reclmation land and requirements in densification.

- Design and acceptance criterial for reclamation fill in terms of relative density , potential of liquefaction and other other factors.
- Selection of dyanamic and vibro compaction methods and their effectiveness on Sri Lankan seasand.
- Mechanism of sand densification by DC and VC
- Optimization of dynamic and vibro compaction process by considering factors, which afffect to outcome of densification
- Aging effect on DC and VC
- Evaluation of densification

Chapter 3 discussed the methodology applied for the research including selected data, type of analysis/evaluations used and flow chart of the reseach work.

Chapter 4 presents the results obtained from analysis/evaluations done for self compaction condition and index properites of reclamaition fill, applicability and effectiveness and optimization and verification of DC and VC .

Chapter 5 presents the conclusion made by the findings of this research.

2. LITERATURE REVIEW

2.1. Off-Shore Reclamation Methods using Sea Sand

Reclamation is either be land based process or by dump trucks tipping fill in to sea or by hydraulic placement of sand from the sea (Babak Hamidi et al. 2012) [1]. Generally, one or few of following discharge or dumping methods are used to fill sand up to the required level.

a. Bottom dumping
b. Subaerial rainbow discharge
c. Pipeline discharge
d. Dumping by trucks or earthmovers

Capacity of Trailer Suction Hopper Dredgers (TSHD) varies from few hundred m^3 to 40,000m^3. In Sri Lanka TSHDs with capacity varies from 10,000m^3 to 20,000m^3 are used for sand dredging and pumping. Due to much higher draught of Trailer Suction Hopper Dredgers, bottom dumping method can only be used in areas having more than 12m depth to the seabed. Thus, shallow areas are filled by above b and c methods (Sladen et al.:1989) [2].

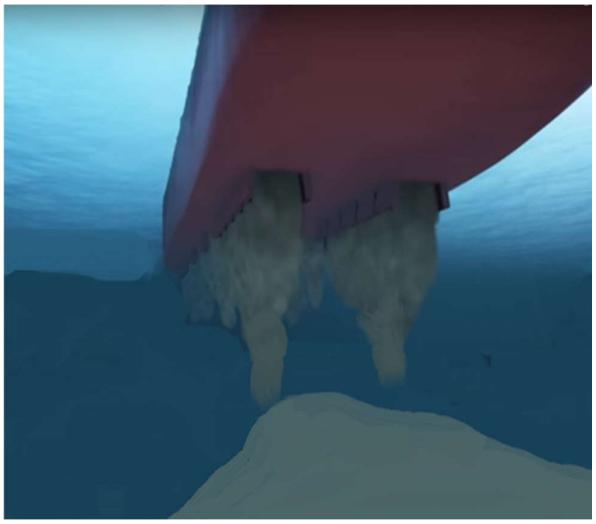

Figure 2-1*:* Sand bottom dumping from TSHD

Figure 2-2*:* Sand Rain bowing from TSHD

The placement methodology of reclamation always plays an important role in shaping the compaction condition of the reclaimed soil. Lack of proper placement causes a risk of proper densification and stratification of the reclaimed fill with subsequent, undesirable consequences in bearing capacities and the settlements. Therefore, it is essential to take special precautions for the placement method in order to achieve better improvement condition in the fill (Ali et al. 2013) [3]. As stated in ROM (Spanish National Port Authorities 1994) [4], the characteristics of hydraulic fill generally depends on the nature of the material remaining after taking placing

the processes of excavation, transport and sedimentation. Some times Hydraulic fill may have quite different characteristics from borrow materials as at the point of origin."

In reclamation of relatively deeper areas, hydraulic placement is able subaqueous by hoppers or bottom dumping barges. When possible, sand can be discharged by using a big door located on the bottom of the hull. However, when water being shallow, pipeline discharge or subaerial rainbow discharge or such alternate methods can be used. Due to lose packing from self-weight sedimentation of sand particles under water, deposited sand by hydraulic filling below water level possesses low to medium relative density of about 20% to 60% in general.

Accordingly, the compaction achieved during reclamation, varies with applied discharging method. As Sladen and Hewitt (1989) [2], Lee et al (1999), Lee et al. (2000), Lee (2001) and Na et al. (2005) reported the density achieved in sand after dumped by trucks and then pushed into the sea by a bulldozer is usually as low as relative density of about 20%. Exceptions might be in thin layers when which had been compacted due to the traffic of earthmoving equipment.

However, when rain bowing is done above water, downward seepage and void ratio reduction occurs. As a result of sliding as well as rolling of sand particles mixture, relative density of the fill varies from 60% to 80%. In pipeline discharge, water-sand slurry pumping velocity is low. However, during the sand rainbow process, the dredgers spray water-sand mixture with high velocity onto the reclamation (Babak Hamidi et al. 2012) [1]. Menge et. Al (2016) [5] has summarized the relative density (Dr) variation with hydraulic fill placement method as follows;

Table 2-1: Typical relative densities as a result of hydraulic fill [5]

Placing method	Dr (%)
Spraying (discharge under water)	20-40
Dumping (discharge under water)	30-50
Land pipe line (discharge under water)	20-40
Rain bowing (discharge under water)	40-60
Land pipelines (discharge above water)	60-70
Rain bowing (discharge above water)	60-80

As Bo et. al. (2009) [6] noted when a fines content of less than 10%, the marine sand fill formed by hydraulic placement being placed in a loose state. Thereof cone resistance values of CPTs are quite low as 5MPa to 7 MPa, of which densification requirements was 12 to 15 MPa (corresponding relative densities are 70% to 75% respectively).

2.2. Index Properties of Reclaimed Sea Sand

In reclamation projects, source material is defined based on properties, which are determined by lab tests such as sieve analysis and hydrometer test, specific gravity tests, etc., in which maximum particle size, fines content, plasticity index (Plasticity Index =Liquid limit -Plastic limit of soil) etc. are checked. Filling material basically consist of fine to coarse sand with trace amount of gravel and silt, which is recognized as liquefiable soil as per the procedures developed by Tsuchida (1970) [7]. In addition, effective friction angle is around 32^0 and unit weight is about 18 kN/m^3 (Y. Tan: 2007) [8]. Mitchell (1982) [9] , who identified soils as per grain size distribution and suggested that most granular soils consist of a fine content (particles sizes< 0.064 mm) lower than 10% could be densified by impact (dynamic) methods or vibratory. Based on Robertson′s SBT chart (2010) [10] as shown in

Figure 2-3: Sand pumping from TSSD

Figure 2-4: Sand dumping and moving by earth movers

Figure *2-5*, soil type used for the reclamation can be identified by CPT data.

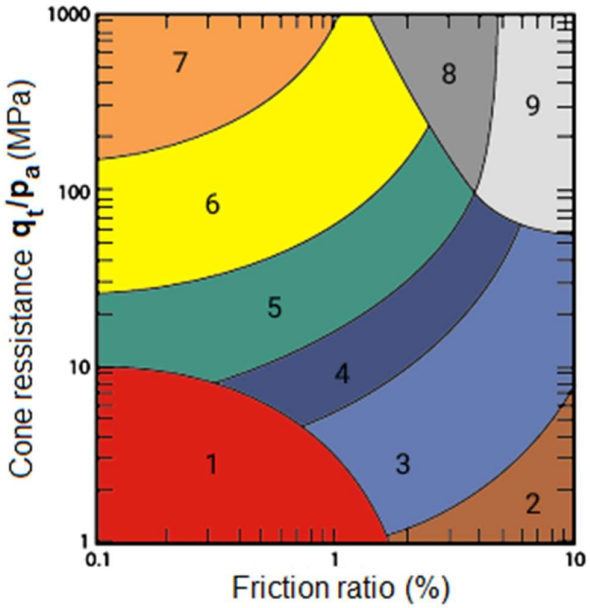

Table 2-2: Soil Types identified by SBT

Zone	Soil Behaviour Type (SBT)
1	Sensitive fine-grained
2	Clay - organic soil
3	Clays: clay to silty clay
4	Silt mixtures: clayey silt & silty clay
5	Sand mixtures: silty sand to sandy silt
6	Sands: clean sands to silty sands
7	Dense sand to gravelly sand
8	Stiff sand to clayey sand*
9	Stiff fine-grained*

** Over consolidated or cemented*

Pa=100MPa

Figure 2-5: Non-normalized SBT chart based on dimensionless cone resistance, (q_c/p_a) and friction ratio, R_f [10]

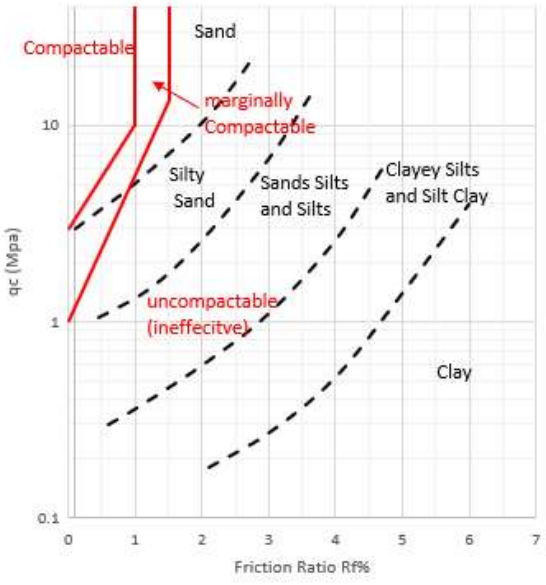

Figure 2-6: Soil identification of backfill for DC improvement (after Massarch 1991) [11]

In order to check the compactability, it prefers to use the compaction criterion developed assuming homogeneous soil conditions by Massarch (1991) [12] based on cone resistance, q_c,

and friction ratio, R_f as shown in Figure 2-6. However, with presence of thin silt and clay layers, the compaction effectiveness will be reduced.

2.3. Potential Failure Modes in Reclaimed Land fill

Basically, following failure modes has to be considered in reclamation;

1. Settlement as residual primary and secondary settlement at seabed or weak fill layers due to presence of organic, clay or silt materials.
2. Insufficient bearing capacity of the top (founding) layer of the land.
3. Stability of edge (retaining) structures against slip failure.
4. Liquefaction due to cyclic loads such as earthquakes.

Reason for above failures can be noted due to weak soil layer or lack of densification of sand fill, where liquefaction potential can be assessed by particle size distribution as presented by Tan (2005). [13]

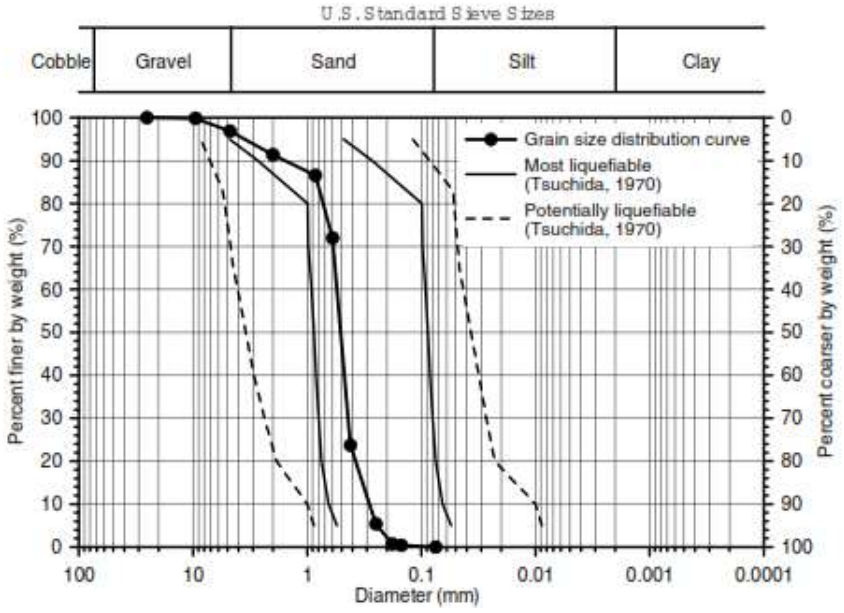

Figure 2-7**:** Potential of liquefiable with grain size distribution of soils **(**Y**.** Tan 2005**) [**8**]**

2.4. Scope of the Improvement in Reclaimed Ground

It was decided to proceed with a ground improvement technique in order to;

a. Provide bearing capacity under static and pseudo static loading condition for the construction of shallow foundations.

b. Keep the anticipated total and differential settlement under tolerable values compatible with demands of the superstructure by increasing the soil stiffness (modulus) and uniformity.
c. Provide shear strength to achieve lateral stability of the retaining structures.
d. Mitigate the liquefaction potential generated by seismic events at design Peak Ground Accelaration (PGA) & return period or due to dynamic response by the soil as a result of dynamic soil-structure interaction in case of dynamically loaded foundation.

2.5. Factors Affecting on the Popularity of Application and Improvements of Efficiency in Sand Densification work

Since it is compelled to use of generally unsuitable lands for construction, ground improvement was the popular solution in many countries. With continuous development of dredging and ground improvement technique, the following factors has contributed the application of soil improvement with much improved efficiency;

- Availability of more powerful construction equipment day by day (e.g. Adjustable vibrators and large and versatile carriers and rigs).
- Possibility to optimize equipment performance with minimized environmental effects such as construction vibrations due to introduction of electronic control systems.
- Availability of well-trained site personnel, essential for operating and maintaining sophisticated construction equipment in most countries.
- Improvement geotechnical investigations qualitatively and quantitatively (availability of efficient methods for field investigation with more powerful data storage, transmission, and evaluation systems, which are particular important for large construction projects).
- Availability of field investigation methods and more reliable results interpretation, such as the cone penetrometer test (CPT), and some correlations between test data and geotechnical design parameters.
- Cost consciousness of project owners, who demanding evaluation of different foundation alternatives for their projects.
- More sensitivity to differential settlements of modern structures and more stringent design requirements.

- Availability of better understandings of the static and dynamic stress-strain behaviour of soils and many advanced analytical tools used for more cost-effective reliable designs, especially with respect to settlement analysis;
- Development of a greater level of understanding in principles of how a foundation design can be benefitted from compaction, how compaction can be performed, and how compaction work can be integrated in the overall construction and performance inspection of an engineering project (K. Rainer Massarsch et al. 2002) [14]

2.6. Improvement of Fill Material

Better understanding of the possibilities and limitations particular to each improvement method is essential for efficient use of compaction methods. Due to the inappropriate application and/or execution of a compaction method for a project, there might be severe technical and economic consequences. Thus, the geotechnical engineers must take more active part in all phases of a project, such as:

- Selection as well as evaluation of applicability of compaction method(s).
- Design of appropriate compaction effort required for the project including compaction verification.
- Selection of the appropriate compaction equipment and techniques and appointing competent and experienced technical personnel to lead the project.
- Assessing and deciding on the optimal compaction process in terms of sequence, duration, point spacing and pattern.
- Preparing specifications for contract to include acceptance criteria based on the verification testing methods to be applied in the project, overview QA & QC of the project as verifying that the results of the treatment to comply requirement in the Design and specifications.

(K. Rainer Massarsch 2002) [14]

2.7. Design and Acceptance Criteria

Since the loose soil thickness in reclaimed ground is quite high, geotechnical engineers should use more meaningful ways to specify design and acceptance criteria as which are more compatible with the objectives of design. Criteria for ground improvement acceptance can be envisaged to be in three main forms based on quality of works, minimum values in the tests or directly on design criteria. The first type of criteria is used when the non-specialized contractor

cannot take responsibility of outcome of the improvement work and the second method is used to verify the improvement by field test such as CPT, which is correlated to the relative density on the densified soils. Under the third criteria, contractor calculates and verify that compaction has achieved all the design requirement such as settlement, bearing capacity etc., without strictly complying to the specified minimum test values (Hamidi et al., 2011) [15].

2.8. Parameters Related to Granular Soil Densification

2.8.1 Relative Density

In the reclamation quality control philosophy, the future stress–strain behaviour of the site can be correlated to the fill density. Quality control is always related to 'adequate densification', which should guarantee that specified certain minimal requirements related to the soil behaviour (shear strength, stiffness or cyclic resistance ratio) will be obtained at the end of the day. Accordingly, this concept is translated into technical requirements in terms of parameters like relative density D_r or Maximum Dry Density (MDD). Then either directly (in situ dry density measurement by e.g. the sand replacement method) or indirectly, densities should be determined on site, based on correlations between density and the cone resistance q_c in CPT. During construction in progress at site, the CPT can be used as a quality control method to identify any additional densification requirement. (Van Impe: 2015) [16]

Relative density, Dr generally indicates the degree of packing of sand and which is applicable strictly for granular soils having less than 12 percent fines (ASTM). [17] For sandy soil the relative density, Dr states the degree of compactness in terms of both the loosest and densest status achieved by the material using slandered laboratory procedures.

$$D_r = \frac{\gamma_{dmax}}{\gamma_d}\left[\frac{\gamma_d - \gamma_{dmin}}{\gamma_{dmax} - \gamma_{dmin}}\right] \quad (1)$$

Generally, the relative density can be expressed with respect to the void ratios (e):

$$D_r = [(e_{max} - e_0)/(e_{max} - e_{min})] \times 100 \quad (2)$$

Where e_{min} = void ratio at the densest state and e_{max}= void ratio related to it is at the loosest state, e_0 = insitu void ratio while e_{max} and e_{min} values with respect the fine content of non-plastic soil has determined in ASTM as follows;

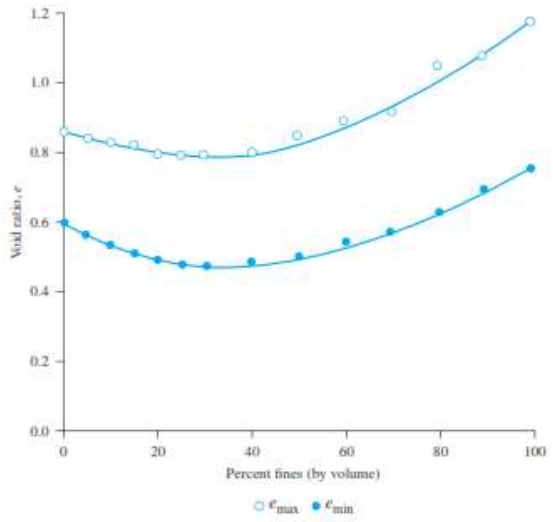

Figure 2-8: e_{max} and e_{min} (for Nevada 50/80 sand) variation against non-plastic fines percentage (Redrawn from Lade et al 1998)

Further, relationship between e_{max} and e_{min} has been defined by Poulos (cited by Youssef et al. 2007, [18]) as follows;

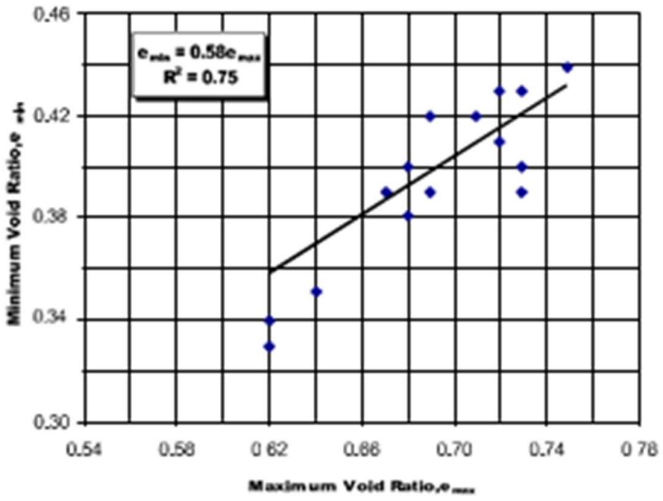

Figure 2-9*:* Relation between e_{max} and e_{min}

Cubrinovski and Ishihara (1999 [19]and 2002) derived the relationship of e_{max}, e_{min} and mean grain size in sand gravelly soils as follows;

$$e_{max} - e_{min} = 0.23 + \frac{0.06}{D_{50}(mm)} \quad (3)$$

Relative compaction, RC is not the same as it can be applied for plastic soils unlike Dr.

Relative density cannot be directly measured in-situ at depth and does not always have a well-defined line with soil behaviour, especially in sandy soil with high fine content. In more recent years CPT has become popular for quality control for deep compaction since it is: fast and cost effective, provide continuous profile, gives reliable and repeatable measurements and provides more than one measurement. Although it is possible to link CPT measurement with Dr the correlations are not unique, apply only to clean sands and can vary considerably with grain mineralogy and characteristics (P.K. Robertson, 2016) [10]. Coefficient of uniformity, C_u is the ratio of grain sizes at passing percentage of sixty, D_{60} and ten, D_{10}.

As per Craig , a well graded soil has a coefficient of uniformity (Cu) bigger than 6 (Craig 1974) [20] while it will be lesser than 6 for poorly graded sands. For poorly graded sands, Gomma et al. ([18]. presented a correlation of e_{min} and e_{max} with Cu as follows;

$$e_{min} = 0.5 - 0.033 \log (C_u) \quad (4)$$

$$e_{max} = 0.81 - 0.037 \log (C_u) \quad (5)$$

The first attempt to correlate the penetration resistance of the cone penetration tests (q_c) to the density of sands has been done by Schmertmann (1976) [21] . He presented the first comprehensive correlation between qc and relative density (D_r) on the basis of CPTs performed in the Calibration Chamber (CC). Such a correlation is applicable to normally consolidated (NC) fine to medium, unaged, clean sands. Schmertmann (1976) [21]suggested a correlation between the cone resistance (q_c) and the relative density with the vertical effective stress (σ'_{vo}), using the results of CPT's performed on sands in the CC of the University of Florida. The analytical expression takes the form:

$$q_c = C_0 (\sigma'_{V0})^{C1} \exp(C_2 - D_r) \quad (6)$$

or

$$D_r = (1/C_2) \cdot ln[q_c/(C_0 \cdot (\sigma')^{C_1})] \quad (7)$$

With σ′ being effective vertical or mean stress (kPa), q_c- cone resistance (kPa) and C_0, C_1 and C_2 are empirical soil constant.

Tom Lunee et al. (2009) [22] established empirical constants for normally consolidated and over-consolidated sand using Ticino sand applying index densities according to ASTM. According to this formulation, an estimation of the relative density in normally consolidated sand requires only the knowledge of the vertical effective stress and the cone resistance. Soil constant are in this case given as: C_0= 181, C_1= 0.55, C_2= 2.61.

Mayne et al. (2007) [23] proposed a correlation for Dr as in equation 8;

$$D_R = 100 \cdot \left[0.268 \cdot \ln\left(\frac{q_t / \sigma_{atm}}{\sqrt{\sigma_{vo}' / \sigma_{atm}}} \right) - 0.675 \right] \quad (8)$$

In which;

$$q_t = q_c + (1-a)\, u_2 \quad (9)$$

Where; 'a' is the net ratio of the cone (a= 0.6 to 0.8) and 'u_2' is pore pressure measured during CPT (at the base of sleeve).

For sandy soils $q_c = q_t$

However, Biryaltseva [24] found above relation seems to constantly underestimate the measured relative density values and proposed more appropriate values for C_o=357, C_1=0.59 and C_2= 1.38 for the correlation suggested by Schmertmann (1976) [21].

2.8.2 Compaction Status of Sand fill by Relative Density

Based on relative density compaction status can be evaluated as follows;

Table 2-3: Qualitative Description in compaction for Granular Soil Deposits

Relative density (%)	Compaction status of sand
0–15	Very loose
15–50	Loose
50–70	Medium
70–85	Dense
85–100	Very dense

Relative density can be considered as a useful parameter to describe the relative behaviour of cohesion less soils. Increasing of relative density, Dr indicates increasing of strength and decreasing of compressibility. when Dr has a negative density value, the soil structure might be collapsible, such as a very loose cemented or calcareous sand and honeycombed soils with e_0 is bigger than e_{max} (Kulhawy and Mayne1990) [25] .

2.9. Assessment of Potential Liquefaction

The method developed by Robertson and Wride (1998) [26] is used for liquefaction evaluation based on the in-situ CPT data, which assumes no liquefaction to occur if F_S is greater than or equal to 1.0 and liquefaction occurs if F_S is less than 1.0. The factor of safety, F_S is defined in Equation 10 as the ratio between Cyclic Resistance Ratio (CRR) and Cyclic Stress Ratio (CSR) (Seed and Idriss 1971) [27].

$$F_S = CRR/CSR \quad (10)$$

in which, CSR can be calculated as:

$$CSR_{7.5} = 0.65 \times (a_{max}/g)(\sigma_{v0} / \sigma'_{vo}) \times r_d \quad (11)$$

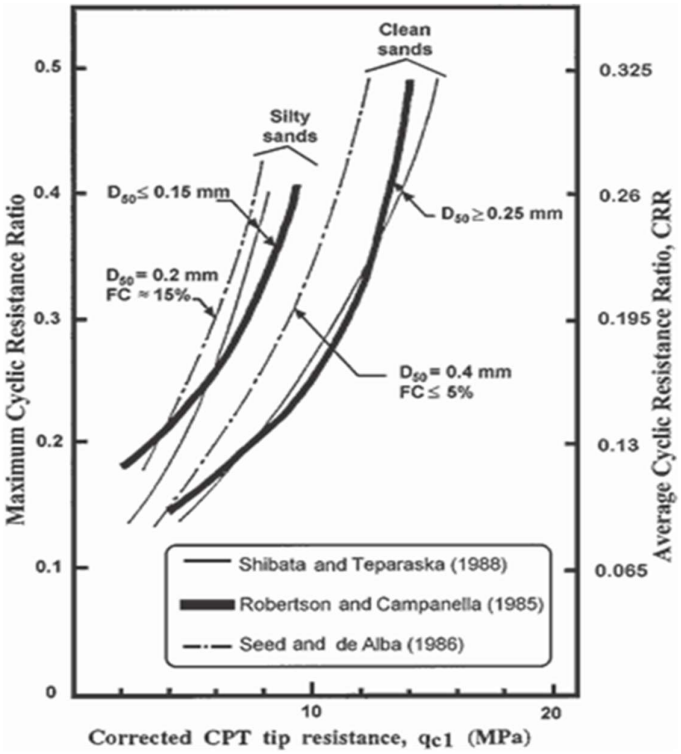

Figure 2-10: CRR vs q_{c1} for different soil types [26]

Where σ_v and σ'_v indicates the total stress and the effective stress of the soil respectively considered at a given depth. while g is the acceleration of gravity having unit for peak ground surface acceleration a_{max}. rd is the depth-dependent shear stress reduction factor.

The value of r_d in Equation (12 a & b) is assessed by following the equations (Liao and Whitman 1986) [28]:

$r_d = 1.0 - 0.00765z$ for $z \leq 9.15$ m (12a)

$r_d = 1.174 - 0.0267z$ for $9.15 \text{ m} < z \leq 23$ m (12b)

Where, z is depth below ground surface in metres.

CRR is calculated for clean sand as suggested by Robertson and Wride 1998) [26]

If $(q_{c1N}) < 50$, $CRR_{7.5} = 0.833[(q_{c1N})/1000] + 0.05$ (13a)

If $50 \leq (q_{c1N}) < 160$, $CRR_{7.5} = 93[(qc_{1N})/1000]^3 + 0.08$ (13b)

Where, $(q_{c1N})_{cs}$ is calculated by Eqn (14) using p_a=100kPa if σ'_{vo} is in kPa and P_{a2}=0.1MPa if q_c is in MPa

$$q_{c1N} = (q_c/P_{a2})(P_a/\sigma'_{vo})^{0.5} \quad (14)$$

In this studied site, compaction requirement is designed to withstand a maximum earthquake magnitude M_w of 7.5 with a two percent probability of being exceeded in fifty years (this implies a mean recurrence interval of 2500years). Since, soils may liquefy in reality even if the calculated safety factor $F_S > 1.0$. Thus, There is a requirment of assessing likelihood of liquefaction (Juang et al., 2002). Accordingly Juang and Jiang (2000) [29] presented the following mapping function to get correlation between the safety factor F_S and the probability of liquefaction P_L, based on the calibration of Robertson and Wride method (1998) [26] using large database of field observed cases, (Y. Tan, 2007) [8]

$$P_L = 1/(1+F_s^{3.3}) \quad (15)$$

2.9.1 Soil Behaviour Type (SBT) Index (Ic) and Normalized Cone Resistance (Qtn)

Massarsch (1991) [12] showed that vibro compaction method tend to be more effective in clean sands and Degan et al. (2005) [30] showed that vibro or vibratory compaction methods become less effective with increasing soils behaviour type (SBT) Index I_c as shown in Figure 2-11. Hence, I_C and be used as guide on potential effectiveness of many vibro or vibratory

compaction methods. Typically, when $I_C > 2.6$ vibro or vibratory compaction method become less effective in terms of improved density as measured by penetration resistance. However, soils with $I_C > 2.6$ can have improved behaviour characteristic due to changes in stress history and K_o.

Normalized CPT cone resistance is determined by Robertson (2016) [10] as follows;

$$Q_{tn} = [(q_t - \sigma_v)/P_a]\, C_N \qquad \text{For clean sands } C_N = (P_a/\sigma'_{vo})^{0.5} \qquad (16)$$

Where:

q_t = cone resistance corrected for water pressure (Campanella and Robertson, 1982)

$(q_t - \sigma_v)/P_a$ = dimensionless net cone resistance

σ_{vo} = the total overburden stresses ;

P_a is a reference atm. pressure in the same units as σ'_{vo}, q_c and σ_{vo}.

$$I_c = [(3.47 - \log Q_{tn})^2 + (\log Fr + 1.22)^2]^{0.5} \qquad (17)$$

Fr is the normalized friction ratio (in percent) and defined as

$$F_r = f_s/[(q_c - \sigma_{vo})] \times 100\%$$

f_s = CPT sleeve friction stress;

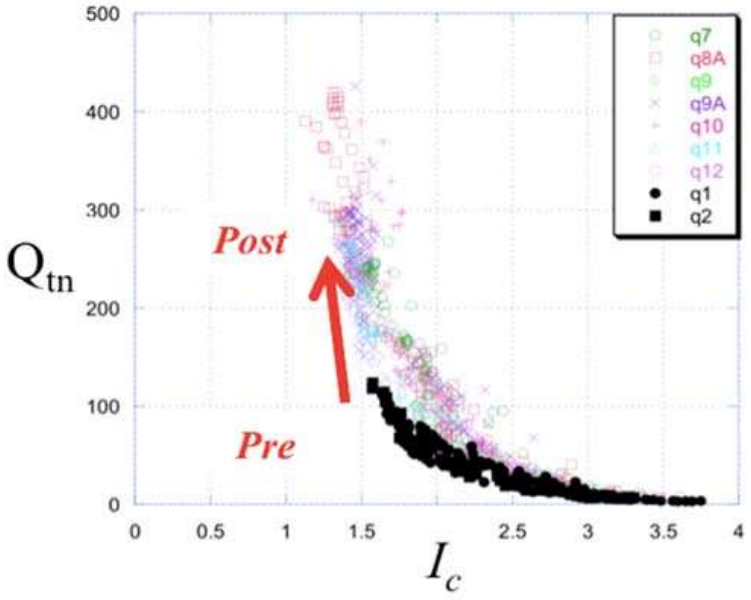

Figure 2-11: Q_{tn} vs I_c graph (Robertson: 2016) [19]

2.10. Methods Apply for Improvement of Reclaimed Sand Fill

When non-cohesive soils are available having insufficient compressibility or strength, compaction is viable. Thus, soil improvement by economical means should be applicable to both shallow and deep foundations. Generally compaction always refers to densification by dynamic methods. However, which will be depending on the manner of imparting the energy to the soil and accordingly can be divided into two main categories as follows:

1. Impact compaction
2. Vibratory compaction.

Impact compaction varies from a heavy roller used for surface-compaction to a heavy weight (Tamper), which is falling from large heights (Dynamic Consolidation) according to a pre-defined grid pattern.

Vibratory compaction ranges from surface-compacting vibratory rollers or plates to deep-acting vibratory probes, which provide lateral or vertical vibration to the ground. These methods and their practical applications, limitation have been discussed extensively in the geotechnical literature by Mitchell (1982) [9], Massarsch (1991) [12], Massarsch (1999) [31], and Schlosser (1999) [32].

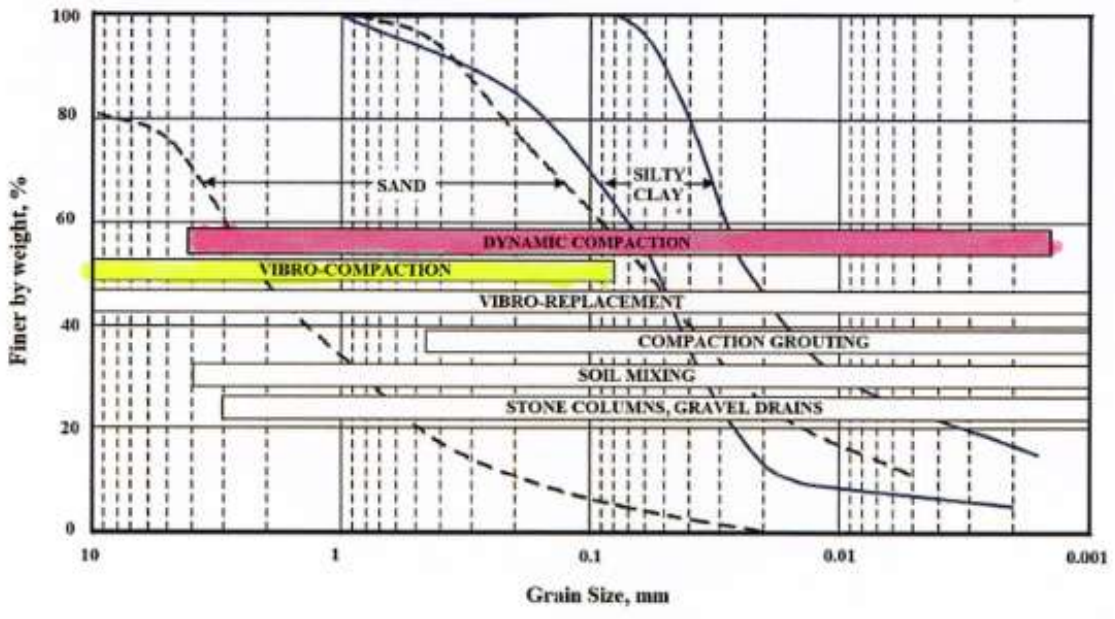

Figure 2-12: Suitability of different ground stabilization methods varies grading range of problem soils (Mitchell et al., 1998) [9]

In this studied area, basically two densification methods were applied, namely dynamic compaction and vibro compaction. Vibro compaction was applied to densify the locations of retaining structures and for the areas close to the existing building and structures while dynamic compaction is applied for rest of the areas. This selection was done based on economic and technical reasons, since DC, which is capable to densify around 12m, is more economical and being a faster compaction method while VC is capable to densify the entire fill thickness with minimum vibration effect to the surrounding structures. Thus, the geotechnical engineer should answer to the most important questions such that whether or not- and to what degree that dynamic methods (vibratory or impact compaction) can improve a soil deposit (Mitchell: 1982) [9]. Moreover, the enveloped developed by Michell et al (1982) , which has been given in Figure 2-12 can be used to check the applicability of the dynamic compaction and vibro compaction.

2.11. Dynamic compaction

In 1957 this method was implemented to evaluate the impact of falling height in degree of compaction of clayey sand by Research Laboratory of the UK (Smoltczyk, 1983) [33]. Menard introduced it as a desirable soil improvement method by 1975, and its application was reported in subgrade improvement of Nice airport, France. Although dynamic compaction has been adopted as a method of improvement for many years, according to Merrifield and Davis (2000) [34], it has been established in practical science literature recently. In this method, compaction engages heavy weight of 5 to 30 tons, which are thrown freely from height of 5 to 30 meters (Mayne et. al.,1984) [35]

Although dynamic compaction is reported to be effective both above and below the ground water table, certain construction difficulties arise if the water table not being maintained at least 2 m below the ground surface. This is achieved by dewatering or raising the grade (Lukas,1986) [36]. Figure 2-13 shows the conceptual illustration of dynamic compaction.

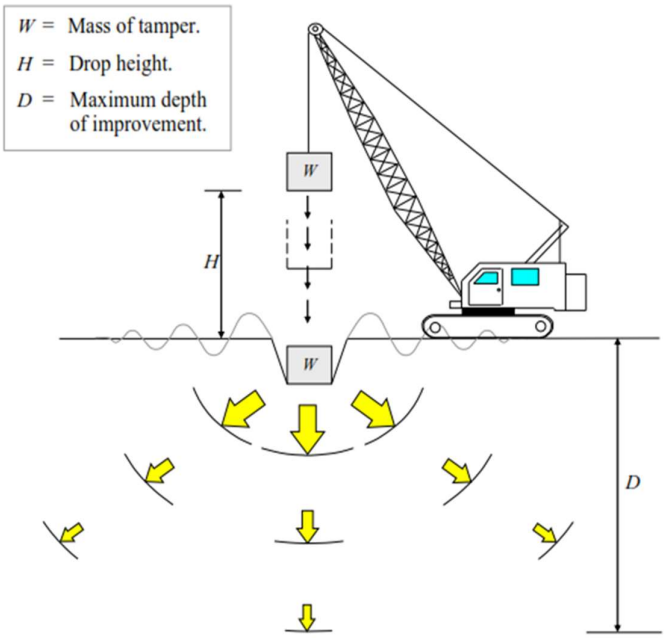

Figure 2-13: Schematic Illustration of deep dynamic compaction (Lukas:1995) [37]

2.11.1 Applicability of Dynamic Compaction

Lukas (1986) [36] has categorized the soil into three zones of improvement based on the soil′s grading i.e. the pervious soils, the semi pervious soils and the impervious soils. In saturated soils the best efficiency and results can be expected in the first Zone, however, dynamic compaction can be used in almost all types of ground conditions, such as for causing pre-collapse in sinkholes and cavities (Chaumeny et al., 2008) [37], compacting large diameter boulders (Menard:1978), [38] sand dune compaction (Varaksin et al.;2004) [39], improvement of collapsible soil (Rollins and Rogers, 1998) [40] , or even for consolidating clay (Perucho and Olalla, 2006) [41] . DC can be used in combination with other technique such as wick drains (Cognon et al., 1983) [42] or surcharging (Menard, 2004) [43] to increase the treatment efficiency. Accordingly, DC can be considered as a feasible solution for sand compaction.

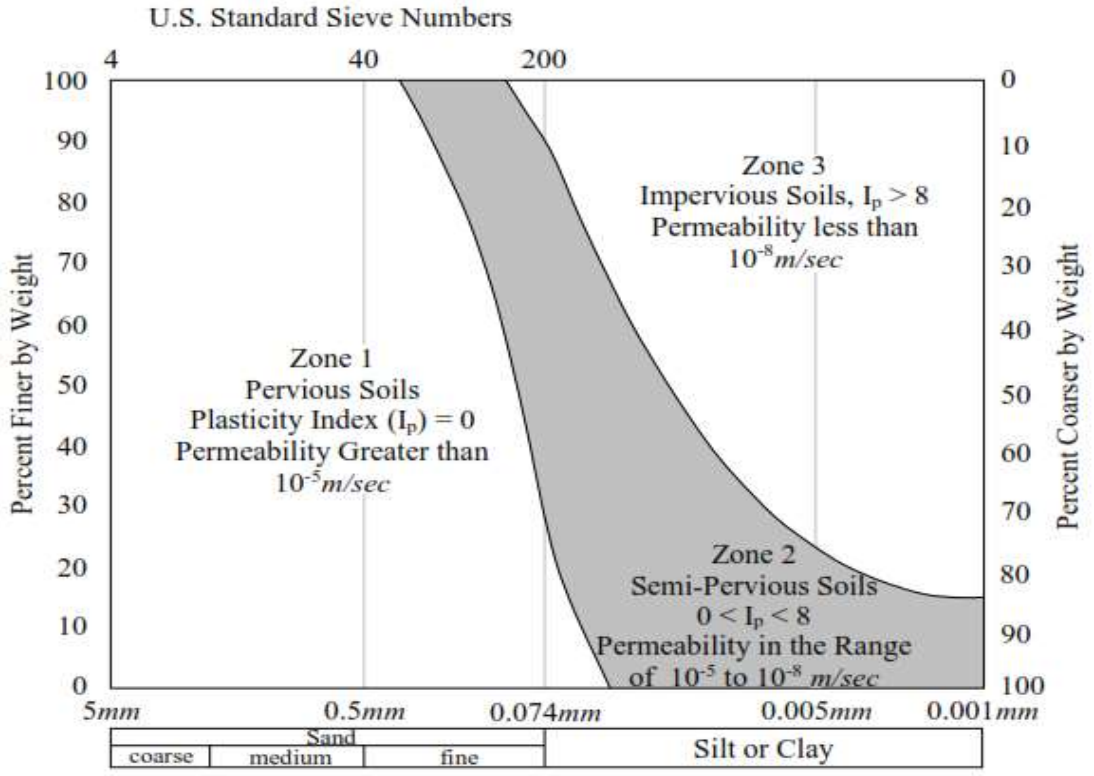

Figure 2-14: Grouping of soils for dynamic compaction (Lukas, 1986) [36]

Lukas (1985) [44]described applicability of dynamic compaction for soils in three zones in above envelope shown in Figure 2-14 and which has been detailed below;

Most Favourable Soil Deposits - Zone 1

On deposits where the degree of saturation is low, the permeability of the soil mass is high, and drainage is good, dynamic compaction works best. Hence deposits such as pervious granular soils are considered as most appropriate for dynamic compaction. When these deposits exist above the water table, those soil particles are rearranged into a denser state by packing immediately. If the deposit exists below the water table, excess pore water pressures generated by the impact of the tamper will dissipate almost immediately as the permeability of the material is sufficiently high. Hence, densification is nearly immediate.

Unfavourable Soil Deposits - Zone 3

Any deposits either natural or fill, that are saturated so that dynamic compaction is not appropriate, would be clayey soils. Improvements in saturated deposits, cannot occur unless

the water content of the deposit is lowered. Generally, permeability of clayey soils will be less than l0^{-8} to 10^{-9} m/s. Thus, excess pore water pressures generated during dynamic compaction cannot be dissipated, except perhaps over a lengthy period of time. This makes applicability of dynamic compaction is impractical for these deposits. Furthermore, the degree of improvement is generally insignificant. But still some improvements have been achieved in clayey fill deposits when are only saturated partially. This happens when fills are elevated well above the water level and having good surface drainage. In that case, improvement occurs by compacting the particles before they became fully saturated. Regardless of the amount of energy applied, no further improvement will happen after saturation occurs. Generally, prior to dynamic compaction, the water content of the clayey soils should not be higher than the plastic limit of the deposit.

Table 2-4: Suitability of soil for dynamic compaction (Lukas, 1986)

Soil Category (Figure 2.7.)	Soil Type	Soil Hydraulic Conductivity /PI	Suitability for DC
Zone 1 Most favourable	Permeable Soil - Sands, gravel, granular fill	$k > 10^{-5}$ m/sec PI= 0	Improvement is achievable
Zone 2 Intermediate	Silty sands, silts and clayey silts	$10^{-5} > k > 10^{-8}$ m/sec $0 < PI < 8$	With adequate dissipation of induced pore pressure
Zone 3 Unfavourable	Impervious clayey soils	$k < 10^{-8}$ m/sec $PI > 8$	Not recommended

Intermediate Soil Deposits - Zone 2

For dynamic compaction, the soils in third zone; which is labelled as Zone 2 on Figure 2-14 , is at intermediate position between the most favourable soils and the unfavourable soils. this catergory conmprises silts, clayey silts, and sandy silts. This soils in Zone 2 normally have a permeability on the order of 10^{-5} to 10^{-8} m/s. When dynamic compaction is applied in these deposits, the energy must be applied using multiple phases or multiple passes due to the lower permeability than desired level. Hence between the phases or passes, adequate time should be

allowed to let despite the excess pore water pressures. Since the excess pore water pressure takes days to weeks to dissipate, sometimes wick drains are installed in such formations for facilitation of drainage.

2.11.2 Main Component of Dynamic Compaction Machine

Dropping weight and lifting crane are the main component of dynamic compaction machine. Those weights have been typically made out of steel plates or concrete filled steel shells and reinforced concrete in dynamic compaction projects. In addition, laboratory systems have been used by several academics to investigate the falling weights' impacts. while Base configuration of those tampers are square, circular or octagonal, the latter two are more suitable for primary tamping phases, since it can form the circular shape crater eventually by wasting little energy. Further, square weights are more suitable for ironing phases. Moreover, special hollow shapes also have been introduced to increase the falling velocity through water for underwater applications .

2.12. Vibro Compaction

Vibro compaction, also known as vibrofloatation developed in 1934 with invention of first vibroprobe by W.L. Degen and S. Steuermann in Germany. This is a deep ground compaction technique and which consists of the application of punctual vibrations at different depths inside a soil layer. These vibrations causing dynamic loadings inside the soil are produced by a device called "vibrator" and can have different amplitudes and frequencies, (Susana López-Querola et al.: 2014) [45].

This technique is most suitable for treating soils consists of less than 18% of fines. However, Woodward (1985) [46] have suggested that soils having less than 10% fines would give best results. This vibroprobe, also referred as vibrating poker, is a hollow steel tube giving a horizontal vibration as it contains an eccentric weight mounted on a vertical axis in the lower part.

This vibroprobe is either flushed down to pre-defined depth in soil as per the design using water jets or air jets or both of them. When it reaches to the required depth, the vibroflot is moved in

an up and down motion at certain intervals while material being added to the ground surface. With reduction of void ratio in the improving area by the horizontal vibrations, compacted cylinder of soil is formed with depression at the surface (Hamidi:2011) [47].

Vibro compaction can be applied to compact natural deposits as well as artificially reclaimed sands. The degree of improvement largely depends on;

- Granular soil type being treated.
- Type of equipment used.
- the effect of vibration with distance from the probe point.
- Time spent amount at each compaction stage.
- Achievable amperage.

Typically, the diameter of influence zone will be from 3 to 4 meters. To ensure the zones of influence get overlapped sufficiently, VC point spacing is designed to achieve minimum requirements throughout the treated area. Infill by granular materials is applied subsequently in area formed depression around the vibrator or the extension tubes. Automatic recording device undertakes the monitoring of each probe point (Myint Win Bo:2013). Benefits of Vibro Technologies over the other densification method as follows;

- Liquefaction and lateral spreading mitigation.
- Site after treatment uniformity.
- Achievability of the specified degree of improvement demanded by the project.
- Saving of cost and time over conventional system.
- Applicability on ground close to existing structures.

2.12.1. Applicability of Vibro Compaction

For the ground, which consists of medium to coarse grained sand with a silt content of less than 12% passing sieve size of 0.074mm (No. 200) and clay content of less than 2 percent passing sieve size of 0.005mm, Vibro Compaction technique would be the ideal. (See grain size curve as in Figure 2-15 (Keller, 2012) [48]. The effectiveness of vibro compaction with soil types in reclamation fill is shown Table 2-5.

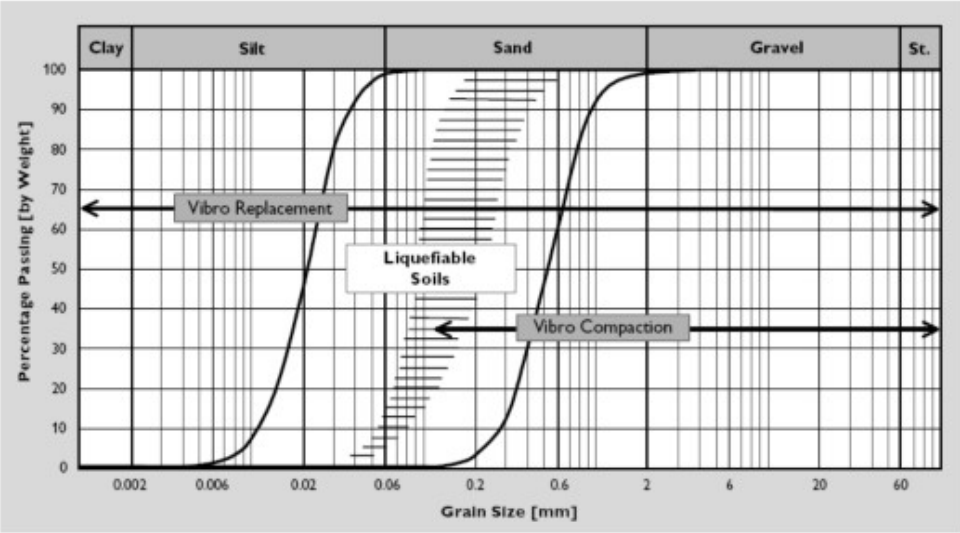

Figure 2-15: Application range of the deep vibratory compaction techniques and liquefiable soils range (Keller; 2012) [48]

Table 2-5*:* Effectiveness of vibrocompaction with soil types *(*Courtesy; Keller*)* [48]

Ground Type to be Improved	**Tentative Effectiveness**
Sand	Excellent
Silty Sand	Marginal to Good
Silts	Poor
Clays	Not applicable
Mine Spoits	Good (if clean granular)
Dumped fill	Dependent on the nature of fill
Garbage	Not applicable

The Vibro Probe, more commonly called a vibroflot is classic vibro compaction method equipment, which consists of a torpedo shaped hydraulic or electric vibrator. Vibro probe is vibrating horizontally at frequencies of up to 3000 rpm and with amplitudes of 10 to 23 mm (1/2 to 1 inch) while typically 2 to 4 m (7-11 ft) in length. The vibrator is attached to a follow up pipe and hose length selected according to the desired improvement depth. (FHWA 2001) [49] . The performance sequence of classic processes can be figure out in three distinguished steps as penetration, compaction and backfilling: (Laynegeo 2012). Typically vibroprobe

method range from 3 to 15m (10 to 50 ft) depth, but it can also be applied as shallow as a one meter (3 ft) and as deep as 36 m (120 ft) (FHWA, 2001) [49].

2.12.2. Use of Brown's suitability index

Applicability of vibro compaction for the sand can be further verified by Brown's suitability number as shown in Table 2-6;

Suitability number, $S_N=\sqrt{(3/D_{50}^2+ 1/D_{20}^2+1/D_{10}^2)}$ (18)

Where D_{50}, D_{20} and D_{10} are particle diameter at 50% passing, 20% passing and 10% passing respectively. Rating of sand for suitability to apply vibro compaction is as follows;

Table 2-6: Rating for vibro compaction on S_N (Brown: 1977) [49]

Range of S_N	Rating
0-10	Excellent
10-20	Good
20-30	Fair
30-50	Poor
>50	Unsuitable

2.12.3. Main component of the Deep Vibrators

The Followings can be considered as the major three elements contain in vibro compaction process:

- Compaction equipment: vibrator or compaction probe (probe and shaft) and power pack, and base machine.
- Compaction Process: compaction point grid pattern and spacing, vibration frequency and duration and mode of probe insertion and extraction.
- Process control and monitoring: control of production (evaluation of vibro graphs record in the machine) and verification of densification effort (CPT/SPT)

To achieve optimal performance, these elements need to be adapted to the site condition and densification requirements (Massarsch:2015) [50].

Essentially, the vibroflot is a long as well as slender steel tube having two parts, i.e. the vibrator and the follow up tubes. By an eccentric weight at the bottom of the vibrator body, which rotates around its vertical axis, horizontal vibrations of the probe are induced. Then the probe is connected to the extension tube supported by a rig; usually a crane. The vibrator (can be taken as the heart of the vibroflot) consists of a 300- 400-millimetre diameter, a hollow

cylindrical body of 2.0 to 4.0m in length. An elastic coupling or universal type point is used to connect the vibrator to the follower tubes while isolating from induced vibration. In the lower part of the vibroflot, eccentric weight is driven by an electric or hydraulic motor induced the required latteral vibration (Griffith: 1991) [51]. Main component of the vibro probe and supporting equipment are listed below (see Figure 2-16).

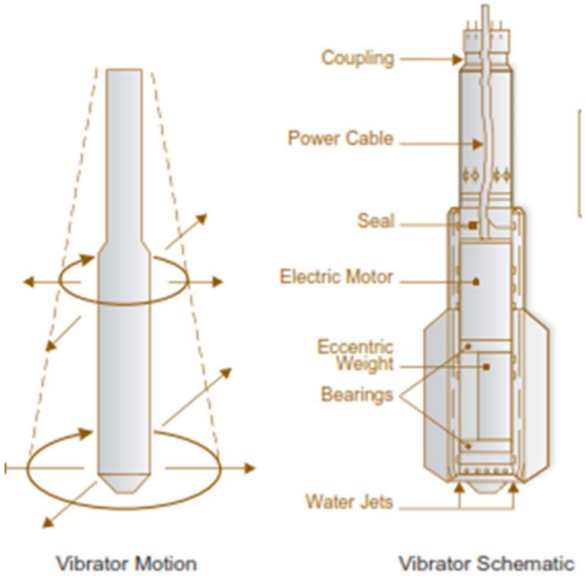

Figure 2-16: Vibrator Motion and Schematic

a. Components of the Vibrator

- Motor gland
- Motor water jet
- Vibrator Motor
- Connecting flange
- Electrical block
- Vibrator spindle
- Vibrator head
- Data logger, data transmitter

b. Supporting equipment

- Hanging head and guide rod
- Shock absorber
- Electric cabinet
- Cable and high-pressure hose
- Clear water pump

- Water tank and level instrument
- Pressure guages and valves
- Generators

2.13. Mechanism of Densification in DC and VC

In simple terms, the increase of density while the decrease of volume occupied by the voids is described as soil densification. After satisfying two conditions, materials shift from a loose state to a dense state. Firstly, the shear resistance force; a function of the normal force, coefficient of physical friction and adhesion force (if available), must be overcome at the points of contact. (Wallays; 1982) [52] . Secondly, the pore water pressure corresponding to the reduction of voids must be able to freely and quickly dissipated, if the soils exist below the ground water table level, or the addition of water occurs (i.e. jetting during vibroflot penetration) [51].

Dynamic compaction can be considered as a ground improvement technique, which transmits high energy impact to loosen soils having low bearing capacity and high compressibility potentials initially to improve their mechanical properties (Hamidi et al., 2009) [53]. Thereof a heavy weight or pounder dropping from a significant height delivers the impact energy. (Hamidi et al., 2009) [53] .

When applying pounder impact on the unsaturated ground surface, impact energy generates seismic radiation, which transmits into the underlying soil mass subsequently. At the moment of impact, the impact energy is transmitted to soil as mainly in body waves, which consist of compression and shear waves. Moreover surface waves also generated in the soil layer while, body waves generated from the source and propagate radially outwards along a hemispherical wave front, as shown in Figure 2-19. Meanwhile the surface waves propagate horizontally along the surface. These shock wave influence on the soil depends on the soil types and the degree of saturation. For dry deposits, the interlocking stresses are overcome by impact induced compressive and shear waves within the loose strata and resulting a void reduction. When profile of sand grains rearrangement by dynamic compaction (see Figure 2-17), surface settlement can be appeared by reduction of volume with densification of non-cohesive soils.

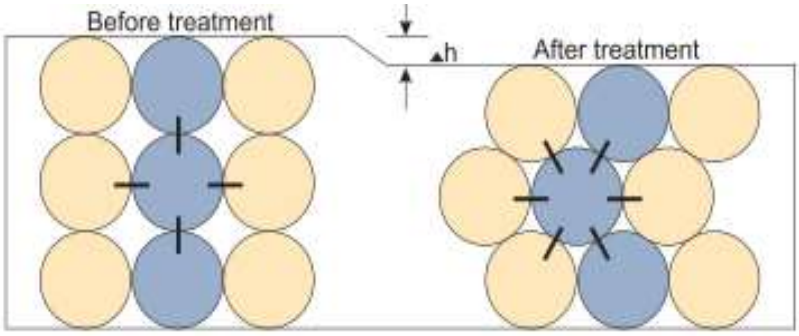

Figure 2-17: Profile of sand grains rearranged by dynamic compaction

For a saturated granular deposit, the mechanism of densification is quite different. During dynamic compaction, DC impact induce compressive stresses, results in a sudden pore water pressure increase, thereby soil is forced into temporary liquefaction state. Then the soil skeleton is travelled by much slower shear wave and Rayleigh waves. Accordingly, the soil particles are rearranged into a dense state by a combination of a temporary loss of contact stresses and dynamic oscillation forces (M.W. Bo et al. 2009) [6] . The falling pounder applies a sudden dynamic loading to the loose granular soil, which can cause the vertical stress to exceed its elastic limit σ_e causing the soil to deform plastically (Yahya Nazhat 2013) [55] .

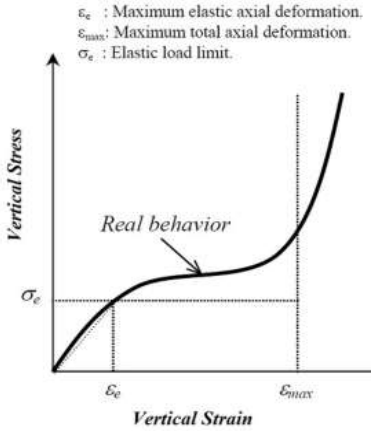

Figure 2-18: Axial deformation of confined compactable loose granular soil [54]

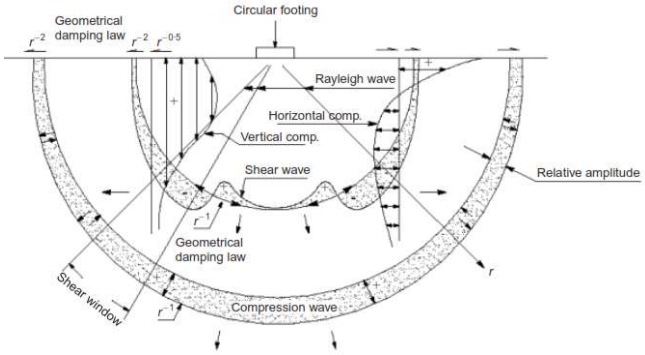

Figure 2-19: Wave Propagation due to dynamic compaction (Wood R.D) [55]

Using trial compaction and in-situ field investigation data, Lukas developed a descriptive compaction pattern down to the influence depth as Figure 2-20. Therefore, it can be noted that the surface deposits become loosen initially and with ironing compaction, it is densified.

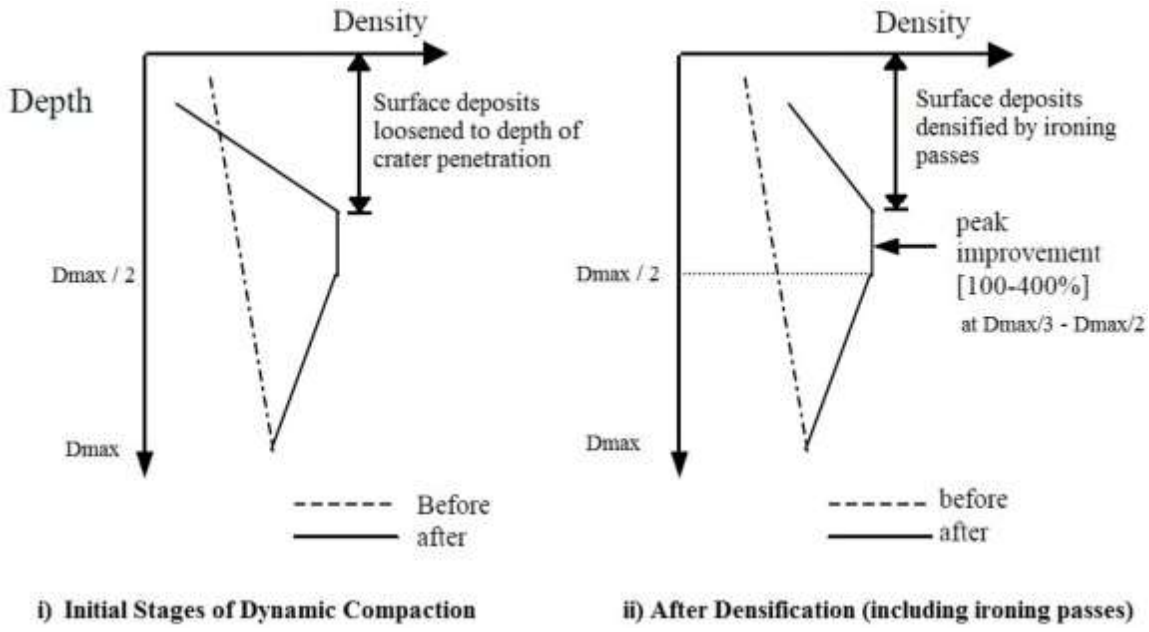

Figure 2-20: Soil Improvement Descriptive Pattern of by DC (Lukas, 1986) [36]

In sand improvement by vibro compaction or dynamic compaction in saturated condition, the following diagrams illustrate the compaction process due to re-arrangment of sand grains.

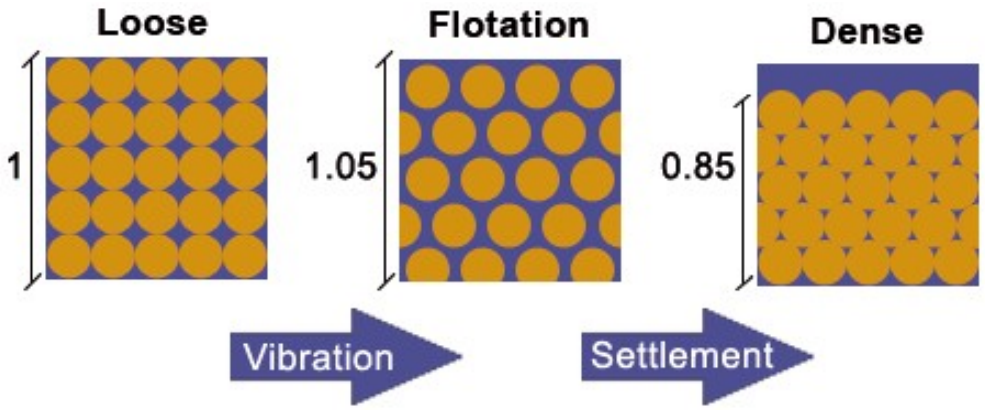

Figure 2-21: Grain rearrangement in Vibro Compaction

As Moretrench, (2012) [56] notified the effects of soil densification by vibro compaction as summarized below;

- The sand and gravel particles are rearranged into a denser state.
- Horizontal and vertical effective stress ratio is significantly increased.
- Depending on many factors, soil permeability is reduced from 2 to 10-fold.
- The friction angle of soil is increased by up to 8 degrees typically.

- In the range of 2 per cent to 15 per cent, typically 5 per cent settlements in the compacted soil mass is forced.
- The modulus of stiffness can be increased by 2 to 4-fold.
- As a result of higher shear strength parameters, a better bearing capacity can be achieved.

2.14. Compaction Sequence of Dynamic Compaction

Dynamic compaction is usually applied as two phases as shown in Figure 2-22. In order to improve the deeper layers, wide spaced impacts is designed under the first phase of the treatment, normally called a pass. These initial phases are also known as the ′high energy phases′ as the compactive energy is concentrated on point distant by at least 3m. Those initial passes are followed by a low energy pass at the end. This lower energy pass is called as ′ironing tamping‘ and which is used to get the surficial layers densified applying in the 0 to 1.5m intervals (Mayne et al:1984) [35]. The treatment by the first phase (also known as first and second pass) can be considered as deep treatment and intermediate treatment while the treatment by ironing tamping is considered as shallow treatment. Figure 2-24 shows the image of 1st pass in DC.

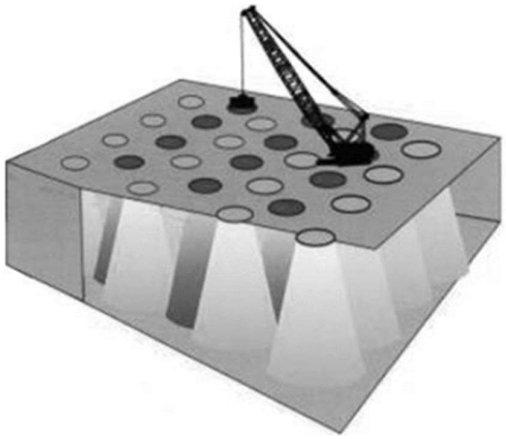

Figure 2-22: Arrangement of compaction point as first and second pass

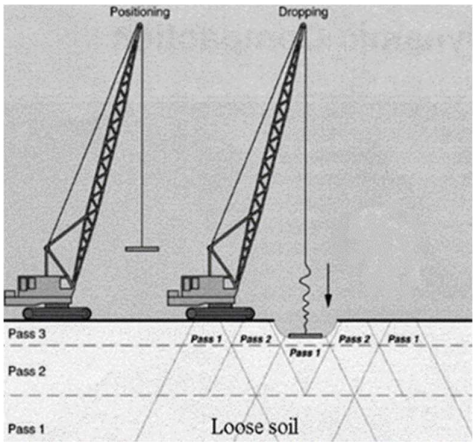

Figure 2-23: Treatment by each pass

The spacing for the first pass of impact is usually equals to the densifiable layer thickness (influenced depth). In order to allow the impact energy to reach the lower part of the layer the second pass is generally made at the centroid prints of the first pass. During each pass, several drops are made at the same point. There is a maximum number of impacts that leads to closure of voids in order to achieve the minimum void ratio. After each pass the created craters during

pounder dropping are backfilled with surrounding materials usually prior to next pass. Finally, ironing pass with low energy impact and reduced drop height is performed to compact the shallow surface layer (M.W. Bo: 2008). [6]. when the craters are backfilled using the surrounding materials , the working platform is lowered gradually by an amount which is proportional to the achieved densification by each pass. In order to get maximize effect from dynamic compaction, cranes are utilized by lifting an available weight to its highest possible drop height while considering operational and structural limitations of the system. However, selection of incorrect spacing and energy at this stage may result in the dense material raft creation at an intermediate level, making difficult, if not impossible to treat underneath loose materials (Mayne et al.:1984) [35].

Figure 2-24: Dynamic compaction done in the project site

2.15. Construction Sequence of Vibro Compaction

As per Figure 2-25, construction sequence of VC can be illustrated as few steps and the four major steps in VC can be described as follows;

Penetration : The vibroflot is suspended by a crane, be lowered by its own weight and penetrated up to the required depth by vibration with aid of jetting water and air. Subsequently the vibrator penetrates to design depth at full water pressure and is surged up and down as

necessary to agitate sand, remove fines and form an annular gap around the vibrator, resulted the water flow get stopped or reduced.

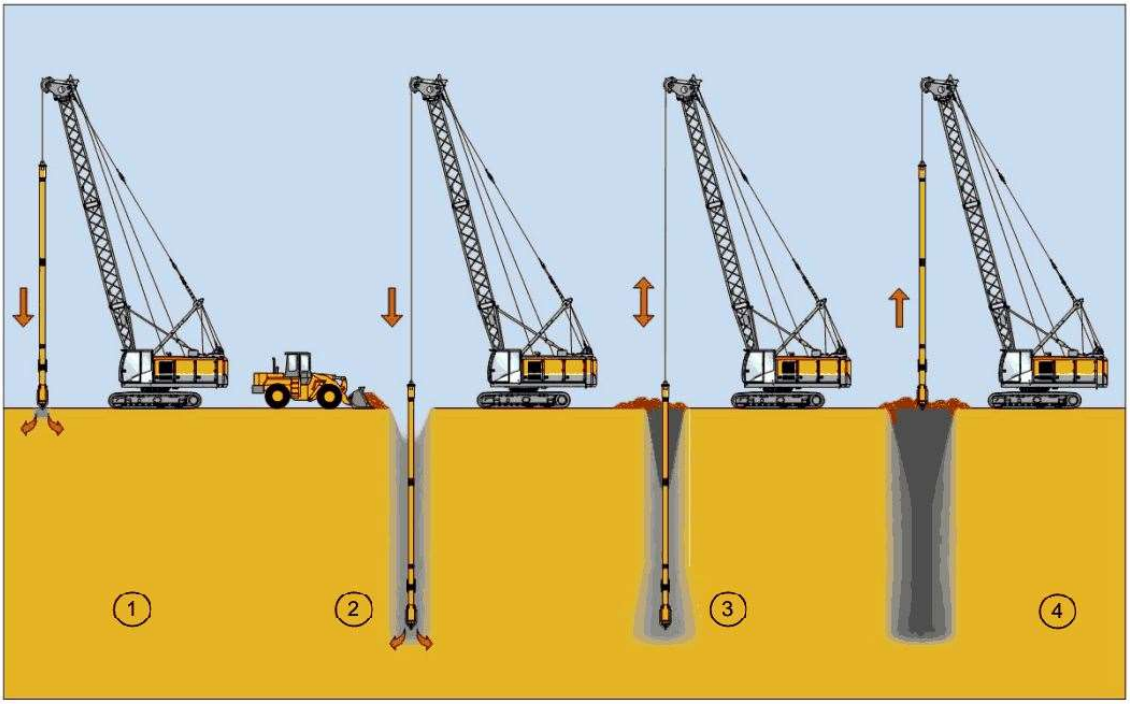

Figure 2-25: Construction sequence of vibro compaction

Compaction : After the vibroprobe reaches the required depth, during withdrawal, the vibroflot is moved in an up and down motion at certain intervals while adding material from the ground surface. Accordingly a compacted cylinder of soil is formed due to horizontal vibrations getting a depression at the surface due to the void ratio reduction in the ground. This soil improved zone extends from 1.5 m to more than 4 m from the vibrator, depending on the vibroflot power.

The vibrator is maintained at a certain depth during the compaction, until either the vibrator's power consumption reaches to predetermined amperage level or to elapse the pre-set time intervals, typically 30–60sec, whichever is the sooner. The vibrator is raised to a pre-determined height, typically 0.5– 1.0m after the amperage/time criterion is satisfied, and is held again in position until the amperage reaches the target level or the pre-set time, whichever is sooner. Then the vibrator is lifted for the next compaction step and this procedure is repeated stepwise till the vibrator comes to the surface (Raju et al.:2008) [57]

The vibro compaction process done by transmission of waves and its affection zone has shown as a schematic diagram by Jaime Peco Culebra et al. (2012) [58] in his numerical analysis as shown in Figure 2-26.

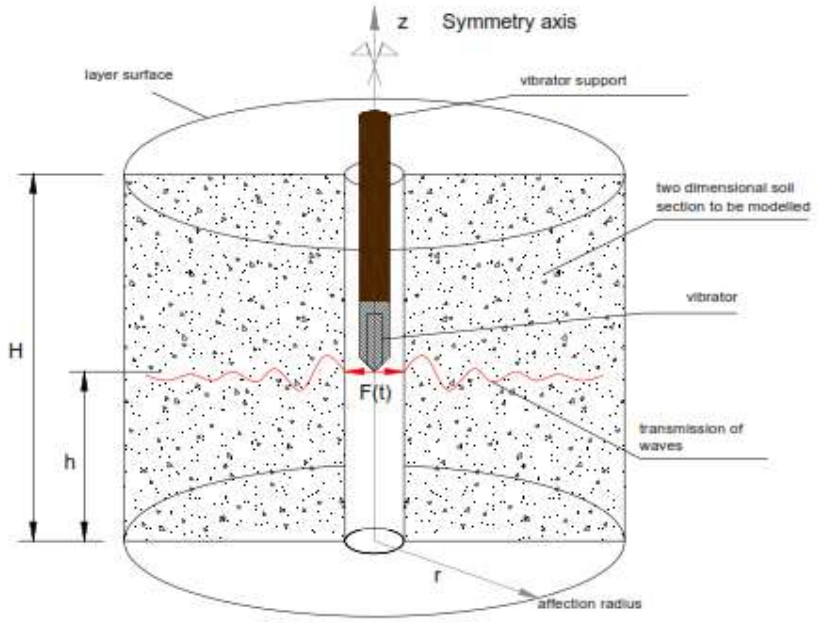

Figure 2-26: Process of vibro-compaction and its affection zone

In this study, upon lowering the vibro float to the required level, while turning off air, water pressure at side wash pipes was reduce to 0.2 to 0.4MPa level to collapse in situ material on the side of the probe. The lifting increment is 0.75m below 6m depth and 0.5m increment in layers at 0 to 6m depth. Hold time is 30s and average maximum amperage is 140 to 150 Amps.

According to sand movement within the affection zone, it can be further divided as in Figure 2-28.

Refilling (Backfilling): backfilling is done using, either imported or insitu material. the compacted surface of the area may be lowered 5% to 15% of the treated depth (influenced depth), if in situ material is used.

Completion : An optimum improvement can be achieved using an economical layout of compaction points. Then the improved area surface is relevelled and again densified with a surface compactor.

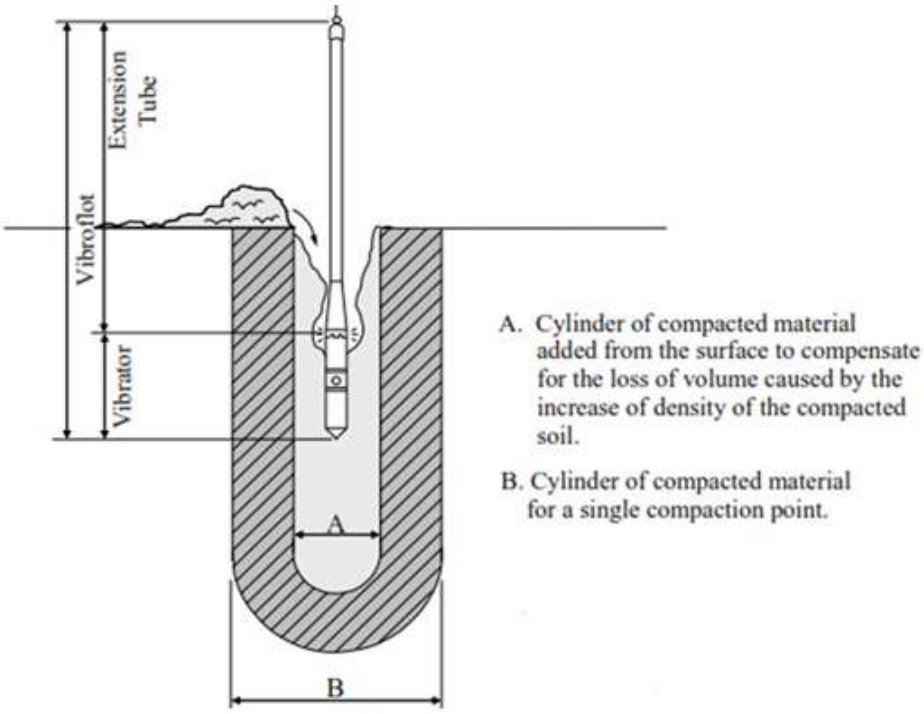

Figure 2-27: Densification zones resulting from vibro compaction (Brown: 1977)

Figure 2-28: Vibro Compaction done in Project Area

2.16. Optimization of Sand Densification

2.16.1. Factors Affecting Dynamic Compaction

Effective factors on efficiency and improvement depth of dynamic compaction was divided into two general categories by a number of researchers, including Lukas (1986) [36] and Luongo (1992) [59] as follows;

1. The ground related factors such as soil type and its layering, presence of a hard layer under or on compacted soil, degree of saturation and ground water level etc.
2. The equipment related factors including weight of tamper, falling height, base area of the tamper tamper and its shape and number of blows (Mehdipour S. et al. 2017) [60].

However, when dynamic compaction is used for thick sand fill in reclamation area, ground related factors do not have much variation. Thus, equipment related factors govern the degree of compaction and influence depth.

Federal Highway Circular I describes following consideration to be considered in the design of dynamic compaction;

- Determining of the energy to be applied over the project site to achieve the desired improvement.
- Selection of the tamper mass and drop height as appropriate to the improvement depth requirements.
- Selection of the area to be densified by DC.
- Determination of the grid pattern, spacing and number of phases (passes).
- Establishment of the maximum number of blows.
- Requirement of a surface stabilizing layer in case of weak ground.

Regardless of whether the project will be completed with a method or a performance specification, these six steps should be addressed. If the project is undertaken as per a method specification, the design agency or their consultant determines the procedure of dynamic compaction with incorporation of an evaluation on these six items. Otherwise, when the project will be undertaken with a performance specification, the specialty contractor addresses these six items based upon the required improvement level. In order to determine whether these items have been adequately considered, the design agency or their consultant should review the plan of specialty contractor.

2.16.1.1. Compaction-Point Spacing

Normally, a square grid pattern for 1st pass and contiguous (square grid) pattern for 2nd pass compaction points is chosen while overlapping low energy is applied for ironing tamping. Grid spacing and drops shall be designed using Equation19.

$$AE = (N.W.H.\ P) / (\text{grid spacing})^2 \quad (19)$$

Where: AE = applied energy, N = number of drops, W = tamper mass,
H = drop height, P = number of passes

The design procedure is as follows;

1. Thickness of loose deposit or the depth of the deposit that needs densification to satisfy design requirements is determined from subsurface exploration.
2. Equation; $D = n\,(WH)^{0.5}$ is used for influenced depth while n value is selected from **Error! Reference source not found.** for each soil type.
3. Tamper mass and drop height is checked use Figure 2-29 as a guide while considering available dynamic compaction equipment.
4. Pounder weight (W) and drop height (H) is selected based on required improvement depth.
5. The energy of unit area/volume is selected using Table 2-7 taking the proper deposit classification into account.
6. Average energy to be applied at ground surface is obtained by multiplying unit energy and the deposit thickness.
7. A grid spacing range is selected from 1.5 to 2.5 times the tamper diameter.
8. Equation 19 is used to calculate the product of N and P. Generally, 7 to 15 drops are made at each grid point. When the calculations indicate significantly more than 15 or less than 7 drops, the grid spacing is adjusted.

Table 2 7: n values recommended for different soil types (Lukas: 1995) [44]

Soil Type	Degree of Saturation	Recommended *n* Value*
Pervious Soil Deposits - Granular soils	High	0.5
	Low	0.5 - 0.6
Semipervious Soil Deposits - Primarily silts with plasticity index of < 8	High	0.35 - 0.4
	Low	0.4 - 0.5
Impervious Deposits - Primarily clayey soils with plasiticity index of > 8	High	Not recommended
	Low	0.35 - 0.40 Soils should be at water content less than the plastic limit.

*For an applied energy of 1 to 3 $^{MJ}/_{m^2}$ and for a tamper drop using a single cable with a free spool drum.

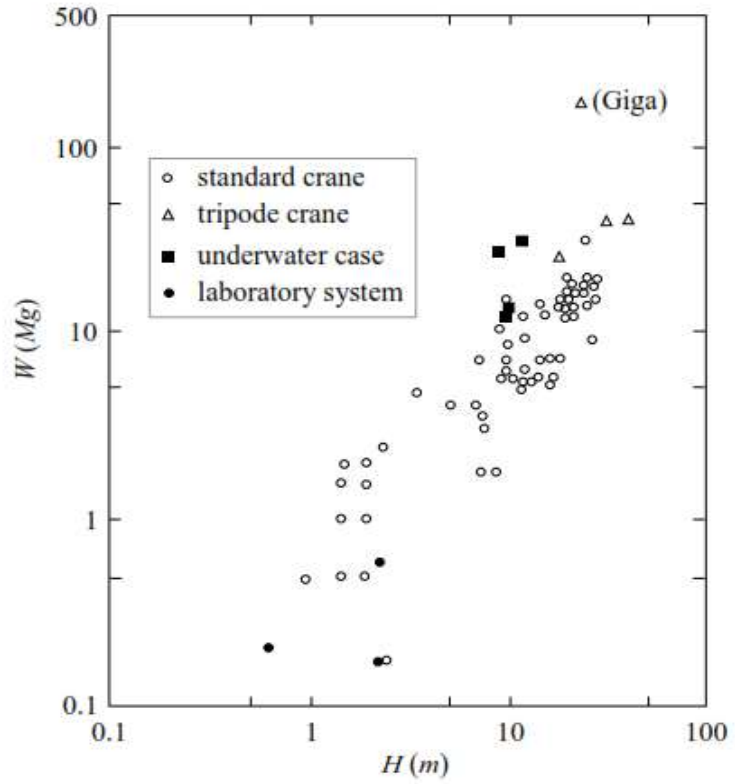

Figure 2-29: Corelation of tamper mass and drop height (Mayne et al.1984)

Table 2-7: Guidelines on applied Energy for densifying various soils (Lukas 1986)

Type of Deposit	Unit Applied Energy (kJ/m^3)	Percent Standard Proctor Energy
Pervious coarse-grained soil (Zone 1)	200 - 250	33 - 41
Semi-pervious fine-grained soils (Zone 2) and Clay fills above the water table (Zone 3)	250 - 350	41 - 60
Landfills	600 - 1100	100 - 180
Note: Standard Proctor energy equals 600 kJ/m^3		

2.16.1.2. Shape of Pounder

Pounders of several different shapes, including square, hexagonal and circular or octagonal have been used in dynamic compaction (M.W. Bo: 2009) [6]. The thickness of pounders may also vary. Some pounders are made up of steel plates which is hold together by studs or nuts and bolts. Pounders are usually made up of steel, though there are a few, which consist of concrete block.

2.16.1.3. Lifting and Dropping Mechanism

In dynamic compaction work, lifting of the pounder is achieved usually by means of a crane having a winch system. Thus, high-capacity cranes with various boom lengths are opted for dynamic compaction works. However, when the pounder is too heavy, tripods will need to be used instead of cranes. The drop point is just in front of the crane, or at the centre of the tripod. When the cable follows with the pounder when the pounder is released, significant friction between the pulley and cable can be expected, resulting in some energy losses. In Equation 21, this effect is taken into account as an empirical coefficient of n. Even in free-fall situations, energy losses arising from friction caused by rapid movement of the pounder in the air can still be expected (M.W. Bo et al. 2008) [6]. Therefore, n value related to dynamic compaction mechanism and machine type can be found by analysing field data.

2.16.2. Factors Affecting Vibro Compaction

The compaction process is an important element of vibro compaction and can influence the technical and economical results significantly. However, in practice, this aspect is not appreciated. The compaction process requires that the following parameters are chosen:

- Vibroprobe capacity
- Lateral vibration impact

- Compaction points spacing
- Probe penetration and extraction
- holding time at each depth interval
- Pressure of water
- Required water jet type and its location

2.16.2.1. Vibro-Probe Capacity

high-powered probe-type vibrators ranging from 12 to 16 inches in diameter and 10 to 15 feet in length are used to achieve the necessary densification in the process. Details of vibro probe under different makes are as in Table 2-8;

Table 2-8: Specifications of several vibrators (Degen and Hussin 2001) [62]

Vibrator	Length m	Dia. mm	Weight kg	Motor kW	Speed rpm	Ampl. mm	Dynamic Force kN
Bauer TR13	3.1	300	1000	105	3250	6	150
Bauer TR85	4.2	420	2090	210	1800	22	330
Keller M	3.3	290	1600	50	3000	7.2	150
Keller S	3.0	400	2450	120	1800	18	280
Keller A	4.3	290	1900	50	2000	13.8	160
Keller L	3.1	320	1815	100	3600	5.3	201
Vibro V23	3.6	350	2200	130	1800	23	300
Vibro V32	3.6	350	2200	130	1800	32	450

An electrically driven motor is usually employed to drive the probe and which is driven by typically in the 100-130 kW range. The vibrations produced as a result of the rotation of the weights, is generated at the nose of the unit and which emanate Dynamic Force radially in the horizontal plane away from the unit. The generate dynamic forces by the unit is from 150 to 450 kN at frequencies ranging from 1,800-3,200 rpm (FHWA: 2017) [61]

2.16.2.2. Compaction-Point Spacing

With respect to practical considerations, such as the overall site geometry, the reach of the compaction machine and the number of compactions passes, the spacing between compaction points is required to be selected.

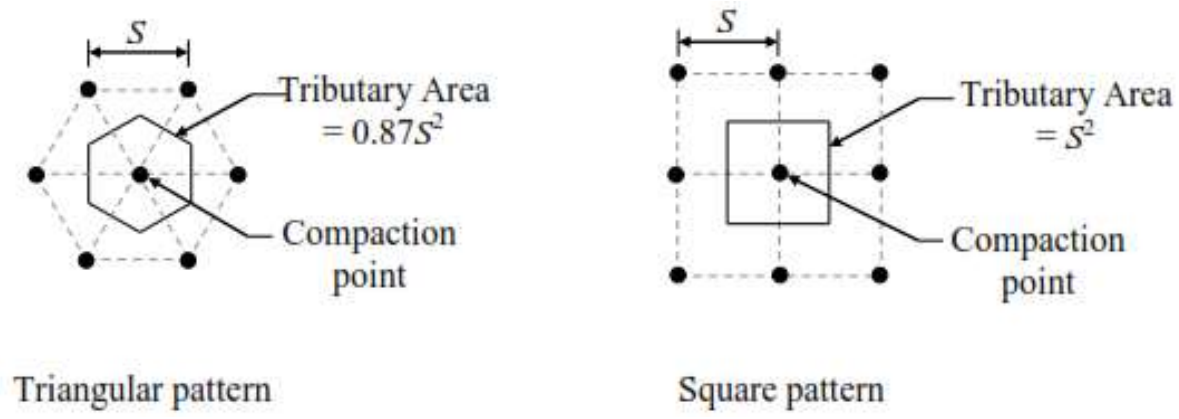

Figure 2-30: Tributary Areas variation with point pattern

If vibro compaction is applied to densify large areas, compaction points are generally arranged in square or triangular grid patterns as shown in Figure 2-30. As shown in Figure 2-31, the approximate post-treated relative density variation can be defined as a function of the tributary area per compaction point as well as soil type. However, though this Figure 2-31 can be used to select the initial spacing of the compaction points, the final design should be selected based on a field tests performed in a trial area.

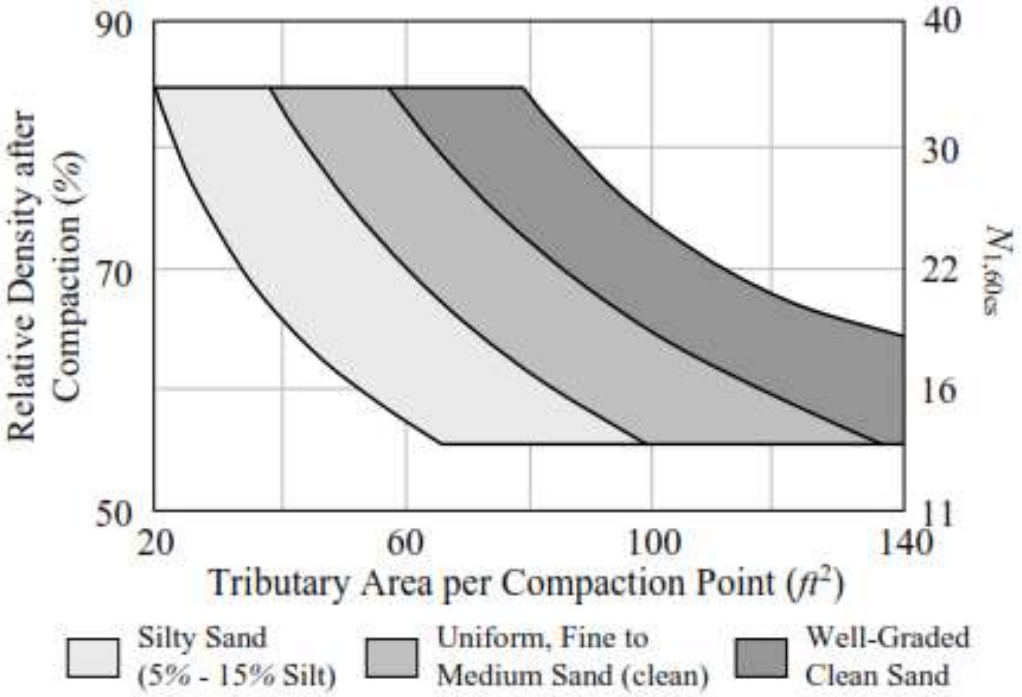

Figure 2-31: Approximate post-compaction relative density variation with tributary area per compaction point (Dobson and Slocombe:1982) [62]

It has been realized that the appropriate grid spacing will likely vary as a function of the type of probe used while a closer grid spacing does not always lead to increased penetration resistance at the centre of the compaction points (Degen and Hussin 2001) [63]. Tip resistance variation of the post-treated CPT is shown as a function of distance from a compaction point as in Figure 2-32.

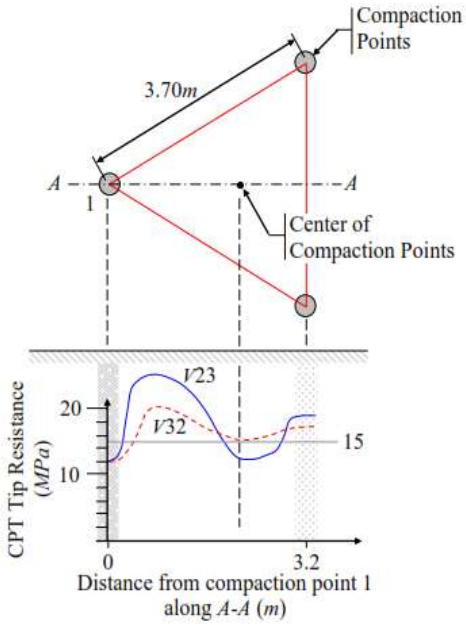

Figure 2-32: Tip resistance (qc) variation of post- treated CPT with distance from compaction point for two different vibrators (Degan and Hussain: 2001) [62]

This figure illustrated; the minimum tip resistance specified for all locations of this particular project was 15MPa. Using the V23 probe, the minimum tip resistance could not be achieved for a 3.7m probe spacing at the centre of the compaction points, but it could be achieved using the V32 probe. However, higher tip resistances were measured in the soil at other locations, if soil is densified with the V23 probe. Adhering to the specified guidelines of a minimum tip resistance of 15MPa at all locations (i.e., densification of the soil using the V32), the best overall improvement of the site may not be achieved in this particular project (Green: 2001) [64].

What spacing to be assigned between compaction points are dependent on several factors, such as the geotechnical site conditions prior to compaction, degree of compaction requirement, the compaction probe size (area of influence), and the vibrator capacity etc. Use of a smaller spacing for a shorter duration of compaction is generally advantageous than that of a larger spacing with longer duration. The former will form a more homogeneous compaction for the

soil deposit. The typical ranges of spacing is between 1.5m and 5 m for vibro compaction. (Massarsch: 2015) [50] . However, depending on the vibroflot power, Hamidi et al (2011) [15]stated that the improved zone extends from 1.5 m to more than 4 m from the vibrator.

2.16.2.3. Lateral Vibration Impact

As a result of horizontal impact of the compaction probe at the lower end the soil is densified during the vibroflotation. Primarily, the compaction action is in the all direction laterally and gives rise to compression waves. Thus, creating of soil resonance using a Vibroflotation probe is not possible. The vertical limit of compaction zone is up to the compaction probe length and the soil improvement is achieved during extraction of the probe. (Massarsch: 2015) [50] .

It was noted that the interaction between the vibroflot and the surrounding soil is very complex, especially when water and backfill materials are introduced into the borehole during vibration. Below Figure 2-33 shows a conceptual illustration of this interaction and thereof induced stresses and strains on the surrounding soils. As seen in the Figure 2-33, the applied horizontal impact force causes both a radial strain (ε_{rr}) and lateral strain ($\varepsilon_{\theta\theta}$) in the soil, resulting in a deviatoric shear strain (γ_{dev}) as given expression in Equation 20.

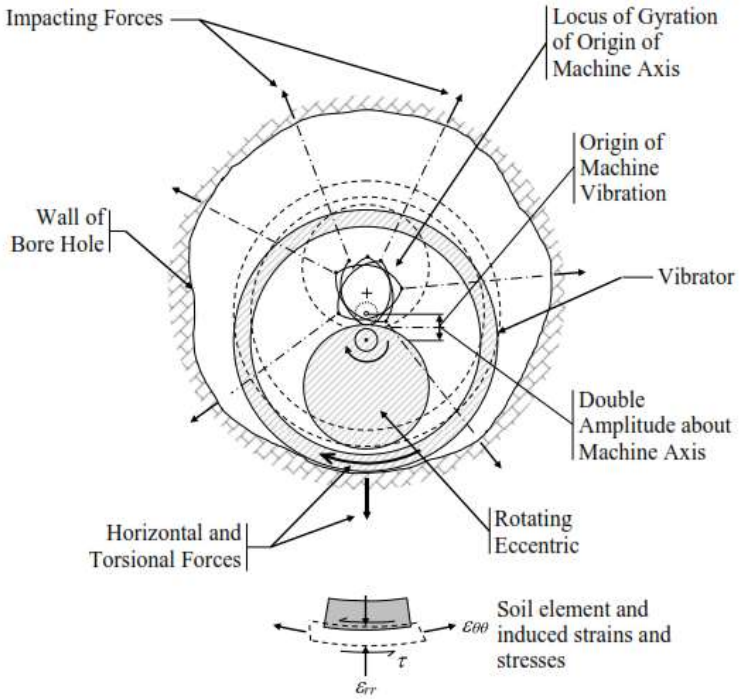

Figure 2-33: Illustration of vibro float induced the horizontal impacting forces and torsional shear (Green wood :1991)

$$\gamma_{dev} = \frac{1}{2} \cdot [\varepsilon_{rr} - \varepsilon_{\theta\theta}] \quad (20)$$

Where:
γ_{dev} = Deviatoric shear strain.
$\varepsilon_{\theta\theta}$ = Lateral strain.
ε_{rr} = Radial strain.

Furthermore, a shear stress (τ) in soil is induced by the torsional motion of the vibroflot. With facilitation by the influx of water that reduces the effective confining stresses imposed on soil, both the deviatoric shear strain and torsional shear stress cause the breakdown of the soil structure, (Green: 2001) [64].

Though vertically oscillating vibro probing mechanism is fully understood, the micro-mechanism in the process of vibroflotation remains poorly understood for horizontally circling deep vibrators while meaningful results being obtained. Since this vibro compaction technique has been successfully applied in many cases, it seems to be essential to develop a rational design approach (Susana López-Querola et al. 2014) [45].

Moreover, it was noted that vibrators operating at lower frequencies in vibro-compaction produce better results in densification usually, than those operating at higher frequencies. The reason is that low frequency vibrators usually have a higher amplitude, which provides a greater compactive effort. Furthermore, most densifiable soils are having the natural frequency closer to 1500 rpm than to 3000 rpm (FHWA:2017) [61].

2.16.2.4. Probe Penetration, Compaction and Extraction

Deep vibratory compaction is a repetitive process, which comprise of three main phases such as compaction probe insertion to the required depth, soil densification by holding probe at that particular depth, and extraction. With assistance of pressure applied by water jet, air jet and self-weight of vibroprobe, the vibro prob is penetrated down to the required depth of compaction while keeping vibration at adequate level. Upon the probe reaching to the design depth, water jetting is reduced and subsequently the vibroflot is extracted slowly, with pauses at regular intervals to ensure achieving compaction at each depth at satisfactory level. Finally the vibroprobe is withdrawn back to the surface after forming cylindrical compacted zone in

ground around the insertion point. In order to fill the formed cone of depression, additional sand will also be added at the top of the hole. The extraction rate is varied to suit the encountered conditions onsite and to ensure achieving correct amount of densification for each project (www.balfourbeatty.com).

Rates applied for the penetration typically varies from 1.0 to 2.0 m /min. After reaching to the required depth the bottom water jets are turned off while the side jets are turned on. This side jets are introduced to liquefy the soil around the vibrator. More importantly, the water volume used for jetting should be sufficient to stabilize the borehole and to compensate seepage looses. This flow rate should be up to 3 m^3 /min and the maximum water pressure is 0.8 MPa. To prevent caving of the sides of the hole, the water level in the borehole should always be kept higher than the groundwater level (Broms:1991) [65].

2.16.2.5. Duration of Compaction

The compaction duration for each point is an important parameter and which is dependent on the properties of soils prior to compaction, the required degree of densification and the amount of vibration energy transferred to the ground (intensity and duration). For the larger projects, the optimal compaction grid pattern and spacing should be determined using few compaction trials.

In water-saturated loose sand deposits, the ground liquefies during the compaction. Shortly after densification had started, a zone adjacent to the compaction probe liquefied and groundwater rose to the surface. During this liquefaction phase, the ground vibrations are almost ceased as no energy transferring from the probe to the surrounding soil. Subsequently with sand densification, ground vibrations gradually increase again. (Massarsch: 2015) [50].

2.16.3. Evaluation of Optimization of Sand Densification for Optimization

After selection of compaction equipment to achieve most efficient compaction, other main factors to increase efficiency shall be considered. In design of ground improvement by DC or VC, the main factors to be concerned for optimization are application of energy, spacing of compaction, pattern of compaction points, use of phase construction or duration etc. When the

design is applied on the sand layer to be compacted, the design has to be verified by trial compaction by measuring few field data directly or indirectly with correlations. Based on that field data, degree of compaction and optimization of compaction can be decided.

Those field data to be concerned in DC is crater depth, influence depth and Ground Improvement index, aging effect etc. the crater depth is the major measurable fact required to evaluate the optimization of compaction and influence depth and Ground improvement Index is required to evaluate influence of compaction with respect to the depth and degree of compaction, which are required to meet the design criteria such as bearing capacity, strength parameters, relative density etc. Except crater depth, other factors are measured based on CPT data and selection of CPT location should be carefully taken to confirm the minimum compaction and the consistency of the compaction. Similarly, in VC, current, time and penetration can be measured at site. Based on those values, design and actual compaction can be evaluated.

2.16.3.1. Evaluation of Dynamic Compaction by Construction Data

To verify the dynamic compaction optimization following factors are to be evaluated;

Crater depth

When the energy by falling weight is applied on a pre-determined grid, induction of the relatively large craters in each compaction point can be considered as the most obvious manifestation of the DC process. Thus, the Crater depth is one of useful items used for quality controlling in DC treatment. During multiple impacts of dynamic compaction, the cumulative crater depth increment is a simple sign of their continual improvement of the process. Mehdipour et al.(2017) [60] conducted a numerical analysis to find a corelation between applied energy and crater depth and result has given in Figure 2-34 comparing that determined by Arslan et al. (2007) [66] using 67N test pounder falling from 2.4m in 1120x760x400mm loose sand in a box.

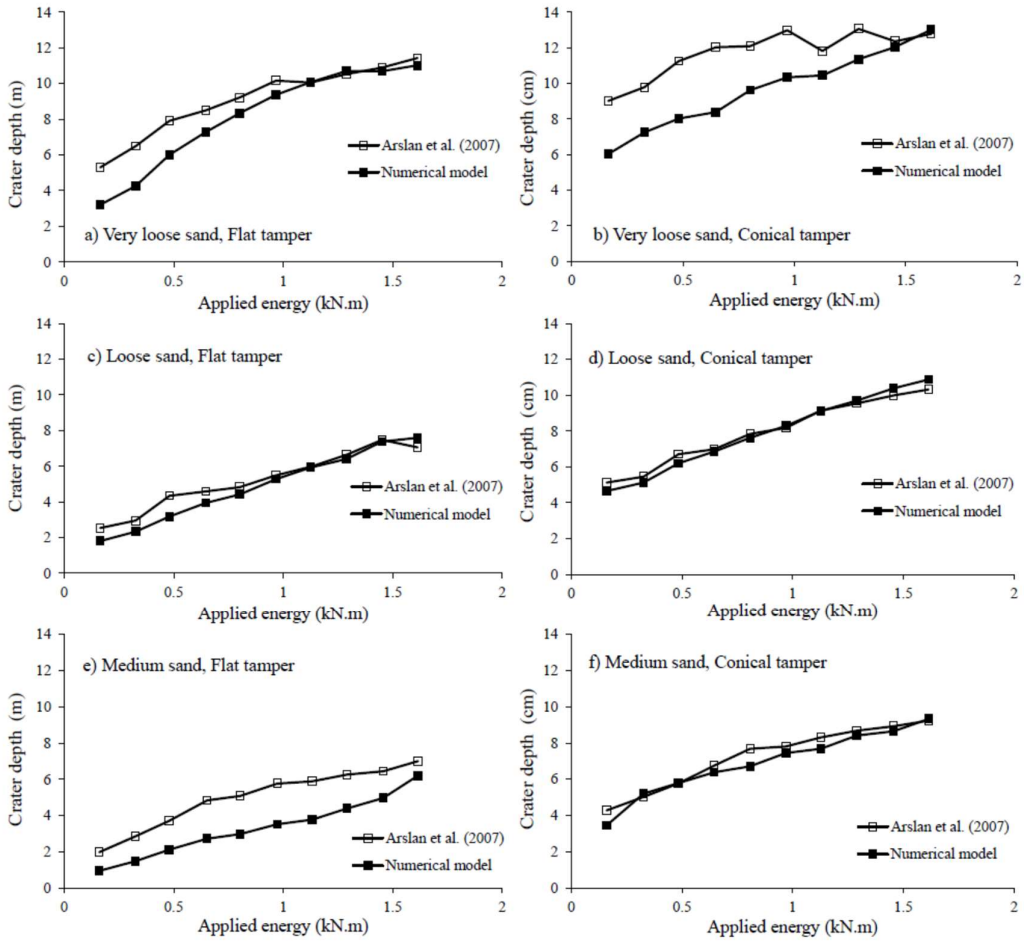

Figure 2-34: Verification of Numerical Model with Experimental Data of Arslan et al. (2007) *[66]*

Moreover, based on empirical data, the following correlation for crater depth, h was proposed by Takada and Oshima (1994) [67] ;

$$h = c.\ m.\ v_0(N)^{0.5}/A \qquad (21)$$

in which N is blow number, m is mass of tamper, v_0 is velocity of tamper at contact time with the ground surface and c is a constant coefficient assumed to be equal to 0.0083 m^2s/ton.

F. Jafarzadeh [68] determined the normalized crater depth by dividing h value with square root of the applied energy to verify the applicability of above Equation 21. The values of normalized crater depth were plotted against the number of drops, N as in Figure 2-35 and it was found that above Takada and Oshima equation predicts low values for a normalized

crater depth, compared with the that of measured in low compaction energy levels (0.2 and 0.5 Kgf tampers) mean while the situation being opposite for high energy levels (1 and 2.3 Kgf tampers). However, for low drop numbers, it was noted a good correlation between the measured and estimated values by above equation.

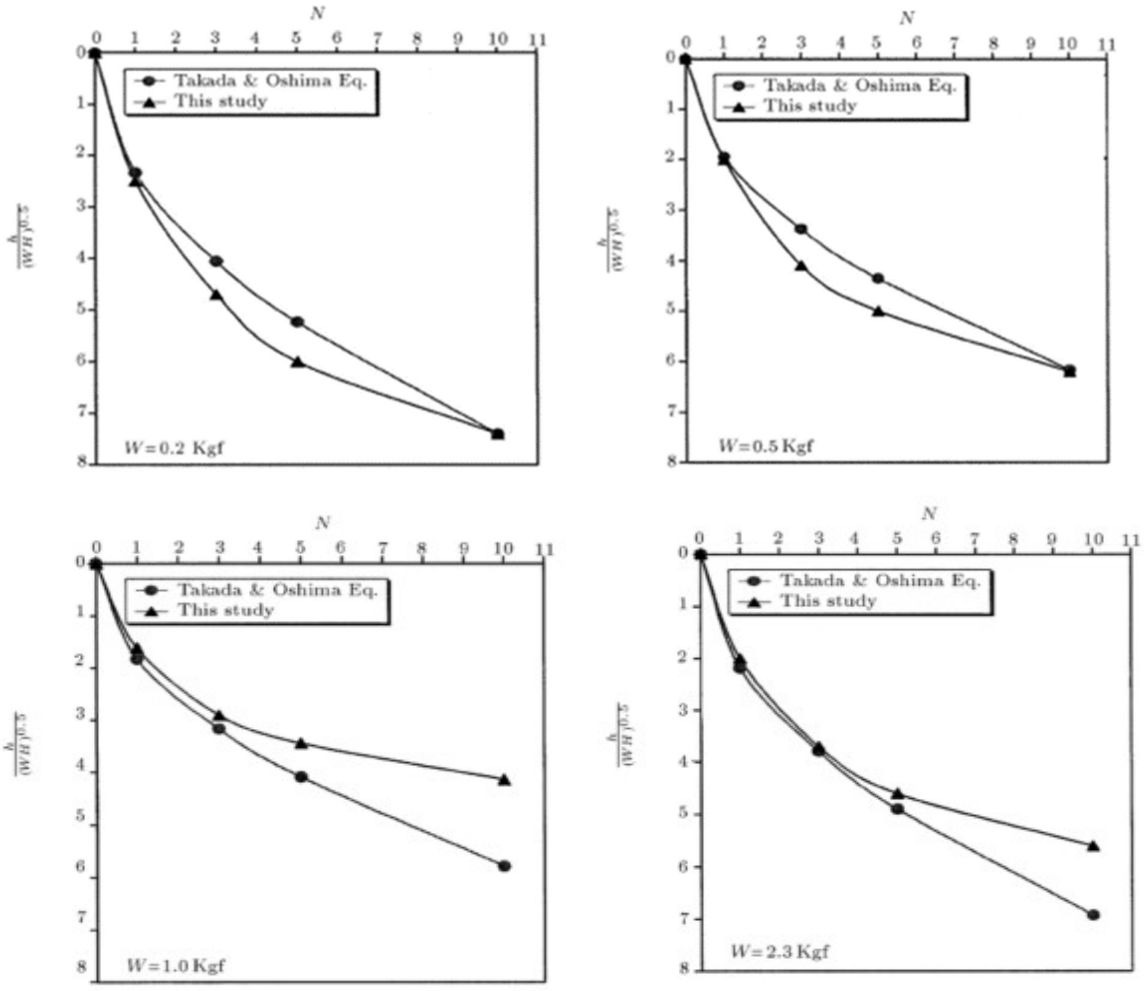

Figure 2-35: Normalized crater depth Correlation with drop numbers measured from model test by F. Jafarzadeh and the Equation introduced by Takada and Oshima for different compaction energy levels. [69]

Y.K. Chow et al.also [69] presented a correlation of number of drops and crater depth found in his numerical analysis with experimentally measure data at Nishiro site by Tanka et al. (1989) [70] as shown in Figure 2-36.

Field measurements of over 120 sites were collected by Mayne et al. to study the response of the ground to DC. As their evaluation, it was showed that the data fall within a rather

narrow band, when the crater depth measurements had been normalized with respect to the square root of energy per drop. On the other hand, they showed that crater depth has a linear correlation with the square root of drop counts.

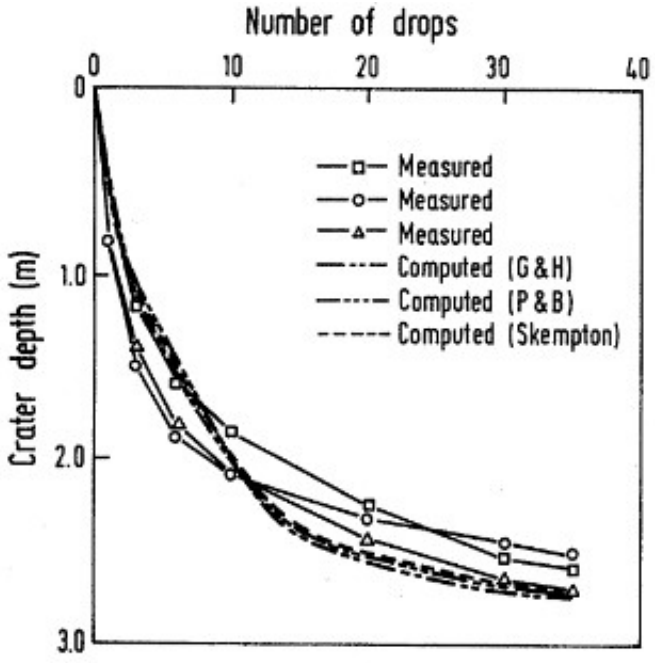

Figure 2-36: Computed and measured crater depths at Nishiro site [70]

The relationship between these measured values and the results of the numerical model carried out by A. Ghassemi et al. [71], varying energy level was plotted in Figure 2-37 as normalized craters depths against the square root of drop number. Then the analysed results by Mayne et al. [35] were compared with those computed normalized results for 300-400 t.m energy per drop from a number of DC sites. ln both the numerical and the experimental data, the linear trends can be seen . The complete overlapping of the lines for different energies in the numerical results can be considered as interesting point as which shows a good agreement with the field measurements as well as numerical values. As such, measured Crater values should be used to select the optimal number of blows per pass and to estimate the average areal subsidence occurred during the process of dynamic compaction. (Mayne et al.,1984) [35].

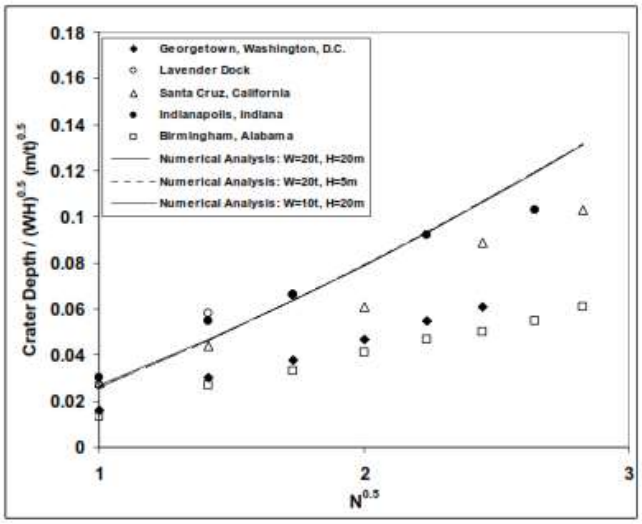

Figure 2-37: Relation between normalized crater depth and √N

2.16.3.2. Evaluation of improvement by Cone Penetration Test

In soil compaction projects, geotechnical field investigation methods play an important role to plan, implement, and verify its performance. The assessment of in-situ characteristics of the soil under before and after compaction condition can be considered as an integral part of the field investigation. In order to assess the sandy coarse-grained soils characteristics, the cone penetration test (CPT) is an efficient as well as operator-independent tool. It is replacing the Standard Penetration Test (SPT) gradually, which dominated previously as the in-situ testing method for this purpose. Accordingly, at Present, CPT can be considered a the most popular field investigation method for compaction projects.

Since CPT provides the entire vertical subsoil formation as a continuous profile it helps to detect the presence of interspersed soil layers. In addtion, since a thin permiable layer also will have a significant influence on the compactability and its time effects, obtaining hydraulic conductivity (permeability) variation of the soil even in thin layers, will be a much important feature of CPT. Since piezocones are able to measure pore water pressure, it is preferred in case of evaluating the efficiency of compaction. moreover, additional sensors such as accelerometers can be added to the CPT equipment to determine velocity of shear waves for special purpose.

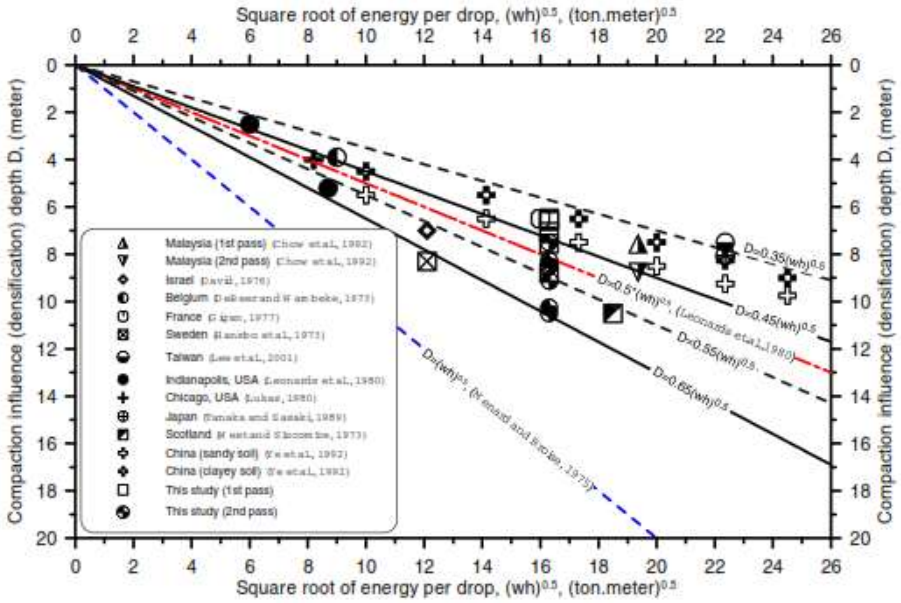

Figure 2-38: Correlation between square root of energy per drop and influence depth (after Leonards et al. 1980) [72]

Influence Depth

By comparing field measurements, improvement depth and degree of improvement are generally evaluated before and after dynamic compaction [35]. Van Impe W.F. [73] pointed out that the influence depth is dependent upon the shape and base area of the pounder. Further, Lukas stated that multi-tamping improves only the zone of influence in lateral directions, and not the influence depth. In dynamic compaction, the degree of improvement of granular soil reaches to its maximum at a critical depth, which is roughly one half of the maximum influence depth as shown in Figure 2-20.

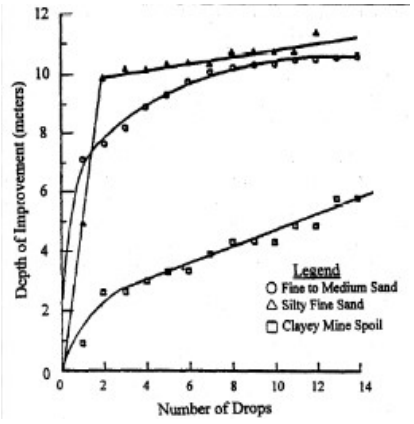

Figure 2-39: Depth improvement as measured at 3m from centre of drop point (Lukas (1995)) [44]

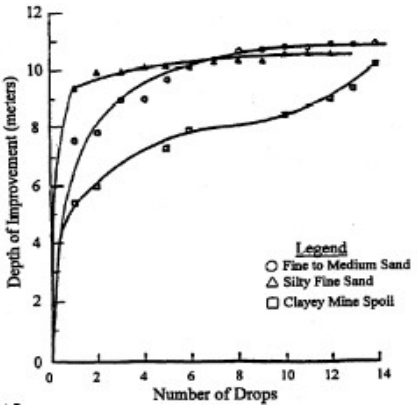

Figure 2-40: Depth improvement as measured at 6.1m from centre of drop point (Lukas (1995)) [44]

Figure 2-39 and Figure 2-40 illustrate the measured depth of improvement for the number of drops of the tamper which shows the total amount of applied energy at a point has some influence upon the depth of improvement. In case of the sandy deposits, after only 2 to 4 drops approximately 90 percent of the maximum influence depth is achieved at one location (Lukas: 1995) [44] .

Despite Lukas (1986) [36] realization that contact pressure (W/A) must affect the depth of improvement, the relationship presented by Menard et al.(1975) [74] was widely used for design, where, applied energy per drop (WH) was the most important factor affected to the influenced depth related to a given ground condition. In addition, there arer many studies , which have found various relations for predicting the maximum influenced depth as a function of energy applied per drop. However, out of those correlations, Menard formula can be considered as the most popular empirical expression among DC practitioners:

$$D = n\sqrt{WH} \qquad (21)$$

Where D is the influenced depth, W is the tamper weight (in tons), H is drop height (in meters) and *n* is an empirical coefficient, which is always less than 1 and appropriate for all the remaining factors affecting DC treatment. *n* was about 0.5 as suggested by Leonards et al. (1980) [72] while value from 0.3 to 0.8 was suggested by Mayne et al. (1984) [35] for 'n'. Though Gambin (1987) (citedby Y. Tan et al. [8]) suggested that n was around 0.5 to 1.0, Ye et al. (1992) (cited by Y. Tan et al. [8]) recommended 0.5 for 'n' value of cohesionless soils. For cohesive soils, it could be 0.35 to 0.5. As suggested by Y. Tan et al. (2007) [8] n value for the granular soils is around 0.35 to 0.55 with an average value of 0.45 at completion of the first pass of DC, while 0.45 to 0.65 with an average value of 0.55 after completion of two passes. Accordinlgy, it was noted that densification after two passes of DC are greater than that as at completeion of first pass. However, Above Menard empirical equation is defined ignoring the effect of applied no of blows and pounder diameter.

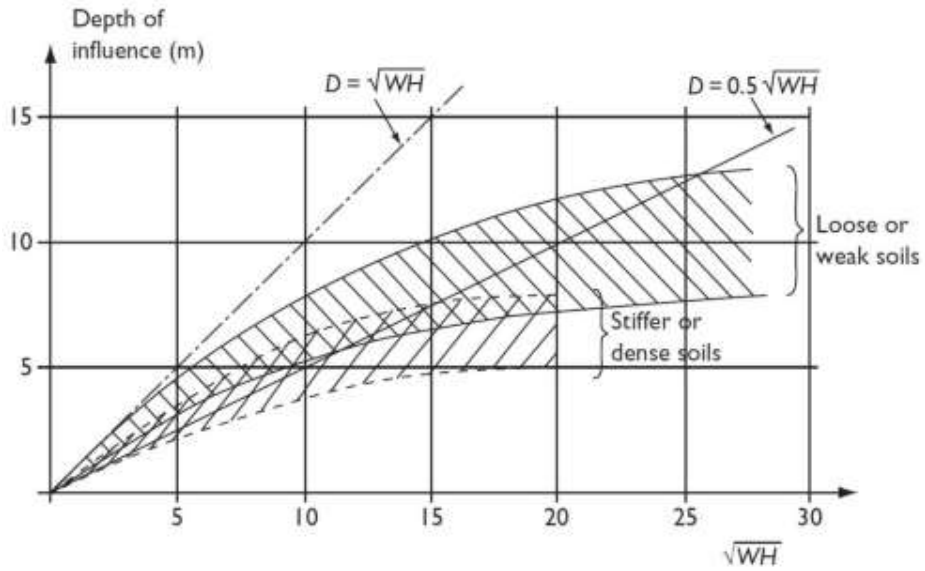

Figure 2-41: Typical Energy -Depth of influence chart for DC (Slocombe, 1993) [75]

As discussed above, the required pounder weight and height of the drop can be selected to achieve the required depth of compaction as per Menard′s equation. Hence, the effectiveness of dynamic compaction depends on the combination of weight (mass) and geometrical shape of the pounder, the drop height, the point spacings, the number of drop and finally the total compactive energy applied in unit volume(M.W. Bo et. al. [6]

Table 2-9: Values of n for various pounders (after Choa et al ; 1997 [1])

	Pounder mass: t			
	15	14	23	23
Drop height: m	20	20	12·5	25
Pounder surface area: m^2	3·87	2·25	5·5	5·5
Energy: t–m	300	280	287·5	575
Influence depth: m	7·5	7	6	8
n^*	0·433	0·418	0·354	0·334

* Determined from CPT.

In order to reduce scale effects, F. Jafarzadeh [68] applied the method proposed by Poran et al. [76] to scale the Improvement Depth (taken as 'DI' here) to tamper diameter (taken as D) and a normalized energy index as, N.W.H/A. DI as shown in Figure 2-42.

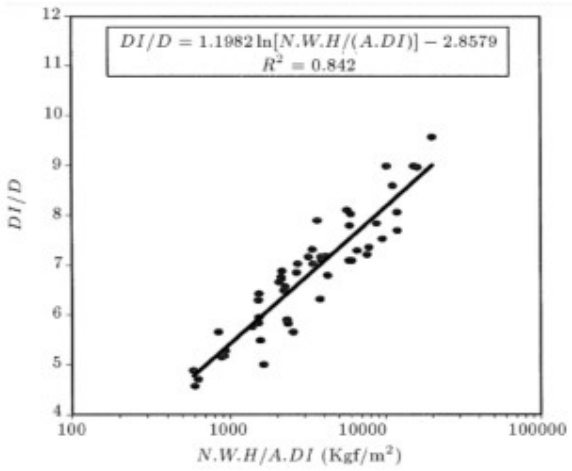

Figure 2-42: Relationship between improvement depth and normalized compaction energy [69]

Ground Improvement Index (I_d)

The widely used criterion for degree of ground improvement is evaluated based on tip resistance, qt values of CPT. Dove et al. (2000) [77] developed such a criterion known as ground improvement index (I_d) and which is calculated as in the following way:

$$I_d = \frac{q_{t,after}}{q_{t,before}} - 1 \qquad (20)$$

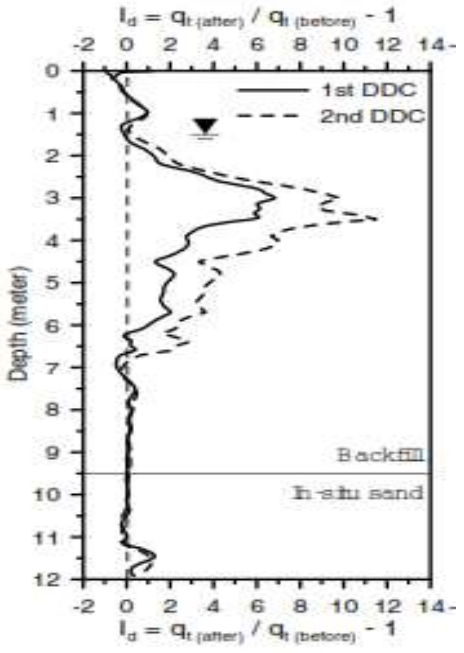

Figure 2-43: Typical I_d graph with respect to the pass number (Y. Tan et al.2007) [8]

Where qt, $_{before}$ is corrected cone (tip) resistance before ground compaction and $q_{t,\ after}$ is corrected cone resistance after densification at the same location. hence, the qt value increment (Id>0.0) always indicates results of the densification effects regardless the applied compaction method. Y. Tan et al. [8] Calculated I_d at twelve compacting locations at U.S. Route 44 for loose saturated granular fill and found based on I_d, influence depth varies from 6.5m to 9.5m after 1st pass and 7.5 to 11 m after 2nd pass.

2.16.3.3. Evaluation of Vibro Compaction by Machine Records

In vibro compaction, the challenge of optimization always involves on determination of the multiple parameters that can be varied generally and but how they lie within a narrow band when they are to deliver the desired results.

It was discussed in section 2.16.2 in this document that vibro compaction is basically affected by Amperage (frequency and amplitude) and duration of compaction. In other words, the total energy released during compaction. In standard vibro compaction machines penetration vs time and amperage can be found.

In addition, quality control work of Vibro compaction can be performed under two stages, namely monitoring of compaction parameters and post-compaction verification testing. During the entire construction process, the compaction parameters (depth, compaction duration and power consumption) are monitored using real-time graphs generate in computerised system. The data recorded in real-time can be checked for each and every compaction point and it comprises probe reference number, date time of compaction and referenced ground elevation. This has ensured the proper documentation of the work done in order to verify desired end product is achieved (Raju et al.:2008) [57] or to identify any quality issues occurred.

2.16.3.4. Energy Transfer from Compaction Probe to Soil

In some researches, the movement of the deep vibrator in all three-directions has been determined while interacting with the compacted soil. Thus, it was noted that an increase of the soil stiffness during the compaction process has caused in the vibrator movement changes. Accordingly, certain process parameters related to vibrator movements can be used for a work-integrated indication of compaction state, would be a valuable tool for the quality assurance of

the compaction works since it is providing on-site valuable information to the machine operator. That means the deep vibrator acts as not only a compaction equipment but also at the same time, serves as a measuring device. (Nagy et al. 2018) [78]. The relationship between the movement of the deep vibrator and the soil compaction state was firstly analysed by Fellin (2000a-b) by simple physical models. Subsequently by Nendza (2006) model tests were performed in saturated sand. However, still it could not be realized a reliable vibrator instrumentation as well as a comprehensive measurement campaign (Nagy et al. 2018) [78].

One of most important issues is variation of its movement due to the changing compaction state of the adjacent soil body rather than the shape of the vibrator movement. below some fundamental findings of the dependency of the vibrator movement on the variation of compaction state of the soil has been presented briefly based on site measurement data from a compaction point, which has been carried out in standard operation mode;

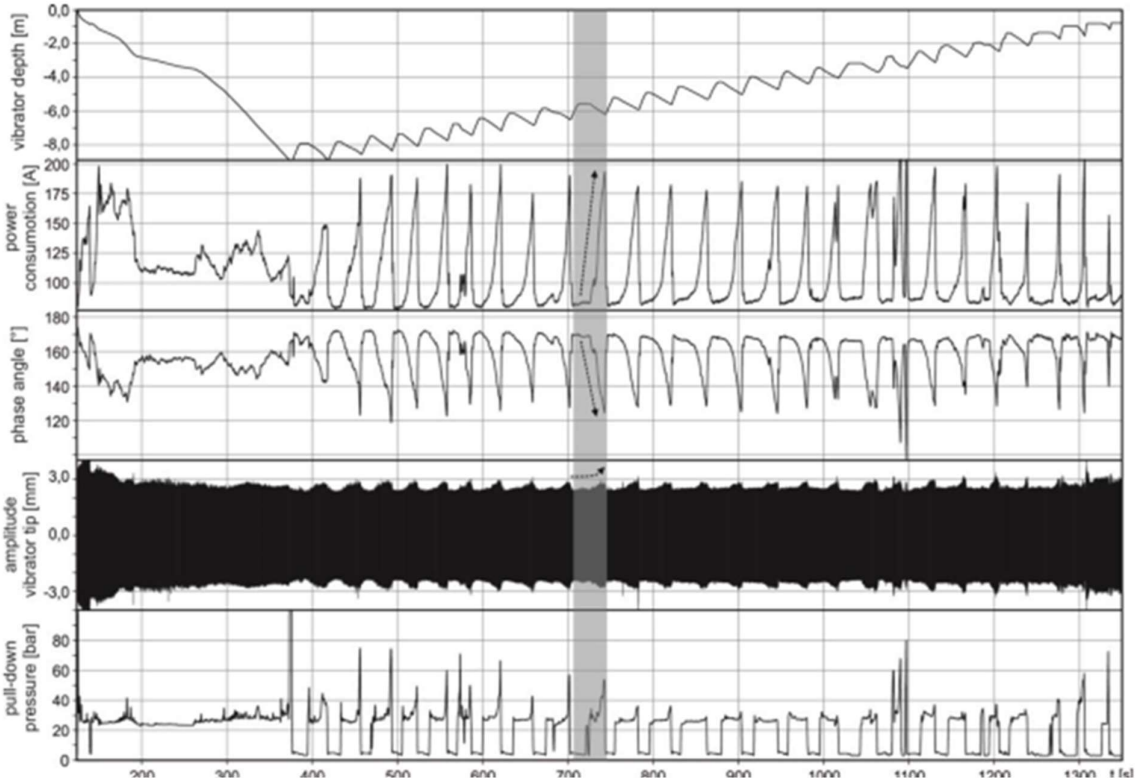

Figure 2-44: Variation the vibrator depth, current power consumption of the electric engine, vibrator tip amplitude, angle of phase and pull-down pressure during deep vibrator compaction against time under standard operation mode (Nagy et al. 2017) [80]

In Figure 2-44, it was illustrated the selected process parameters and the vibrator movement during the lowering and the compaction process. thereof the most established parameters are the time history of the vibrator depth and current power consumption of the electric engine,

which are considered together with the amount of backfill material for quality assurance of the compaction works. On the other hand, movement of the vibrator is characterized by two parameters known as the vibrator's amplitude and the phase angle. the current angle between the position of the rotating eccentric mass and the direction of the vibrator movement is defined as the phase angle.

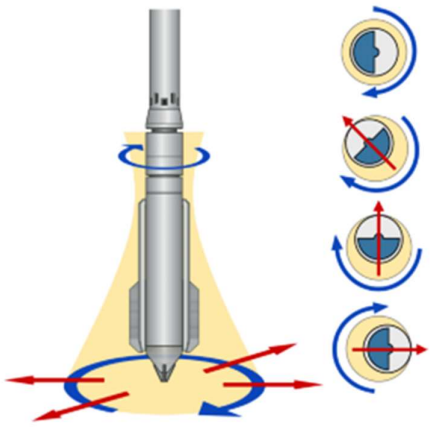

Figure 2-45: position of eccentric mass with respect to the vibrator contact location

As per Nagy et. al 2018 [78] application of impulse force on surrounding soils with respect to the rotating mass position is shown in Figure 2-45. However, this mass positions are contradicted with what was earlier published by Keller [48].

With both lateral vibration and penetration of the vibrator probe while lowering process, the soil was compacted and displaced lateral as well as downward directions. In Figure 2-44 such a compaction step is highlighted exemplarily. It was noted that the power consumption of the vibrator motor increases during the lowering process with increase of soil resistance. When the vibrator probe is being withdrawn, the power consumption is dropping again quickly. Accordingly, a significant change in vibrator movement can be observed in all three-direction (increasing amplitude of the vibrator tip and decreasing phase angle) during increment of power consuption . At the beginning and end of the lowering process, the horizontal movement of the vibrator tip can be seen as in Figure 2-46 during the highlighted compaction step. In both cases the vibrator tip describes almost a perfect circular shape; however, at the end of the lowering process the amplitude of the vibrator tip is higher than that at the beginning, and the movement becomes more irregular. However, since all process parameters are maintained constant during the compaction process, the changes in the vibrator movement only due to the compaction

state changes in the influenced cylindrical soil body. According to the outcomes of the above described test confirmed that the changing compaction state of the soil will have a decisive influence on the movement of the vibrator (Nagy et al. 2017) [79].

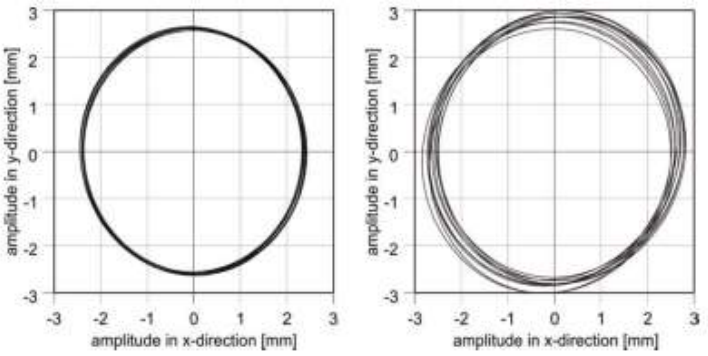

Figure 2-46: Recorded lateral movement of the tip of vibro probe at the commencement (left) and at the end (right) in the lowering process during the highlighted compaction step in Figure 2-44 (Nagy et al. 2017)

Moreover, soil response and formation of different zones around the vibro probe and its acceleration is as shown in Figure 2-47.

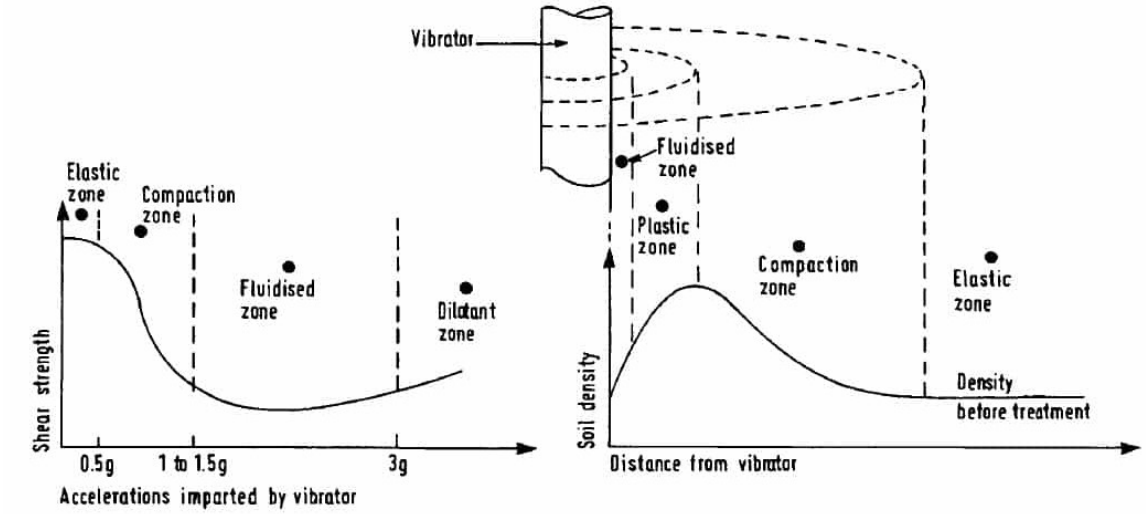

Figure 2-47: Soil Response of vibro-floatation (civildigital.com) [80]

The complex movement of vibro probe during vibration was also analysed using a video recorded during compaction works of the Port of Calais, France in 2017.The vibroflot in that video was operated at 1800 RPM (30 Hz) while the video was shot at the frequecy of 25 Hz (25 frames per second). This small frequency difference in the vibroflot and the video has formed a slow-motion effect, which makes the vibroflots motions are better visible in the video than what can be seen by bare eyes on site. The differential movement of the upper, middle and

lower parts of the vibro probe were an artifact of the scanning, which made by the video recorder that sequentially scanned from top to bottom. Due to very complex lateral movement of vibro probe in different radial direction, the appearance of the very stiff steel probe leads to be like which made out of rubber [81]. As described in Brown (1977) [49] and D'Appolonia (1953) [82], the current draw of the vibrator in electrically driven motors, indicates the state of compaction process: where the current draw increases as the soil gradually densifies. When the current draw reaches to its "peak," the vibroflot is raised to the next (upper) elevation. Subsequently at the next elevation, when vibro compaction starts and current draw drops suddenly and increasing again as compaction begins. in Figure 2-48 (Degen and Hussin 2001) [63] this process is illustrated with the current log;

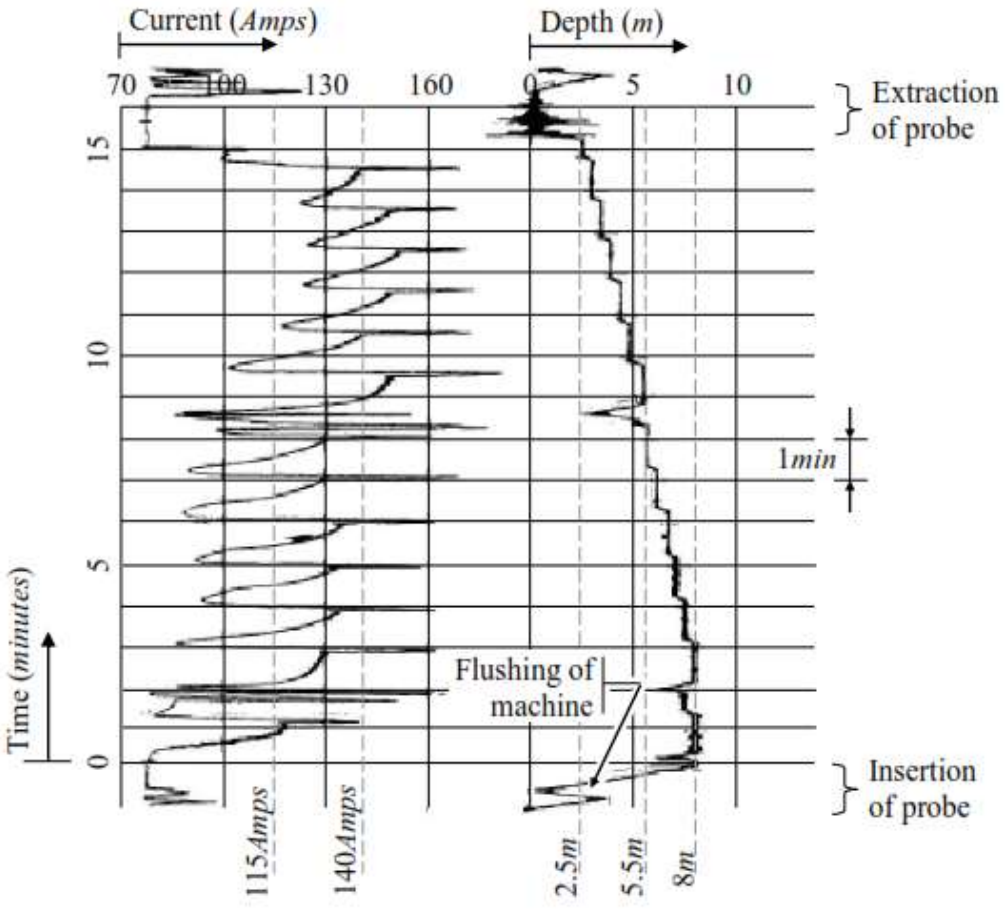

Figure 2-48: Current log recorded during vibro compaction (Degan and Hussin 2001)

Figure 2-48 illustrates the rapid penetration of the vibroflot in soil profile to the desired depth of 8m with one up-down flushing of the machine after reaching 4m. The penetration time was just over one minute. After reaching desired depth of 8m, the compaction phase has begun and

has been indicated in this figure as t = 0min. Subsequently, the probe was raised in 0.5m intervals while being held at each designated elevation for about 45sec.

Using Equation 23, which was derived by Puchstein et al. (1954), the average work rate (i.e., power) performed during vibro compaction in soil can be assessed;

$$P = I \cdot E \cdot pf \cdot eff \cdot \frac{\sqrt{3}}{1000} \tag{23}$$

Where: P = Average work rate performed during vibro compaction (i.e., power) (kW, kJ/sec).
I = Average current of the line ($Amps$).
E = requirment of Phase-to-phase voltage of vibrator ($volts$).
pf = Average power factor (≈0.8).
eff = Electric motor Efficiency (i.e., motor consumed portion of the electrical power to do mechanical work, ≈0.9).
Based on the average current draw as well as the amplitude of the peaks, the profile can be considered as two layers as from 2.5 to 5.5m and from 5.5 to 8m. The estimated average current draws for the top layer and bottom layer are to be about 140$Amps$ and 115$Amps$, respectively. Thus, using Equation 23, the rates of work (P) performed during vibro compaction on the top and bottom layers were estimated to be about 77 and 63kW, respectively for the V23 vibrator (i.e., 440$volts$). Since the compaction rate, the performed rate of work, and tributary area per compaction point are known, the required mechanical energy to treat a unit volume of soil can be determined. From Figure 2-48, the compaction rate can be assessed as 0.37m/min (i.e., (8m to 2.5m)/15min and probe was at 2.5m the it has been withdrawn from the ground (Green: 2001) [64] . This is in reasonable agreement with the typical rate of 0.3m/min given in Mitchell (1981) [83].

Variation of PPV with power

Under the circumstance that probe movements , frequency and relevant ampherage has not fully understood yet, lateral vibration generated during vibro compaction has been determined as empherical equations with the intension of controlling vibration on nearby structures during

the compaction work. An expression for PPV in terms of distance, d, and energy, E has been suggested by Wiss (1981) [84] has proposed as given in Equation 24.

$$PPV = K\left(\frac{d}{\sqrt{E}}\right)^{-n} \tag{24}$$

Where, K is the intercept with the ordinate and n is the slope or attenuation rate. 1.5 is used as a relatively common value for n while it generally lies between 1.0 to 2.0.

$d/\sqrt{E}$ = scaled distance.

Since power, P, is defined as energy per unit time, it is possible to express vibro compaction generated PPV in terms of vibroflot power and distance. It could be estimated that n is from 1.52 to 1.64 while average value is 1.59 by applying Equation 25 to each of the PPV measurements by Wood and Jedele (1985) [46], Dowding (2000) [85] and Babak et al.(2011) [47]. As Calculation showed range of K was from 2.08 to 8.16 with its average value as 6.2 for the four set of curves. While it was noted that the lowest K value was for the 24 kW vibro probe, the average K for the other 3 vibroflots was 7.5. Since, the 24 kW vibro probe is less commonly used than the other types of vibro probes. Hence, when P is in kW and d is in metres a large K value will be more conservative. Accordingly, Babak et al. has modified that Equation 24 to determine the PPV at ground surface as follows;

$$PPV = 7.5\left(\frac{d}{\sqrt{P}}\right)^{-1.59} \quad \text{mm/s} \tag{25}$$

In that study trend of variation in PPV was noted with the depth as given in Figure 2-49(cited by Babak et al. [47]) below. However, the scatter of data does not allow the realization of curve fitting processes with high amounts of reliability.

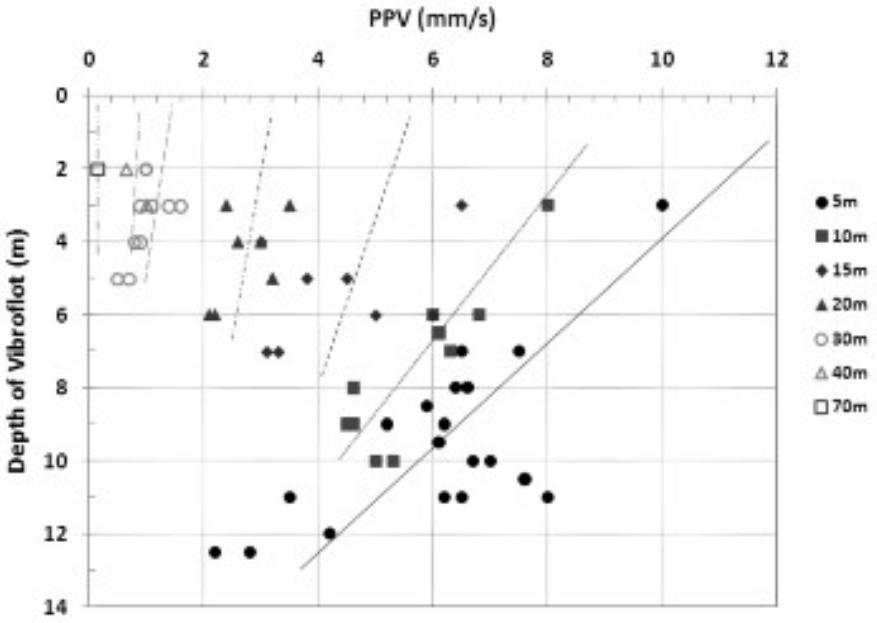

Figure 2-49: Variation of PPV measured in different distance with respect to the depth (Babak: 2011)

2.16.3.5. Compaction Evolution in Time of Vibration at a Point

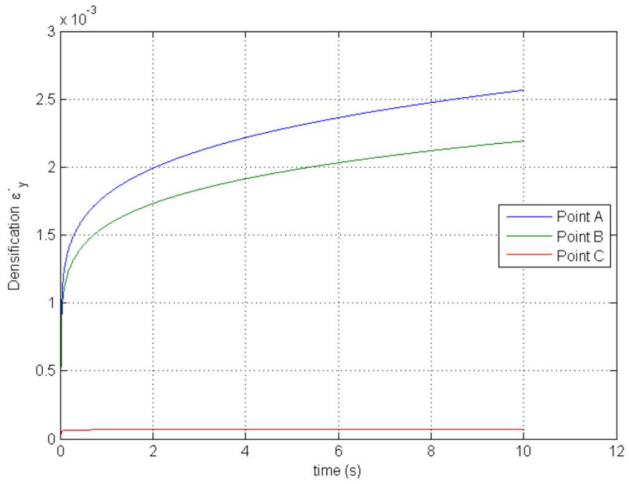

Figure 2-50: Compaction evolution in time of vibration at a point

(Jaime Peco Culebra et al.:2012) *[59]*

Figure 2-50 shows the numerical analysis done by Jaimpe Culebra et al.(2012) *[59]* for evaluation in time of vibration (holding time) in three points of the geometrical points as 'A' at right on the vibration, 'C'on the boundary of the vibrated area and 'B' at the intermediate

point. Sand properties used in the analysis belongs to Crystal Silica having relative density 45%. As per the above graph, it was found 10 second seem to be enough to get a final densification result.

2.16.4. Other Influencing Factors for Optimization of Sand Densification

In addition to already discussed factors influencing for sand densification, following factors would also affect on the final result of the compaction.

2.16.4.1. Ageing Effect

More and more evidences are becoming available to indicate that in many sands time-dependent increases in strength and decreases in compressibility develop after densification by any of the deep compaction methods. Because these effects continue over periods of many weeks or months, they cannot be explained in terms of pore pressure dissipation, which continues only for periods of several minutes at the most in the case of clean sand. The aging effect has been shown to give substantial increase in the strength of sands under cyclic loading, as may be seen in Figure 2-51.

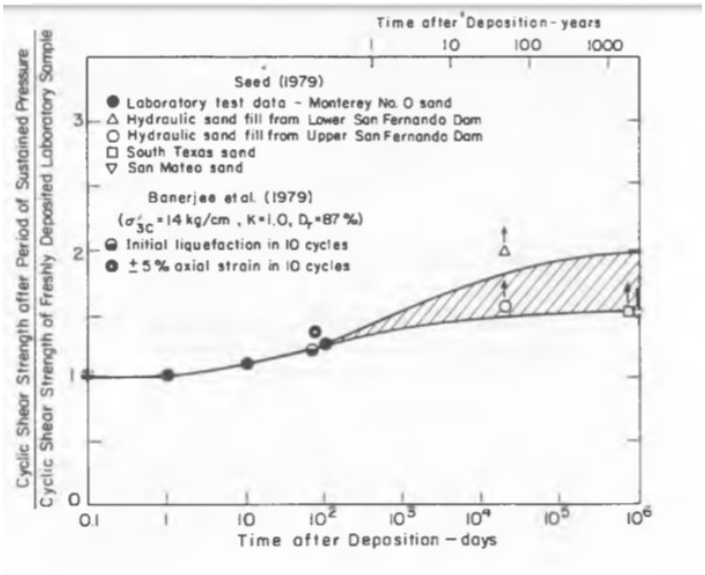

Figure 2-51: Influence of period of sustained pressure on stress ratio causing peak cyclic pore pressure ratio of 100% ([88]

Although a number of hypotheses have been advanced to explain this behaviour; e.g., thixo-tropic hardening, chemical cementation, the effects of dissolved gases, the mechanism is not

yet completely clear. From a practical standpoint, however, it would be reasonable to conclude that evaluations of the ground shortly after the completion of deep densification will give conservative results (Michel: 1981). [83]

However, as M.W. Bo et al (2008) [6] assessed on dynamic compaction, no significant increase in strength or softening or ageing is expected after compaction, which was often performed in passes to let pore pressure dissipate during the pause period. Under the condition of granular soil is highly permeable, there is rapid excess pore pressure dissipation, particularly if fissures develop. Therefore, a minor increase in cone resistance may occur as a result of the slow re-deposition of soluble silica at grain contacts, which act as natural cementation. Accordingly, increases in penetration resistance over time after a densification treatment have been reported. According to M.W. Bo et al., in the Changi East reclamation project CPTs had been carried out at 14 days and 3 months after compaction, but the change in the cone resistance was scarcely noticeable. Thus, he recommended that CPT after 14days can account the ageing effect, if any.

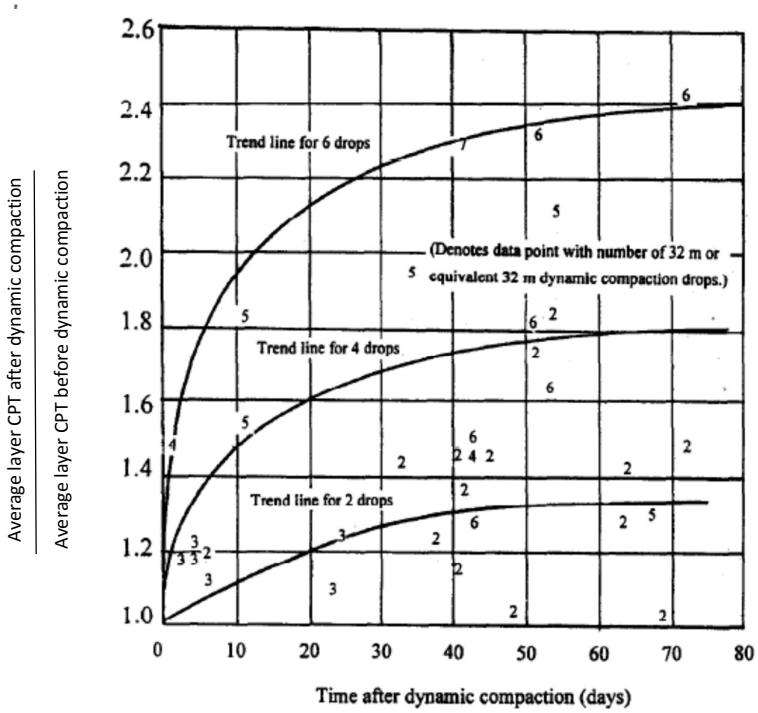

Figure 2-52: Effect of time upon relative improvement in CPT values in sandy soil in range of depth from 2 to 8m ([38]

As observed for sands densified by vibro and heavy tamping, the penetration resistance may increase with time after treatment, even though densification and surface settlement are essentially complete at the end of treatment. Experience at the Kwinana Terminal in Western Australia (Contracting and Construction Engineer, 1974) is a good case in point. At this site 12,500 vibroflotation probes were made full depth into a sand deposit about 25m thick. Cone penetration resistance values increased by 10 to 15 percent over the three weeks following treatment (Mitchel:1981) [9] .

2.16.5. Evaluation of Densification

2.16.5.1. Least Compacted Point in Dynamic Compaction

Most specifications in a dynamic compaction contract require that verification for acceptance of the compaction works be based on an in-situ test performed at the centroid point, based on the assumption that least compacted soil is present at centroid location. However, if a correct spacing is used for the centroid point often will turn out to be the mostly compacted point, and right under the exact compaction point (foot print) will be the least compacted point (M.W. Bo et al. 2008) [6].

Chow et al. (1994) [69] proposed the use of an improvement ratio, which is defined by resistance expressed as function of the ratio of the peak angles of shear at any point in the soil and that underneath the pounder ($\Delta\Phi/\Delta\phi_b$) . This ratio again varies with ratio of X/D. In their proposal, $\Delta\Phi$ represent the extent of improvement at a distance X from the centre of impact, $\Delta\Phi_b$ is that underneath the pounder and D is the diameter of the pounder. According to Chow et al.(1994) [69], the extent of improvement can be taken as zero at X/D > 3.5 and 1.0 at X/D < 0.5 as per data from Changi East reclamation project, Singapore. M. W. Bo noted that for 6 m x 6 m and 7 m x 7 m square grid spacing having two passes of pounding, the X/D ratios of the centroid locations are between approximately 1.5 and 1.75. In general at centroid points the average qc value is the lowest and the soil is the least compacted, although a thin layer of highly compacted sand between 2 and 3 m depth is present. It was found that the compacted soils at the centroid point were most homogeneous with depth. Though, the degree of densification by for the single pounding reduces gradually as increasing the distance from the

pounding point, for the multiple pounding, the soil mass at the centroid of the compaction grid was generally well compacted owing to multiple pounding effects from all four adjacent pounding points after the correct grid pattern and spacing was used. From predicted contours of Chow et al. for X/D of 2.5 and 4, a greater extent of improvement was achievable at the centroid point, where X/D becomes smaller. Therefore, the centroid point may not be necessarily the ideal point for verifying the extent of improvement.

2.16.5.2. Sand fill densification by Vibro Compaction

Design point spacing in vibro compaction is considered as a function of desired relative density, particle distribution of the material, fines content and power capabilities of the vibro probe. The spacing is selected so that improved columns from each compaction point location get overlapped. The process effectiveness decreases exponentially as increasing distance from the vibroflot in radial direction. In order to determine a suitable spacing for vibro compaction work, an arbitrary number, which is called as a coefficient of influence, is determined based on the relative compaction with respect to the radial distance from the compaction point. For one vibroflotation probe location, this coefficient of influence is a function of distance and relative density, and which increases as decreasing the distance to the probe. For considered design patterns, the coefficients of influence are displayed around the probe location and represent an equivalent value at the corresponding radial distance. The critical point is determined based on the greatest distance from the surrounding probe locations. Accordingly the sum of the coefficients at considered centroid point due to each of the compaction point, must be greater than the required minimum coefficient value. Figure 2-53, which is from the International Mineral and Chemical Corporation Phosphate Plant case study shows the sum at the critical point, A, is calculated as 4 + 4 + 4 = 12. For this project, a minimum influence coefficient was determined to be 10, based on achieved relative density. Hence, the value of 12 indicates that this design point spacing was adequate (D'Appolonia et al., 1953) [82].

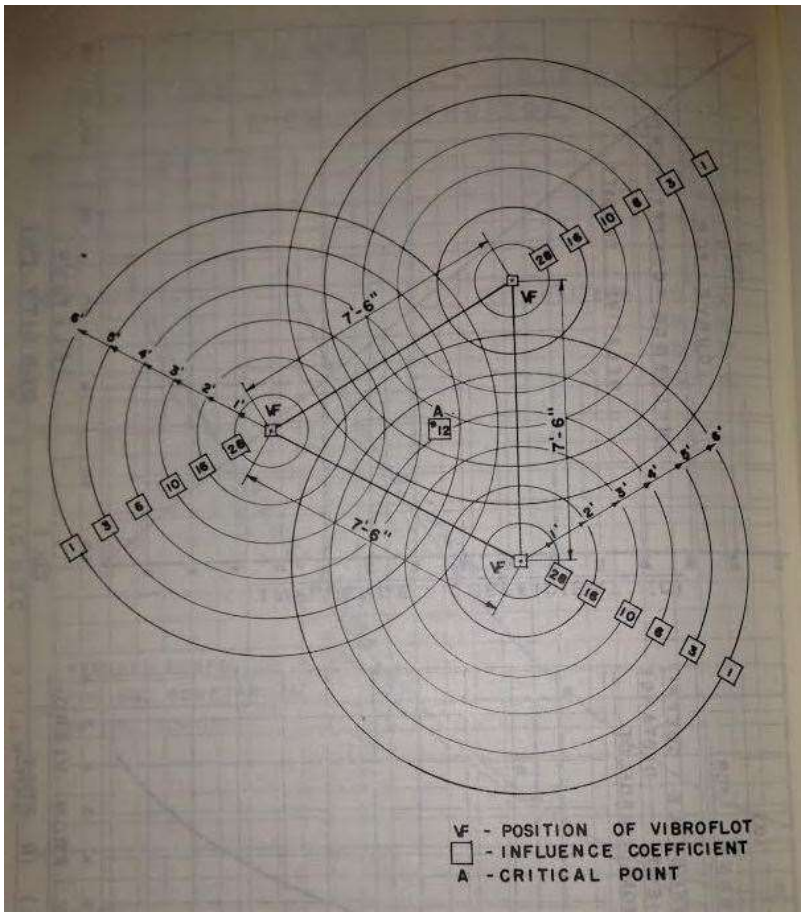

Figure 2-53: Sum of coefficients of influence at critical point for triangular spacing pattern (D'Appolonia et al., 1953) [82]

3. METHODOLOGY

Figure 3-1 shows the sequence of the research work. At the outset, index properties of the fill material, i.e. reclaimed sea sand were evaluated using laboratory test results of over 3000 samples taken from trailing suction hopper dredgers and from the reclaimed land regularly. During the reclamation period an average of four samples per day was jointly collected and tested for bulk density, for particle distribution and for silt content. Particle distribution was done by sieve analysis and hydro-meter test and specific gravity test. For this study, only 62 results out of 3000 were randomly selected. The selected samples reasonably represented different areas and different elevations reclaimed by considered time period. In addition, sample of fill material collected along the canal wall and marina sea wall area were tested for friction angles under different compaction conditions pre-defined as Dr= 40% and 55%. Moreover, samples taken from road areas were tested for lab CBR tests.

In the meantime, self-compaction during sand placing by hydraulic and other methods were evaluated using 28 nos of pre-CPTs conducted in different areas of the reclaimed land. Subsequently, by plotting Pre-CPT data such as cone resistance and friction ratio in Roberson's Soil Behaviour Type Chart, soil types consist of reclaimed fill material were determined. Similarly, soil behaviour type index (I_c) was plotted against normalized cone resistance (Q_{tn}) to find the status of self-compaction and effectiveness of application of compaction methods. In addition, particle distribution curves were plotted in the envelope developed by Lukas and Keller for dynamic and vibro compaction respectively to check the applicability of above compaction method for this material. For vibro compaction Browns suitability number for vibro compaction was checked using data extracted from particle distribution curve data.

After confirmation of applicability of dynamic and vibro compaction for densification of fill material, optimization of both methods was considered. In order to optimize the dynamic compaction, measurement such as Crater depth, Net volume change variation was evaluated with the blow number while influence depth and Ground Improvement Index (I_d) was evaluated using pre-compaction and post compaction CPT data.

Accordingly, crater depth was plotted against the blow number (N) along with previous crater depth data found in literature, generally which were measured or computed in loose sand.

Moreover, the already derived equation for crater depth is also evaluated with the crater depth data found from the actual site condition in this reclaimed land.

Further, influenced depth due to the different energies of 4000kNm, 2000kNm and 1000kNm was evaluated using post compaction CPT data at trial site. Variation of influenced depth against square root of energy was assessed under different envelopes. Using pre-compaction and post compaction CPT data, Ground Improvement Index in Dynamic compaction was evaluated for different energies such as 4000kNm, 2000kNm and 1000kNm.

To optimize the vibro compaction, amperage and holding time effect on vibro compaction was evaluated with machine records and CPT results.

To check the aging effect on dynamic and vibro compaction, results of CPTs conducted at the same location with different time lags after completion of compaction were evaluated.

Finally, selection of compaction verification (CPT) points in dynamic and vibro compaction was evaluated using CPT data, which were conducted at four different locations with respect to the compaction points.

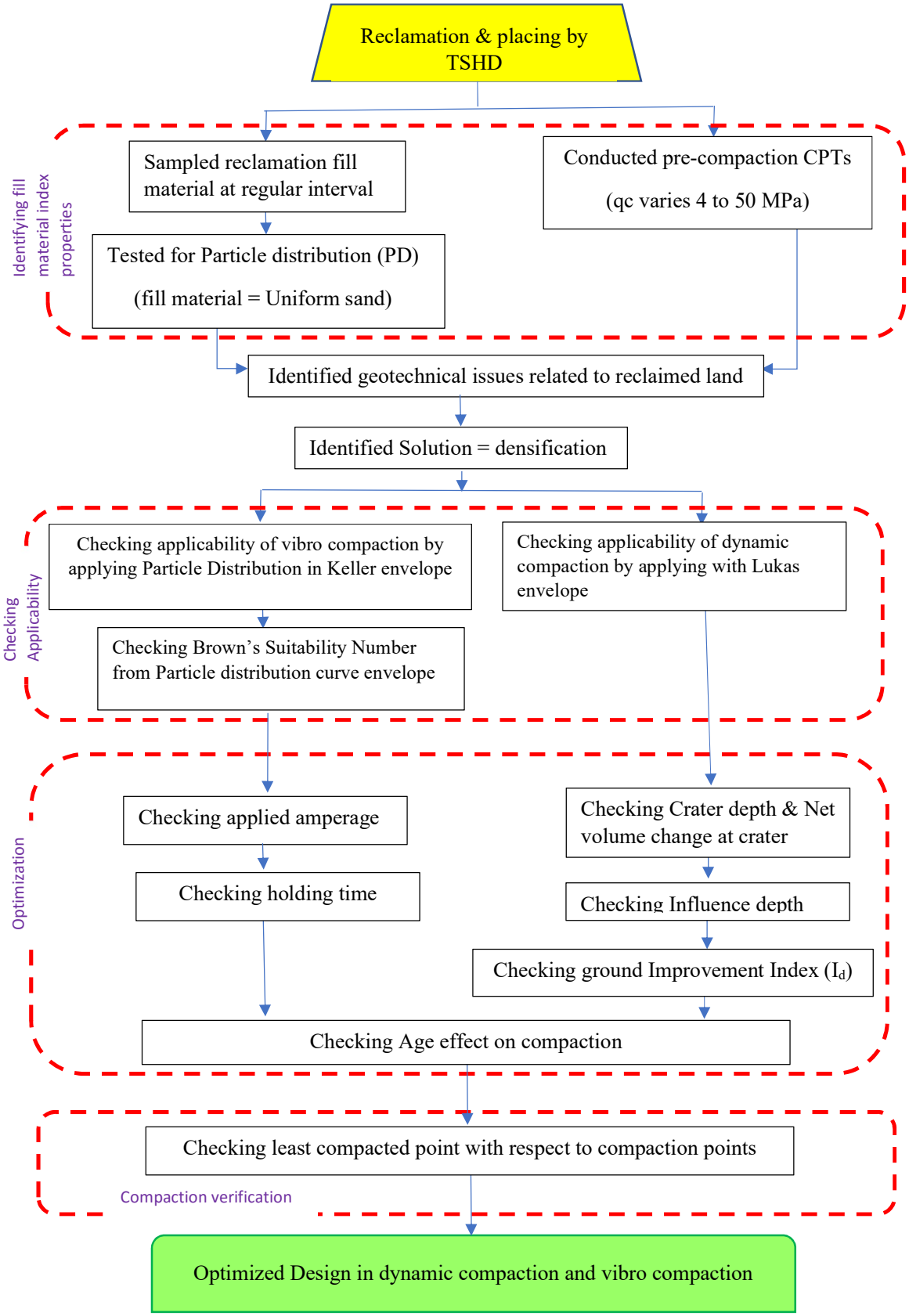

Figure 3-1: Flow chart of research

4. RESULTS AND DISCUSSION

This analysis was carried out using construction data related to the project such as laboratory test results, trial compaction, pre-compaction and post compaction field tests etc.

4.1. Evaluation of Properties and Self-Compaction of Sand While Being Reclaimed by Different Methods.

Basically, properties of borrow sand which were dredged using TSHDs and self-compaction during placing by hydraulic and dumping methods were evaluated.

4.1.1. Index Properties of Reclaimed Sand

The sand borrow pit used for this project was 10 km from shore of Negombo and which is 38 km off from Colombo. Totally 72 Million cubic meter of sand volume was dredged and placed in the reclamation land. During this reclamation project over 3000 sand samples were taken from dredgers and reclaimed land on daily basis and found almost similar materials over the project duration.

The basic properties of reclaimed sand are as follows;

- Silt content <2%
- Non-plastic
- Particle density ≈2.7Mg/m^3
- Poorly graded sand having D_{50} = 0.6mm and soil is fairly homogeneous.

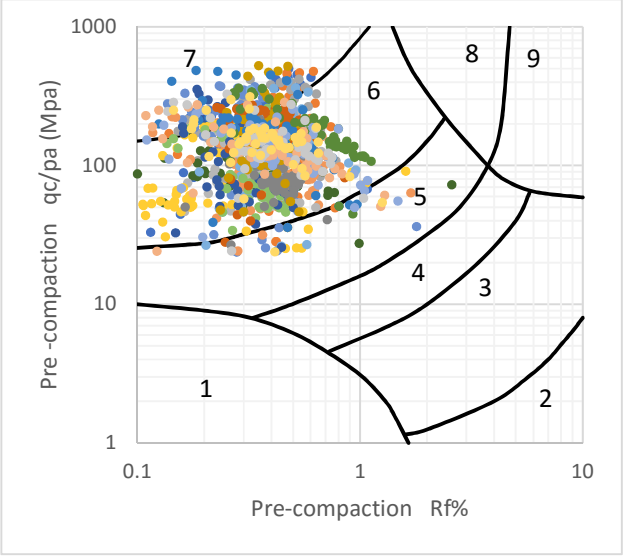

Zone	Soil Behavior Type
1	Sensitive, fine grained
2	Organic soils - clay
3	Clay – silty clay to clay
4	Silt mixtures – clayey silt to silty
5	Sand mixtures – silty sand to sand
6	Sands – clean sand to silty san
7	Gravelly sand to dense sand
8	Very stiff sand to clayey sand
9	Very stiff fine grained*

* Heavily overconsolidated or cemented

P_a = atmospheric pressure = 100 kPa = 1 tsf

Figure 4-1: Soil behaviour of filling material in this project as per SBT chart by Robertson et al. (2010) prepared based on pre-compaction CPT data.

Based on Pre-compaction CPT data as shown in **Error! Reference source not found.** in Appendix I, relevant soil parameters were plotted on Roberson's SBT chart as shown in Figure 4-1. The fill materials behaviour generally varies from clean sand/ silty sand to gravelly/dense sand.

Table 4-1: grading indices of reclaimed sand

Index	Range
D_{10}	0.178 – 0.495
D_{30}	0.287 – 0.763
D_{60}	0.431 – 1.512
Cu	2.424- 3.058
Cc	1.076 – 0.779

Considering variations in reclaimed sand particle distribution curves as shown in Figure 4-1 range of grading indices are shown in Table 4-1. Since all uniformity coefficient values obtained are less than 5, this reclaimed sand can be considered as "uniformly graded sand".

According to correlation presented by Gomma et al. (2007) [18]e_{min} and e_{max} values were calculated as follows;

By equation 4 & 5:

$$e_{min} = 0.5 - 0.033 \log (C_u)$$

$$e_{max} = 0.81 - .037 \log (C_u)$$

Variation of e_{min} and e_{max} were 0.484 to 0.487 and 0.792 to 0.796 respectively. Values found from laboratory test was 0.5 and 0.8 respectively.

$$e_{max} - e_{min} = 0.309$$

Using Cubrinovski and Ishihara's (1999 and 2000) correlation this value was verified as follows;

$$e_{max} - e_{min} = .23 + 0.06/D_{50} \text{ (mm)}$$

$$= 0.23 + 0.06/0.6 = 0.33$$

4.1.2. Self-Densification during Reclamation

In this project, seabed elevation varies from -3m to -20m and hence, all generally applied reclamation (discharging or dumping) methods such as bottom dumping, subaerial rainbow discharge, pipeline discharge and dumping by trucks or earthmovers were used. Restrictions for application of above methods have been noted as lack of draught for large ships, avoiding

sand spreading by heavy wind during rainbowing, lack of required space for the operations, disturbance to the on-going operation at site and controlling of required elevations etc.

.

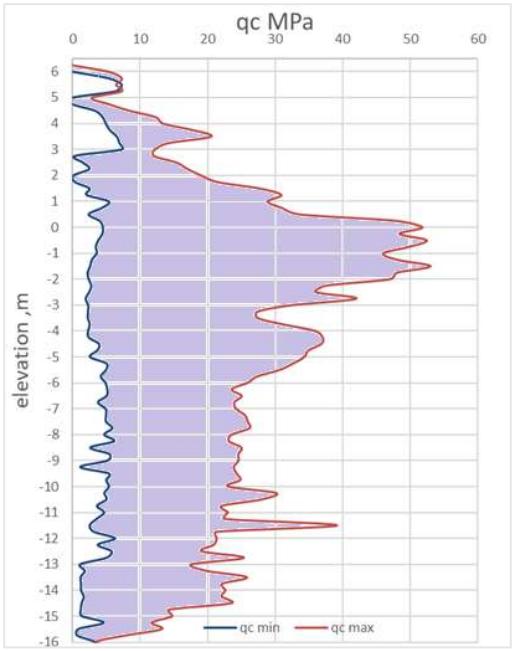

Figure 4-2: qc range in pre-compaction CPT curves

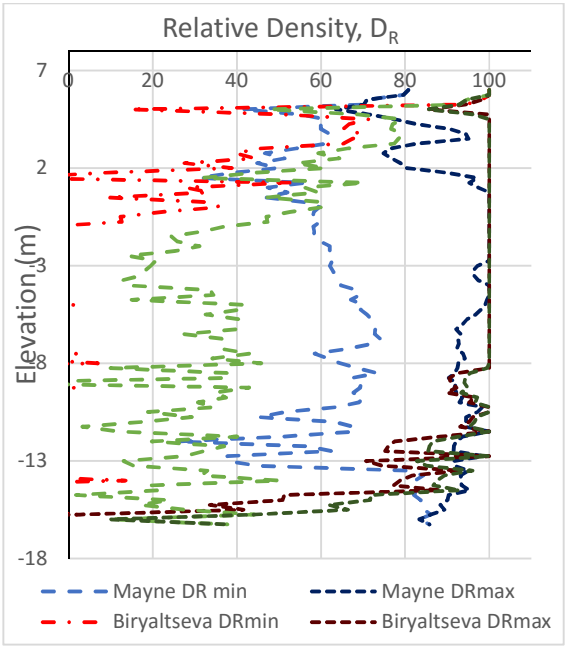

Figure 4-3: Maximum and minimum D_R values varies with depth in pre-compaction CPTs

As earlier discussed, though there might be some relationship between discharge method and natural densification during discharging, it was difficult to identify such relationship in this project as mixture of rainbowing, bottom dumping, pump ashore and by earthmoving machines were used for different elevations of the reclamation work. Therefore, separation based on discharging methods was not possible for this project.

However, variation in cone resistance was noted showing self-densification based on the results of Pre-compaction CPTs as shown Figure 4-2 (See all Pre-compaction CPTs on Figure A- 1 in Annex I). Maximum natural densification can be seen between +1.0 to -3.0m and it was mainly due to densification achieved by direct sand rainbowing rather than sand particles deposit after passing through water. On the other hand, densification in lower elevations was found to be lower as compared to those sand particles deposit after going through a thick water body. Moreover, top layers were mainly reclaimed by pump ashore and earth movers. Hence, densification of top layers is significantly low. Figure 55 shows the maximum and minimum q_c values in pre-compaction CPTs. As per these curves, cone resistance (q_c) basically varies from 4 MPa to 50 MPa while lower q_c values such as 2 MPa are also noted in some areas.

In this analysis relative density of the pre-compaction sand fill was calculated using methods presented by Mayne (2007), Biryaltseva (2007) and Tom Lunee (2009) and those maximum and minimum D_r values were plotted in Figure 56 (see Figure A- 2 in Appendix I). As per D_r values form Tom Lunee method minimum Dr below -1.0 elevation, vary from 20 to 40. Accordingly, liquefaction potential (probability) of sand fill was evaluated by Juang and Jiang (2000) method (see Appendix A) and in the summary, all of pre-CPT locations had more or less potential for liquefaction while considerable points of them are having high potential.

4.1.3. Evaluation of the Properties of Dredged Sand

4.1.3.1. Compactability

Compactability of reclaimed sand is shown in the Robertson SBT chart (1986) with Massarch's compactability envelope in Figure 4-4 and found vast majority of them are within compactable area. The rest of the areas are within marginally compactable area.

As per the laboratory test results, maximum dry density according to modified proctor test was 1.85Mg/m^3. Friction angle variation was 35^0 to 42^0 with variation of relative density from 40% to 55%.

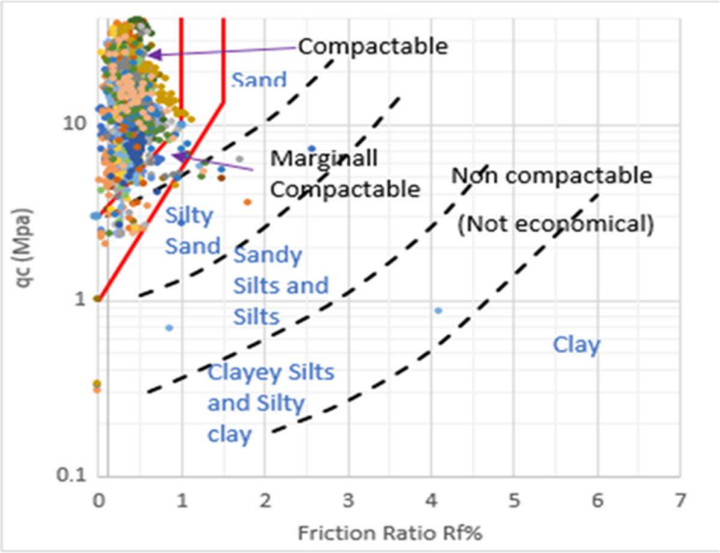

Figure 4-4: SBT chart for dredge sand with compactability envelope.

4.1.3.2. Potential of Liquefiability

To prepare the grain size distribution graph, results of 62 samples were selected randomly out of the results of 3000 fill material, to cover different stages of the project.

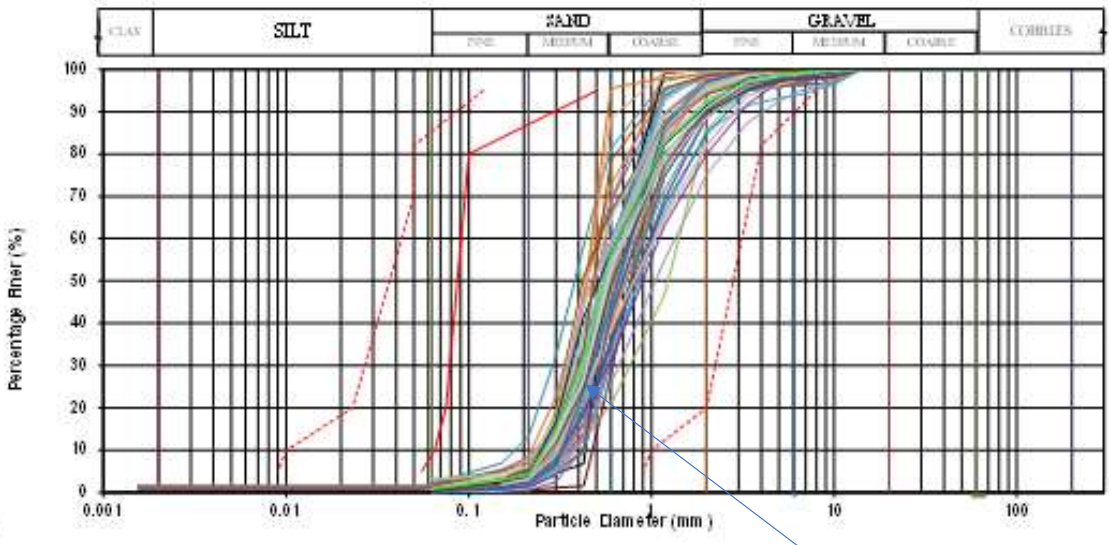

------Potentially liquefiable (Tsuchida 1970)

———— Most liquefiable (Tsuchida 1970)

Figure 4-5: Grain size distribution of sand used for port city reclamation.

The sand has a D_{50} varies from 0.4 to 1.2mm.

As per average curve,

D_{60}=0.71

D_{30}=0.44

D_{10}=0.29

Coefficient of uniformity, $C_u=D_{60}/D_{10}=2.448<5$

Coefficient of Curvature, $Cc=D_{30}^2/(D_{60}xD_{10})$ =0.303

Above particle distribution curves have laid in most liquefiable zone as per above Tsudhida (1970) [7] envelope. Based on q_c values obtained from 28nos pre-compaction CPTs, potential of liquefaction was evaluated and summary of evaluation was given in Appendix I. As per the evaluation result, all the areas covered by pre-compaction CPTs are more or less liquefiable.

By further evaluation of those CPT parameters, Normalized cone resistance (Q_{tn}) and Soil Behaviour Type Index (I_c) plotted in Robertson chart found that most of material are having I_c less than 2.5 while Q_{tn} varies up to 900 (see Figure 4-6). Hence, vibro compaction is effective

for this sand. However, still Q_{tn} of vast majority points were below 400. Hence the fill ground is required to be densified using appropriate compaction methods.

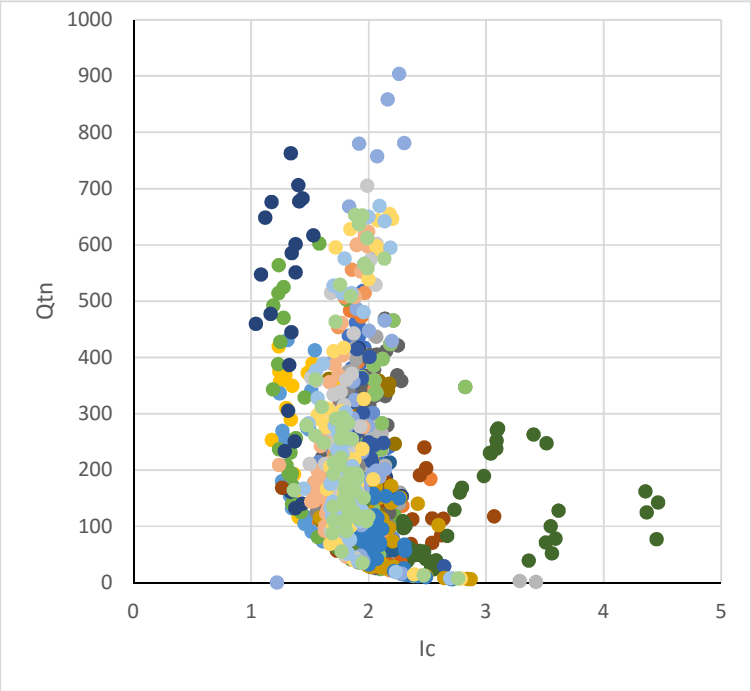

Figure 4-6: I_c Vs Q_{tn} graph for pre-compaction reclaimed sand

4.2. Evaluation of the effectiveness of Dynamic and Vibro Compaction of the Reclaimed Sea Sand Fill

Optimization of dynamic and vibro compaction was carried out using trial and permanent compaction data of this project. Basically, field records, field tests and machine records provided the construction data in numerical and graphical formats.

4.2.1. Application of Dynamic and Vibro Compaction

Since the self-compaction during reclamation was not adequate to meet the design requirement in bearing capacity, settlement, stability and liquefaction, the loose sand was densified using dynamic compaction and vibro compaction. Application of dynamic compaction with different energies and vibro compaction at the project site in phase 1 compaction is as shown in Figure 4-7. Generally, in development areas where dynamic compaction was applied, the selection of energy level with land usage of the reclamation ground is as follows;

- Dynamic compaction with 4000kN.m. (Road areas)
- Dynamic compaction with 2000kN.m. (Development areas)
- Dynamic compaction with 1000kN.m. (Development areas having higher self-compaction)

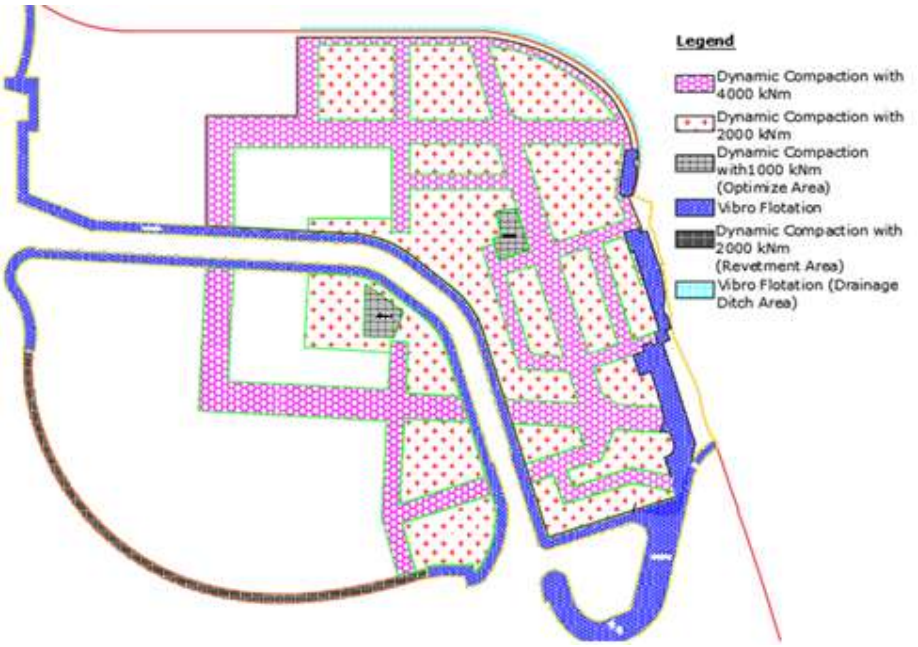

Figure 4-7: Ground Improvement Areas compacted by different san densification methods

4.2.2. Applicability of Dynamic Compaction for the Project

Based on particle distribution curves drawn from randomly selected reclamation material (sand) samples, applicability of dynamic compaction and vibro Compaction for the project was verified as given in Figure 4-8 using Michel's envelope;

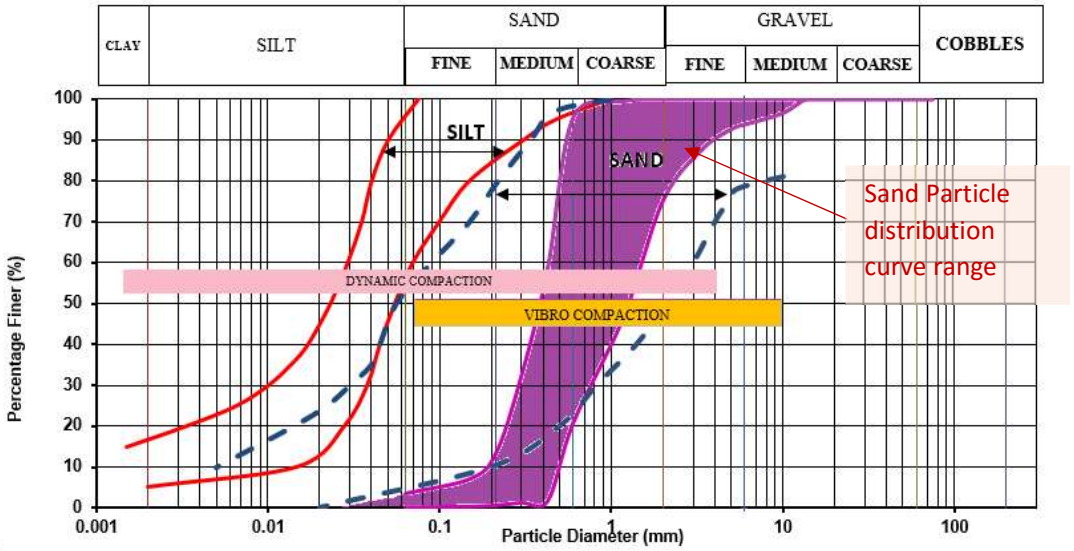

Figure 4-8: Applicability of dynamic compaction and vibro compaction.

As per Figure 4-8, dynamic compaction can be applied within a large range. However due to requirement of ground improvement in deeper elevations in order to increase the stability of retaining structures, vibro compaction was applied. In addition, vibro compaction was applied

in the areas, where important structures such as archaeological buildings exist or to avoid disturbance to the smooth functioning of existing buildings.In order to check the effectiveness of DC , particle distribution curve range was applied in Lukas soil grouping envelope shown in Figure *4-9*.

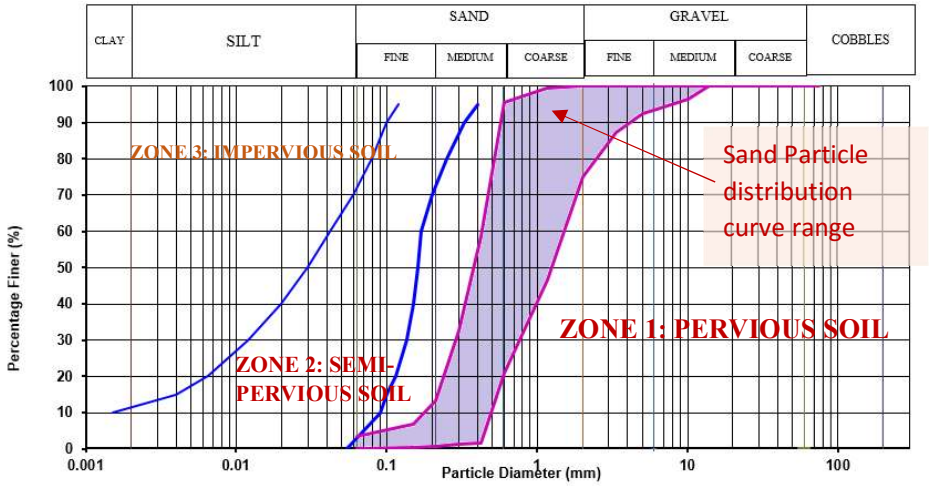

Figure 4-9: Sand behavior within Lukas' Grouping of soils for dynamic compaction

As per Figure 4-9 , filling sea sand in this project lies within favourable pervious soil zone and effectiveness of DC was confirmed.

4.2.3. Applicability of Vibro Compaction

As indicated below in Figure 4-10, grain size curves have fallen to vibro compaction applicable zone, which is within a part of liquefiable area. Hence, effectiveness of vibro compaction in this sand was primarily confirmed.

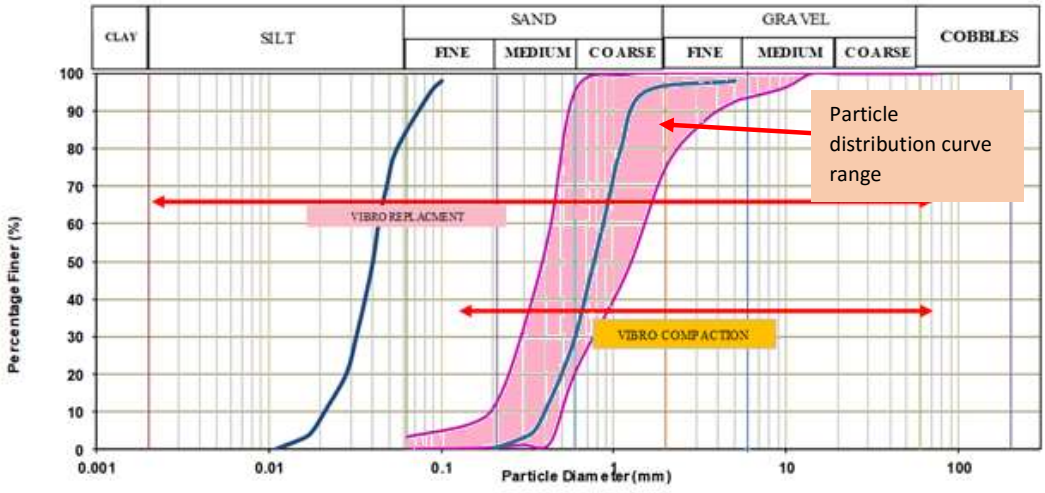

Figure 4-10: Particle distribution curves range of this reclaimed sand in Keller envelope for vibro compaction

Further confirmation of the applicability of vibro compaction for the sand was done by checking the Brown's suitability number by the Equation 18 as follows;

Suitability number, $S_N=\sqrt{(3/D_{50}^2+ 1/D_{20}^2+1/D_{10}^2)}$

Where D_{50}, D_{20} and D_{10} are particle diameter at 50% passing, 20% passing and 10% passing respectively.

As per the average particle distribution curve;

D_{50}=0.67 mm

D_{20}=0.45 mm

D_{10}=0.29 mm

$S_N= (3/0.67^2+1/0.45^2+1/0.29^2)^{0.5}$

S_N=4.85

As per the Brown's rating (see Table 2-6), this sand is "excellent" for use of vibro compaction.

4.2.4. Evaluation of Dynamic Compaction in Reclaimed Sea Sand for Optimization

Optimization of dynamic compaction was evaluated based on trial compaction data such as applied energy, point arrangement, created crater depth and net volume change etc.

4.2.4.1. Detail of Tamper Used for Dynamic Compaction

Dynamic compaction was applied using four pounders and their details are as follows;

Table 4-2: Pounder details

Pounder Label	Diameter (m)	Contact area (m2) *	Weight (ton)	Shape
DC1	2.5	4.406	21.59	Circular -flat
DC2	2.5	4.406	21.23	Circular -flat
DC3	2.5	4.406	20.89	Circular -flat
DC4	2.5	4.406	20.86	Circular -flat

*Contact area=4.406 m^2 (consist of 4 nos. of 0.4m dia. Pressure release holes)

Since the above pounder details are almost the same, the applied energy was fixed while adjusting the dropping height slightly. Accordingly, there is no significant variation in pounder weight and drop height.

Figure 4-11: Application of dynamic compaction

4.2.4.2. Design details of Dynamic compaction

Details of applied energy in DC is as in Table 4-3;

Table 4-3: Design of Dynamic compaction

Energy (kNm)	Founder weight (ton)	Drop height (m)	Spacing (m)	DC pattern	No blows	Total Energy (kNm)	Tributary Area (m^2)	Energy applied in unit area (kN/m^2)
4000	21	19.416	6.5	Staggered square	10	40000	21.125	1893.5
2000	21	9.708	5.0	Staggered square	11	22000	12.500	1760
1000	21	4.854	2.0	Staggered square	1	3000	4.000	750

To get uniform compaction at the ground finish level, two blows of $1000kN/m^2$ is applied as square pattern at 2m interval. Figure 4-13 shows the remoted controlled DC machnines operated in thi Port City project and typical tamper used thereby is shown in Figure 4-12.

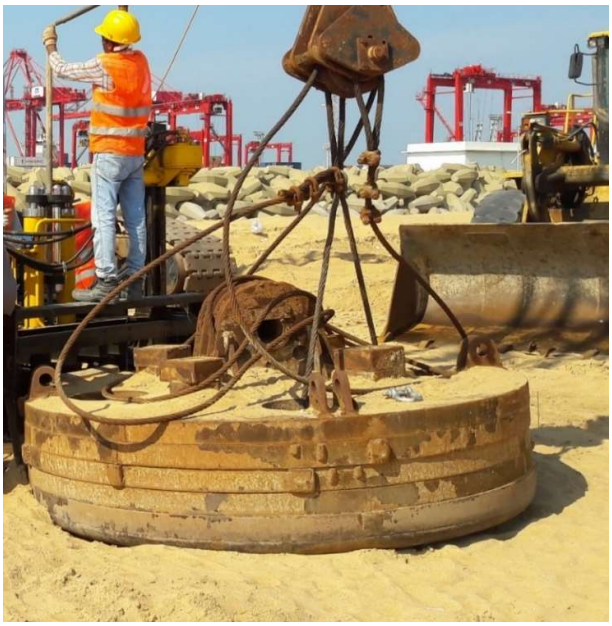

Figure 4-12: Typical pounder used for dynamic comaction

Figure 4-13: Typical dynamic compaction machine used in Port City project

4.2.4.3. Compaction Pattern Applied in Trial Dynamic Compaction

During the trial dynamic compaction 4000kNm and 2000kNm was applied under 6.5m and 5.0m interval staggered grid lines. The point to point spacing for two energies were 4.738m and 3.535m respectively. Point arrangement of trial dynamic compaction is as follows in Figure 4-14;

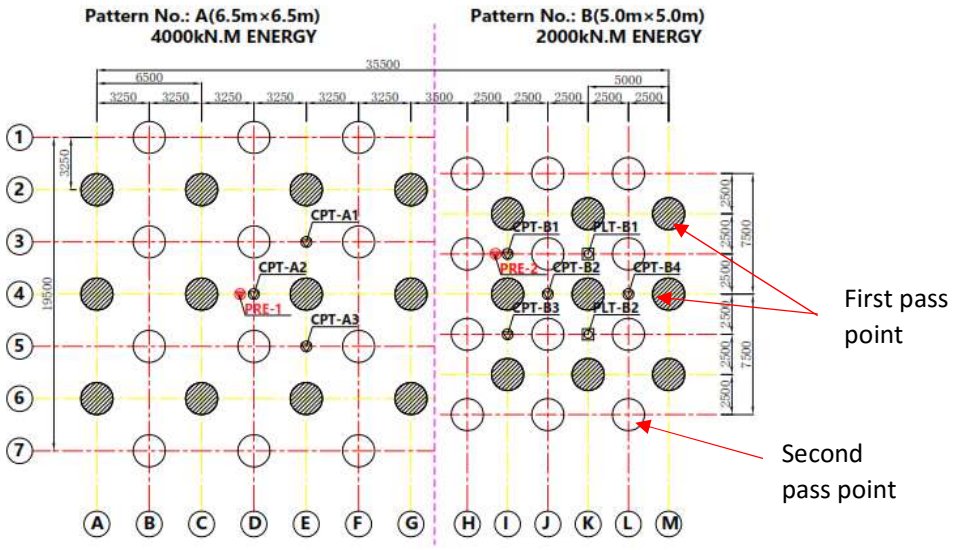

Figure 4-14: Compaction point arrangement for Trial dynamic compaction by 4000 kNm and 2000kNm

Ironing tamping application for 4000kNm and 2000kNm trial areas was carried out as shown in Figure 4-15, where grid spacing was 2.0 x 2.0m.

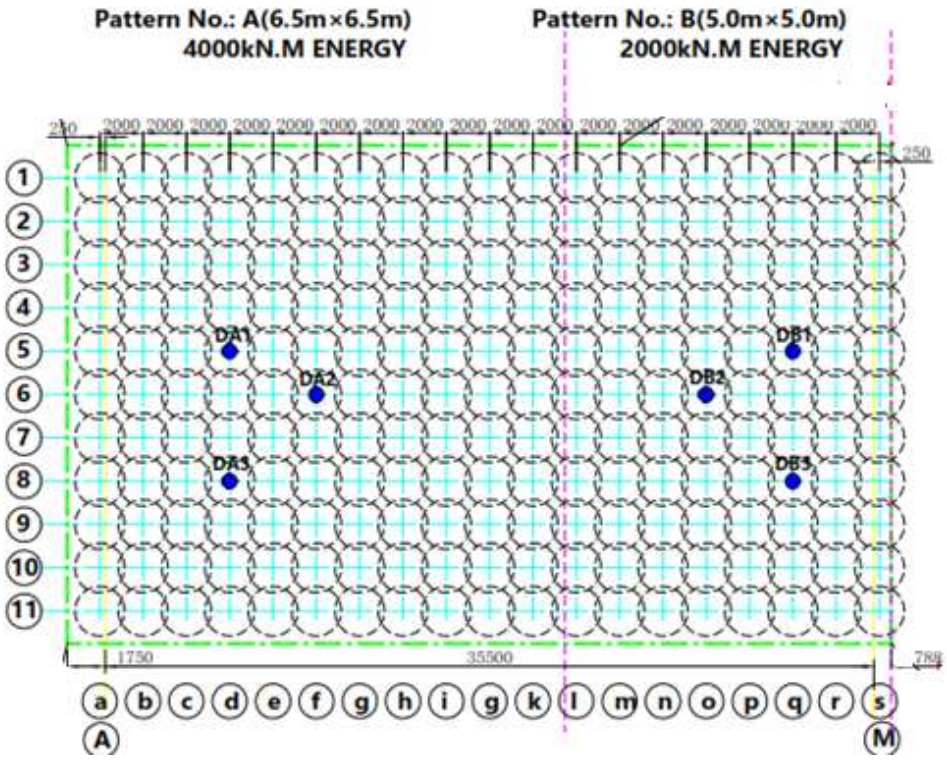

Figure 4-15: Ironing tamping pattern in 4000kNm and 2000kNm applied area.

1000kNm energy applied as the same interval of ironing tamping with single additional blow in Figure 4-16.

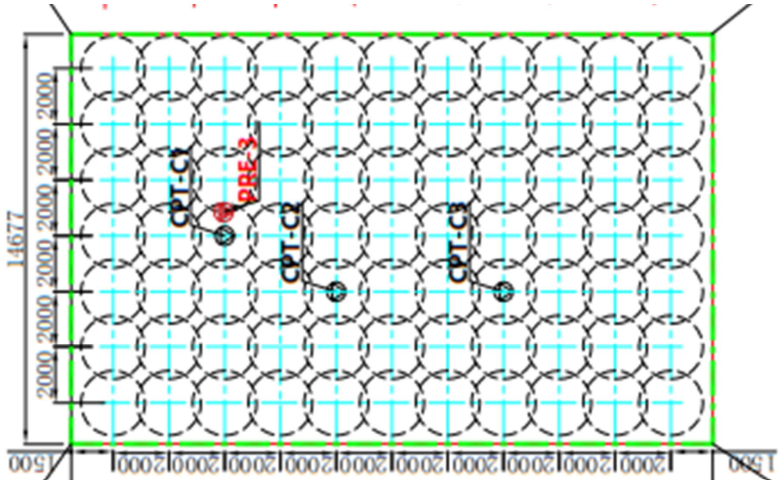

Figure 4-16: compaction pattern in 1000 kNm energy applied area

4.2.4.4. Identification of the Optimum Number of Blows in Dynamic Compaction by Crater Depths

Figure 4-17: typical crater seen during dynamic compaction

When DC is applied in sand fill, it forms a crater as shown in Figure 4-17. During trial dynamic compaction, crater elevation was taken by engineering level and the crater depth was measured with each blow of dynamic compaction. The crater depth variation with blow number and the increment observed in crater depth are referred to Figure A- 3: to in Appendix II and Figure 4-18 respectively.

Average crater depth variation with number of blows in trial area of this project was plotted along with actual site measured crater depth data of 48 compacted points and computed crater depth by wave equations of Gibbs and Holtz (1957), Peck and Bazaraa (1966) and Skempton (1986) in Noshira Thermal Power plant site in Japan. In that site 7m thick loose sand layer was compacted by dynamic compaction using 4900kNm (20ton by 25m) as a single phase. According to the graph shown in Figure 4-18, recorded average crater depth in this study is almost half of the value got in Noshira site (ignoring compaction energy level). According to SBT graph given in Figure 4-1 considerable portion of pre-compaction sand can be considered as dense sand. Hence, considerable reduction of crater depth could be predicted.

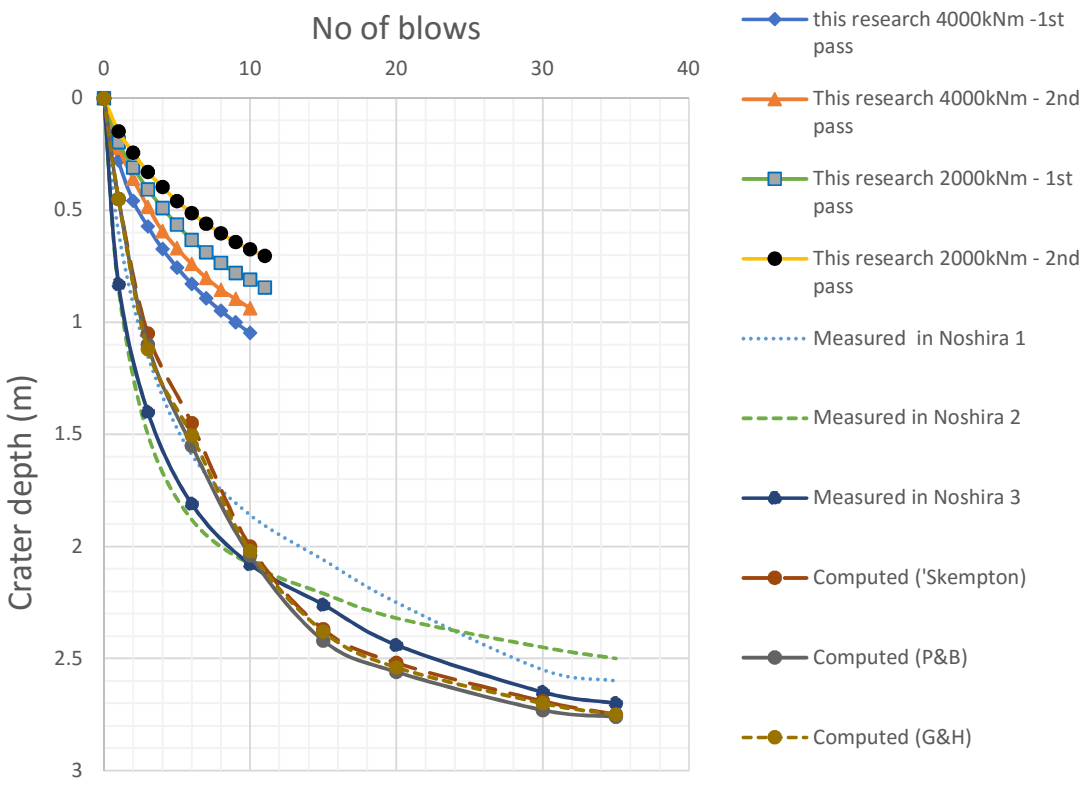

Figure 4-18: Crater depth variation with blow number

Crater depth increment with blow numbers is shown in Figure 4-19. Rapid increment in crater depth was observed up to three blows. From 3 to 8 blows moderate increment was noted and after 8 blows very low increment in crater depth could be seen.

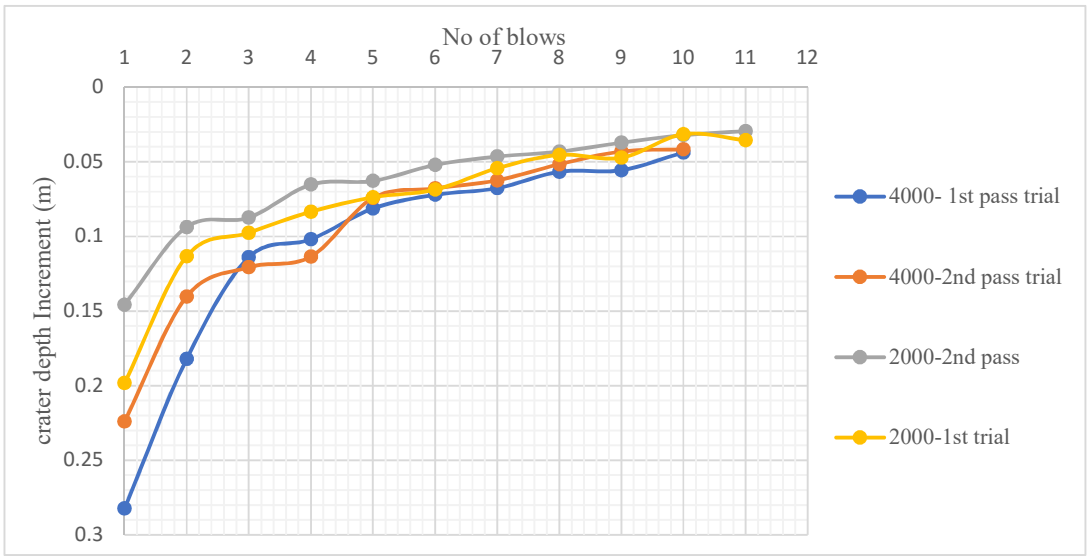

Figure 4-19: Increment in crater depth with respect to blow number

According to Takada and Oshima (1994) [67] using lab trials, crater depth can be calculated as follows;

$$\text{Crater depth, } h = c.\, m.\, v_0 (N)^{0.5}/A \qquad (26)$$

Where

N = blow number, m = tamper mass (ton), v_0 = tamper velocity at contact time with the ground surface and c =0.0083 m^2s/ton, A=contact area of pounder.

Accordingly, computed crater depths for 4000kNm and 2000kNm energy were plotted along with actual average crater depth related to 4000kNm and 2000kNm as shown in Figure 4-20. It can be seen that the computed values are deviated from measured values at site. In this project dynamic compaction was applied as 4000kNm over 20,000 points and 2000kNm over 45000 points. However, there was no significant deviation from the crater depth of trial area throughout the project.

The above equation has been derived taking impulse force at a blow proportionate to crater volume. Though it was valid for very loose to loose soils, when medium dense sand is taken in to account, it was suggested to take the impulse force at a blow proportionate to energy change during forming of crater volume. Accordingly, the Takada's correlation is suggested to change considering moving soil mass up to craft depth.

$$h^2 = c_1.\, m.\, v_0 (N)^{0.5}/A \qquad (27)$$

Taking velocity of pounder just before ground as $v_0=\sqrt{(2gH)}$

$$h = c'_1 \sqrt{(m.\, H\, N/A)} \qquad (28)$$

With this modified equation, most reliable crater depth values could be determined as shown in Figure 4-20 .

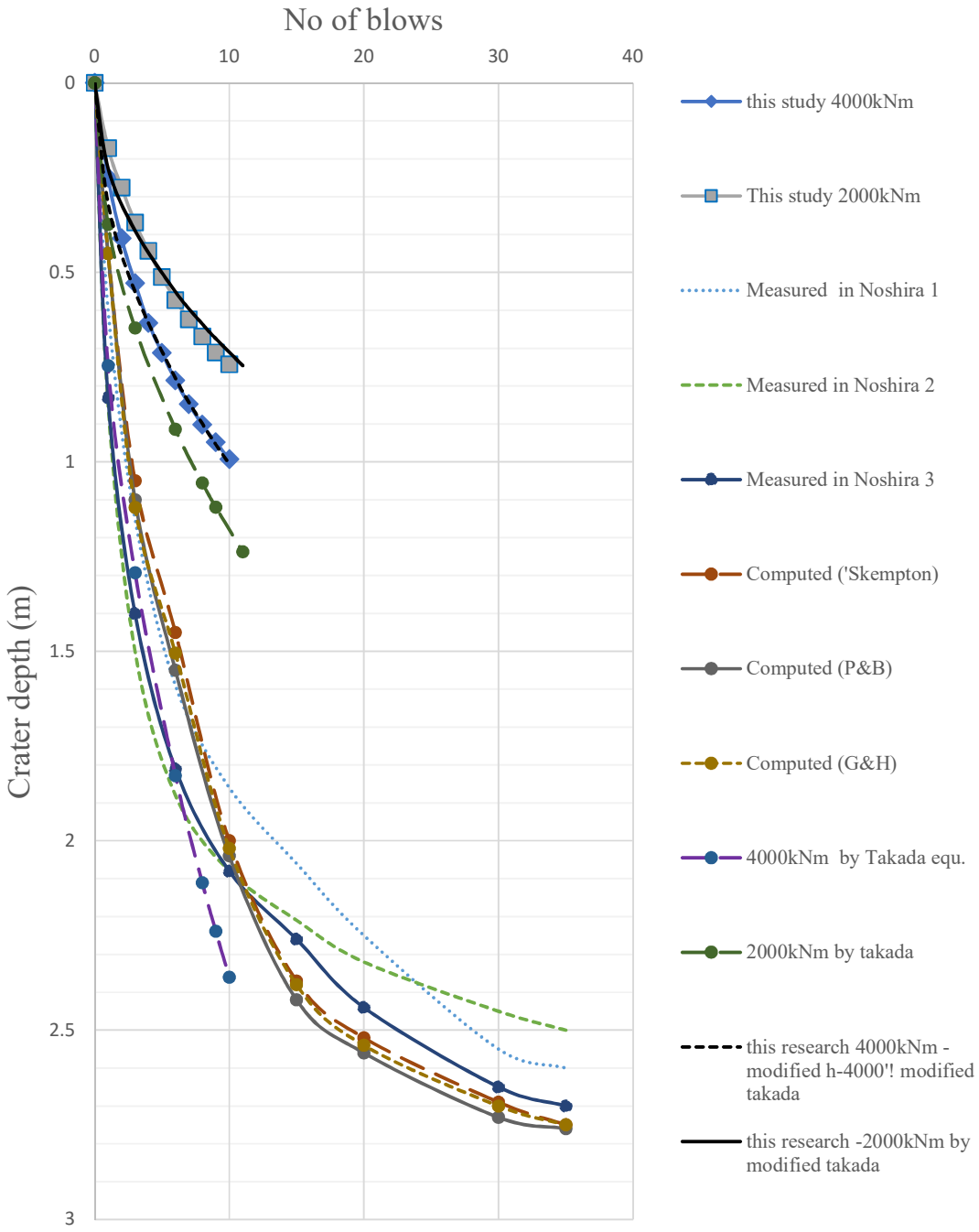

Figure 4-20; comparison of crater depth found from modified Takada equation.

Accordingly, within this range of data, C_1'was found as approximately 0. 034. In order to analysis more accurate crater depth with blow numbers, normalized crater $[h/(WH)^{0.5}]$ depth was determined and plotted below. Where, W & H are pounder weight and drop height respectively.

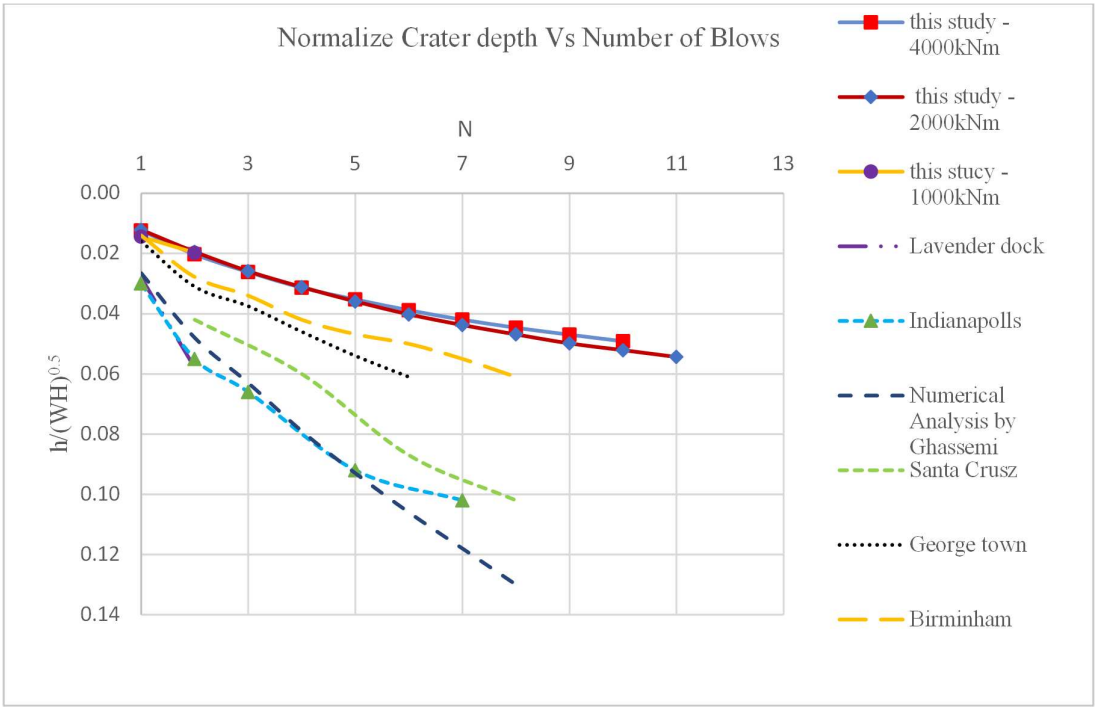

Figure 4-21: Normalized Crater Depth Vs Blow Number (N)

4.2.4.5. Evaluation of Normalized Crater Depth Variation with No of Blows (N)

Using crater depth data for 24 compaction points in each 4000kNm and 2000kNm area and 60 points in 1000 kNm area, the liner relationship originally suggested by Mayne was checked as shown in Figure A- 4 to Figure A- 8: in Appendix II. The average crater depth against each dynamic energy application was plotted as in Figure 4-20. In addition, the results of numerical analysis done by A. Ghassemi (2009) [86], were also plotted as shown in Figure 4-22.

In site studies by Mayne, it was reported that deep crater up to 2m was created during application of dynamic energy such as 300tm to 400tm. However, the crater depths measured in this study was significantly low when compared to the Mayne's crater depth values measured at different sites in the US. There might be some differences in properties of filling material (silty sand, sand, rubble, rock fill and coal spoil), and their pre-compaction conditions. In this study, the curve between normalized crater depths to square root of number of blows (see Figure 4-22) was approximately a linear relationship as suggested by Mayne. Since it should go through the origin, the following relationship can be defined;

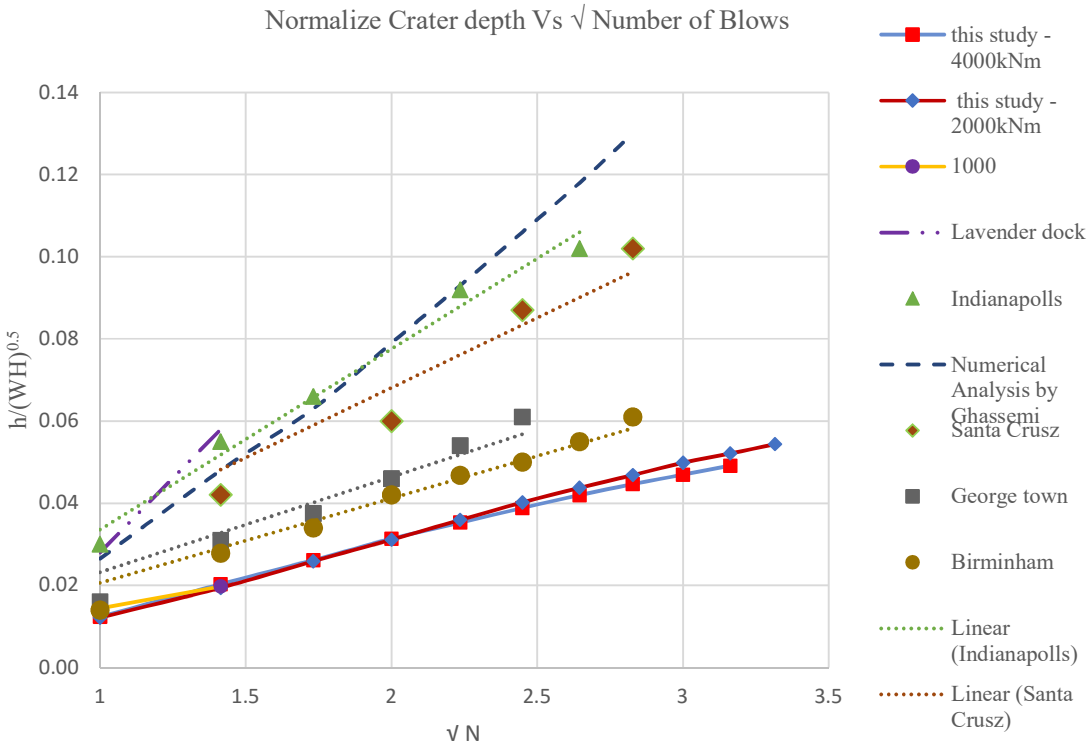

Figure 4-22: Normalized crater depth variation with √N

$$h/(WH)^{0.5}=k_1 (N)^{0.5} \quad (29)$$

With rearrangement of the above equation following relationship and be taken;

$$h=k_1(WHN)^{0.5} \quad (30)$$

This Equation 30 is almost identical to the equation 28, in which the pounder contact area, only additional parameter is a constant for a single pounder. The coefficient k_1 may depend on other factors such as sand properties, degree of self-compaction during reclamation and fill thickness for thinner fill layers.

In this study, trial compaction of 4000kNm, 2000kNm was applied in adjacent land plots, hence material condition, pre-compaction condition and fill thickness were noted as almost the same. Under that condition, linear correlation between normalized crater depth and square root of blow numbers relevant to 2000kNm and 4000kNm (see Figure 4-22) are almost overlapping and it verified the relationship given above. Similar overlapped linear relationship between normalize crater depth and square root of no of blows for different

energies was found by numerical analysis by A. Ghassemi et al. (2009) [71] by modelling dry and moist granular material fill.

Accordingly, considering slope of the trend line going through the origin of axis, k_1 could be found.

Slope of trend line $=k_1$

In this study $k_1$was determined as follows using liner relationship in Figure 4-23;

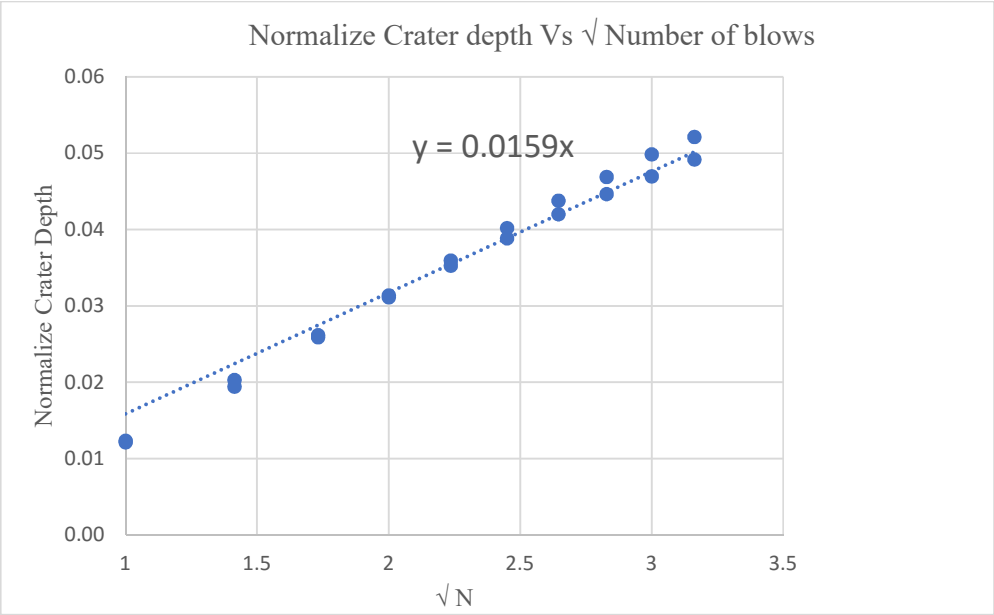

Figure 4-23: liner variation between Normalized crater depth and √N

k_1=0.0159

When k_1 value attributed to C_1' in Equation28:

$C_1'=k_1 \times \sqrt{A}=0.0159 \times \sqrt{4.406}=0.033375$

Accordingly, it can be noted that both values are almost identical. Based on the above relationship, the crater depth vs √ N graph can be extended if required. In other words, as per Equation 28, it can be identified that there is no maximum crater depth value. This is because of upheave of the surrounding area of the crater while increasing crater depth. Thus, final decision on blow number selection has to be taken by net volume change instead of crater depth. However, after finalizing the Blow Number (N) considering Ground Improvement Indices, which is discussed later, crater depth relevant to that particular blow number can be determined by this Equation 28. Since, there are facilities to measure crater depth in current tamping machines, crater depth values can be used for quality control work.

4.2.4.6. Identification of the Optimum Number of Blows in Dynamic Compaction by Net Volume Changes at the Compaction Point

To measure the volume change in the dynamic compaction, in addition to the crater bottom level, levels of four points outside the crater were measured in perpendicular directions as shown in Figure 4-24;

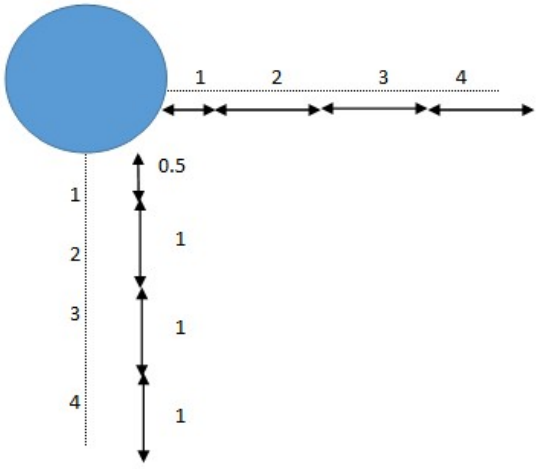

Figure 4-24: Ground level measured point in perpendicular directions at dynamic compaction point

As such crater volume, up heave volume and net volume were calculated at each blow number of dynamic compaction (see Appendix C) and summary of which has been plotted as follows;

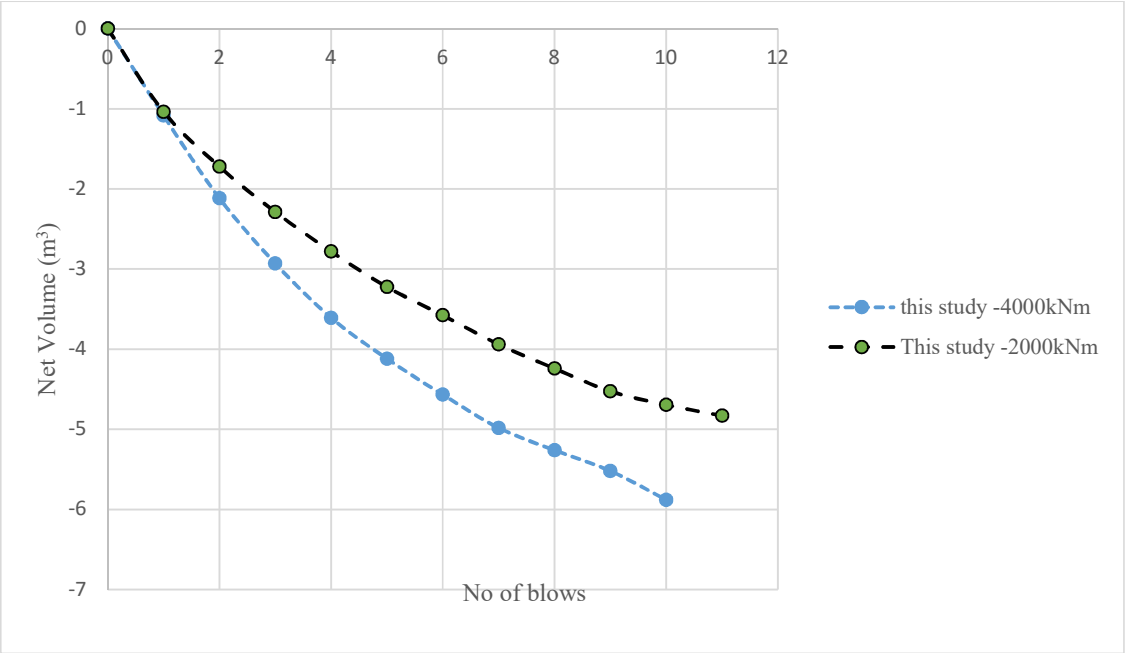

Figure 4-25: Net volume variation with blow number

Net Volume increment in ground movement by DC is shown in Figure 4-26;

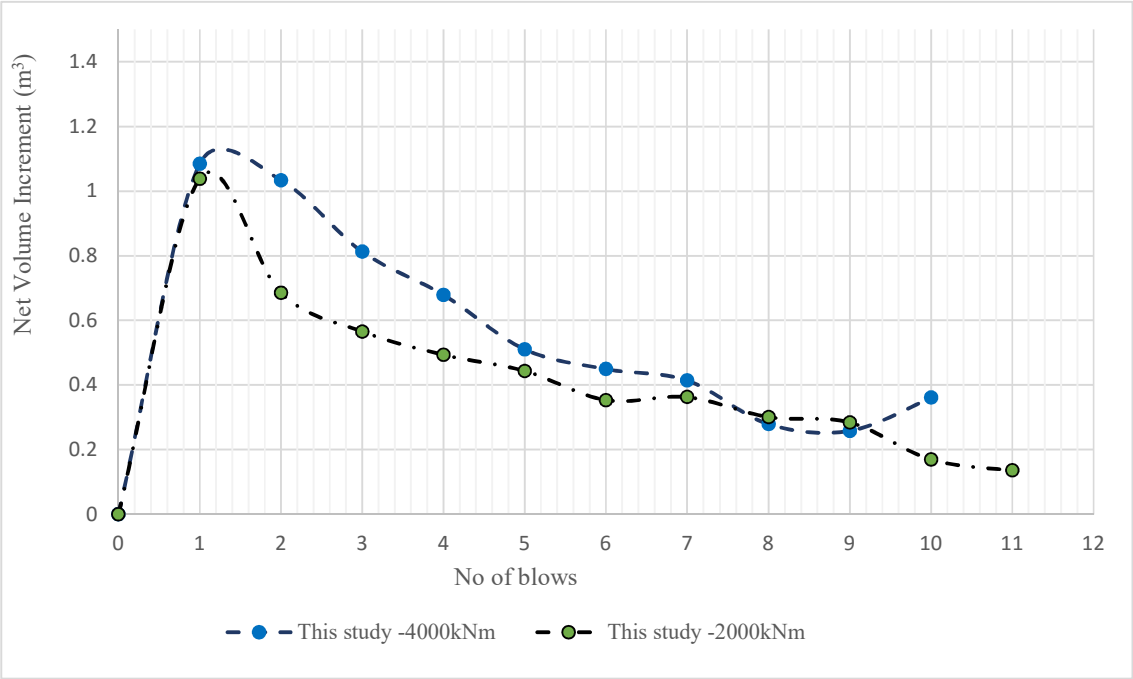

Figure 4-26: Net volume increment variation with no of blow

As per the above graphs, even after applying 10 or 11 blows still net volume change has not reached to zero. In other words, the peripheral ground heave was less than the change in crater volume. However, since net volume increment is low at the last blow of each 4000kNm and 2000kNm energy level, applying of further blows is no longer effective. According to the field data of trial compaction, 8 No of blows was the most optimum value despite the applied energy level in heavy tamping in reclaimed sand. Achieving of required qc values based on Ground Improvement indices is discussed later .

4.2.4.7. Influence Depth in Dynamic Compaction with Applied Energy

In this assessment, influence depth due to 4000kNm and 2000kNm energies were taken by considering the depth, in which significant improvement in cone resistant, qc values are noticeable.

(a) Influence Depth at Trial compaction

Based on pre and post compaction CPTs carried out in 2000kNm and 4000kNm dynamic trial compaction areas, influence depth was assessed as follows in Figure 4-27. The location of CPTs can be referred to the Figure 4-14.

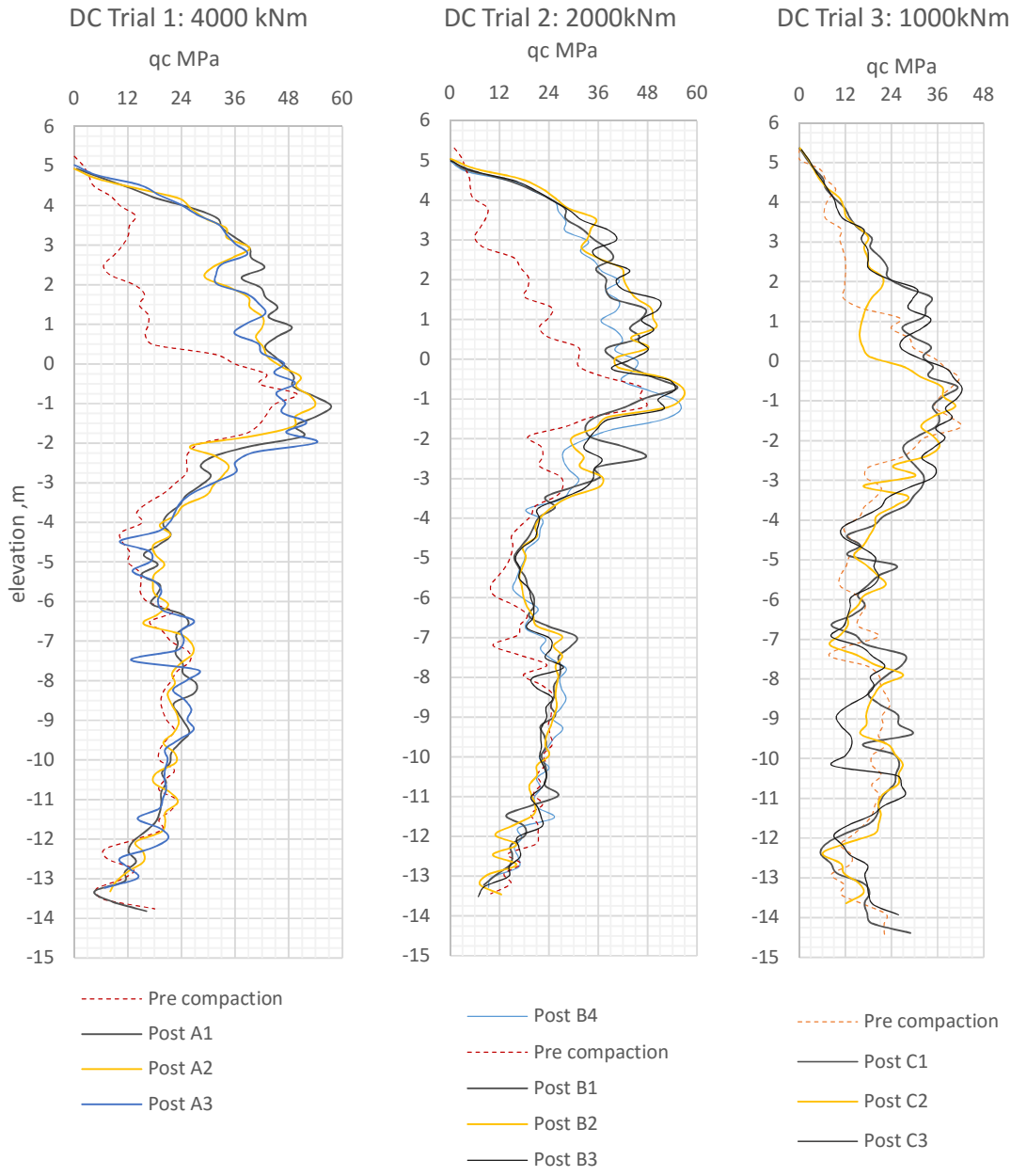

Figure 4-27: Comparison in influence depth considering improvement in qc after applying DC

Considering significant increase of qc in above post compaction CPT graphs, influence depths relevant for application of different energies were determined and summarized in Table 4-4 below. Accordingly, Menard's n value was assessed for different applied energies;

Table 4-4: Summary of influence depth with respect to the applied energy and estimated n values

Energy level	CPT No	Influence depth, (m)	Average (m)	n	Average n
4000kNm	A1	10.23	10.23	0.51	0.51
	A2	10.93		0.54	
	A3	9.52		0.47	
2000kNm	B1	8.33	8.48	0.58	0.58
	B2	8.54		0.60	
	B3	8.59		0.60	
	B4	8.47		0.59	
1000kNm	C1	4.66	4.45	0.46	0.44
	C2	4.06		0.40	
	C3	4.62		0.46	

As per above data average n value despite the energy level was 0.52 and which tally with the value proposed by Leonard et al (1980) and Ye et al. (1992). In addition, influence depth and n values were assessed using permanent DC works as follows;

(b) Influenced Depth and parameter "n" for permanent work with Different Energies

Based on the result of 19 no of CPTs advanced at locations given in Figure 4-28, where 4000kNm was applied for dynamic compaction, the influence depth varies from 6.78m to 9.83 m, while average influence depth was at 8.47m. Considering Menard equation, n value was estimated and found to be vary from 0.336 to 0.487. The average n value was observed as 0.419 (refer to Appendix IV for details).

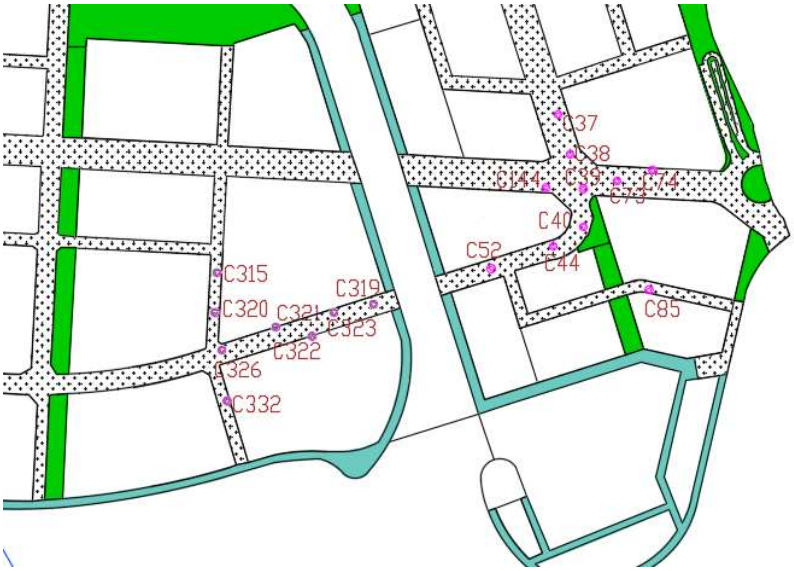

Figure 4-28: CPT locations in 4000kNm applied area

Similarly, analysing result of 57no of CPTs conducted at locations shown in Figure 4-29 in 2000kNm energy applied area, it was found that influence depths are having a much larger variation from 4.82m to 8.92m leading to average of 6.86m. Accordingly, Menard n value varies from 0.34 to 0.63.

Figure 4-29: CPT locations in 2000kNm applied area

Figure 4-30 shows the influence depth related to dynamic compaction in both 2000kNm and 4000kNm applied areas and the same observed in the trial areas belongs to 2000kNm, 4000kNm and 1000kNm.

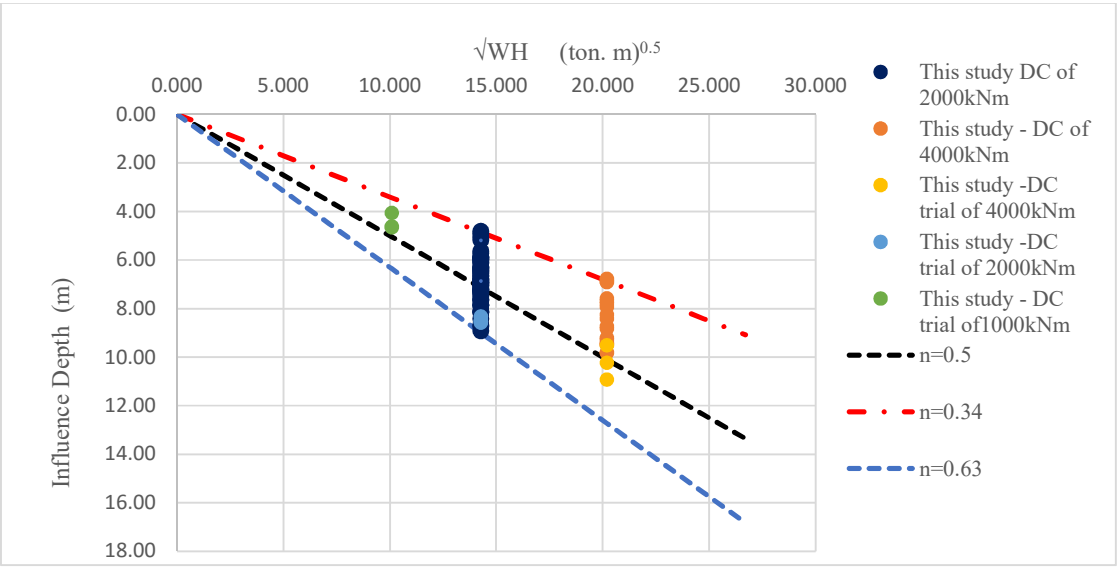

Figure 4-30: Variation of influence depth with √WH for this study

To compare the influence depth values found in this study with already published data of same found in different countries such as Malaysia, Israel, Taiwan, USA, Japan, China, Sweden, Scotland and Belgium, that data was plotted together with the values found in this study along with different Menard n value variation lines belong to 0.34, 0.5, 0.55 and 0.63. Though influence depth variation with square root of energy is generally considered as linear as per Menard n value for design work, according to following graph (Figure 4-31), this relationship can be identified as slightly non-linear. With increase of square root of energy, the rate of increment in influence depth has decreased and hence, the relationship has become slightly non-linear.

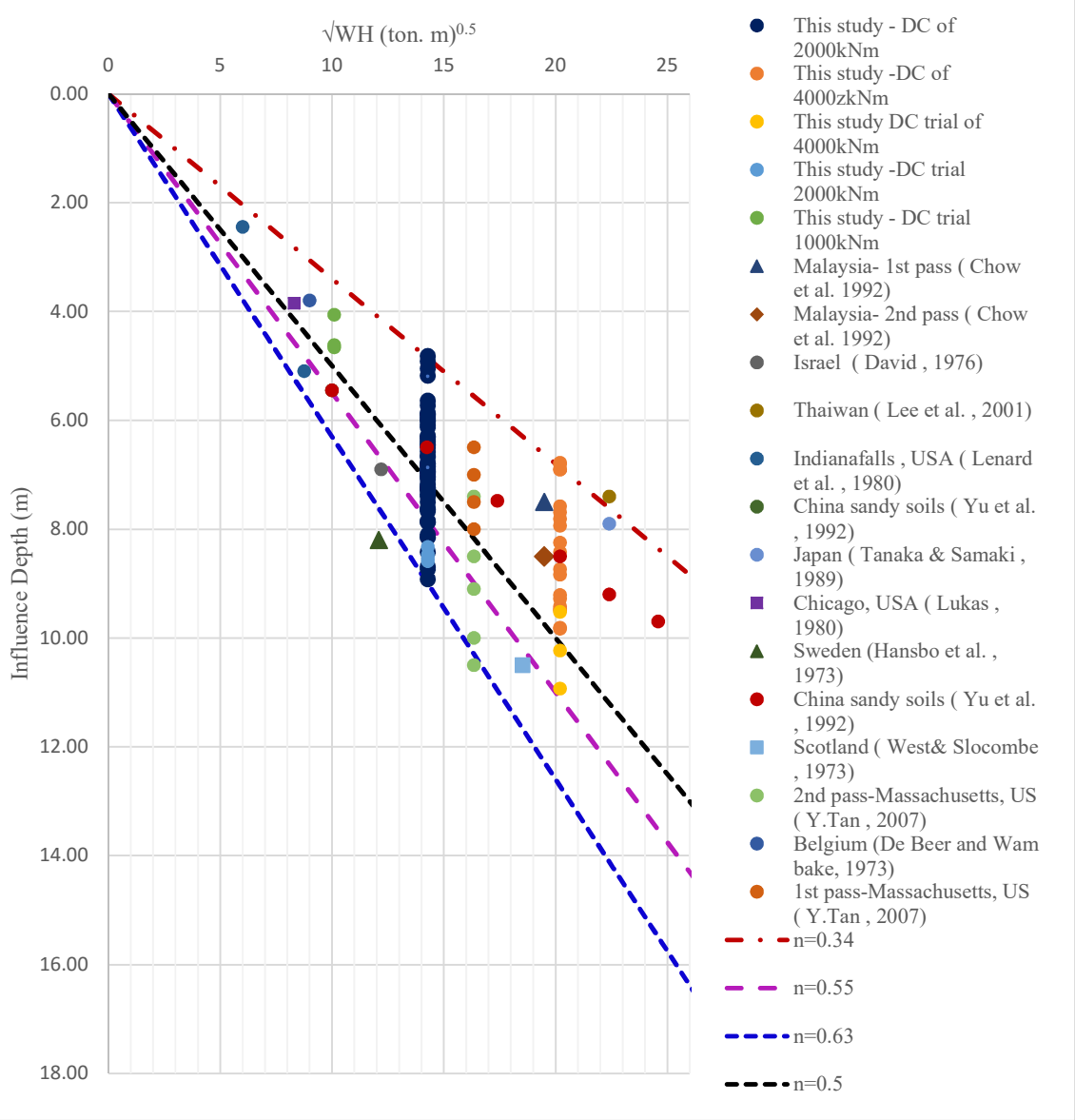

Figure 4-31: influenced depth variation with √WH in this study along with previous studies data

This non-linear behaviour of influence depth was introduced by Slocombe (1993) [75] and data in this study was applied in Slocombe chart as shown in Figure 4-32. Further, it can be observed that the data from the current study also fits well with the published data plotted in Figure 4-31.

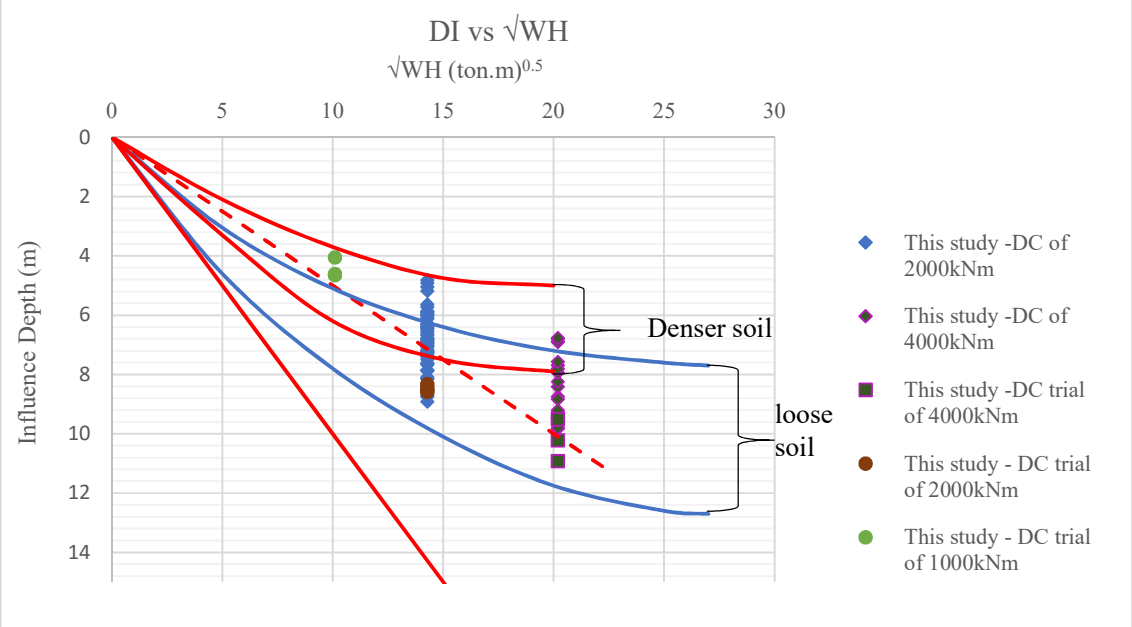

Figure 4-32: Influenced depth variation with square root of energy

Due to considerably wide range of influence depth shown in Figure 4-32 for each single energy levels (i.e. 4000kNm, 2000kNm or 1000kNm), the influence depth might be affected by some other factors such as initial soil condition. As Slocombe described, influence depth varies with initial strength, soil type, position of water table, number of drops etc. However, in this study, it was able to compare the influence depth achieved for each energy at an area having all the factors almost the same. During this study, the 'influence depth' and 'improved depth' as per Ground Improvement Index could be compared. It was observed that a significant ground improvement was observed at a depth (improved depth), which is shorter than the influenced depth (see Figure 4-33) and i.e. almost half of the influenced depth. This implies that when initial compaction of the fill is higher than the compaction that could have been achieved by dynamic compaction, no further improvement (relevant to qc) could be observed by dynamic compaction. This confirms the Menard suggestions on influence depth, which says "only applied energy at a time decides influence depth, while contribution from other factors are negligible for influence depth. However As per Lukas (Figure 2-39 & Figure 2-40), depth of improvement is achieved within first few blows (first two blows at a point 3m away from the centre) and further improvement is not significant.

4.2.4.8. Ground Improvement Index (Id)

A criteria for ground improvement evaluation based on CPT tip resistance q_t values has been widely used. Dove et al. (2000) [77] developed the ground improvement index (I_d), which is calculated in the following way:

$$I_d = \frac{q_{t,after}}{q_{t,before}} - 1$$

For sandy soil q_c equals to q_t. Ground improvement index related to each energy of trial dynamic compaction is as follows and pre and post compaction cone resistance ($q_{t,\,before,}$ $qt_{\,after}$) in trial area has been given in Figure 4-27;

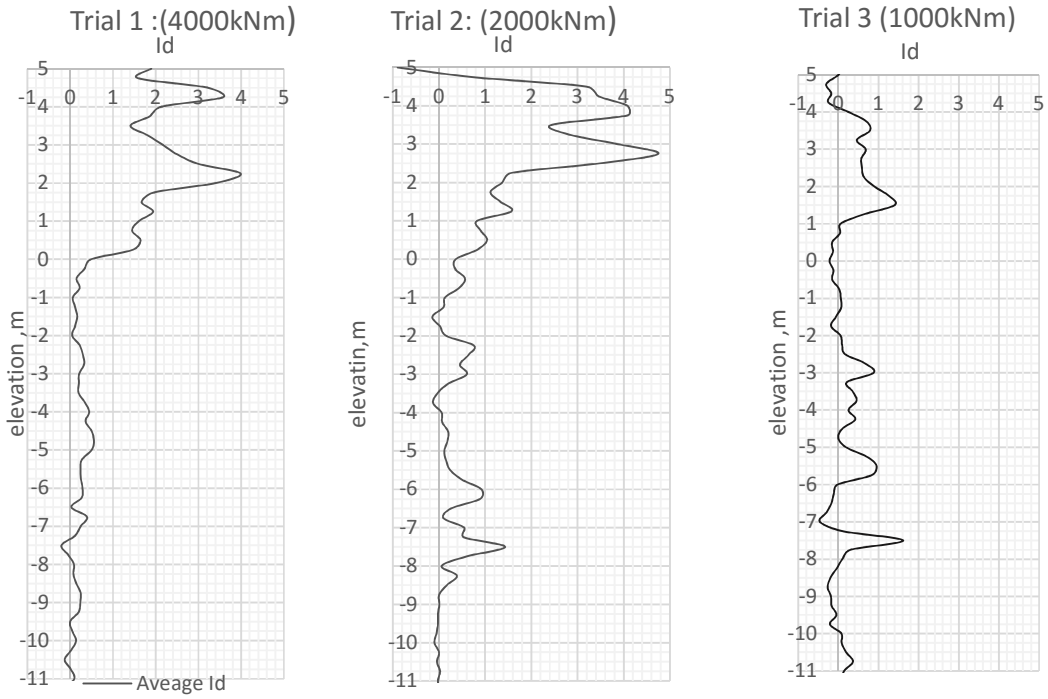

Figure 4-33: Ground Improvement Index variation with depth in trial area of this study

As per above result, it can be noted that ground improvement is limited only to a small depth when compared to its influence depth. In addition, according to the number of blows applied over unit tributary area, the improvement is up to 1 to 4 times for 1000kNm. 4000kNm and 2000kNm respectively. Earlier it was noted that no further improvement can be achieved when initial strength of soil is higher than the achievable strength. Moreover, when initial qc is very low I_d value is very high and there is no any sense of target improvement. Thus, the ground

improvement index does not truly reflect the effect of the energy application in dynamic compaction. However, that ground improvement index provides some idea about the achieved ground improvement with respect to the initial strength rather than required target strength. Thus, if such a similar improvement index based on final and target q_t values is introduced, it would be helpful to assess the ground improvement with respect to the target strength. Accordingly, Ground Improvement Index upon target improvement was suggested as follows;

$$I_t = \frac{q_{t,after}}{q_{t,target}} - 1$$

Considering target improvement defined in this project as shown in Table 4-5, it was evaluated for the trial dynamic compaction as illustrated in Figure 4-34.

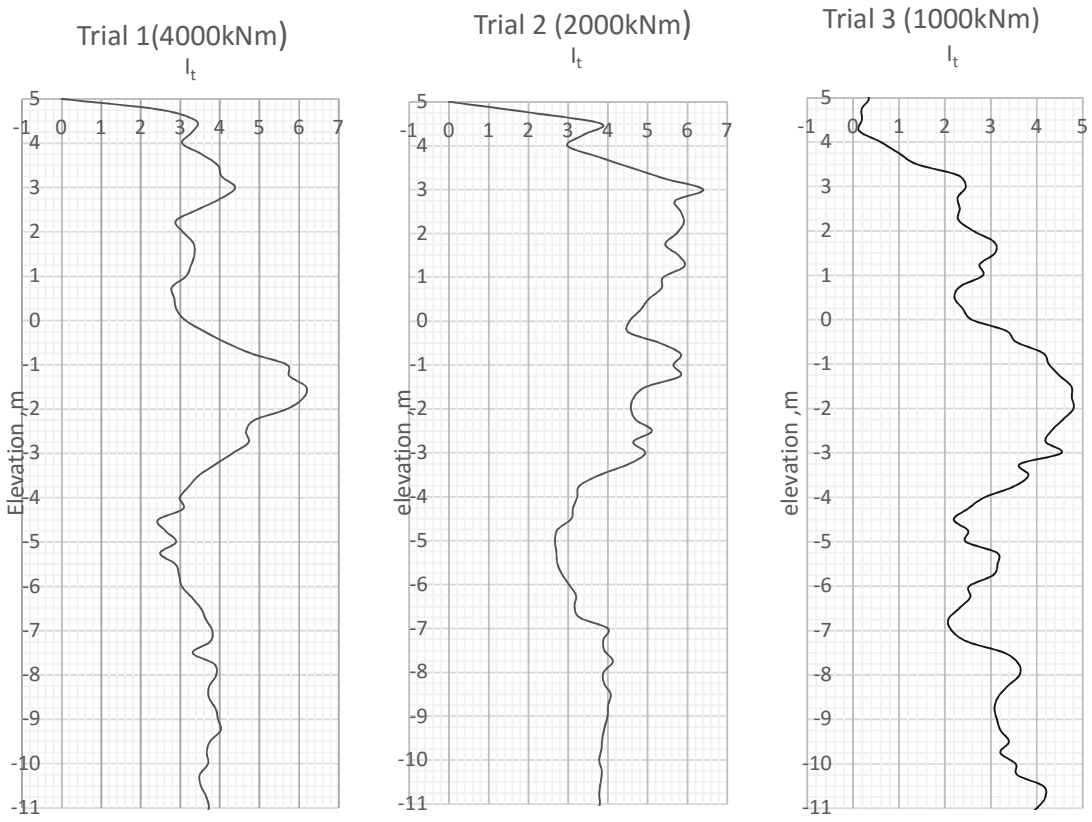

Figure 4-34: Variation of Ground Improvement Index upon target with depth in trial area

For sandy soils target qt equals to target q_c values, which was designed in development area and road areas are given in Table 4-5.

Table 4-5: Target q*c* values applied in different areas of this project

Development Area			Road Area		
Depth (m)	**Target Dr %**	**Target q_c**	**Depth (m)**	**Target Dr%**	**Target q_c**
1	75	6.3	1	75	6.3
2	50	4.8	2	65	731.0
3	50	6.0	3	65	8.9
4	50	7.0	4	65	10.4
5	50	7.9	5	65	11.7
6	50	8.4	6	50	8.4
7	40	6.8	7	40	6.8
8	40	7.1	8	40	7.1
9	40	7.4	9	40	7.4
10	40	7.7	10	40	7.7
11	40	8.0	11	40	8.0
12	40	8.3	12	40	8.3
13	40	8.6	13	40	8.6
14	40	8.8	14	40	8.8
15	40	9.1	15	40	9.1
16	40	9.3	16	40	9.3
17	40	9.6	17	40	9.6
18	40	9.8	18	40	9.8
19	40	10.1	19	40	10.1
20	40	10.3	20	40	10.3
21	40	10.5	21	40	10.5
22	40	10.7	22	40	10.7
23	40	11.0	23	40	11.0
24	40	11.2	24	40	11.2

Accordingly, Figure 4-34 illustrates the achieved compaction with respect to the target compaction upon the application of each energy. While dynamic compaction can be considered as successful based on I_t>0, requirement in degree of densification is evaluated by ratio between corrected cone resistance (q_t) at pre-compaction stage and target q_t. That ratio can be defined also by I_d and I_t as follows;

$$\frac{I_d + 1}{I_t + 1} = \frac{q_{t,target}}{q_{t,before}}$$

The above ratio describes the requirement of densification to achieve target qc (or qt). In this trial area if the above ratio was given below in Figure 4-33;

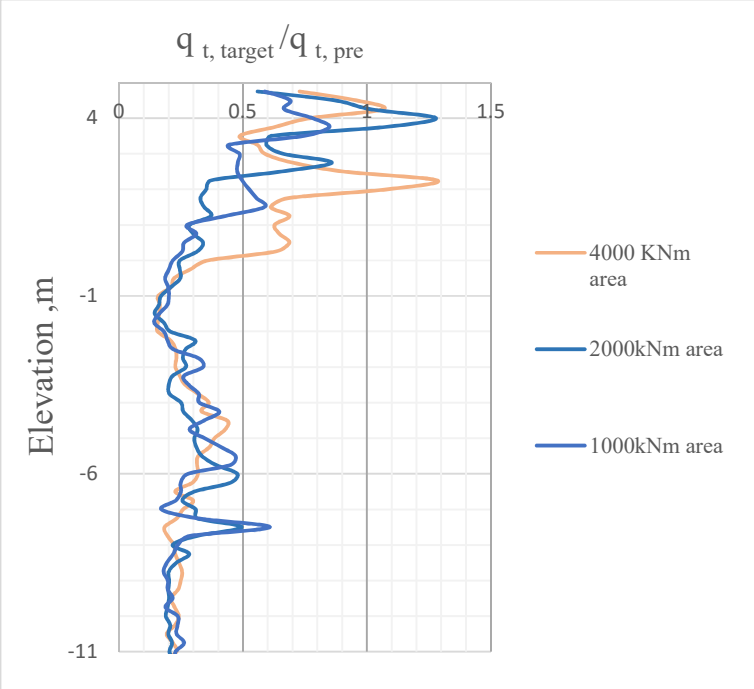

Figure 4-35: $q_{t\text{-target}}/q_{t\text{- pre}}$

As per above graph, self-compaction during reclamation has achieved its target improvement ($q_{t\text{-target}}/q_{t\text{ -pre}}<1$) in the most part of the depth except few layers up to +2.0m in this trial area. However, minimum qc values noticed in Pre-compaction CPT data belong to entire site shows in Figure 4-35 that generally there is a lack of compaction with respect to the target qc values.

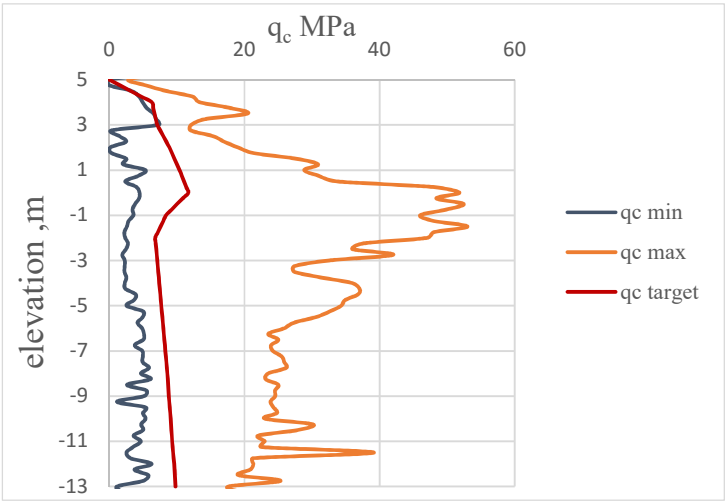

Figure 4-36: Target q_c plotted along with minimum qc values in pre-compaction CPT

Since certain blow numbers are required to achieve the target influenced depth as per Figure 2-39 & Figure 2-40, over compaction up to some extent cannot be avoided in the design of dynamic compaction. Accordingly, based on I_t index and influenced depth, optimum number

of blows can be selected based on a trial compaction. However, in order to confirm the pre-compaction condition at trial area reasonably represents the entire dynamic compaction applying area, adequate pre-compaction CPTs shall be advanced. Further, I_t index can also be applied for ground improvement by vibro compaction to assess the compaction work. As per trial compaction , it was revealed that the most optimum blow number is 8 and requirement of furthe improvement was not noticed during the analysis of Ground Improvment Indices (I_d and I_t)

4.2.5. Evaluation of the Effectiveness of Vibro Compaction in Reclaimed Sea Sand for Optimization

As per the literature discussed in section 2.16.2 in this document, vibro compaction is basically affected by probe capacity, point spacing and pattern, Probe penetration and extraction rates, power (amperage) applied, holding time in compaction phase and water and air pressure applied. Since the capacity of probe was fixed in this study, effect of other factors was analysed below.

4.2.5.1. Effect of Point spacing and Pattern

In this study trial vibro compaction conducted at adjacent locations using triangular pattern for all cases with three different spacing (3.9m, 4.2m and 4.5m) were used in three areas having grids as PA, PB and PC was compacted. Achieved ground densification in three cases were measured using CPTs at centroids of three compaction points shown in Figure 4-37.

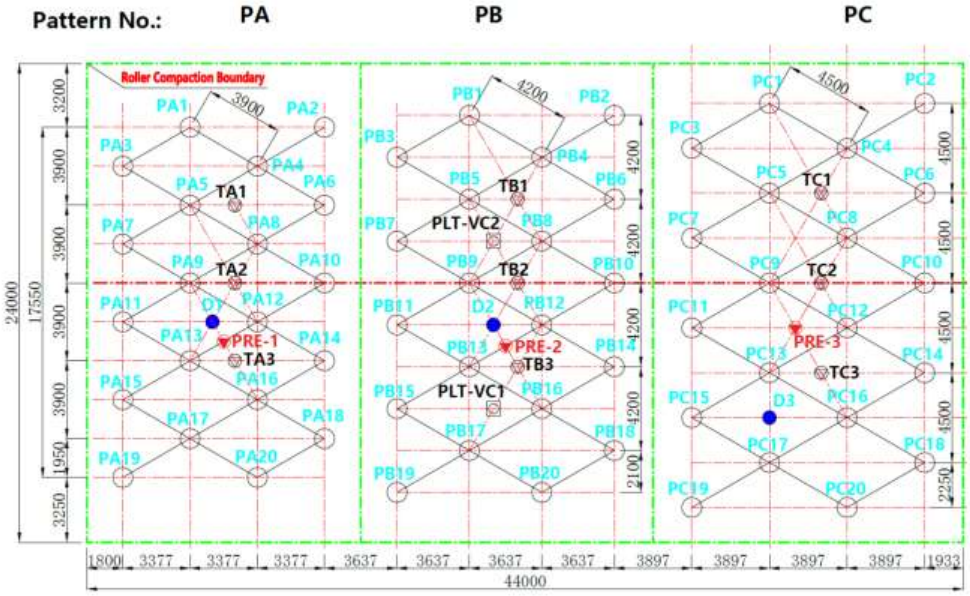

Figure 4-37: layout of trial points

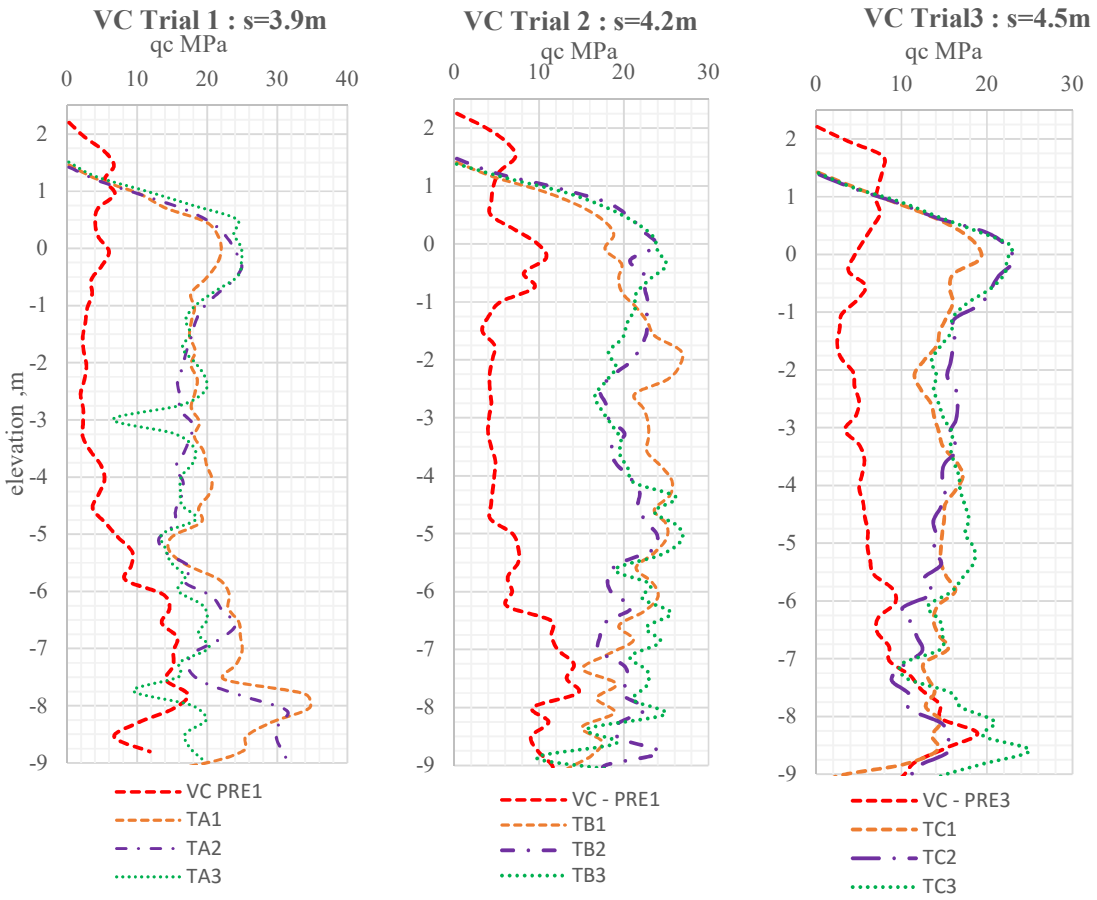

Figure 4-38: Comparison of achieved compaction (q_c) for different point spacing

Above Figure 4-39 shows achieved compaction (q_c) variation with spacing for trial VC area with compared to the pre-compaction q_c values. However, during VC operation, sand was subjected to liquefaction. Hence, original self-compaction condition of the sand fill was fully disturbed and there is no relationship between achieved final densification and original compaction condition.

In Figure 4-40, average post compaction qc curves relevant to 3.9m, 4.2m and 4.5m spacing has been plotted. Accordingly, it was observed that maximum compaction was achieved at 4.2m spacing while lower compaction was noted at 3.9m and 4.5m spacing. Since there is no significant difference in applied amperage, this varition implies that some kind of optimum point spacing for vibro compaction.

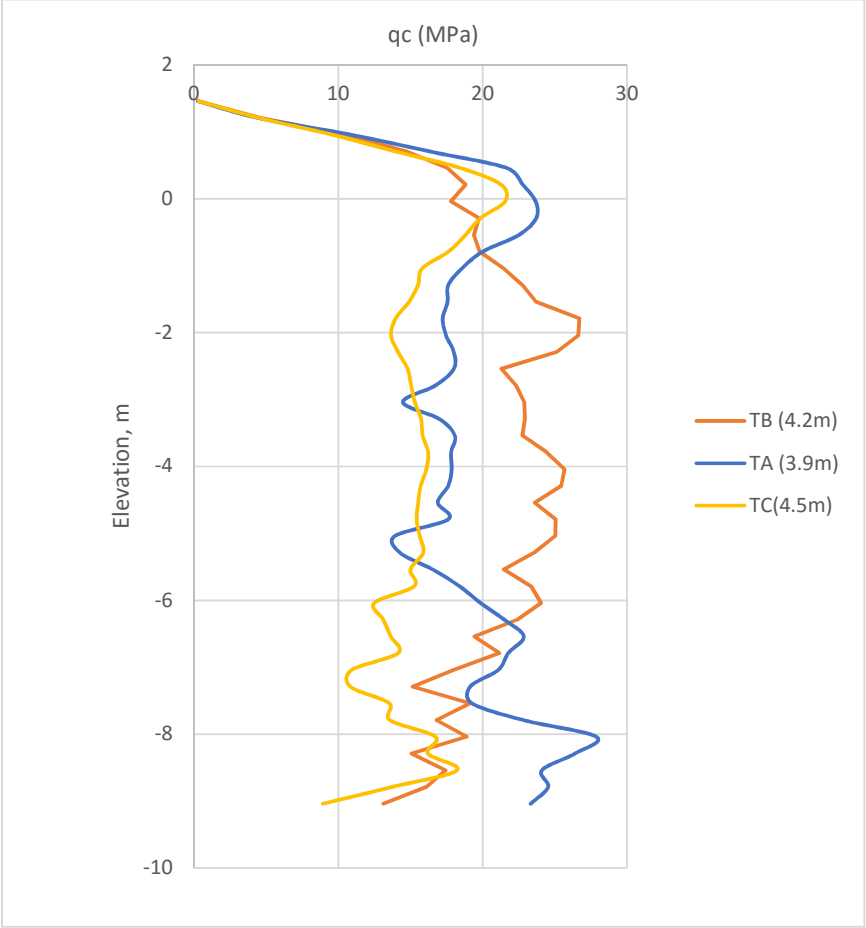

Figure 4-39 : Average compaction (q_c)variation with different spacing

As per the literature, resonance frequencies are not considered in vibro compaction unlike other vibratory compaction methods, because occurrence of oscillations cannot be found. However, point spacing(s) is always related to the capacity of vibro probe. Hence, this output should be further verified with trial compactions.

Most of the literature has given very small spacing such as below 3m. However, with this finding, it is required to evaluate those recommended values, since capacities of vibro probes have been much improved currently with upgraded technology.

4.2.5.2. Effect of Amperage (Power) Consumption, Time Consumption and Depth on Vibro Compaction

Evaluation of Amperage and Holding Time

To evaluate the effect of power consumption, time consumption (holding time) and depth on the sand densification, over 9000 compaction data logs (17000 points) and related 75 CPTs

were studied. Majority of them had similar curves as shown in Figure 4-40 on vertical probe movement against time and power consumption (used amperage) against depth. Basically, both of the curves can be separated as penetration phase and compaction phase as shown in orange and blue colour respectively.

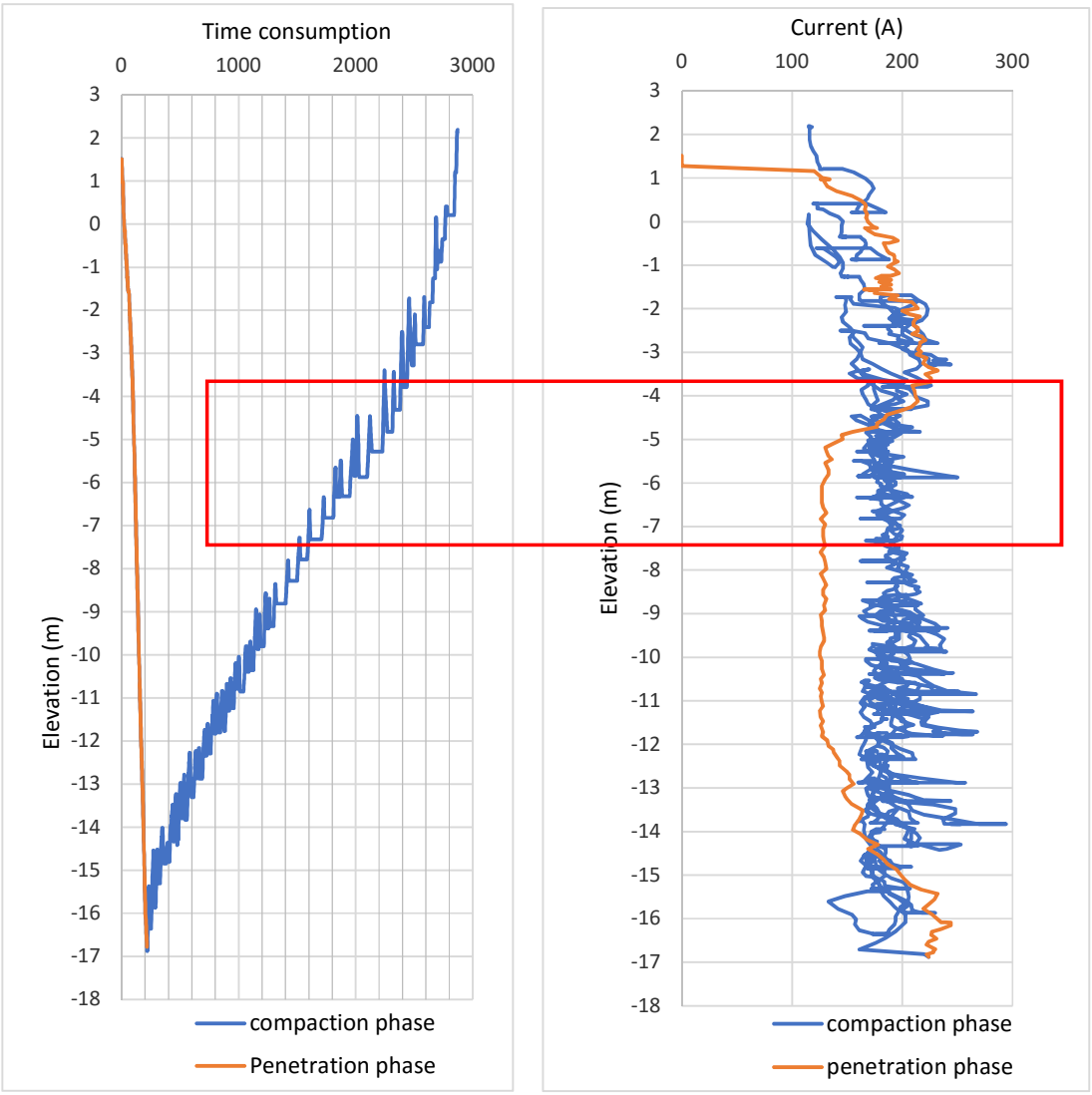

Figure 4-40: Typical time and amperage consumption curve

Since it is focused on compaction phase in this study, the highlighted part of the curves in Figure 4-40 was enlarged as shown in Figure 4-41.

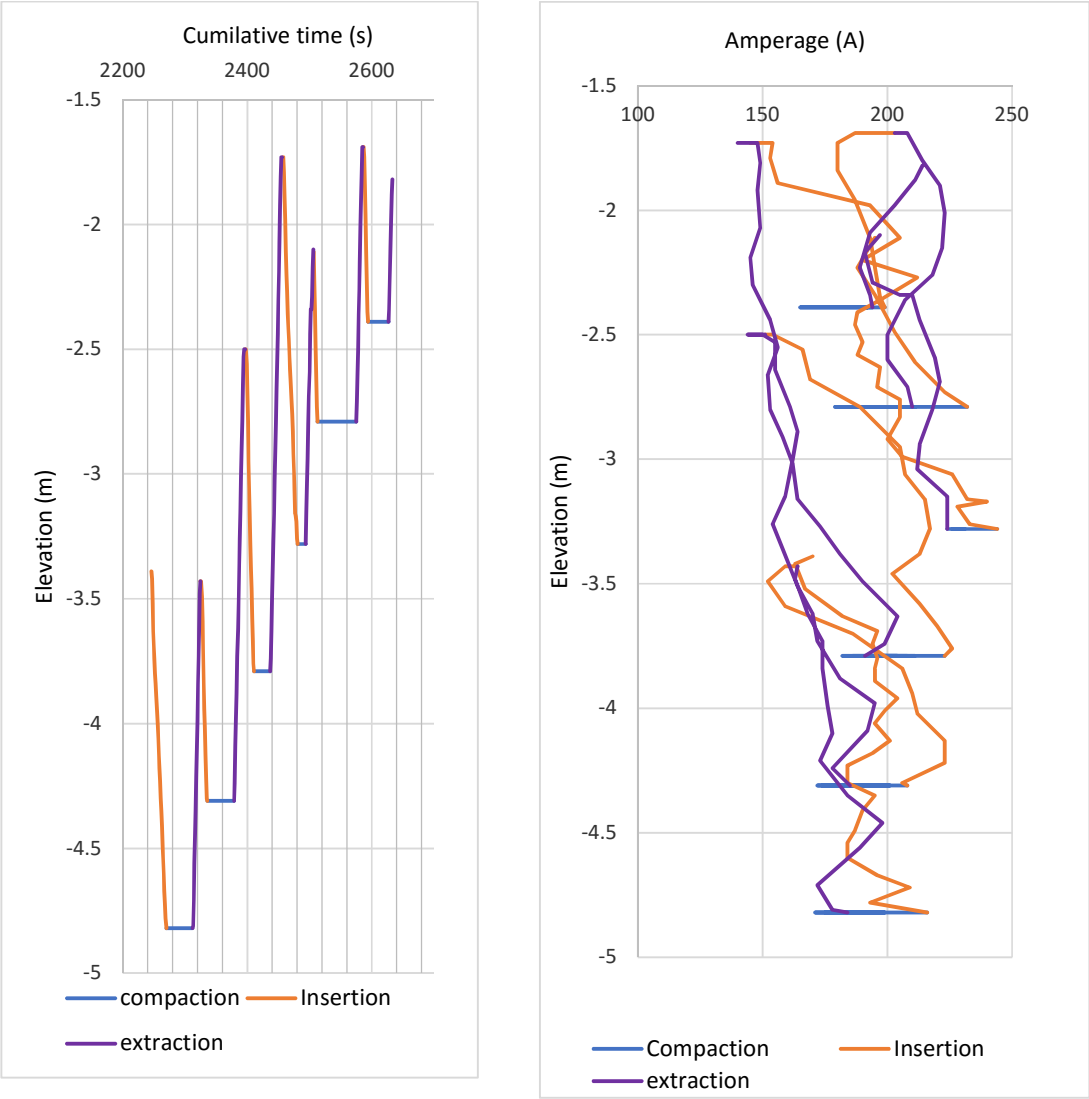

Figure 4-41: Amperage consumption (right) and time consumption (left) with elevation in compaction phase

As per the above graphs in Figure 4-41, three sub phases can be identified as insertion, compaction and extraction based on the vibro-compaction procedure applied as 0.5m insertion, compaction for 30s, and extraction of 1m during compaction phase.

Further, it can be seen that slightly higher amperage was used for insertion to generate higher amplitude and slightly low amperage was used for compaction and extraction. In vibro compaction, power is finally applied on soil as impact force with horizontal vibration. Generally, with low frequency causes for high amplitudes and which will be helpful in applying much higher lateral impact on surrounding soils.

To check the variation of amperage during compaction, amperage was plotted against time as shown in Figure 4-42. In that graph, it can be noted that with densification of sand amperage was increasing.

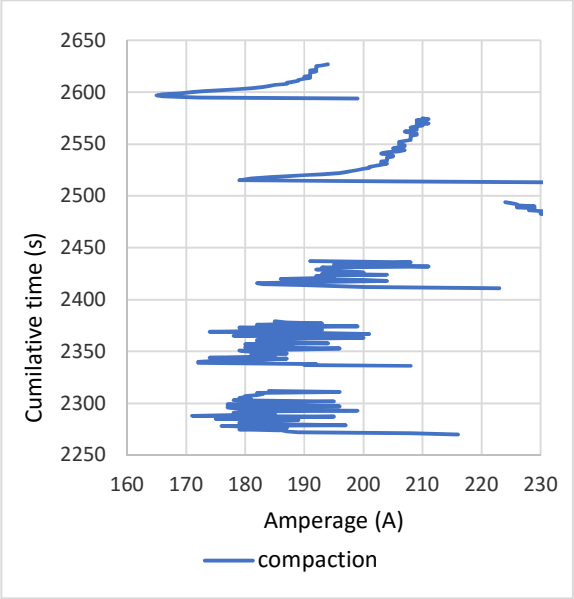

Figure 4-42: Amperage variation during compaction

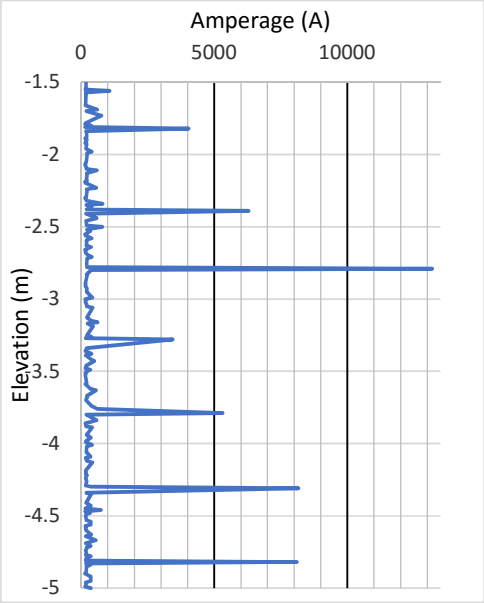

Figure 4-43: Cumulative amperage applied within considered elevation

However, using same data, when the amperage is plotted against the elevation ignoring its execution time, no significant variation was noted in applied energy with a single layer. This tendency can be seen in most of other graphs given in Appendix V (Figure A- 21**Error! Reference source not found.** to Figure A- 29).

Using Equation23 presented by Puchstein et al. the average rate of work (i.e., power) performed on a soil by a vibroflot was estimated considering

Average I =190.4 A while E=400v.

P=190.4x400x0.8x0.9x√3/1000

P=95.0 kW.

Where I= Average line current (A), E= phase to phase voltage requirement of vibrator (volts) and P=Average rate of work (W)

To compare the compaction condition with applied energy, qc values of CPT done in centroid of three compaction points and the relevant amperage data is shown in Appendix V.

4.2.5.3. Understanding of Complexity in Energy and Time Application on Vibro Compaction

As per the literature and practice, the effect of amperage, holding time and depth on the compaction is clear. Generally, that data is recorded in the machine and they are very useful to evaluate the actual compaction procedure and consistency of the compaction. However, due to many reasons described below, compaction output data (q_c) is inconsistent and always very conservative approach is followed for real work in practice.

In this study, considerable number of machine data logs, which consist of amperage (power), holding time and elevation data recorded at every second were evaluated with respect to achieved compaction at each elevation. Further, effect of the depth on power requirement was also considered. Though most of data are recorded in present vibro compaction machines, the correlation of above factors is not simple as one can assume due to following reasons;

1. Compaction requirement varies with depth in most project due to bearing capacity requirement for founding layers. However, the controlling of vibro probe is done as manual control and with the competence of the operator, he totally decides the holding time and insertion and extraction rates using amperage as the only guidance. Thus, possibility of over application energy and time cannot be ruled out.
2. Path of the lateral movement of Vibro probe is not a circle as seen in the Figure 2-46 and of which 3D movement was confirmed by very complex video analysis as discussed in literature review.
3. Since amplitude varies from bottom to top the impact over the surrounding soils also varies along the probe.
4. Generally, during vibro- compaction, sand boiling can be seen at even already compacted locations quite away from the nearest compaction points (beyond the tributary limits). Hence their contribution vibro compaction at considered point cannot be ignored.
5. Impact of vibration is applied along a 2m of vibro probe while extraction and insertion depths are 1m and 0. 5m respectively. Thus, with repeated energy application at each level, total energy applied on each elevation is very complex and difficult to be evaluated since ground improvment achievement is not limited to raidal direction.
6. Sand is aways deposited with denser condition at the bottom part of the vibration probe.

7. when vibro compaction is performed for subsequent points using trangular pattern, perimeter material (sand) of already compacted points will be disturbed and re-compacted based on its previous denser state. Due to this, energy used for the compaction is not uniformly distributed in surounding soils.
8. When vibro compaction is done by couple of vibro probes, a combined effect of vibration is applied on the ground.

4.2.6. Ageing Effect on Sand Densified by DC and VC

In order to determine the ageing effect in dynamic compaction and vibro compaction, 8 repeated CPT results were plotted with their initial post-compaction CPTs (See Appendix VII). Those CPTs had been repeated due to their premature termination.

Table 4-6: Summary of repeated CPTs

Post-compaction CPT				Time difference (days)	Applied Compaction method	Applied Engergy (kNm)	Average increment in qc
Initial		Repeated					
CPT No.	Conducted date	CPT No.	Conducted date				
C18	7-Jul-17	C18.2	25-Aug-17	49	DC	2000	0.38
C29	4-Aug-17	C29.2	25-Aug-17	21	DC	2000	3.52
C47	9-Sep-17	C47.1	9-Mar-18	181	DC	2000	1.49
c73	3-Nov-17	c73.1	26-Dec-17	53	DC	4000	0.01
C282	6-Mar-18	C282.1	20-Oct-18	228	DC	2000	0.61
C291	8-Mar-18	C291.1	18-Jan-19	316	DC	2000	2.65
c300	26-Mar-18	c300.1	28-Mar-18	2	VC		4.68
C203	24-Jul-18	C203.1	19-Jan-19	179	VC		0.44

As per above Table 4-6, the gain in q_c generally, varies 0.38 MPa to 3.5 MPa. But this gain is not increasing significantly with age of the compaction. Thus, in soil like clean sand having fine content less than 2%, age effect on densification is insignificant.

4.3. Evaluation of Ground Improvement Achieved in Dynamic and Vibro Compaction by CPT

4.3.1. Selection of CPT Locations

To achieve the design requirement such as bearing capacity, slope stability, settlement, differential settlement, liquefaction etc. through ground improvement process, the assessment of the improvement in the ground is required. Thus, after the application of dynamic compaction and vibro compaction, the achieved compaction is assessed by insitu tests such as

CPTs advanced at the least compacted points in each compacted area. This least compacted point is generally identified with respect to the compaction grid pattern. In this study 60 CPTs and 43 CPTs were separately evaluated in dynamic compaction and vibro compaction based on its four types of locations with respect to the compaction points as follows;

4.3.1.1. Summary of CPTs Advanced with Respect to the DC Point

The selected four types of CPT locations with respect to the Dynamic Compaction points are shown in Figure 4-44, in which the first pass locations are hatched. The selected point location represents the centre of the compaction point and the farthest point from them (i.e. centroid of the four compaction points) and two middle positions. Since there were adequate number of CPTs to evaluate the improvement with respect to the location of dynamic compaction in 2000kNm energy applied area, those q_c graphs in the same category was plotted separately as shown in the Figure A- 30 to Figure A- 34 in Appendix VI.

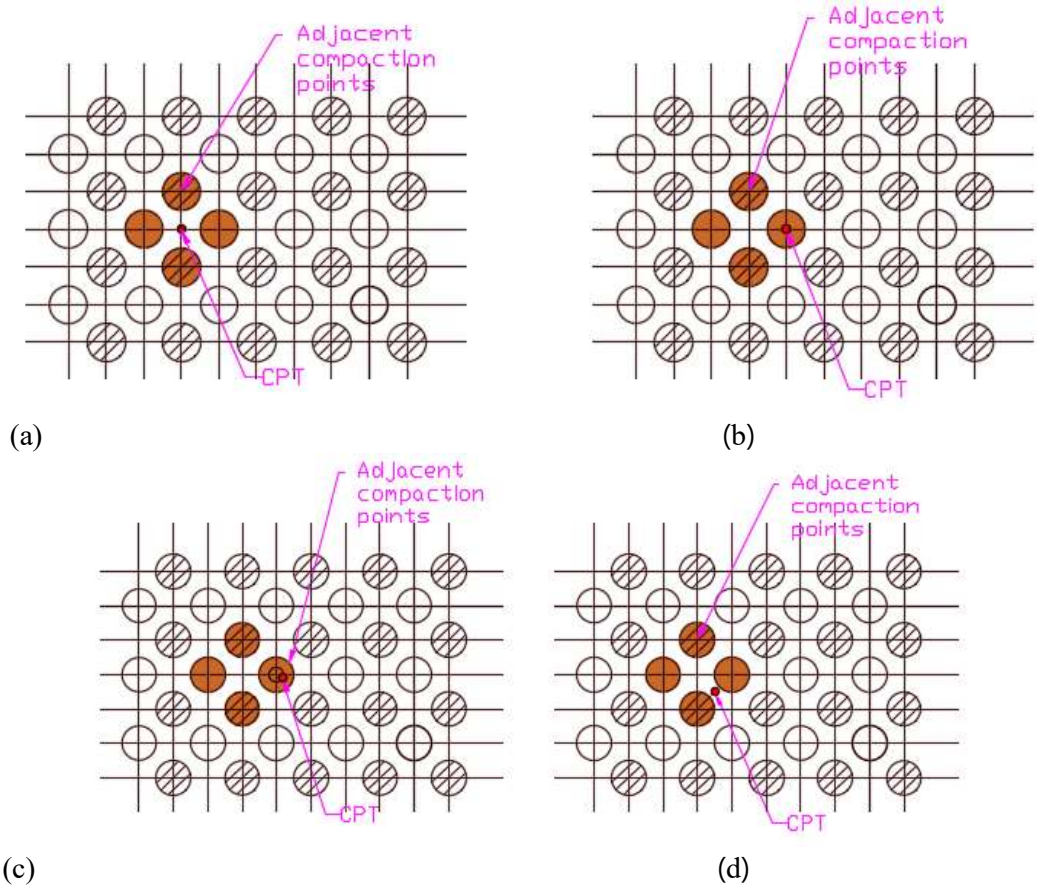

Figure 4-44: Advanced CPT locations with respect to the compaction points

The summary of the CPTs used for the above evaluation in 2000kNm applied area is given in Table 4-7.

Table 4-7: Summary of advanced CPTs with respect to the compaction points in 2000kNm DC area.

	CPT location w.r.t DC point	CPT Nos	Reference figure
1	Mid of four compaction points (Centroid)	34	Figure 4-44 (a)
2	Centre (Right on) the compaction point	8	Figure 4-44 (b)
3	1m away from the centre of compaction point	11	Figure 4-44 (c)
4	Centre of the two points	7	Figure 4-44 (d)

To compare the ground improvement achieved based on q_c values, the average q_c curves in each location type are plotted along with the average of the all q_c value of 60 CPTs in Figure 4-45.

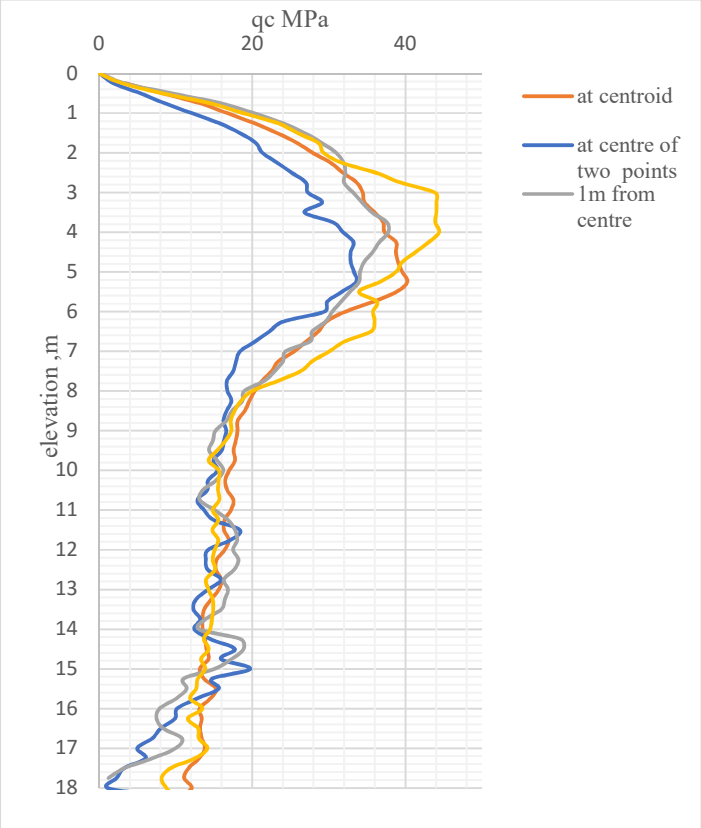

Figure 4-45: Comparison of qc curves in 2000kNm DC applied area with respect to the compacted points

As per the above graph, it was revealed that q_c at centroid does not give the minimum values as expected in general, but the least q_c values belong to CPTs advanced at mid of two dynamic compaction points. It is understandable that the centroid of the four-compaction point was predicted as least compacted point considering it as the farthest point from nearby dynamic compaction points. However, with the above outcome, it was revealed that the least compaction point will not be the centroid always due to overlapping of influence zone as shown in Figure 4-45. As illustrated in Figure 4-46, the over lapping of two, three or four influenced point make them more compacted than each compacted point if the point spacing are too closed. If point spacing are much larger not to overlap the influence zones, the centroid will become the least compacted point.

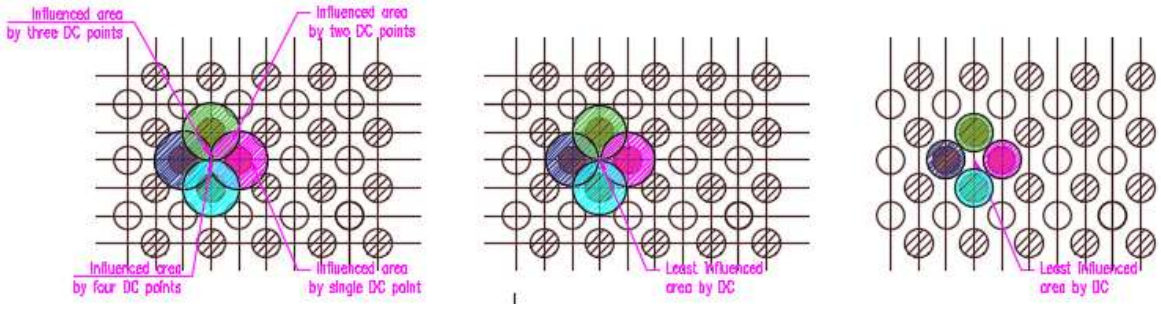

Figure 4-46: Effect of laterally influenced zone in dynamic compaction

As per above graphs, least compacted points were recorded at mid of two DC points. Therefore, least compacted points shall be determined during trial work to verify the achievement of minimum compaction requirement on site.

Though there are 60 CPTs advanced at different locations with respect to the compaction points in 2000kNm energy dynamic compaction area as mentioned above, relatively smaller number of CPTs were advanced in 4000kNm energy applied area. Moreover, most of them are advanced at centroid of the four DC points. Hence CPTs were difficult to categorize with respect to the advanced locations as above and only q_c values obtained from CPTs at centroid point was plotted as follows;

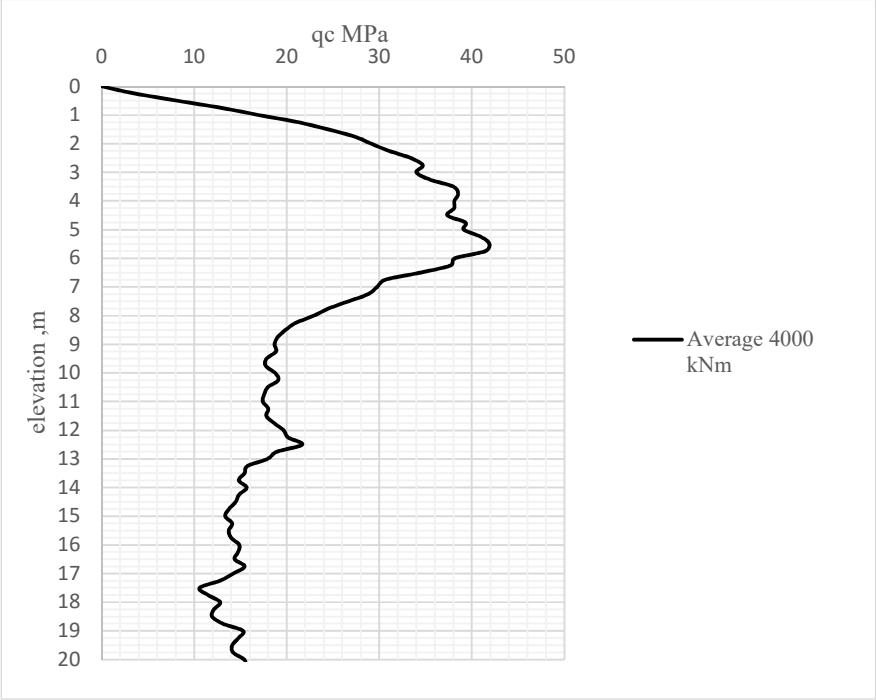

Figure 4-47: Average q_c values of CPT conducted at centroid of nearby compaction points in 4000kNm applied area

In order to assess the achieved improvement due to 4000kNm and 2000kNm dynamic compaction, average q_c curves belong to CPT's conducted at centroid along with average pre-compaction CPTs were plotted as in Figure 4-48;

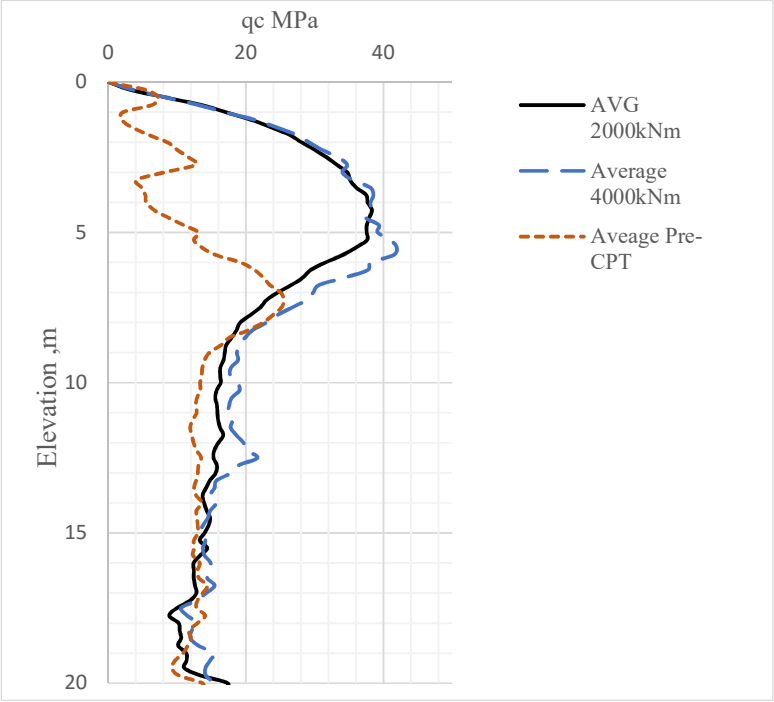

Figure 4-48: achieved qc improvement in 2000kNm and 4000kNm applied dynamic compaction areas

4.3.2. Summary of CPTs Advanced with Respect to the Vibro Compaction Points

Similar to dynamic compaction, ground improvement during vibro compaction was evaluated based on CPT location with respect to the compaction point as follows;

1. Centroid of three surrounding compaction points
2. Midpoint of two consecutive compaction points
3. Centre of the compaction
4. 1m away from centre of the compaction point

The selected four types of CPT locations with respect to VC points are as shown in Figure 4-49;

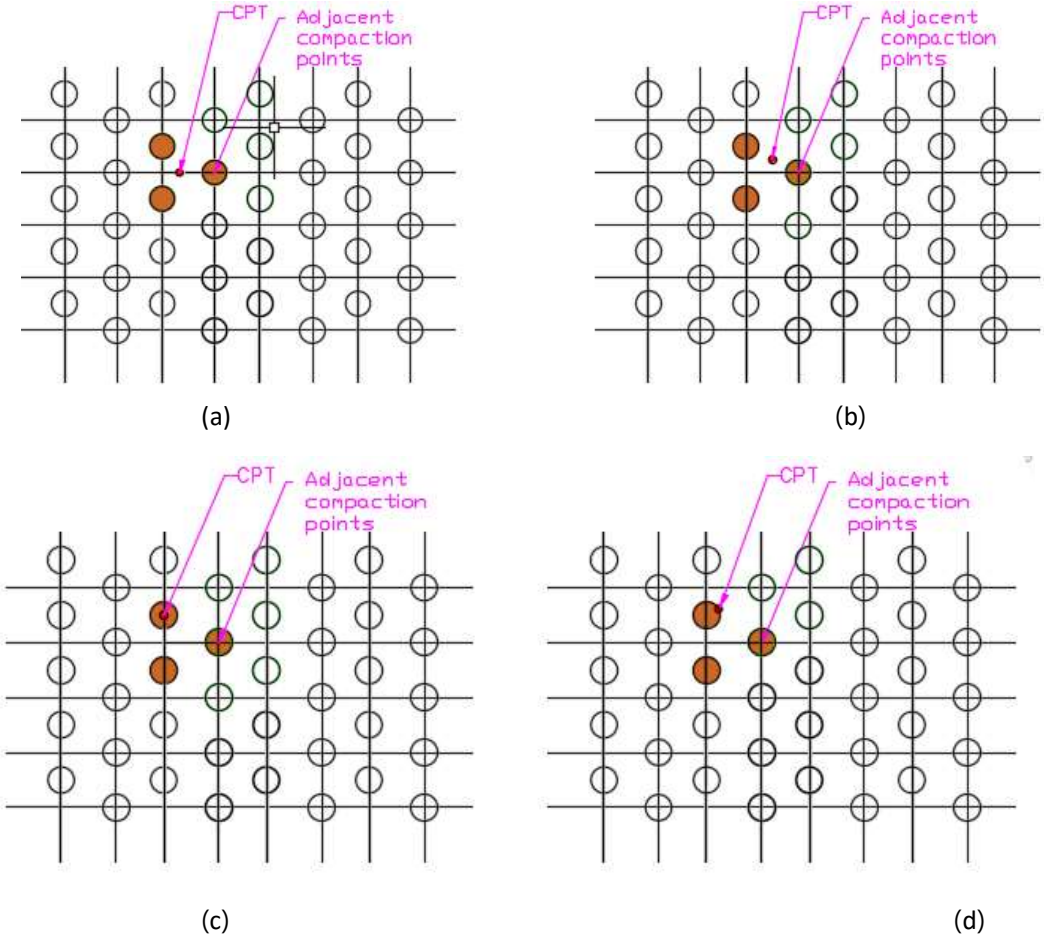

Figure 4-49: Selection of CPT location with respect to the nearby vibro compaction point

The details of CPTs with its relative positions with compaction points are given in Table 4-8.

Table 4-8 : Summary of CPT advanced with respect to the compaction points

	CPT location w.r.t VC point	CPT Nos	Reference figure
1	Mid of four compaction points (Centroid)	13	Figure 4-49 (a)
2	Centre of the compaction point	7	Figure 4-49 (b)
3	1m away from the centre of compaction point	7	Figure 4-49 (c)
4	Centre of the two points	15	Figure 4-49 (d)

Those qc graphs in the same category was plotted separately as shown in Figure A- 35 to Figure A- 38 in Appendix VI. The average graphs of each category were plotted in Figure 4-50;

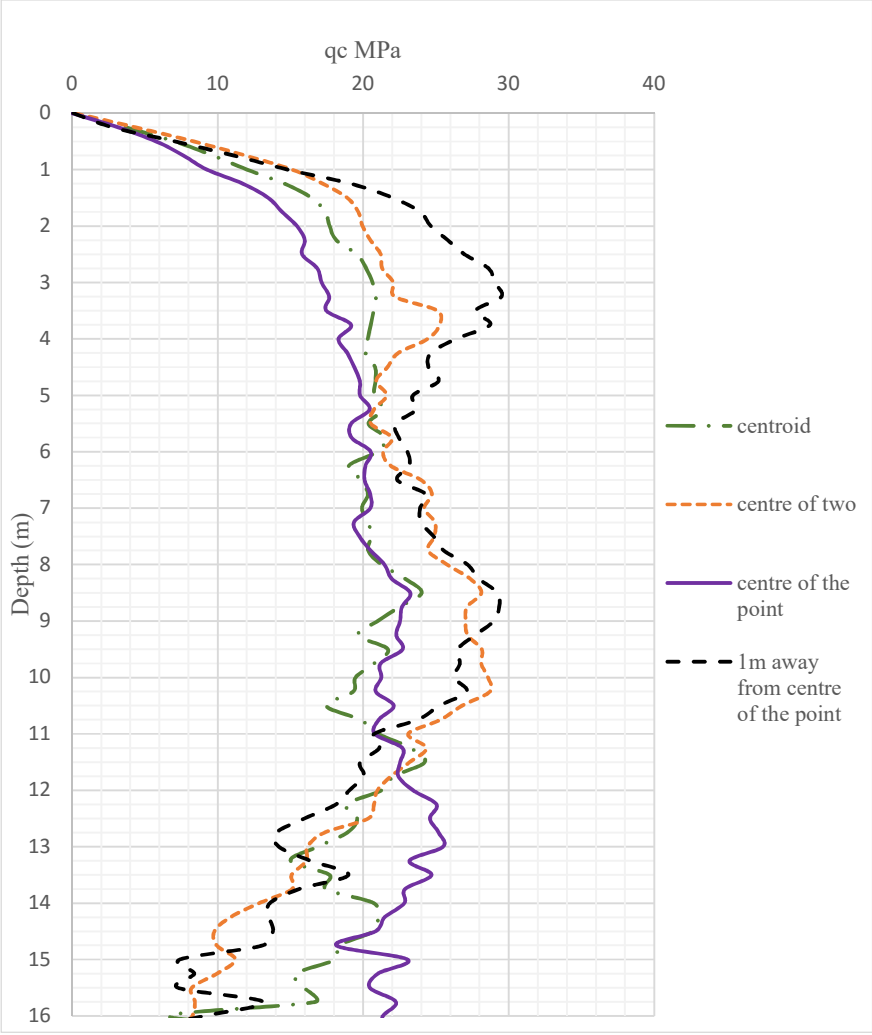

Figure 4-50: qc variation with CPT location with respect to the compaction point

As per above graphs, least compacted points were recorded at centroid and centre of the VC point. Thus, it is obvious that least compacted point is totally dependent on the spacing of compaction points. To illustrate this, the variation of possible laterally influenced areas of VC can be presented as follows;

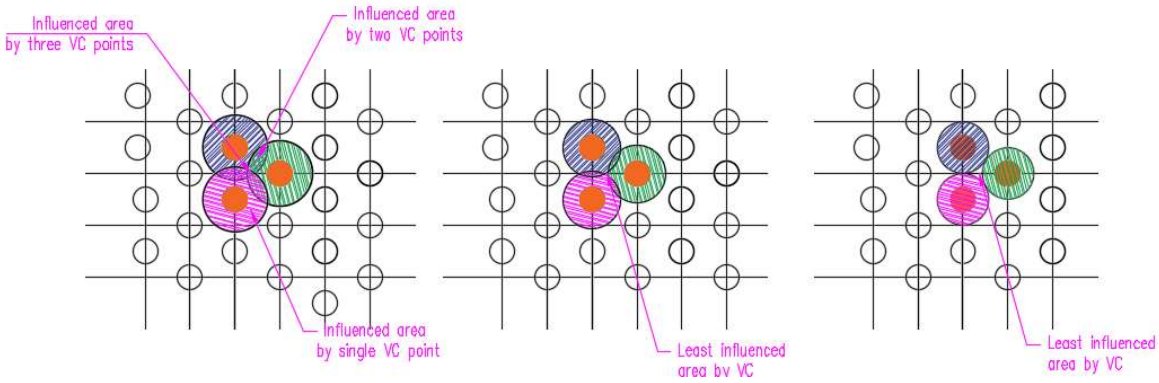

Figure 4-51: Possible variation in laterally influenced zones with change of grid spacing

5. CONCLUSIONS

To achieve the objectives of the research, construction data such as pre-compaction data, index properties of fill material, site records as well as post compaction data of this study area was analysed. Based on the outcome of those analysis, the following conclusions can be made.

According to the pre-compaction CPT results, compaction condition of reclamation fill varies from loose to medium dense sand based on the method used for sand placing. Cone resistance of fill varies in a wide range such as 4MPa to 50MPa and maximum self-compaction exists between +1.0 to -3.0m. Since thickness of the reclaimed fill was high as much as 25m, lower elevations such as -5m to -19m will not be easy to improve by most economical dynamic compaction methods. Since, self-compaction provided by bottom dumping and rainbowing is generally adequate for the requirement in lower elevations, those method should be utilized. Generally, reclamation project operated as turnkey projects and Turnkey Contractor is responsible for sand dredging, placing as well as ground improvement work while keeping design finish level after accounting for residual settlements. Therefore, with selection of right placing method at the right elevation, achievement of required densification by self-compaction is not difficult. On the other hand, usage of earth moving vehicles should be minimized at site, since it always forms fill of loose sand.

In this study, properties of fill material were identified as clean uniform sand (D_{50}=0.6mm) having fines lesser than 2% by Robertson's Soil Behaviour Type chart and particle distribution curves. Particle density is around 2.7Mg/m^3. MDD was 1.85Mg/m^3 while friction angle varies 35^0 to 42^0 relevant to Dr from 40% to 55%. Cu and Cc ranges are 2.424 to 3.058 and 1.076 to 0.776 respectively. This sand belongs to previous zone in Lukas soil grouping and is highly liquefiable. Further the fill material is excellent for application of vibro compaction with having 4.85 of Brown's suitability number. Hence dynamic compaction and vibro compaction can be applied on this sand efficiently. It is believed that Sri Lanka is rich with natural sea sand deposits, there of sand index properties seems to be almost same, especially in the off-shore area from Puttalam to Trincomalee through South-West coast. Hence, these index properties will be useful for the future design of reclamation projects in Sri Lanka.

In order to optimize the dynamic compaction, first of all crater depth and net volume change at crater was analysed using construction data. In dynamic compaction it was confirmed that selection of energy level is merely based on required influence depth. Using Menard equation for low energy or Slocombe envelope for higher energy, mass and drop height can be selected. Thus, the optimization of dynamic compaction is all about the selection of optimum blow number. The analysis results show that most effective ground improvement occurs up to 8 number of blows and after that further improvement occurs is not significant when compared to the applied energy. Influence depth upon different energies was evaluated using trial and construction data and Menard's n values found for 4000kNm, 2000kNm and 1000kNm were 0.419, 0.48 and 0.44, respectively. Since n value range increases for higher energy, this non-linear behaviour of Influence depth shall be derived by further trials of dynamic compaction with different energies.

Ground improvement index (I_d) was analysed using post compaction CPT data and found it to vary from 1 to 4. As per newly introduced index, I_t (for 4000kNm I_t =3, for 2000kNm I_t=3 to 6 and for 1000kNm I_t=2), over compaction can be seen within influenced depth. To achieve the target compaction while minimizing over compaction, crater depth, net volume change, influenced depth and improvement indices should be effectively applied in a trial area, which represents the fill condition of the site in general.

The estimated crater depths in actual reclaimed fill of loose to medium dense sand have to be determined by the Equation 28 or 30 suggested in this research. In which coefficient of C_1' and k_1 for this fill material were 0.334 and 0.0159, respectively. According to this analyis, it was revealed that crater depth continuely increases with number of blows despite reaching to its maximum compaction level. This is because of upheaving of the surrounding area of the crater while incrasing crater depth. Thus, checking of net volume change will be the better option to finalize the number of blows. After evaluation of ground improvement indices, this number of blows can be further curtailed if possible.

Currently, ground improvement by dynamic compaction is not designed using performance-based design. Instead energy level selected according to the soil type as per pre-defined charts is applied over the site after validation with a trial. However, if the design is optimized using cost effective performance-based design, energy and time consumed for entire site can be significantly reduced.

During the vibro compaction data analysis, it was observed that qc values in the area of 4.2m spacing are larger than that of 3.9m spacing area. This shall be further verified by field trials. In vibro compaction, data such as amperage and compaction time is recorded in the machine at every second. However, during the analysis, it was found that there is no simple correlation between those factors and fill compaction during very complex compaction process in vibro compaction. Therefore, for further analysis in vibro compaction shall be done after some of variable are getting fixed.

To identify the other critical factors which affect the outcome of dynamic and vibro compaction, ageing effect was evaluated and found that the improvement due to age effect is very minimal (qc increment varies from 0.38 to 3.5 MPa) in this fill sand. The reason for lower improvement might be the low fine content of filling sand. Accordingly, age effect will not play a big role in improvement in reclaimed ground using sea sand material having low fine content like in Sri Lanka.

For quality control and quality assurance work, compaction is verified by post compaction CPTs at centroid of nearby compaction points conventionally, after considering it as the least compacted point. However, in this analysis, it was noted that centroid is not always the least compacted point. Further, the variation of qc with point spacing could be understood as influence of overlapped laterally influenced area.

As such, the sequence of finalization of dynamic compaction design would be;

1. Selection of tamper mass and drop height based on required influence depth.
2. Identification of most effective number of blows based on estimated net volume change (the 8 number of blows identified in this study shall be further verified).
3. Selection of point pattern (staggered square in this study) and point spacing for trial work.
4. Conducting pre-compaction CPTs.
5. Applying of dynamic compaction design on trial area.
6. Checking the achieved densification through CPTs to be compacted at different (four) locations with respect to the compaction points as considered in this study.
7. As per the least qc values and the location, evaluate the point spacing.

8. Checking the ground improvement indices (Id and It) and deciding the possible reduction in number of blows, if the improvement is highly over designed.
9. Repeating of few more trials to finalize the point spacing and number of blows.

Accordingly, in order to get an optimized design for dynamic and vibro compaction, trial compaction shall be effectively used rather than validation of already completed design. At the outset by evaluation of pre-compaction data, general compaction condition of reclamation fill can be identified. During the trial construction, improvement of the ground and consistency of the improvement can be monitored closely through construction data recorded on site.

REFERENCES

[1] Chaa V., Bo M.W. ArulrajahA. , Na Y.M., "Overview of densification of granular soil by deep compaction methods," in *International Conference on Ground Improvement Technique*, Macau, 1997.

[2] Babak Hamidi , Hamid Nikraz and Serge Varaksin, "Application of Dynamic Compaction in Reclamation Roads," in *Australian Geomachanics Society Sydney Chapter Symposium*, Sydney, 2012.

[3] Sladen, J.A. & Hewitt, K.J. , "Influence of Placement Method on the In-situ Density of Hydraulic Sand Fills," *Canadian Geochnical Journal,* vol. 26, no. 3, pp. 453-466, 1989.

[4] H.E. Ali and J.S. Damgaard, "GEOTECHNICAL ASPECTS OF COASTAL RECLAMATION PROJECTS," in *7th International Conference on Asian and Pacific Coasts* , Indonesia, 2013.

[5] "Geotechnical recommendations for the design of maritime and harbour works - Maritime Works Recommendations," Spanish National Port Authorities, 1994.

[6] P. Menge, K. Vinck , M. Van den Broeck, P.O. Van Impe & W.F. Van Impe, "Evaluation of relative density and liquefaction potential with CPT in reclaimaed calcareous sand," *Geotechnical and Geophysical Site Characterisation5,* 2016.

[7] M.W. Bo Duc, Y.M.Na, A. Arulraj and M.F. Chang, "Densification of Granular Soil by Dynamic Compaction," in *Institute of Civil Engineers -Ground Improvement*, 2009.

[8] H. Tsuchida, "Predictions and countermeasure against the liquefaction in sand deposit," in *Seminor on Port and Habour*, Yokohama, 1970.

[9] Y. Tan, G. Lin , S.G. Paikowsky and J. Fang, "Evaluation of Compaction Effects on Granular Backfill Using CPT," in *Geotechnical Special Publication No172, American Society of Civil Engineers*, Denver, Colorado, 2007.

[10] J. Michell, "Soil Improvement -State of the Art," in *10th International Conference o Soil Mechnics and Foundation Engineering* , Stockholm, 1982.

[11] P. K. Robertson, "Soil Behavior Type from the CPT: an update," 2010.

[12] K. R. Massarsch, "Deep Soil Compaction Using Vibratory Probes," in *ASTM symposium on Design, Construction and Testing of Deep Foundation Improving: Stone Columns and Related Technique*, 1991.

[13] Y. Tan, "Sheet pile wall design and performance in peat," Doctoral Thesis, University of Massachusetts Lowell.

[14] Massarsch, K.R., Fellenius, B.H., "Vibro Compacction of Coarse Grained Soils," *Candian geotechnical Journal,* vol. 39, no. 3, pp. 695 -709, 2002.

[15] Hamidi, B. , Nikraz, H & Varaksin, S., "Ground Improvement Acceptance Criteria," in *14th Asian Regional Conference on Soil Mechenics and Geotechnical Engineering*, Hong Kong, 2011.

[16] P.O. Van Impe , W.F. Van Impe, A. Manzotti, P. Menge, M. Van den Broeck, K. Vinck, "Compaction control and related stress-strain behaviour of off-shore land reclamation with calcureous sands," *Soils and Foundations,* vol. 55, no. 6, pp. 1474-1486, 2015.

[17] American Society for Testing and Materials, "Standard Practice for Wet Preparation of Soil Samples for Particle Size Analysis and Determination of Soil Consultants," *Annula Books of Standard,* vol. 4.08, pp. 270- 272, 1989.

[18] Youssef Gomma and Gihan Abdelrahman, “Correlations Between Relative Density and Compaction Test Parameters,” in *12th International Colloguium on Structural and Geotechnical Engineering*, Egypt, 2007.

[19] Cubrinovski, M. & Ishihara, K., “Emperical Correlation between SPT N-value an Relative Density of Sandy Soils,” *Soils and Foundations,* vol. 39, no. 5, pp. 61-71, 1999.

[20] P. K. Roberson, “Suggested QC criteria for deep compaction using the CPT,” in *Geotechnical and Geophisical Site Charactersation 5*, Sydney, 2016.

[21] R. Craig, Soil Mechenics, London: Chapman & Hall , 1974.

[22] J. Schmertmann, “An Updated Correlation between Relative Denisity Dr and Fugro-Type Electric Cone Bearing , qc,” Contract Report DACW, Wes.Vicksburg. Miss., 1976.

[23] Tom Lunne , Peter K. Robertson, John J.M. Powel, “Cone Penetration Testing in Geotechnical Practice,” *Soil Mechanics and Foundation Engineering,* vol. 46, no. 9, 2009.

[24] P. W. Mayne, “Cone Penetration Testing State-of-Practice,” Transportation Research Board , 2007.

[25] Biryaltseva, T., Lunne, T Kreiter, S., Moerz,T., “Relative density prediction based on in-situ laboratoryu measurements of shear wave velocity,” in *International conference of geotechnical and geophysical site characterization*, ISC'5.

[26] Kulhawy, F.H. & Mayne, P.H. , “Manual on Estimating Soil Properties for Foundation Design,” Electric Power Research Institute (EPRI), 1990.

[27] P.K. Robertson , C.E.Wride, “Evaluation cyclic liquefaction potential using the cone penetration test,” *NRC Canada,* pp. 442-459, 1998.

[28] Seed, H.B. and Idriss, I.M. , “Simplified procedure for Evaluating Soil Liquefaction potential,” *Journal of Soil Mechanics and Foundation Division (ASCE),* vol. 97, no. SM9, pp. 1249-1273, 1971.

[29] Liao, S.S.C, and Whitman, R.V., “A catalog of liquefaction and non-liquefaction occurances during earthquake,” Cambridge , Mass., 1986.

[30] Juang, C.H. and Jiang, T., “Assessing probabilistic methods for liquefaction potential evaluation.,” in *Soil Dynamics and Liquefaction* , Reston, V.A, ASCE, 2000, p. GSP107.

[31] Degan ,W. , Baez, F., Rose, M, “Dry bottom freed stone columns at Pier 400 -An evaluation of CPT based soil classification before and after treatment,” in *US-Japan Workshop on " New Application and Challenging Soils for Ground Improvment Technologies*, Kyoto, Japan, 2005.

[32] K. Massarsch, Deep compaction of granular soils, State- of- art report,Lecture Series: A Look Back for Future Geotechnics, New Delhi & Calcutta: Oxford & IBH Publishing Co. Pvt. Ltd., 1999, pp. 181-223.

[33] F. Schlosser, “Improvement and reinforcement of soils,” in *4th International Conference on Soil Mechanics and Foundation Engineering , ICSMFE*, Hamburg, 1997.

[34] Smoltczyk, U, “Deep Compaction,” in *8th European Conference on Soil Mechanics and Foundation Engineering*, Finland, 1983.

[35] Merrifield, C.M. and Davis, M.C.R., “A study of low energy dynamic compaction: Field Trials and centrifugal modelling,” *Geotechnique,* vol. 50, no. 6, pp. 675-681, 2000.

[36] Mayne, P.W., Jones, J.S. and Dumas, J.C. , “Ground response to dynamic compaction,” *Journal of Geotechnical Engineering , ASCE,* vol. 110, no. GT6, pp. 757-773, 1984.

[37] R. Lukas, “Dynamic Compactionfor highway construction Vol. 1: Design and Construction Guide Line,” Report No. FHWA/RD-86/133 Federal Highway Administration, Department of Transport, Washington D.C. USA, 1986.

[38] R. G. Lukas, “Geotechnical Engineering Circular 1(Dynamic Compaction),” Federal Highway Administration, US, 1995.

[39] Chaumeny. J.L., Hechat, T., Kirstein, J. Krings . M., Lutz, B., “Dynamic Consolidation for the intersection of an Active Sinkhole area in the Course of the Federal Highway,” in *4th Hanz Lorenz Syposium* , Berlin, Germany, 2008.

[40] M. Soltraitement, “Uddevalla Shipyard (Sweden) Dynamic Consolidation Final Report,” Menard Soltraitement, 1978.

[41] Varaksin, S., Hamidi, B. & Aubert, J., “Abu Dhabi's New Corniche Road Ground Improvement,” in *2nd Gulf Conference on Roads*, Abu Dhabi, UAE, 2004.

[42] Rollins, K.M., Rogers, G.W., “Mitigation Measures for Small Structures on Collapsible Allovial Soil,” *Journal of Geotechnical Engineering ,* vol. ASCE, no. 120, pp. 1533 - 1533.

[43] A. O. C. Perucho, “Dynamic Consolidation of a saturated plastic clayey Fill,” *Ground Improvement ,* vol. 10, pp. 55-68, 2006.

[44] Cognon, J., Liausu, P., Vialard, R., “Combination of the Drains and Surcharge Method with Dynamic Compaction,” in *8th European Conference on soil Mechanics and Foundation Engineering* , Helsinki, Findand, AA Balkema Rotterdam, Netherlands, 1983.

[45] M. Soltraitement, “Palm Island STP Tanks Final Report,” Dubai, 2004.

[46] Susana López-Querol, Jaime Pecob, Juana Arias-Trujillo, “Numerical modeling on vibroflotation soil improvement techniques using a densification constitutive law,” *Soil Dynamics and Earthquake Engineering,* vol. 65, 2014.

[47] Woods, R.D , Jedele, L.P., “Energy Attenuation Relationships from Construction Vibration,” Detroit, MI,, 1985.

[48] Babak Hamidi, Serge Varaksin and Hamid Nikraz, “A case of vibro comapction monitoring in reclamation site,” in *Advances in Geotechnical Engineering*, Perth, Australia, 2011.

[49] “www.kellerholding.com,” Keller Holding GmbH, [Online]. Available: https://www.wtcb.be/homepage/download.cfm?lang=en&dtype=services&doc=tc17_presentation_04.pdf.

[50] FHWA, “Ground improvment technical summaries Vol. II. Publication No. FHWA-SA-98-086R, 1-84,” FHWA, 2001.

[51] B. R.E., “Vibroflotation compaction of cohesionless soils,” *Journal of the Geotechnical Engineering Division,* vol. 103, no. 12, pp. 1437-1451, 1977.

[52] K. Rainer Massarsch, Bengt H. Fellienius, “Deep vibratory compaction,” in *Chaper 4, Ground Improvement Case Histories , Compaction, Grouting and Geosynthetics*, Elsevier Ltd, 2015, p. 111 ro 135.

[53] C. J. Griffith, “Soil Improvement through vibro compaction and vibro replacement,” Department of Civil Engineering, University of Maryland, 1991.

[54] M. Wallays, “Deep Compaction by Casting Driving .,” in *ASCE Symposium on Recent Development in Ground Improvment Techniques*, Bangkok, 1983.

[55] Hamidi, B. Nikraz, H. & Varaksin, S., "A Review on Impact Oriented ground Improvment Techniques," *Astralian Geomechanics Journal,* vol. 44, no. 2, pp. 17-24, 2009.

[56] Y. Nazhat, "Behavior of sandy soil subjected to dynamic loading," University of Sydney, Sydney, 2013.

[57] W. R.D., "Severing of surface wires in soils," *Journal of Soil Mechanics and Foundation, ASCE,* vol. 1968, no. NO SM4, DSI-098.

[58] Moretrench, "www.moretrench.com".

[59] Raju V.R.,Sridhar Valluri , "PRACTICAL APPLICATIONS OF GROUND IMPROVEMENT," in *Symposium on ENGINEERING OF GROUND & ENVIRONMENTAL GEOTECHNIQUES*, HYDERABAD, INDIA, 2008.

[60] Jaime Peco Culebra , Susana Lopez- Querol, "Application of endochronic densification law for designing vibroflotation soil improvement technique," in *The 2012 World Congress on Advances in Civil, Environmental, Materials Reseach*, Seoul, Korea, 2012.

[61] V. Luongo, "Dynamic compaction : Predicting depth of improvement," *Geotechnical Special Publication,* vol. 2, no. 30, pp. 927-939, 1992.

[62] Mehdipour, S. , Hamidi, A., "Impact of tamper shape on the efficiency and vibration induced during dynamic compaction of dry sands by 3D Finite Elemant Modeling," *Civil Engineering Infrastrucures Jounal,* vol. 50, no. 1, pp. 151-163, 2017.

[63] Degen, W.S. and J.D> Hussain, "Soil Densification," in *ASCE Geo-Odyssey Confenece*, Backsburg V.A., 2001.

[64] Vernon R. Schaefer, Ryan R. Berg, James G. Collin, Barry R., "GEOTECHNICAL ENGINEERING CIRCULAR NO. 13," U.S.Department of Transportation Federal Highway Administration, U.S., 2017.

[65] Dobson, T. and B. Slocombe, "Deep Densification of Granular Fills," 2nd Geotechnical Conference and Exhibit on Design and Construction , Las Vegas, Nevada, 1982.

[66] R. A. Green, "Energy based evaluation and remediation of liquefiable soils," Virginia Polytechnic Institute and state university, USA, 2001.

[67] B. B. BROMS, "DEEP COMPACTION OF GRANULAR," in *Foundation Engineering Handbook*, New York, Springer Science + Business Media , 1991, pp. 814-831.

[68] Arslan, H., Baykal, G. and Ertas, O., "Influence of tamper weight shape on dynamic compaction," *Ground Improvement,* vol. 11, no. 2, pp. 61-66, 2007.

[69] Oshima, A., Takada, N., "Effect of ram momentum on compaction by heavy tamping," *Internation Conference on Soil Mechanics and Foundation Engineering,* vol. 13, no. 3, pp. 1141-1144, 1994.

[70] F. Jafarzadeh, "Dynamic Compaction Method in Physical Model Test," *Science Iranica,* vol. 13 , no. No2, pp. 187-192, 2006.

[71] Y.K. Chow, D.M. Yong, K.Y. Yong, S.L. Lee, "Dynamic compaction of loose sand deposits: effect of print spacing.Improvement of granular soils by high energy impact," *Journal of Geotechnical Engineering, ASCE,* vol. 120, no. 7, pp. 1115-1133, 1994.

[72] Tanaka, S. and Sasaki, T., "Sandy Ground improvement for Liquefaction at Noshiro Thermal Power station," *Soils and Foundation,* vol. 37, no. 3, pp. 86-90, 1989.

[73] A. Ghassemi, A. Pak and H. Shahir, “A numerical tool for design of dynamic compaction treatment in dry and moist sands,” *Iranian Journal of Science and Technology , Tranasaction and Engineering,* vol. 33, no. B4, pp. 313-326, 2009.

[74] Leonards, G.A., Cutter, W.A., Holtz, R.D., “Dynamic compaction of Granular Soils,” *Journal of Geotechnical Engineering Division,* vol. 106, no. No. 6, pp. 35-44, 1980.

[75] W. Van Impe, Soil Improvement Technique and Their Evaluation, Rotterdam: A.A.Balkema, 1994.

[76] Menard, L., Broise, Y. , “Theretical and practical aspects of dynamic compaction,” *Geotechnique,* vol. 25, no. 1, pp. 3-18, 1975.

[77] Slocombe, “Dynamic Compaction,” in *Ground Improvement*, Boca Raton, Florida, CRC Press Inc, 1993, pp. 21-39.

[78] Poran, C.J. and Rodriguez, J.A., “Design Dynamic Compaction,” *Canadian Geotechnical Journal,* vol. 29, no. 5, pp. 796-802, 1992.

[79] Dove, J.E., Boxil, L.E.C., and Jarrett, J.B., “A CPT based index for evaluating ground improvement,” *Advances in grouting and ground modification,* vol. 104, pp. 296-310, 2000.

[80] Nagy Peter,ADAM Dietmar,KOPF Fritz and FREITAG Peter, “Experimental and theoritical investigation of deep vibro compaction,” in *European Conference on Geotechnical Engineering*, Macedonia, 2018.

[81] P. Nagy, “Investigation soil-machine interaction during deep vibro compaction,” in *6th International young Geotechnical Engineer's Conference* , Seoul, Republic of Korea, 2017.

[82] A. Paul, “civildigital.com,” [Online].

[83] “http://www.betterground.com,” Betterground Inc., 2017. [Online]. Available: http://www.betterground.com/en/vibro-compaction/.

[84] D'Appolonia, E., Miller Jr., C.E., & Ware, T.M., “Sand Compaction by Vibroflotation,” *Geotechnical and Environmental Engineering,* vol. 79, no. 200, pp. 1-23, 1953.

[85] J. MITCHEL, “Soil Improvement — State-of-the-Art Report,” in *10th ICSMFE*, Stockholm, 1981.

[86] J. Wiss, “Construction Vibrations :State of Art (ASCE),” vol. 107, no. 2, pp. 167-182, 1981.

[87] C. Dowding, Construction Vibrations, 2000, p. 610.

[88] A. Ghassemi, A.Pak and H. Shahir, “A Numerical Tool for Design of Dynamic Compaction Treatment in Dry and Moist Sand,” *Iranian Journal of Science and Technology , Transaction B, Engineering ,* vol. 33, no. Islamic Republic of Iran, pp. 313-326, 2009.

[89] P.O. Van Impe , W.F. Van Impe, A. Manzotti, M. Van den Broeck, K. Vinck, “Compaction control and related stress-strain behaviour of off-shore land reclamation with calcareous sand,” *Soils and Foundation, The Japanese Geotehnical Society,* pp. 1474 - 1486, 2014.

[90] Gray Mullins, Manjriker Gunaratne, Pamela Stinnette and Saman Thilakasiri, “Prediction of Dynamic Compaction Pounder Penetration,” *Soils and Foundations, Japanese Geotechnical Society ,* vol. 40, no. Oct. 2000, pp. 91-97, 2000.

[91] S.M. Mackiewicz , W.M. Camp, “Ground Modification : Howmuch improvement”.

[92] Massarsch,K.R., Westerberg, E., “The Active Design Concept Applied to Soil Compaction,” in *Symposium in Geotechnical Engineering*, Singapore, 1995.

[93] Jamiolkowski, M. Lo Presti, D.C.F. , Manassero, M., “Evaluation of Relative Density and Shear Strength of Sands from CPT and DMT,” ASCE Geotechnical Special Publication No119, 2001.

[94] K. Massarsch, “Effect of Vibratory Compaction,” in *Trans Vib 2002- International Conference on Vibratory Pile Driving and Deep Soil Compaction*, Louvain-la-Neuve, 2002.

[95] Bodare, A. and Orrje, O., “Impulse load on a circular surface in an infinite elastic body -Closed solution according to the theory of ealsticity .,” Royal Institute of Technology (KTH), Stockholm, Sweden, 1985.

A1. APPENDIX I: Analysis for Properties of Fill Material and Self-Compaction While Placing

A1.1 Summary of q_c values in Pre-compaction CPT

Pre-compaction CPTs carried out in reclaimed area has been plotted in a single graph to find the Average pre-compaction CPT as shown in Figure A- 1;

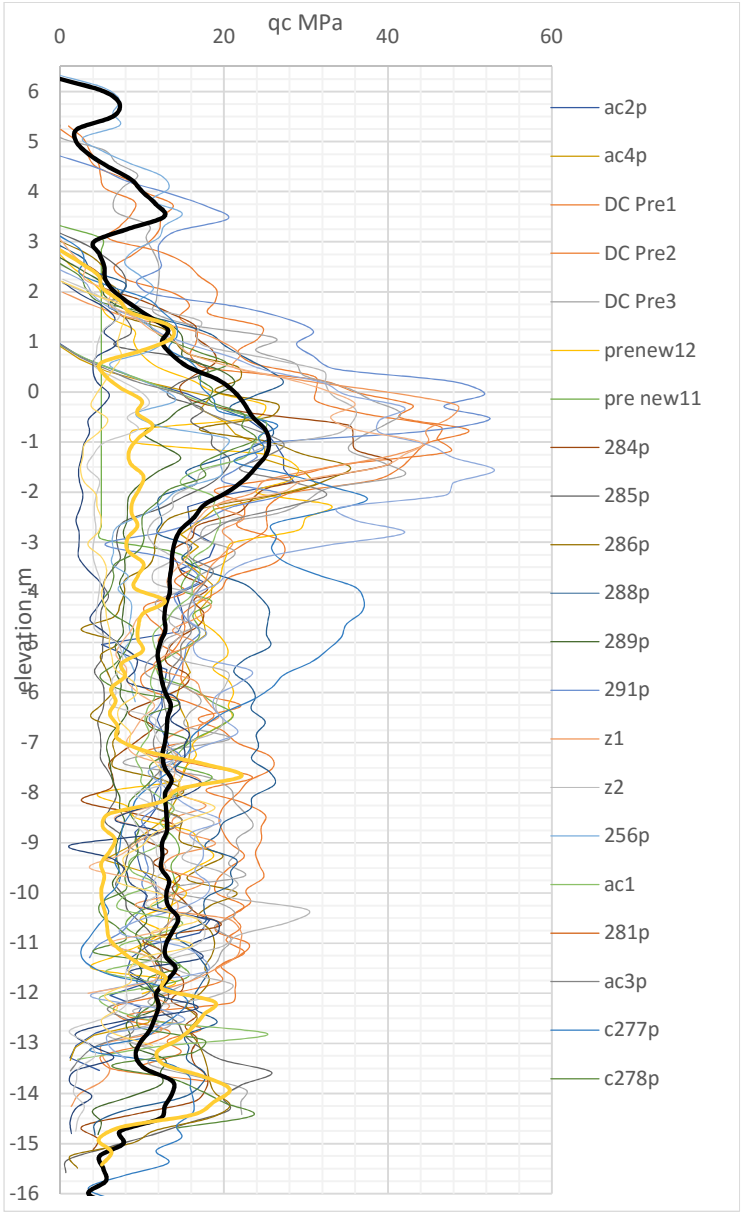

Figure A- 1: Pre-compaction CPT Results

A1.1. Variation of relative density by different methods

Relative Density (D_R) of fill material as estimated from q_c values in pre-compaction CPTs using three different methods are as follows;

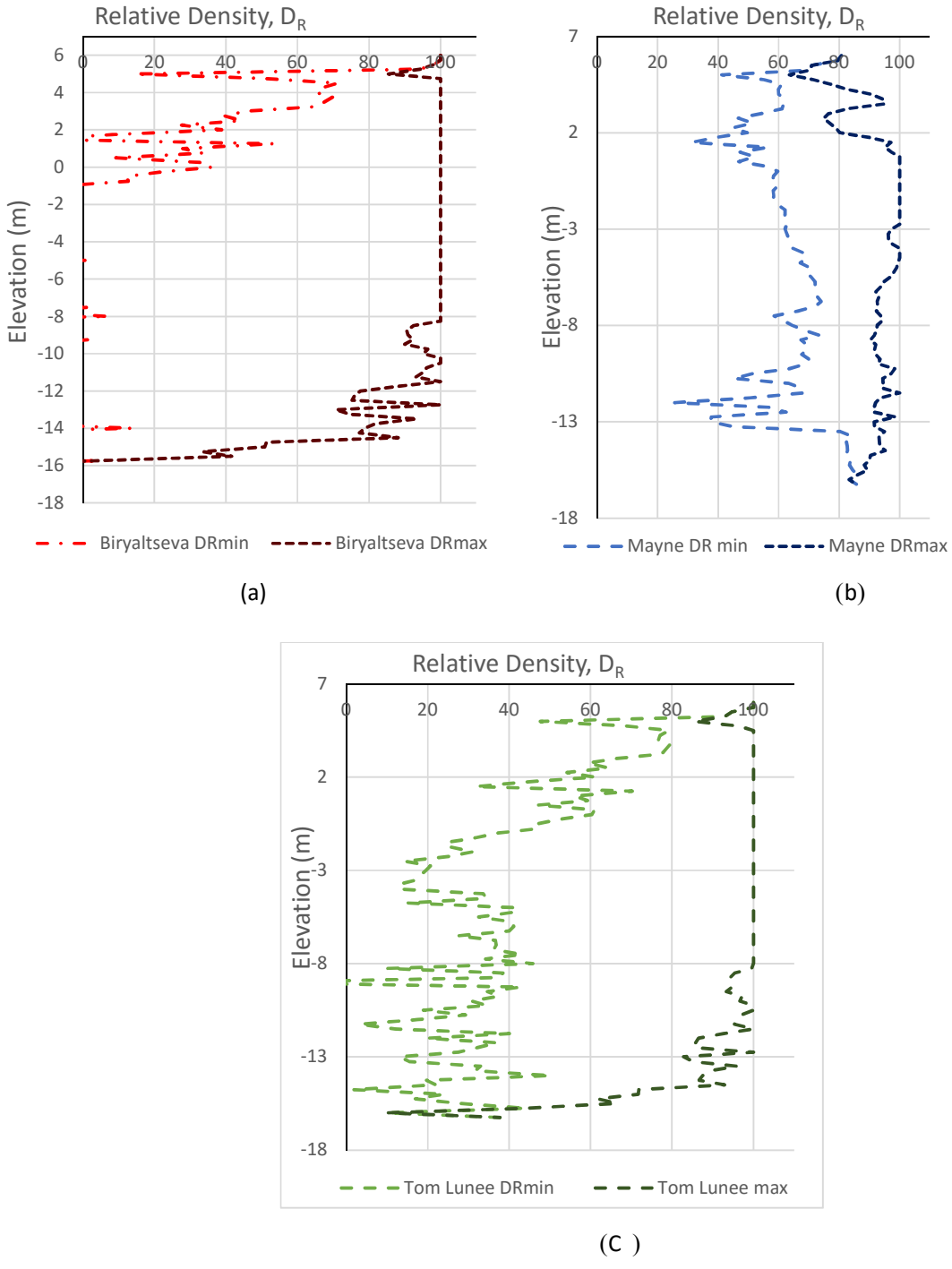

Figure A- 2: Variation of DR before compaction by (a) Biryaltseva method (b) Mayne method (c) Tom Lunee method

A2. APPENDIX II: Crater Depth Analysis

Increase of crater depth with dynamic compaction blows are as follows;

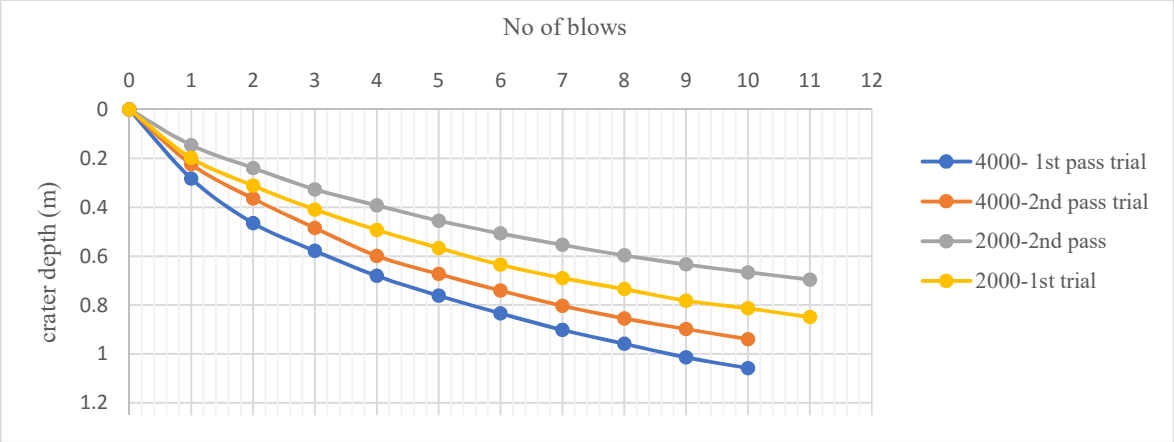

Figure A- 3: Cumulative crater depth variation with blow number

To identify the approximate linear variation as suggested by Mayne, normalized crater depth values were plotted against the √N separately for 2000kNm, 4000kNm and 1000kNm energies as follows. In this trial dynamic compaction area, filling material and self-compaction condition can be considered as almost the same.

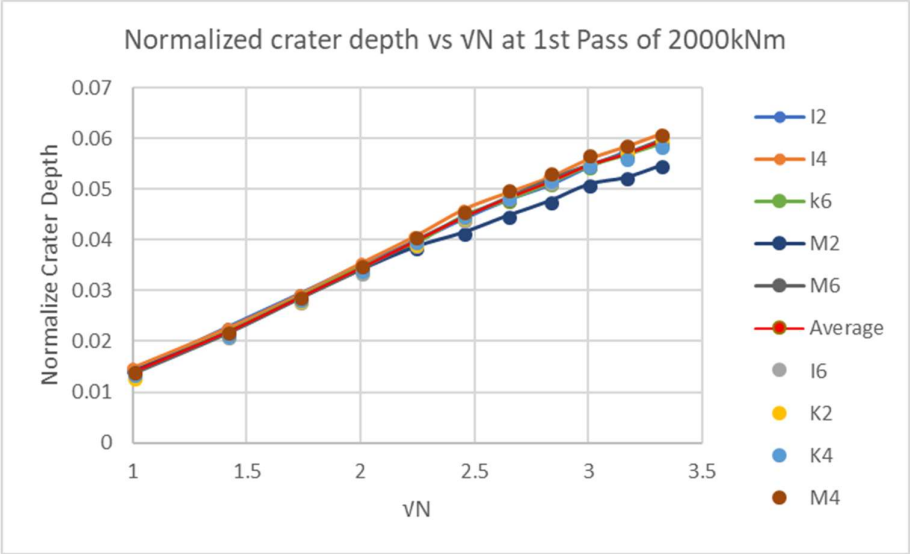

Figure A- 4: Normalized crater depth variation with square root of blow number in 1st pass of 2000kNm

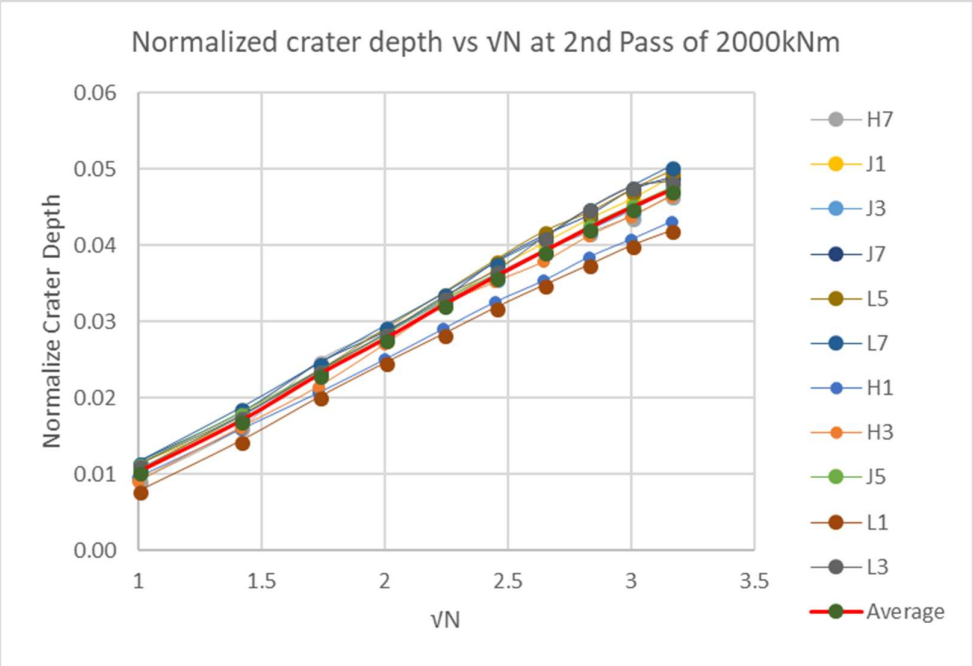

Figure A- 5: Normalized crater depth variation with square root of blow number in 2nd pass of 2000kNm

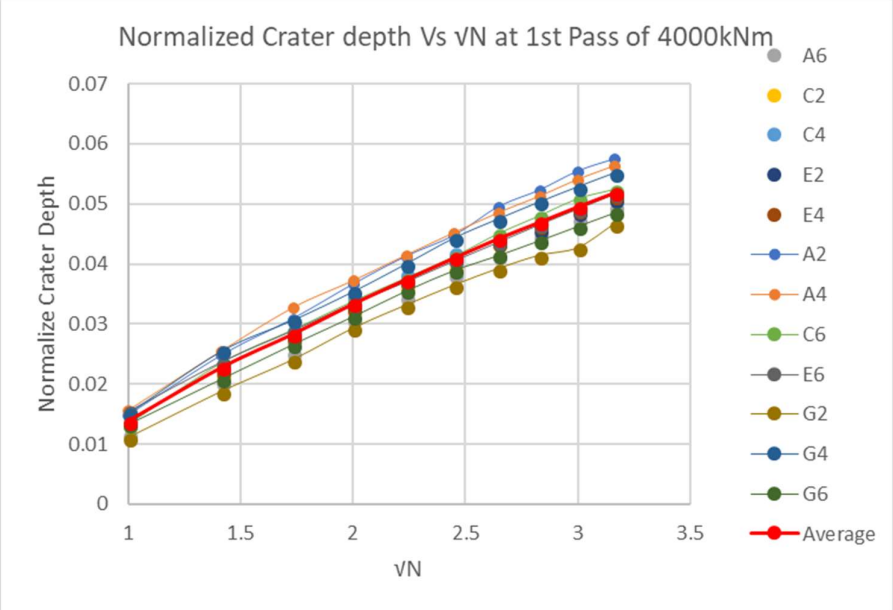

Figure A- 6: Normalized crater depth variation with square root of blow number in 1st pass of 4000kNm

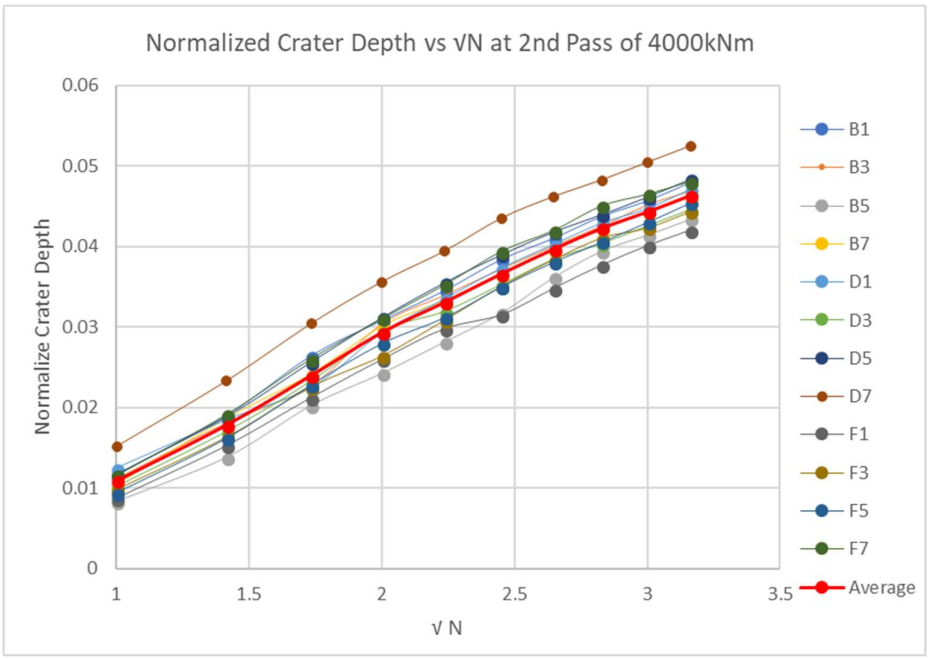

Figure A- 7: Normalized crater depth variation with square root of blow number in 2nd pass of 4000kNm

Average normalized crater depth at different energies and phases are shown as follows;

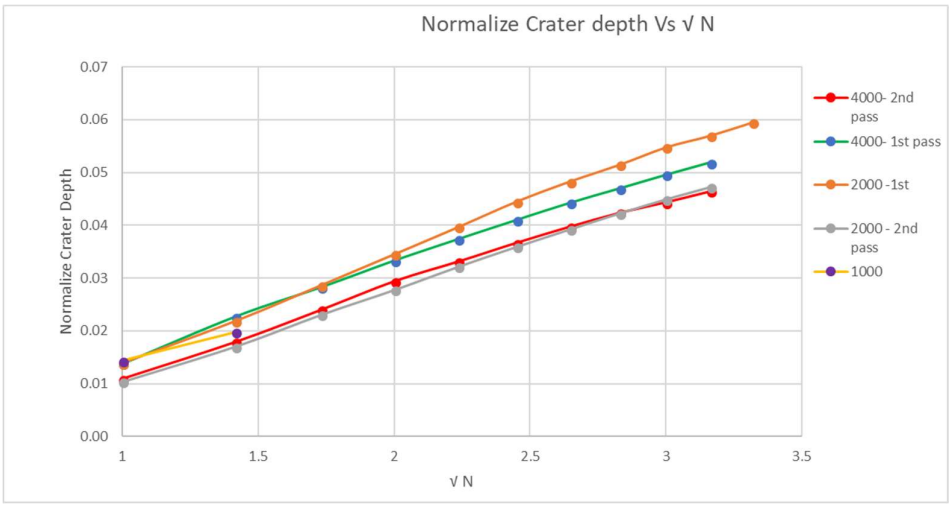

Figure A- 8: Average normalized crater depth Vs √N

A3. APPENDIX III: Net Volume Change Analysis at Dynamic Compaction Point

Crater, heave and net volume changes were assessed based on measured site data at randomly selected points in trial area with blow numbers for each pass of 4000kNm and 2000kNm dynamic compaction area as follows;

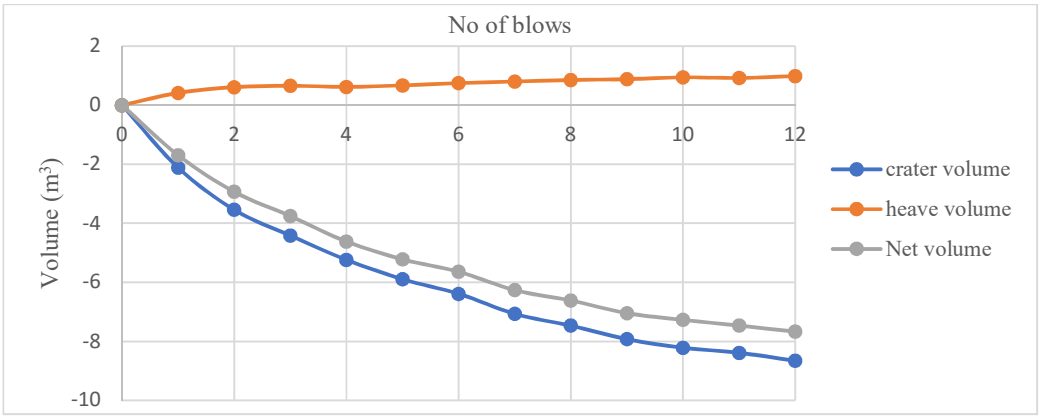

Figure A- 9: Crater, heave and net volume variation at A2 point in 4000kNm DC area for 1st pass

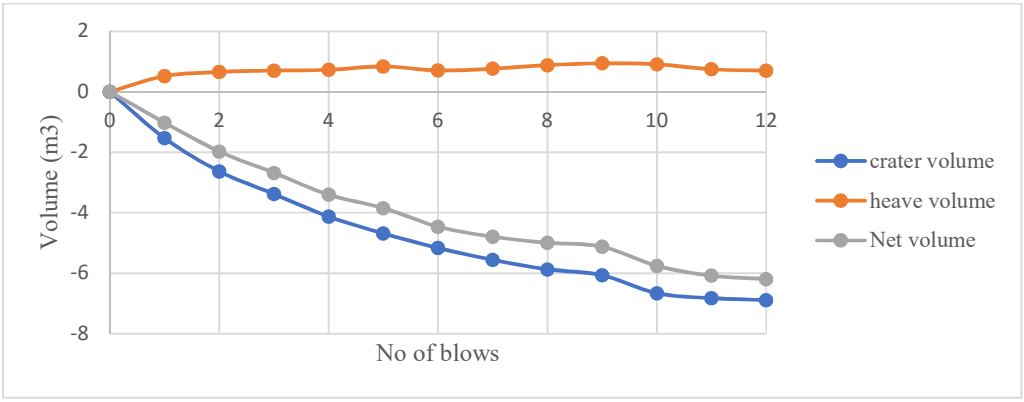

Figure A- 10: Crater, heave and net volume variation at G2 point in 4000kNm DC area for 1st pass

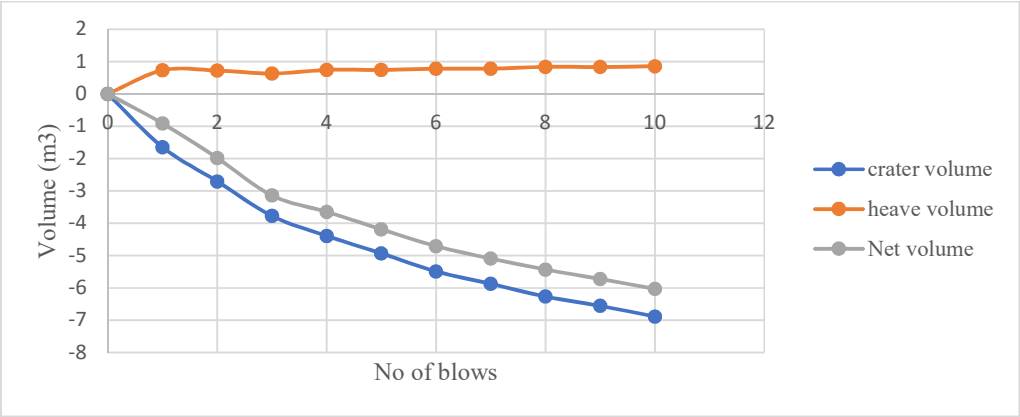

Figure A- 11: Crater, heave and net volume variation at B1 point in 4000kNm DC area for 2nd pass

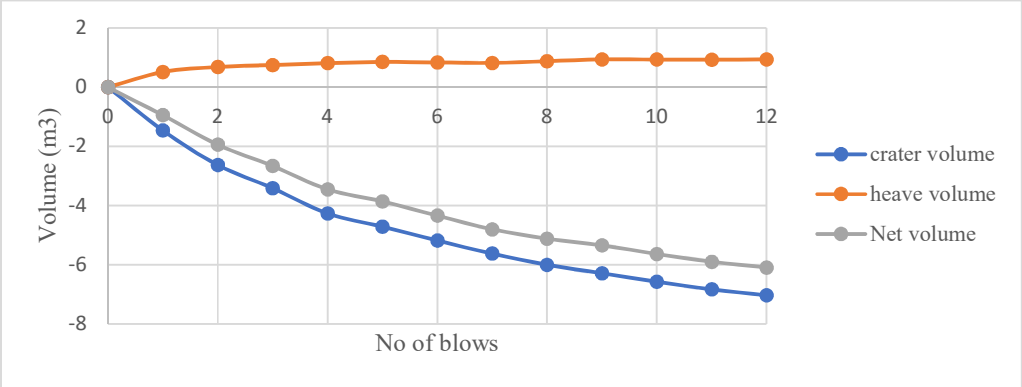

Figure A- 12: Crater, heave and net volume variation at B7 point in 4000kNm DC area for 2nd pass

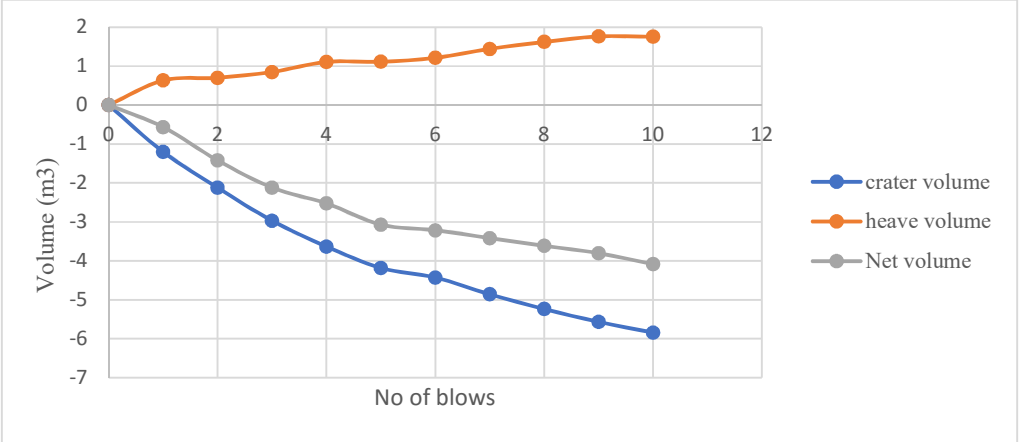

Figure A- 13: Crater, heave and net volume variation at F1 point in 4000kNm DC area for 2nd pass

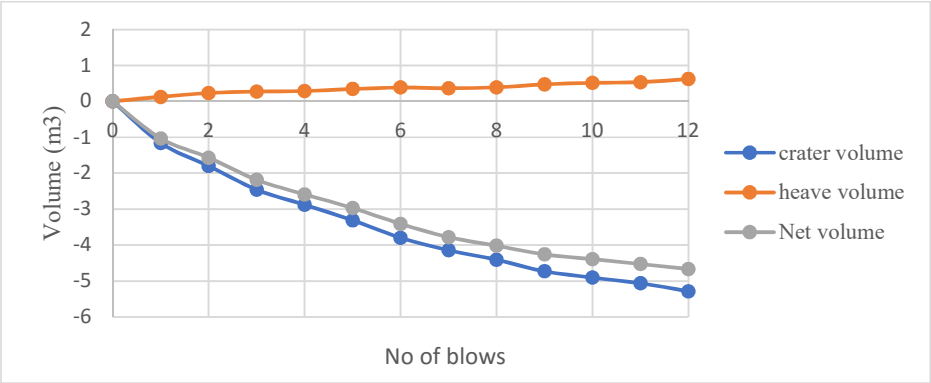

Figure A- 14: Crater, heave and net volume variation at J7 point in 4000kNm DC area for 2nd pass

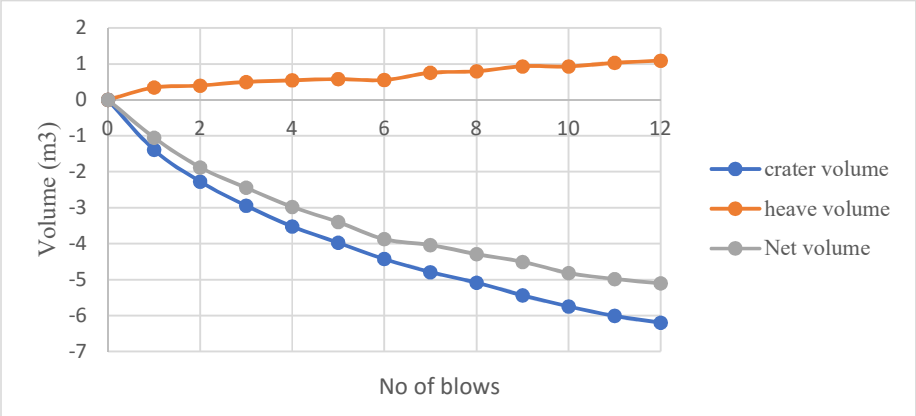

Figure A- 15: Crater, heave and net volume variation at I2 point in 2000kNm DC area for 1st pass

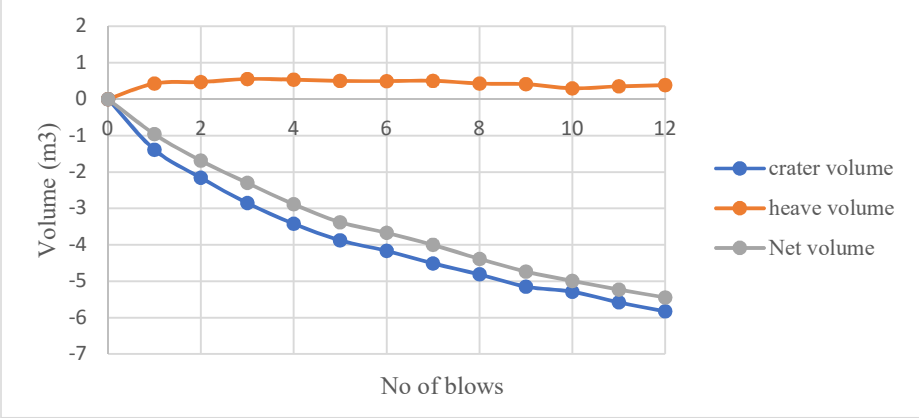

Figure A- 16: Crater, heave and net volume variation at M2 point in 2000kNm DC area for 1st pass

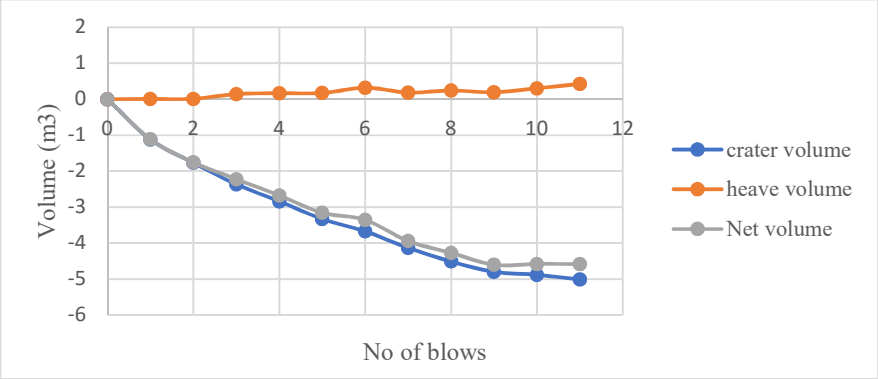

Figure A- 17: Crater, heave and net volume variation at L3 point in 2000kNm DC area for 2nd pass

Based on above data, average net volume data was estimated and which were plotted against blow numbers as follows;

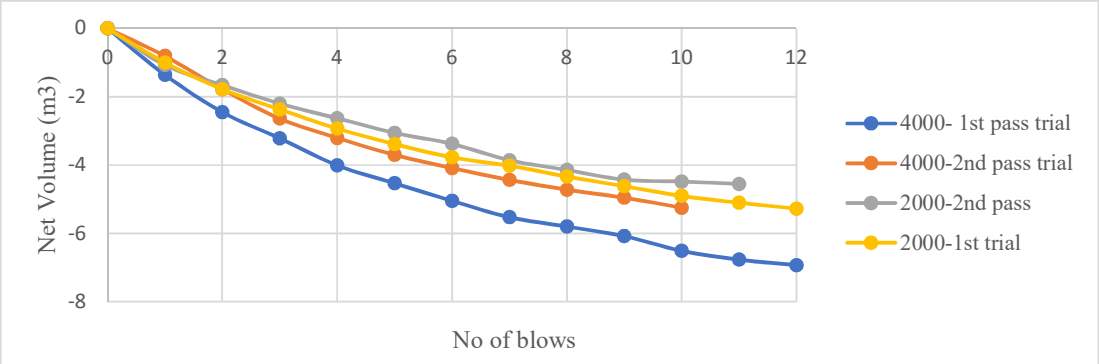

Figure A- 18: Average net volume variation

Accordingly, net volume increment in ground movement by DC is given by,

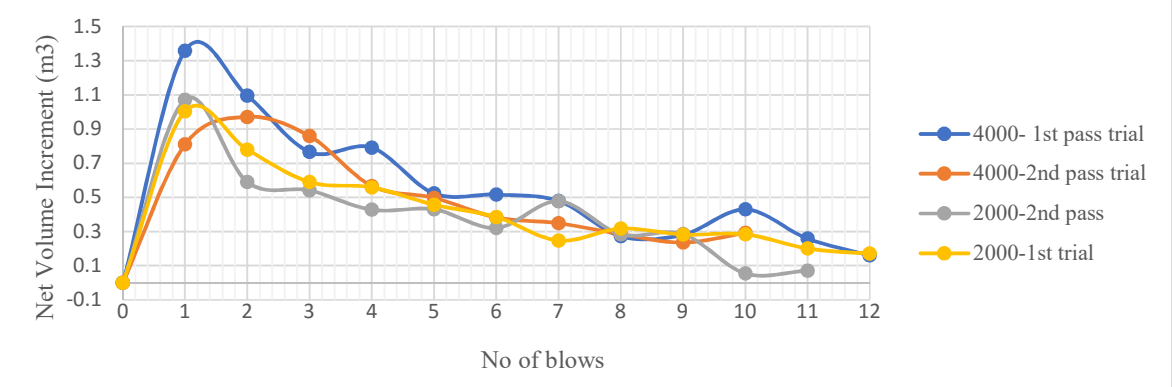

Figure A- 19: Net volume increment in ground movement by DC

A4 APPENDIX IV: Influence Depth and the Parameter "n" For Permanent DC Work

Influence depth calculated from CPT data in 4000kNm, 2000kNm and 1000kNm energy areas is as follows;

Table A- 1: Influence depth assessed from CPT results in 4000kNm energy applied area.

CPT No	Compaction Area	CPT location w.r.t DC point **	Influenced depth (m)	√WH	n
C37	A1-3	1	8.74	20.19	0.433
C38	A1-3	1	9.83	20.19	0.487
C39	A1-3	1	8.42	20.19	0.417
C40	A1-3	1	7.69	20.19	0.381
C44	A1-3	1	9.42	20.19	0.467
C52	A1-3	1	8.25	20.19	0.409
C73	A1-3	1	7.94	20.19	0.393
C73.1	A1-3	1	7.81	20.19	0.387
C74	A1-3	1	6.91	20.19	0.342
C85	A1-3	1	6.81	20.19	0.337
C144	A1-5		8.84	20.19	0.438
C315	A2-1	1	9.81	20.19	0.486
C319	A2-1	1	9.28	20.19	0.460
C320	A2-1	1	9.49	20.19	0.470
C321	A2-1	1	7.58	20.19	0.375
C322	A2-1	1	9.47	20.19	0.469
C323	A2-1	1	6.90	20.19	0.342
C326	A2-1	1	9.21	20.19	0.456
C332	A2-1		6.78	20.19	0.336
			8.47		**0.419**

Note **

1. Mid of four compaction points (Centroid)
2. Centre the compaction point
3. 1m away from the centre of compaction point
4. Centre of the two points

Table A- 2*:* Influence depth assessed from CPT results in 2000kNm energy applied area.

CPT No	DC area	CPT location w.r.t DC point **	Influenced depth, (m)	√WH	n
C19.1	A1-1	2	7.67	14.278	0.537
C20	A1-1	3	6.65	14.278	0.466
C21	A1-1	3	7.24	14.278	0.507
C22	A1-1	3	6.94	14.278	0.486
C23	A1-1	3	7.85	14.278	0.550
C24	A1-1	3	5.91	14.278	0.414
C25	A1-1	3	5.18	14.278	0.363
C28	A1-1	3	8.15	14.278	0.571
C29.2	A1-1	1	6.50	14.278	0.455
C30	A1-1	3	4.92	14.278	0.345
C31	A1-1	3	5.73	14.278	0.401
C32	A1-1	4	6.30	14.278	0.441
C35	A1-1	2	6.29	14.278	0.441
C36	A1-1	1	6.97	14.278	0.488
C41	A1-3	4	7.04	14.278	0.493
C42	A1-3	3	7.29	14.278	0.511
C43	A1-3	4	4.82	14.278	0.338
C45	A1-3	1	6.67	14.278	0.467
C46	A1-3	1	7.24	14.278	0.507
C47.2	A1-3	4	6.45	14.278	0.452
C49	A1-3	1	7.27	14.278	0.509
C50	A1-3	1	8.74	14.278	0.612
C51	A1-3	4	7.36	14.278	0.515
C53	A1-3	1	7.02	14.278	0.492
C54	A1-3	4	5.88	14.278	0.412
C55	A1-3	4	7.08	14.278	0.496
C58	A1-3	1	6.83	14.278	0.478
C59	A1-3	1	6.89	14.278	0.483
C62	A1-3	1	6.34	14.278	0.444
C63.1	A1-3		8.42	14.278	0.590
C69	A1-3	1	6.38	14.278	0.447
C70.2	A1-3		7.22	14.278	0.506
C77.2	A1-3	1	6.01	14.278	0.421
C78	A1-3	1	6.57	14.278	0.460
C81	A1-3	1	5.99	14.278	0.420
C82	A1-3	4	7.17	14.278	0.502
C83	A1-3	1	5.95	14.278	0.417
C86	A1-3	1	6.43	14.278	0.450
C89	A1-3	3	5.05	14.278	0.354
C134	A1-5	1	6.13	14.278	0.429

Table A-2: Influence depth assessed from CPT results in 2000kNm energy applied area (Contd...)

CPT No	DC area	CPT location w.r.t DC point **	Influenced depth, (m)	√WH	n
C135	A1-5	1	7.87	14.278	0.551
C142	A1-5	1	7.87	14.278	0.551
C143	A1-5	1	8.15	14.278	0.571
C316	A2-1	1	7.64	14.278	0.535
C317	A2-1	1	8.92	14.278	0.625
C318	A2-1	1	6.78	14.278	0.475
C324	A2-1	1	8.10	14.278	0.567
C327	A2-1	1	8.69	14.278	0.609
C328	A2-1	1	6.93	14.278	0.485
C329	A2-1	1	6.08	14.278	0.426
C330	A2-1	1	7.50	14.278	0.525
C333	A2-1	1	6.79	14.278	0.476
C334	A2-1	1	7.62	14.278	0.534
C335	A2-1	1	6.85	14.278	0.480
C336	A2-1	1	5.87	14.278	0.411
C339	A2-1	1	5.64	14.278	0.395
C342	A2-1	1	7.40	14.278	0.518
			6.85		**0.480**

A5 Appendix V: Evaluation of Vibro Compaction

A5.1 Trial VC Compaction

The typical amperage usage in surrounding vibro compaction points related to values related to Vibro compaction at 3.9m (TA), 4.2m (TB) and 4.5m (TC) spacing are given below;

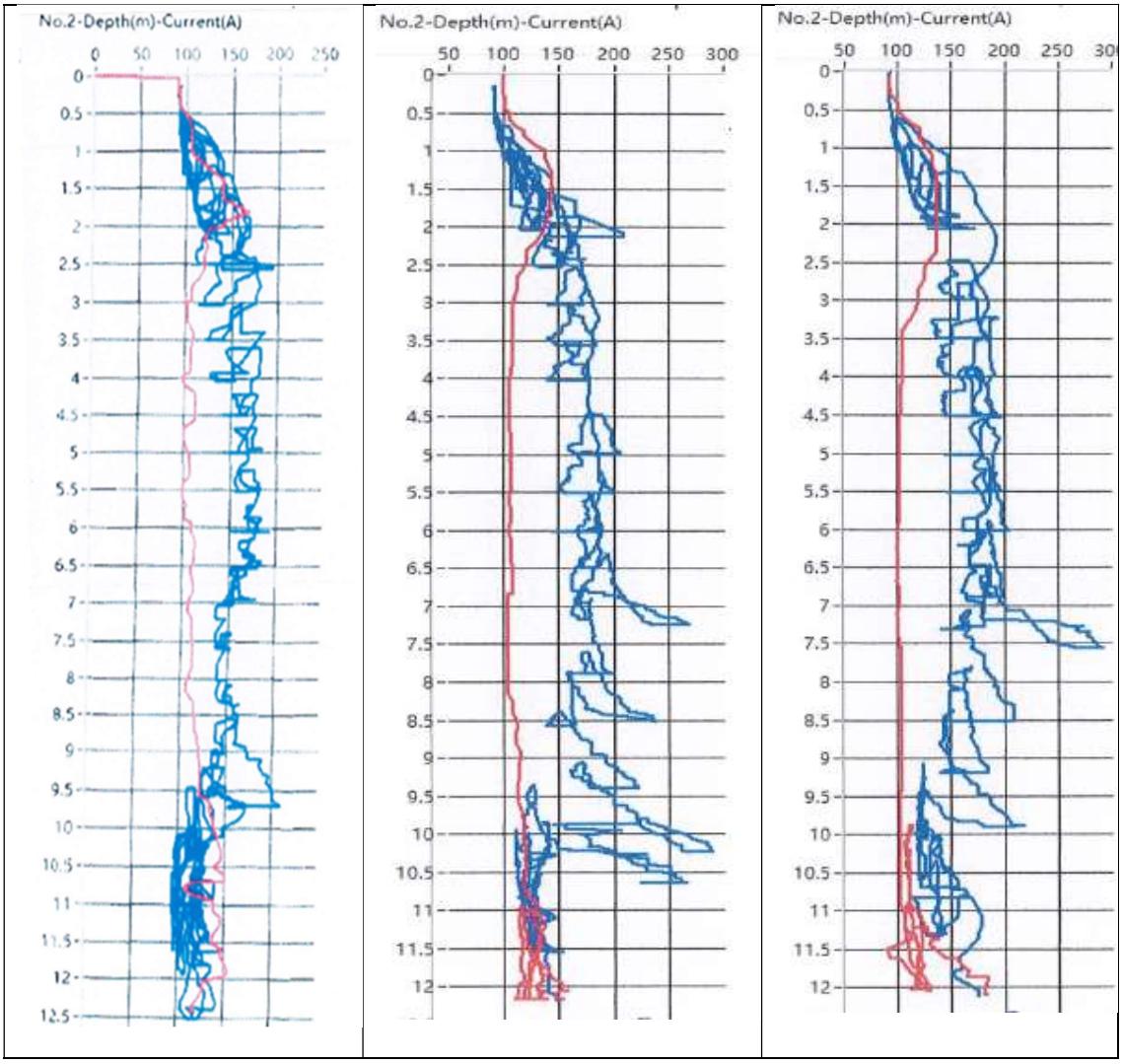

At 3.9m spacing **At 4.2m spacing** **(c) At 4.5m spacing**

Figure A- 20: Typical Amperage usage in nearest VC points

A5.2 Evaluation of Compaction (qc) at Centroid of Three Surrounding Compaction Points with Respect to the Amperage Applied

Variation of compaction (qc values) were evaluated with applied amperage in different elevation of the sand densified depth and plotted below from Figure A- 21 to Figure A- 29**Error! Reference source not found.**;

a. VC at C93

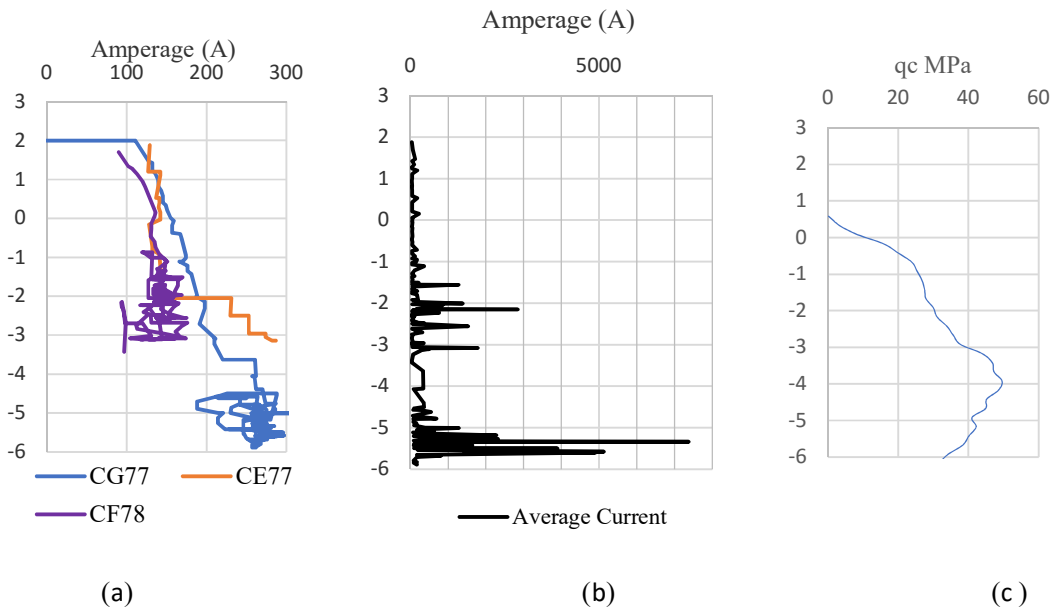

Figure A- 21: (a) Applied amperage (b) Applied average cumulative amperage at each elevation (c) qc variation in the depth at C93

b. VC at C95

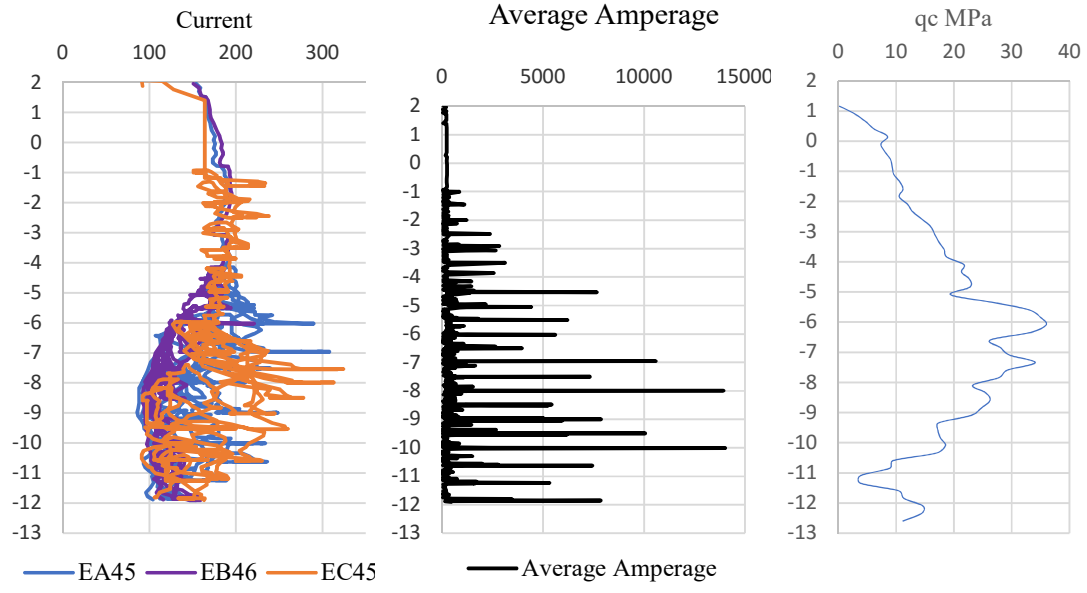

Figure A- 22:(a) Applied amperage (b) Applied average cumulative amperage at each elevation (c) qc variation in the depth at C95

c. VC at C97

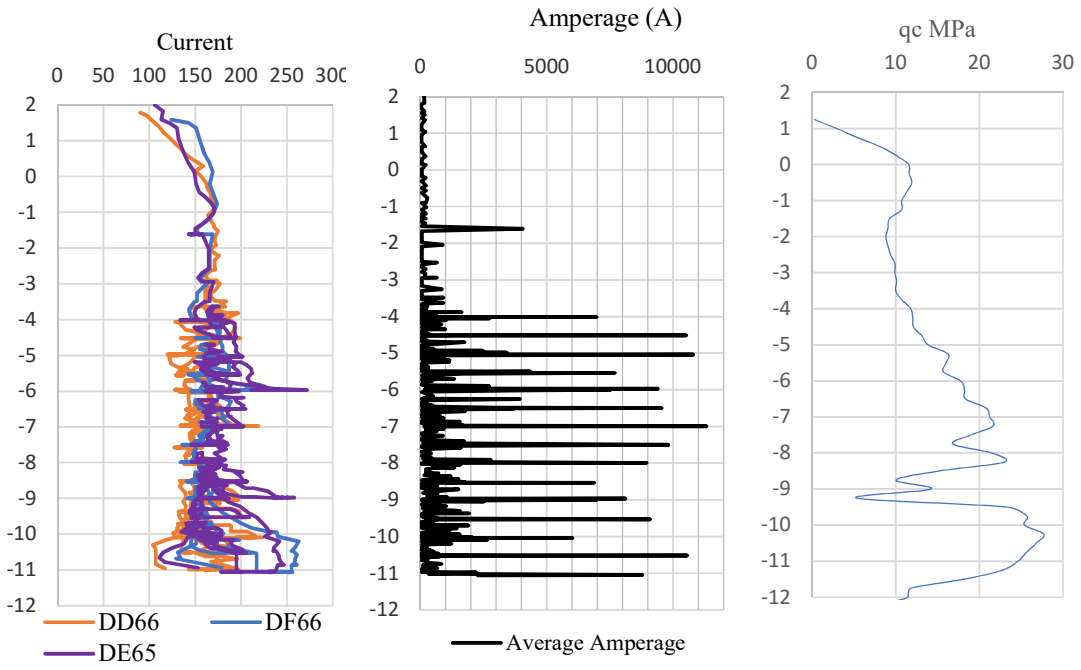

Figure A- 23: (a) Applied amperage (b) Applied average cumulative amperage at each elevation (c) qc variation in the depth at C97

d. VC at C102

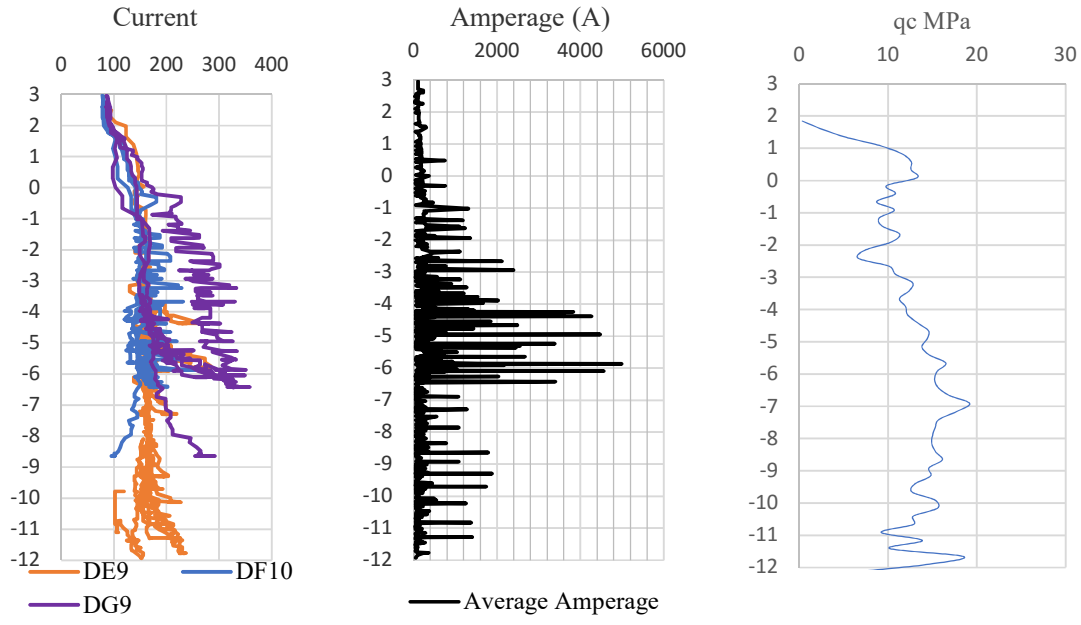

Figure A- 24: (a) Applied amperage (b) Applied average cumulative amperage at each elevation (c) qc variation in the depth at C102

e. AC6

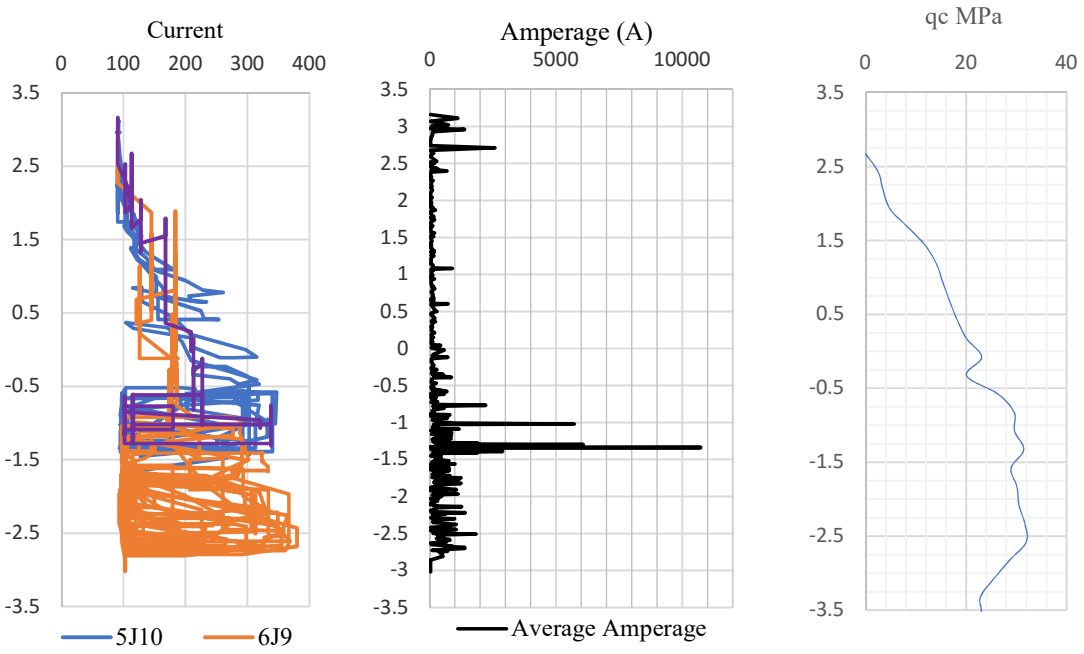

Figure A- 25: (a) Applied amperage (b) Applied average cumulative amperage at each elevation (c) qc variation in the depth at AC6

f. AC29

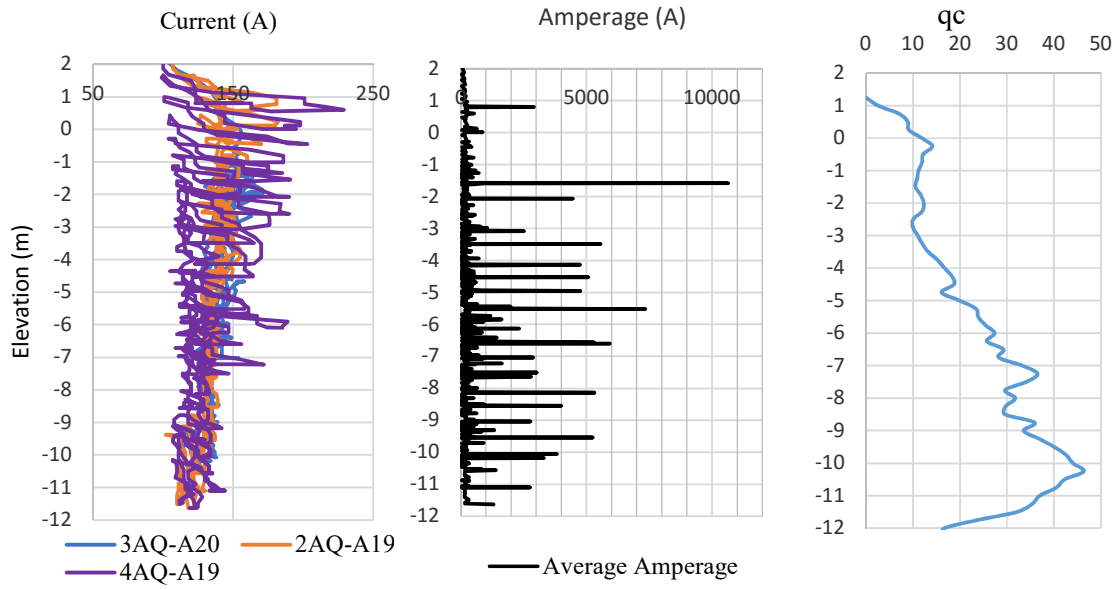

Figure A- 26: a) Applied amperage (b) Applied average cumulative amperage at each elevation (c) qc variation in the depth at AC29

g. VC at AC30

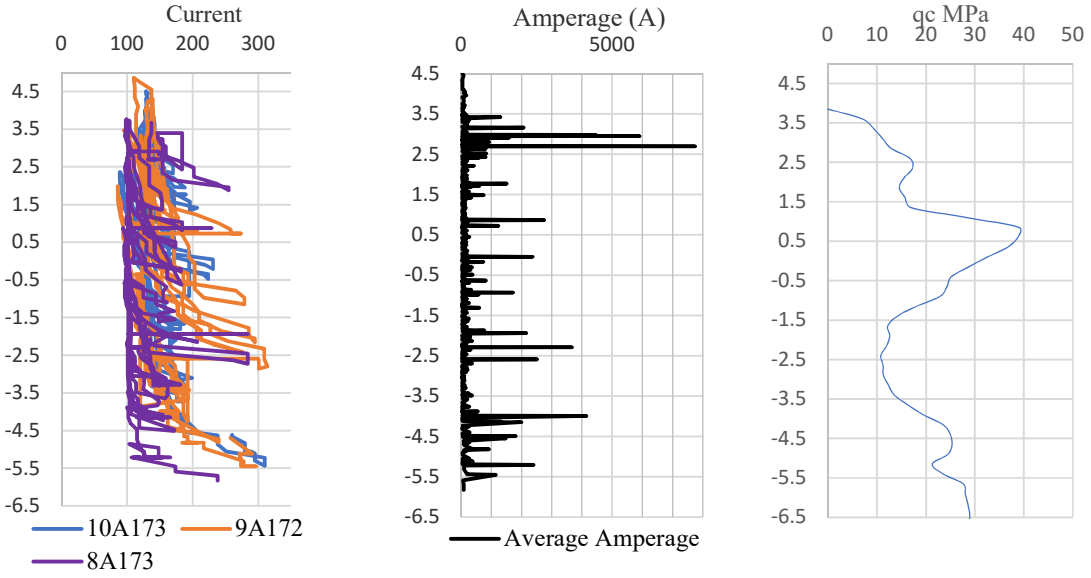

Figure A- 27: a) Applied amperage (b) Applied average cumulative amperage at each elevation (c) qc variation in the depth at AC30

h. C384

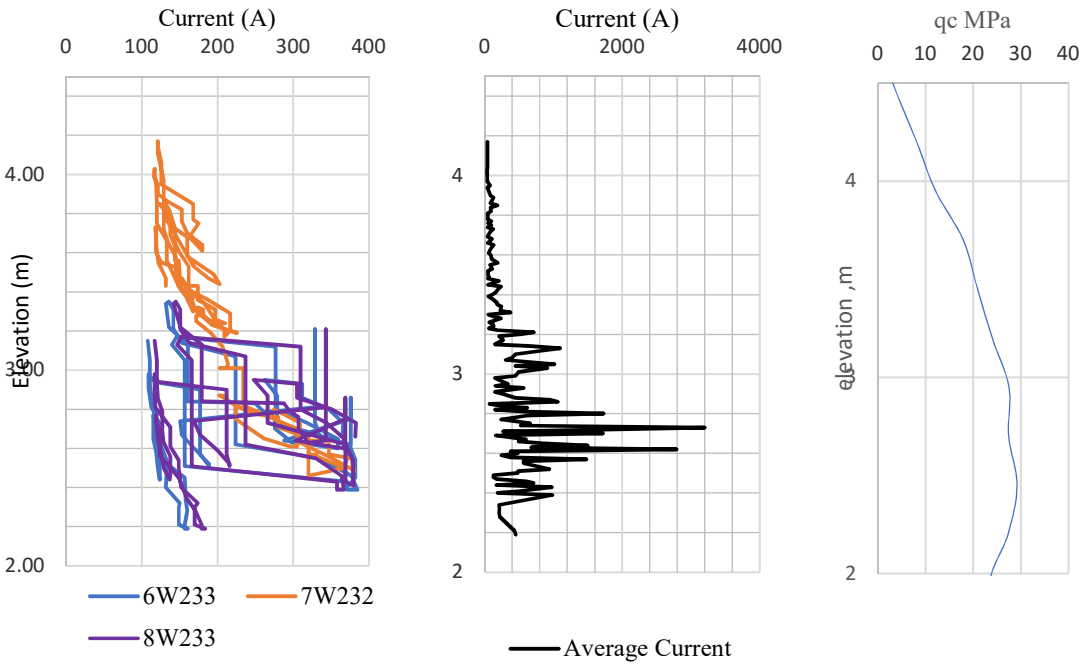

Figure A- 28: a) Applied amperage (b) Applied average cumulative amperage at each elevation (c) qc variation in the depth at AC384

i. C386

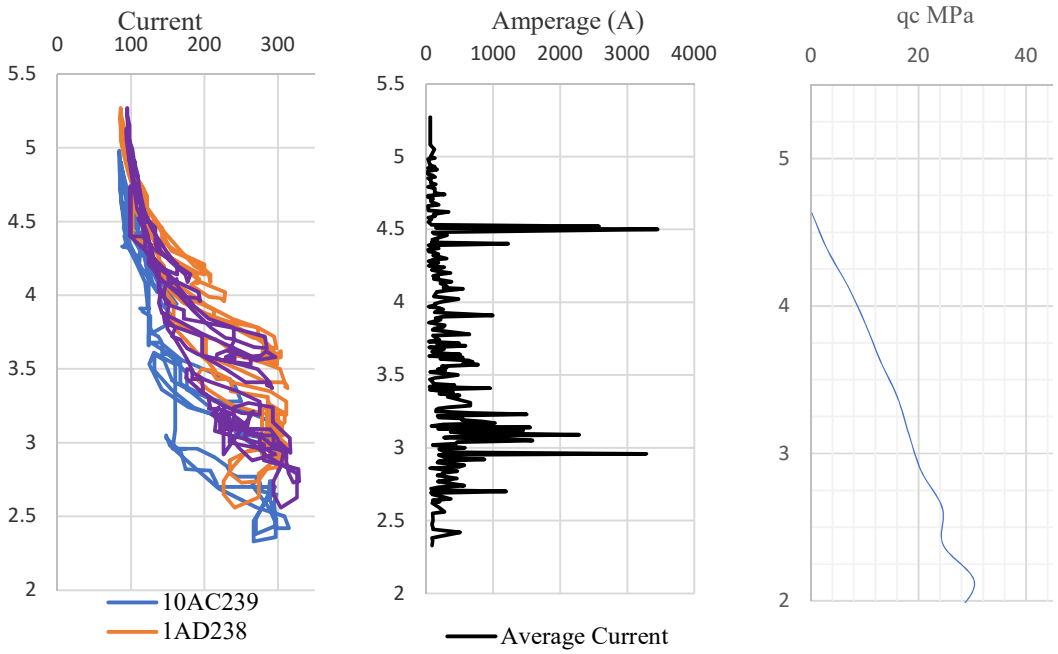

Figure A- 29: a) Applied amperage (b) Applied average cumulative amperage at each elevation (c) qc variation in the depth at AC386

A6 APPENDIX VI: Cone Resistance (qc) Variation at Different Locations with Respect to the Compaction Point

A6.1 In 2000kNm dynamic compaction area

a. Values of q_c of CPT's conducted at the Centroid of four DC points

By following the conventional way, most of CPTs in this project too, were advanced at the centroid of the four points and all q_c curves of them have been plotted in the same graph shown in Figure A- 30 along with its average curve.

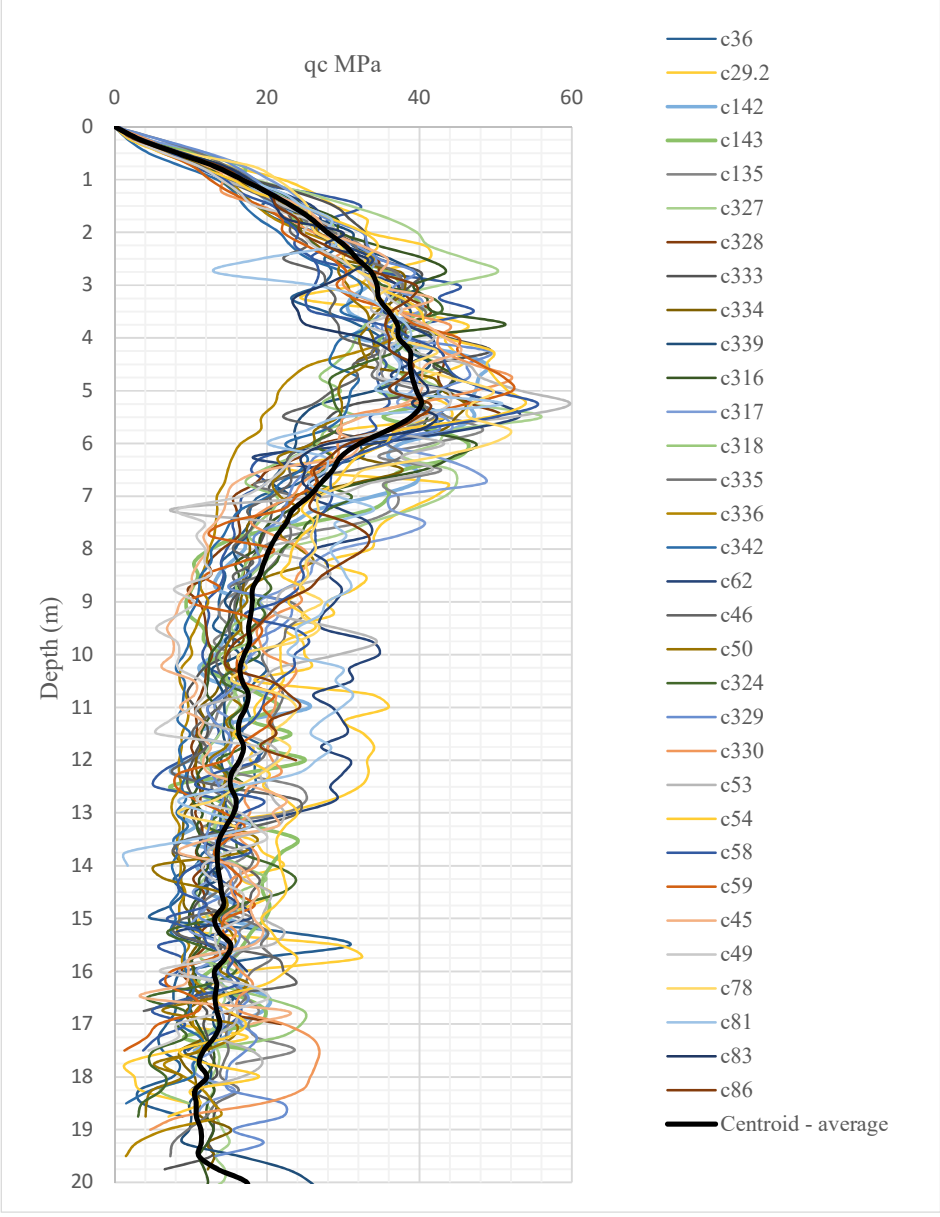

Figure A- 30: Average qc at centroid w.r.t compaction point in 2000kNm DC Area

b. The value of q_c of CPT's conducted at the Centre of DC points

Similarly, q_c curves related to CPTs conducted at middle of the compaction point was plotted in Figure A- 31 along with its average.

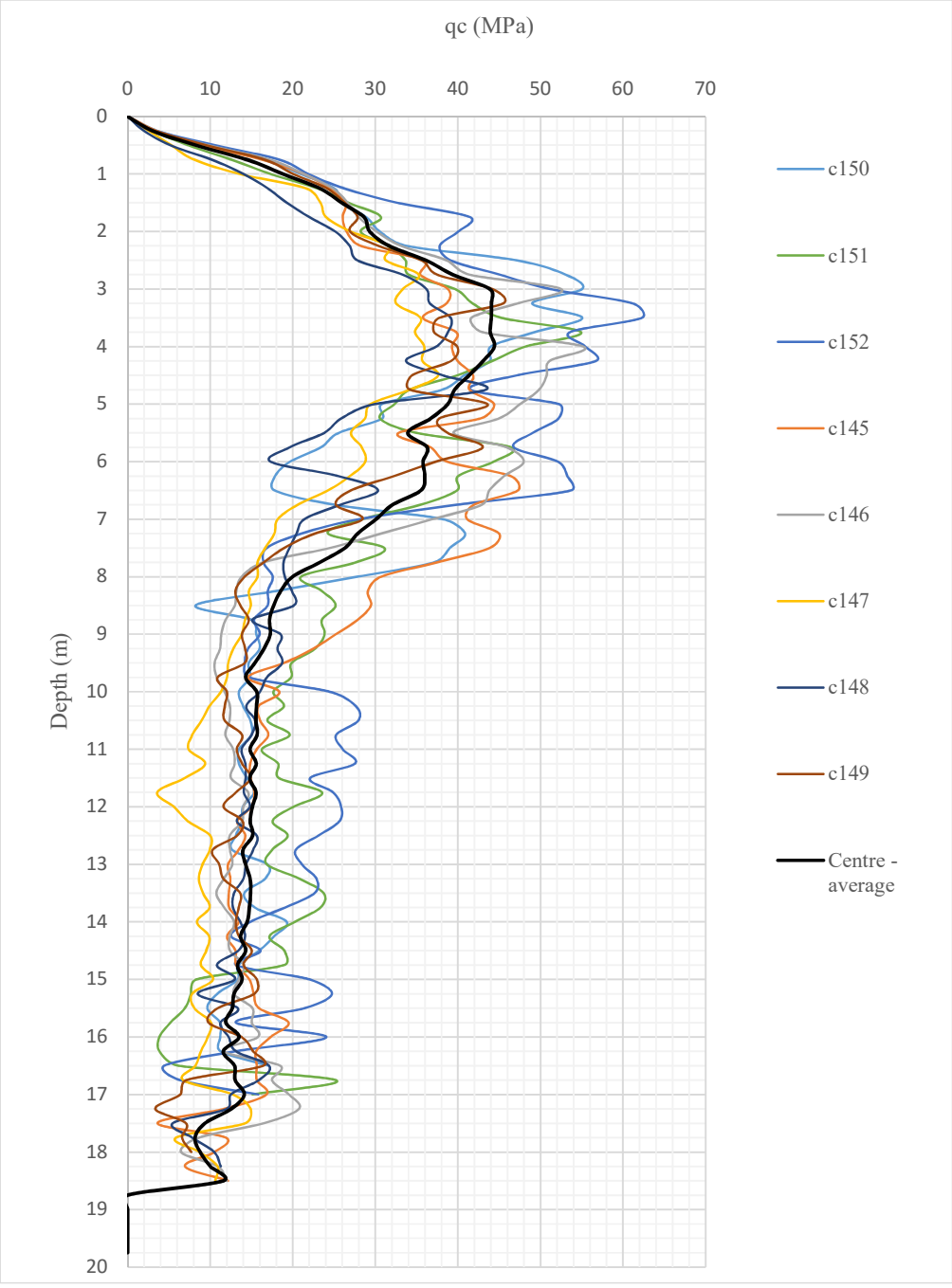

Figure A- 31: Average qc at centre w.r.t to compaction points in 2000 DC area

c. The values of q_c of CPT's conducted at 1m away from the Centre of DC points

The value of q_c curves at 1m away from DC points with average q_c curves have been plotted as shown in Figure A- 32.

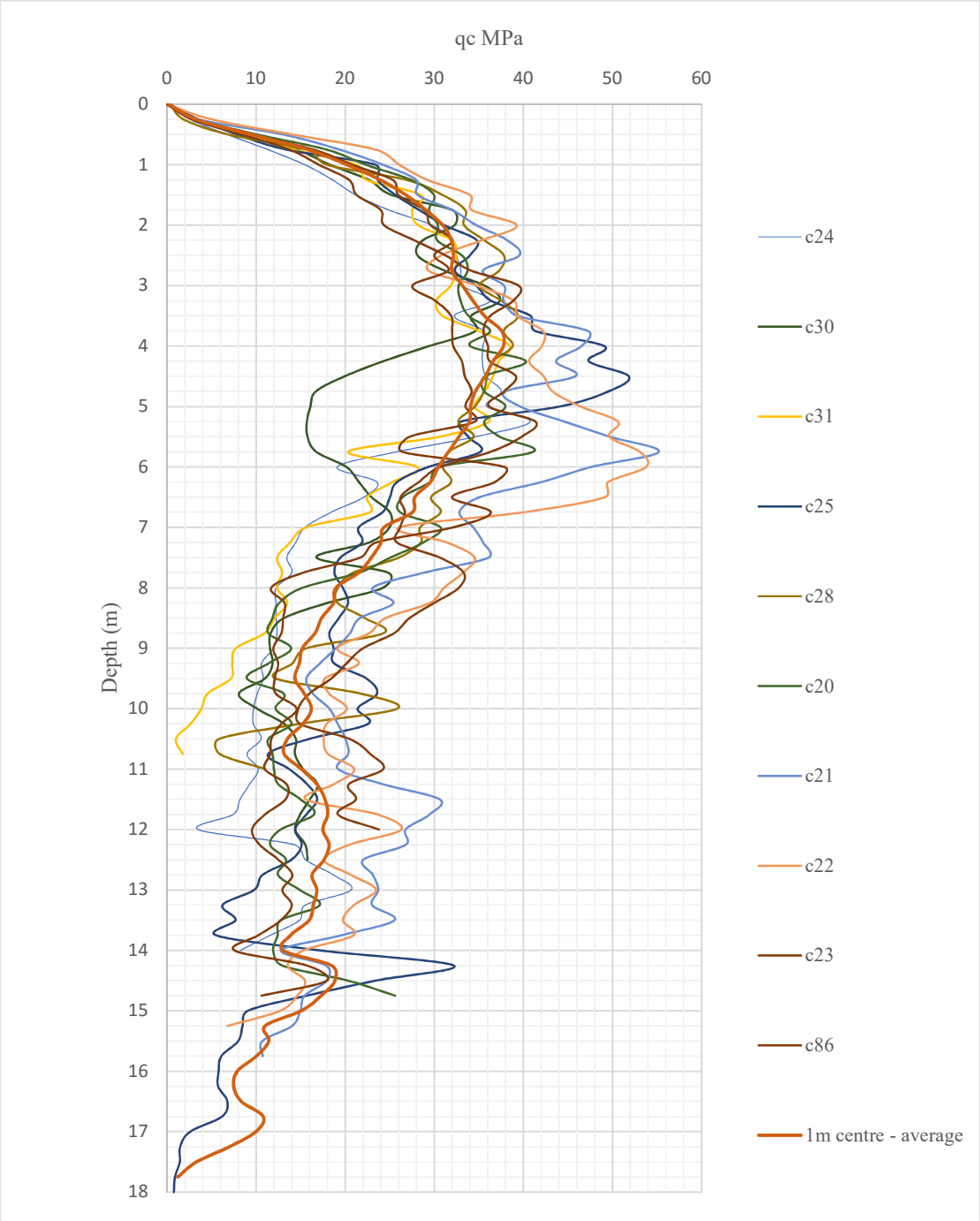

Figure A- 32: qc curves at 1m away from DC points.

d. The values of q_c of CPT's conducted at the midpoint between two DC points

The value of q_c at midpoint between two DC points with its average curve is shown in Figure A- 33.

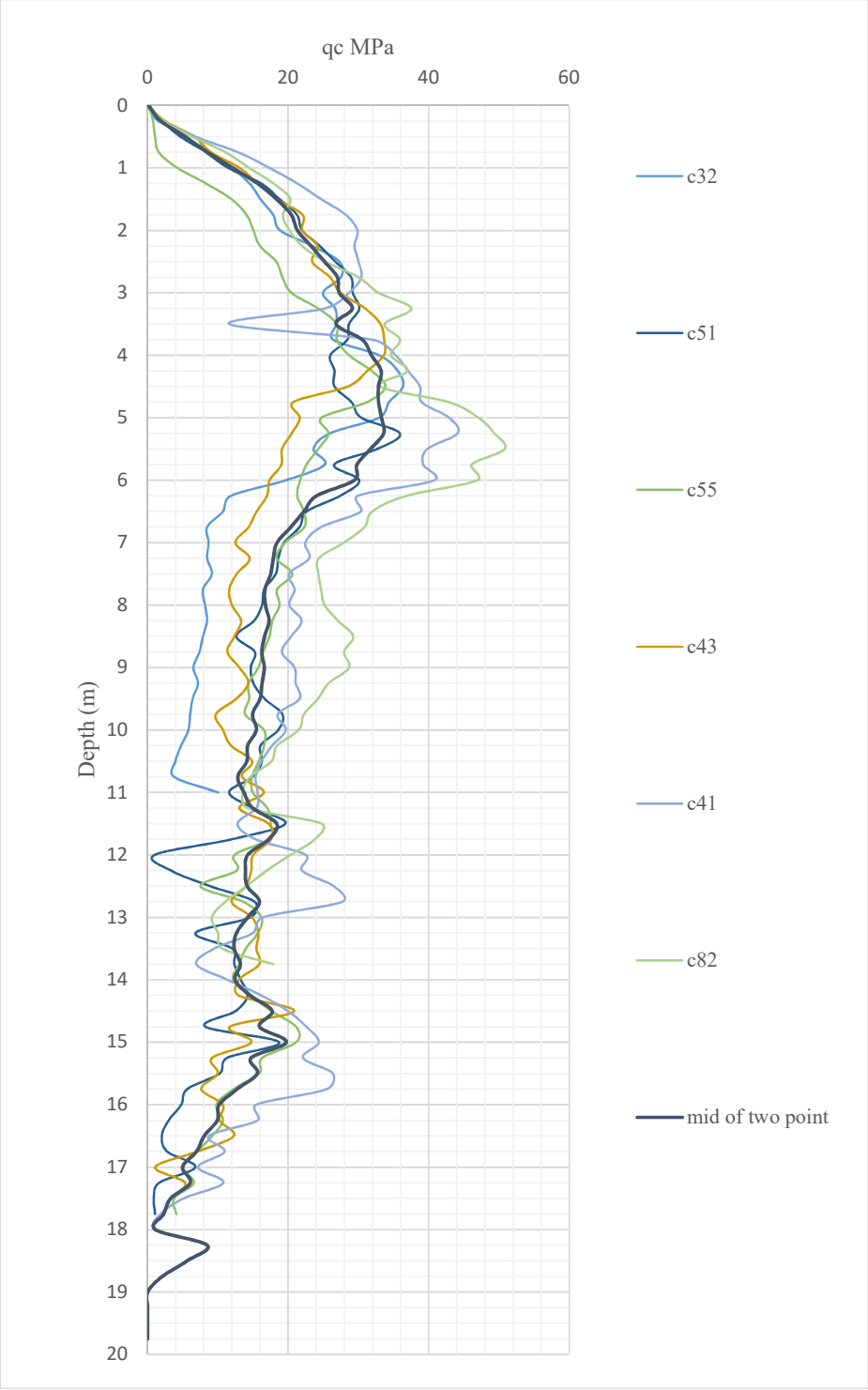

Figure A- 33: q_c curve at mid of two 2000kNm DC point

A6.2 In 4000kNm- dynamic compaction area

e. The qc values of CPT conducted at centroid of four compaction points

qc values of CPT conducted at centroid of four compaction points in the area compacted by 4000kNm of dynamic compaction were plotted along with its average curve in Figure A- 34.

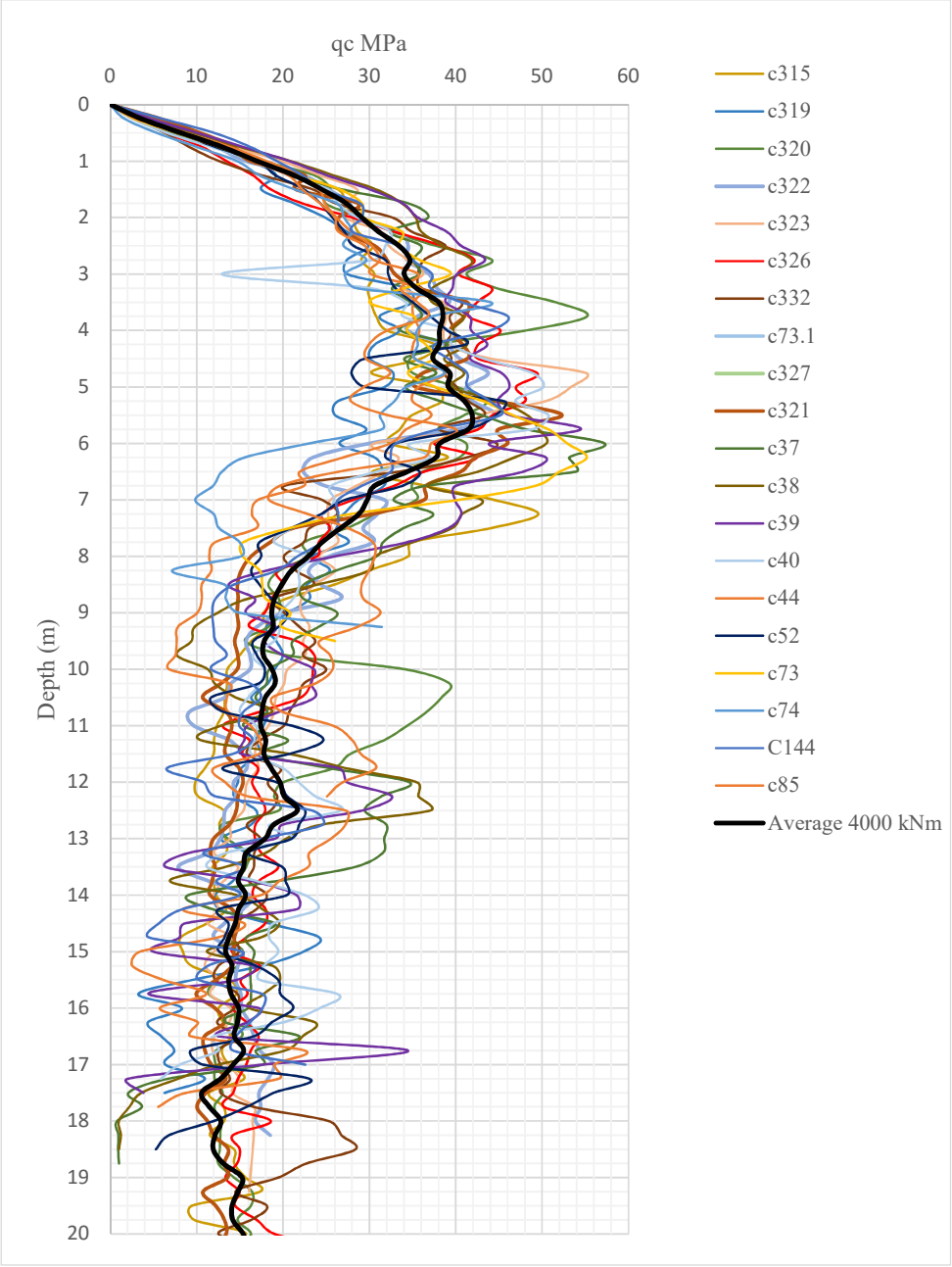

Figure A- 34: qc at centroid w.r.t. compaction points in 4000kNm DC area

A6.3 In vibro compaction area

j. Centroid of three surrounding vibro compaction points

As conventional way, in vibro compaction area of this project, most of CPTs were advanced at the centroid of the four points and all q_c curves of them have been plotted in the same graph shown in Figure A- 35 along with its average curve.

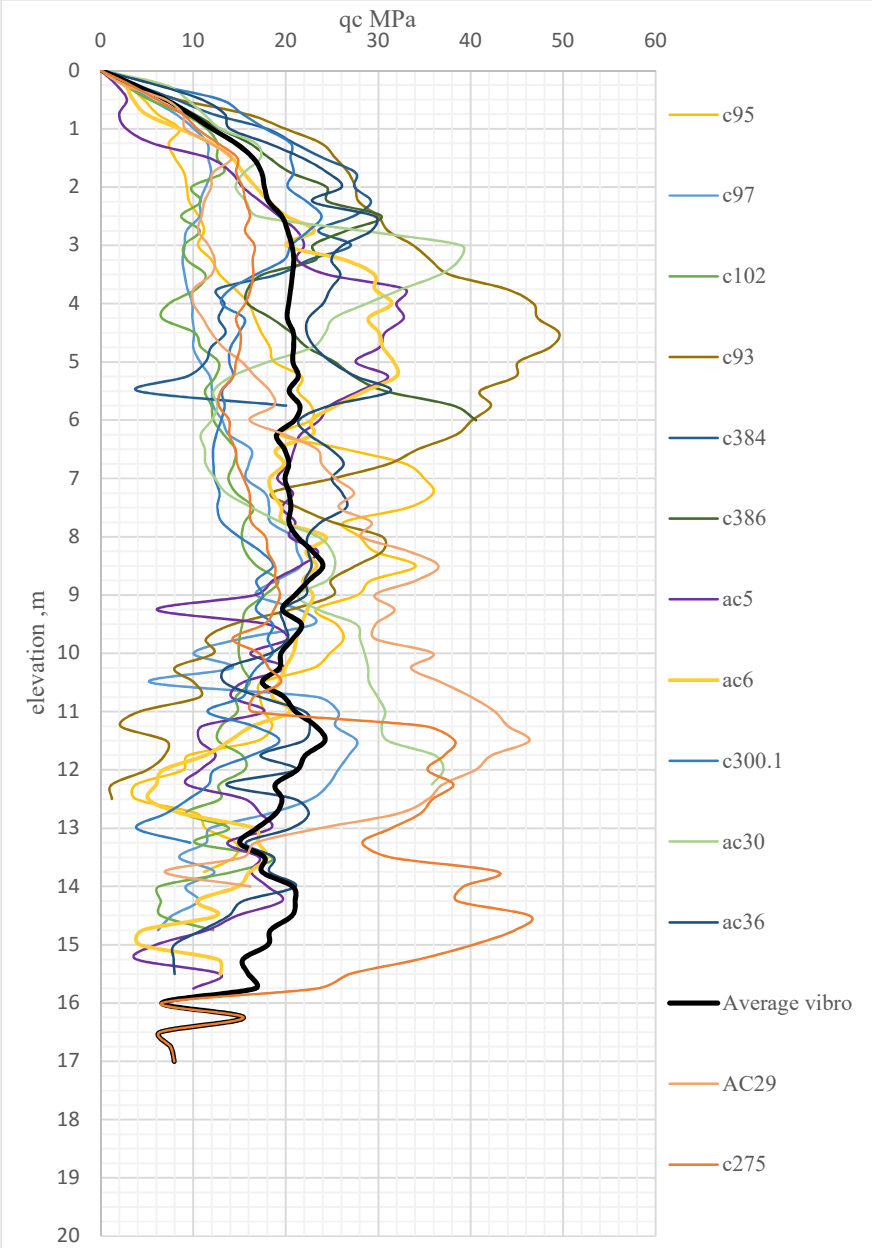

Figure A- 35: qc variation at centroid w.r.t. the VC points

b. Midpoint between two consecutive compaction points

qc values of CPT conducted at mid of two compaction points in the vibro compaction area were plotted along with its average curve in Figure A- 36;

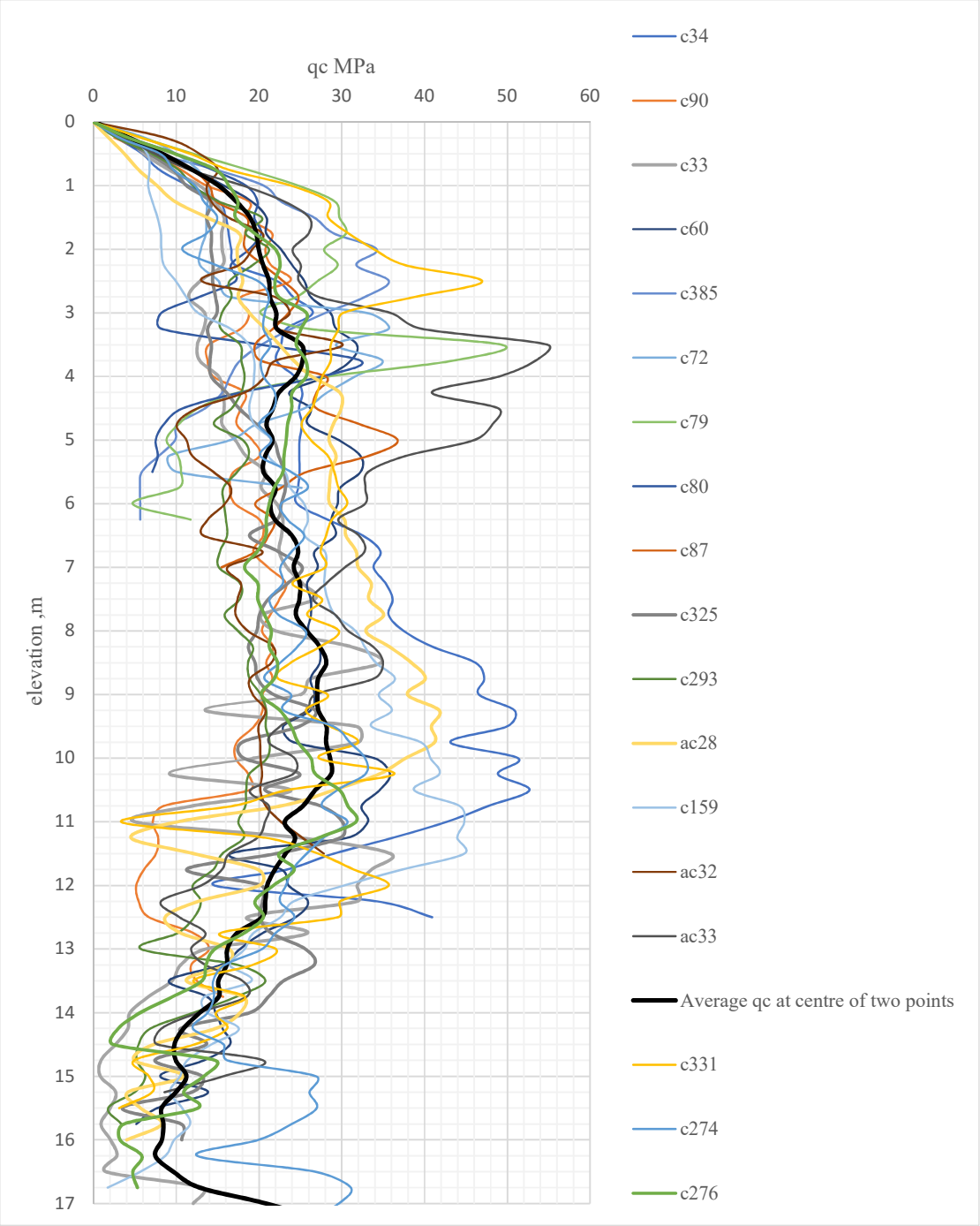

Figure A- 36: qc at mid of two VC points

c. Centre of the compaction

q_c curves of CPT conducted at centre of the compaction points are plotted along with its average curve in Figure A- 37;

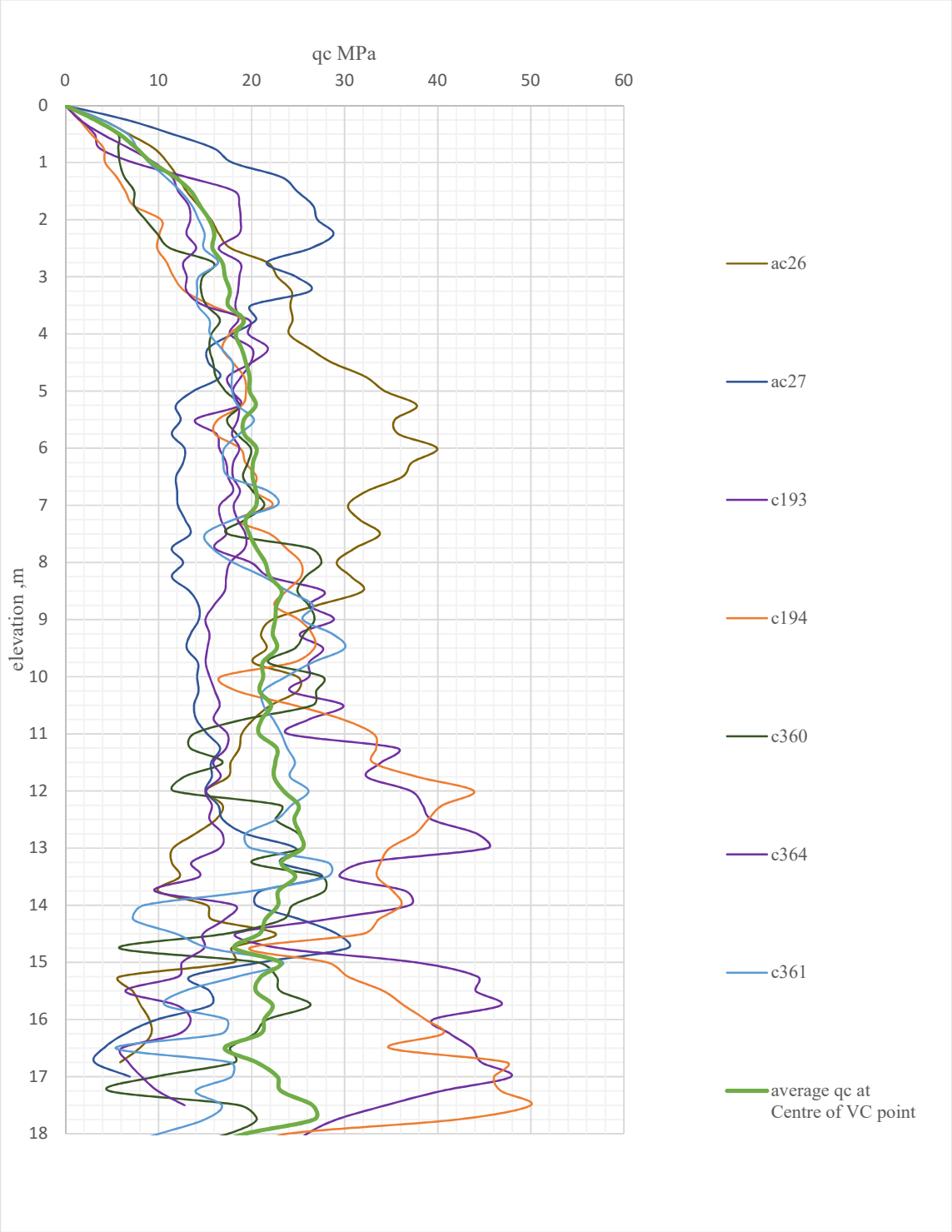

Figure A- 37: qc variation at centre of VC point

d. A distance of 1m away from Centre of the compaction point

q_c curves of CPT conducted at 1m away from centre of the compaction points are plotted along with its average curve in Figure A- 38;

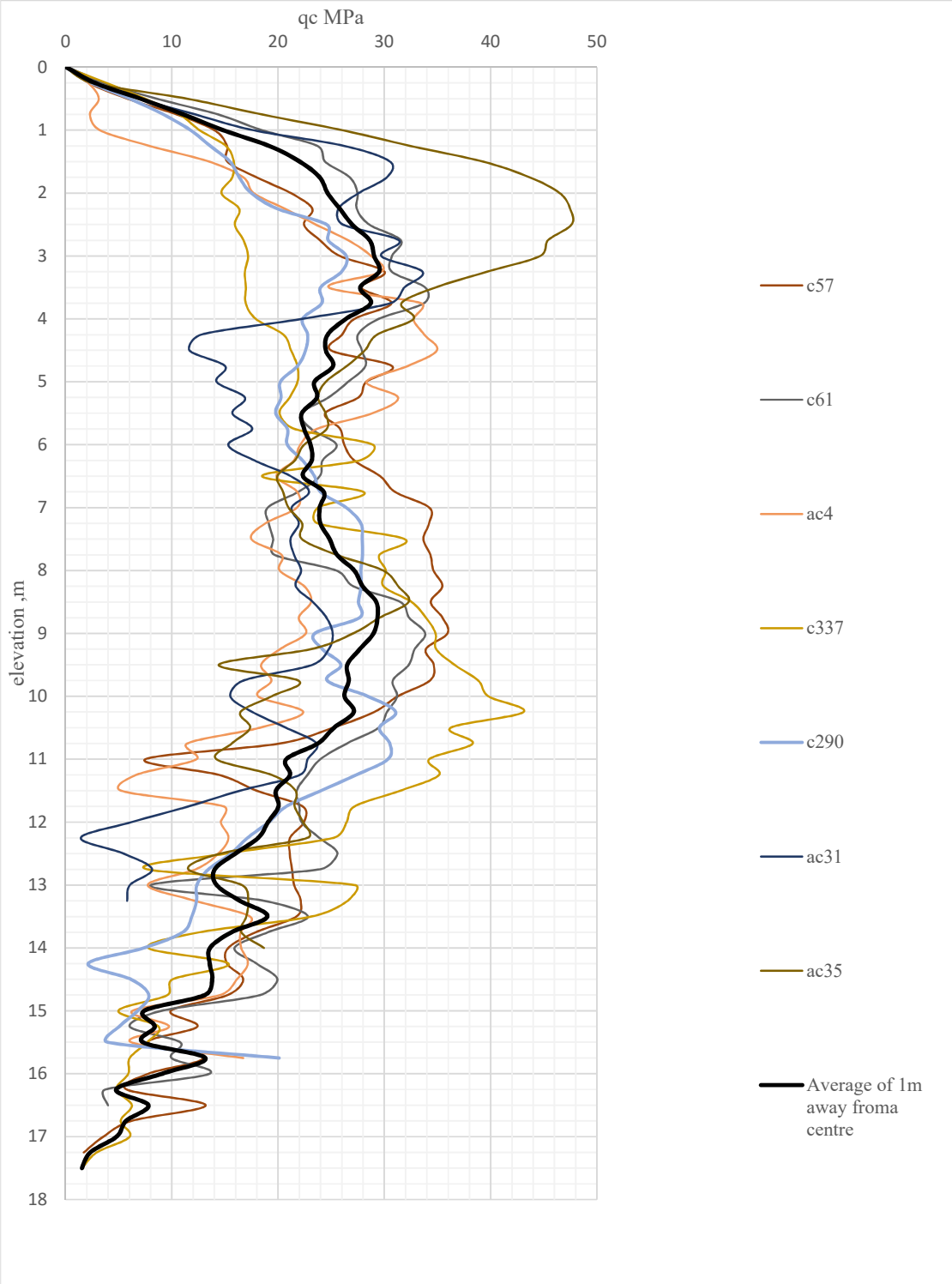

Figure A- 38; q_c variation at 1m away from a centre of VC point

A7 APPENDIX VII: Age Effect on Sand Densification

A7.1 Age effect on Dynamic Compaction

1. Variation of qc when Age of compaction below two months;

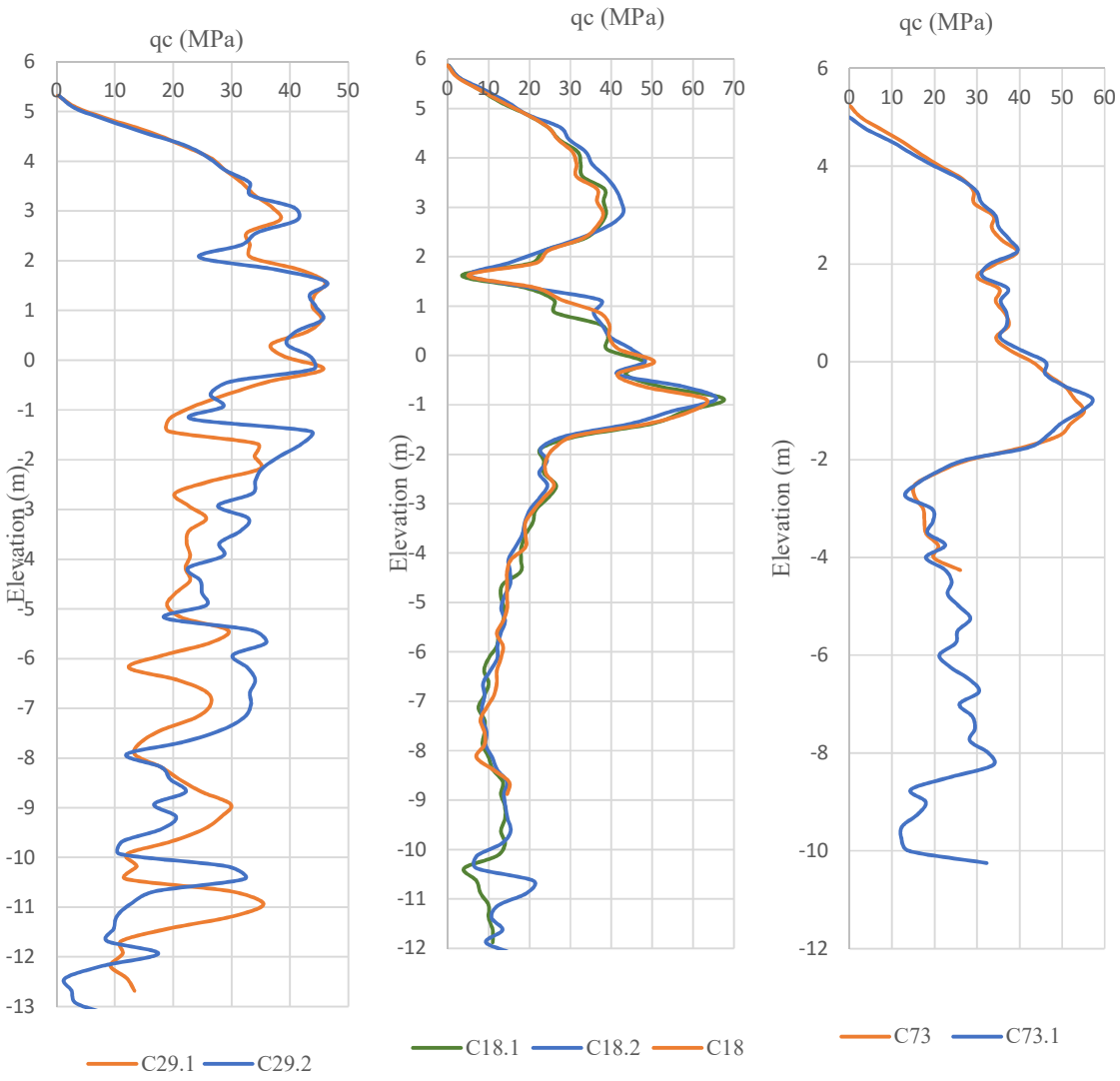

At age of 21 days (C29) At age of 49 days (C18) At age of 53 days (C73)

Figure A- 39: qc variation when compaction below 2 months

2. Variation of qc when Age of compaction above five months

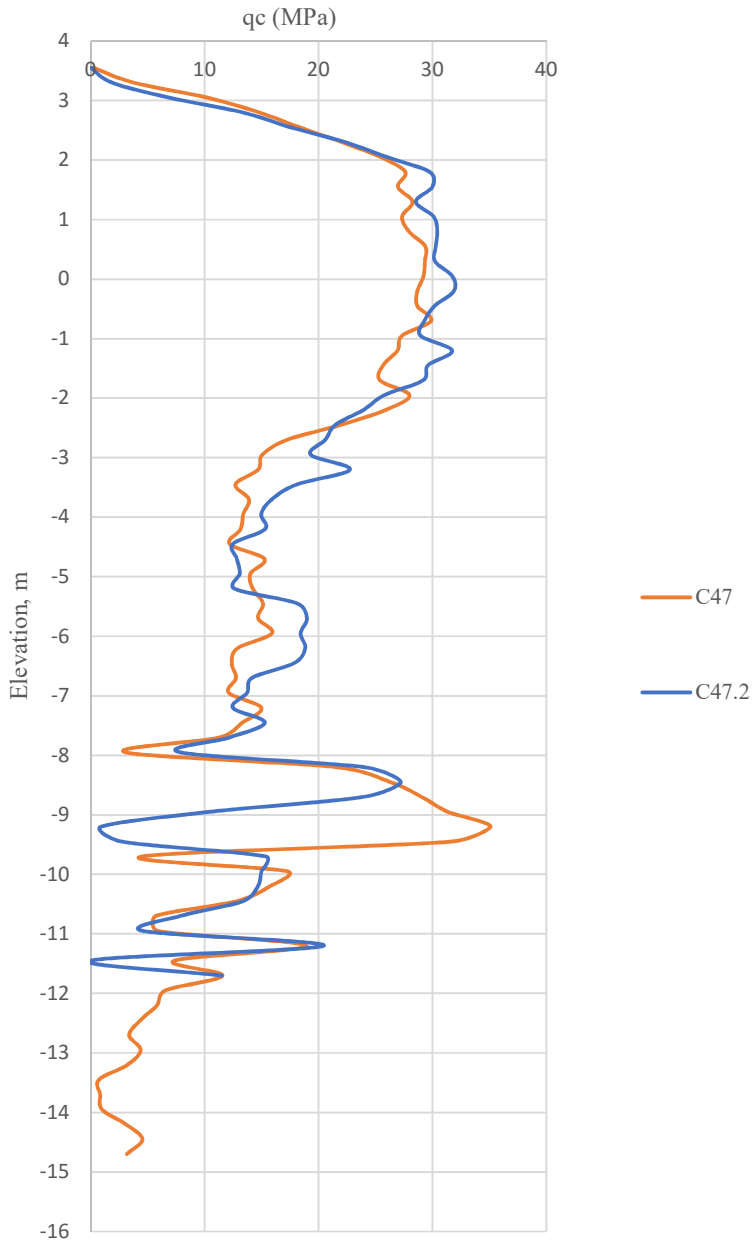

qc at age of 180 days (C47)

Figure A- 40: Variation of qc when compaction below 180 days

3. Improvement in compaction when Age of compaction above 7 months

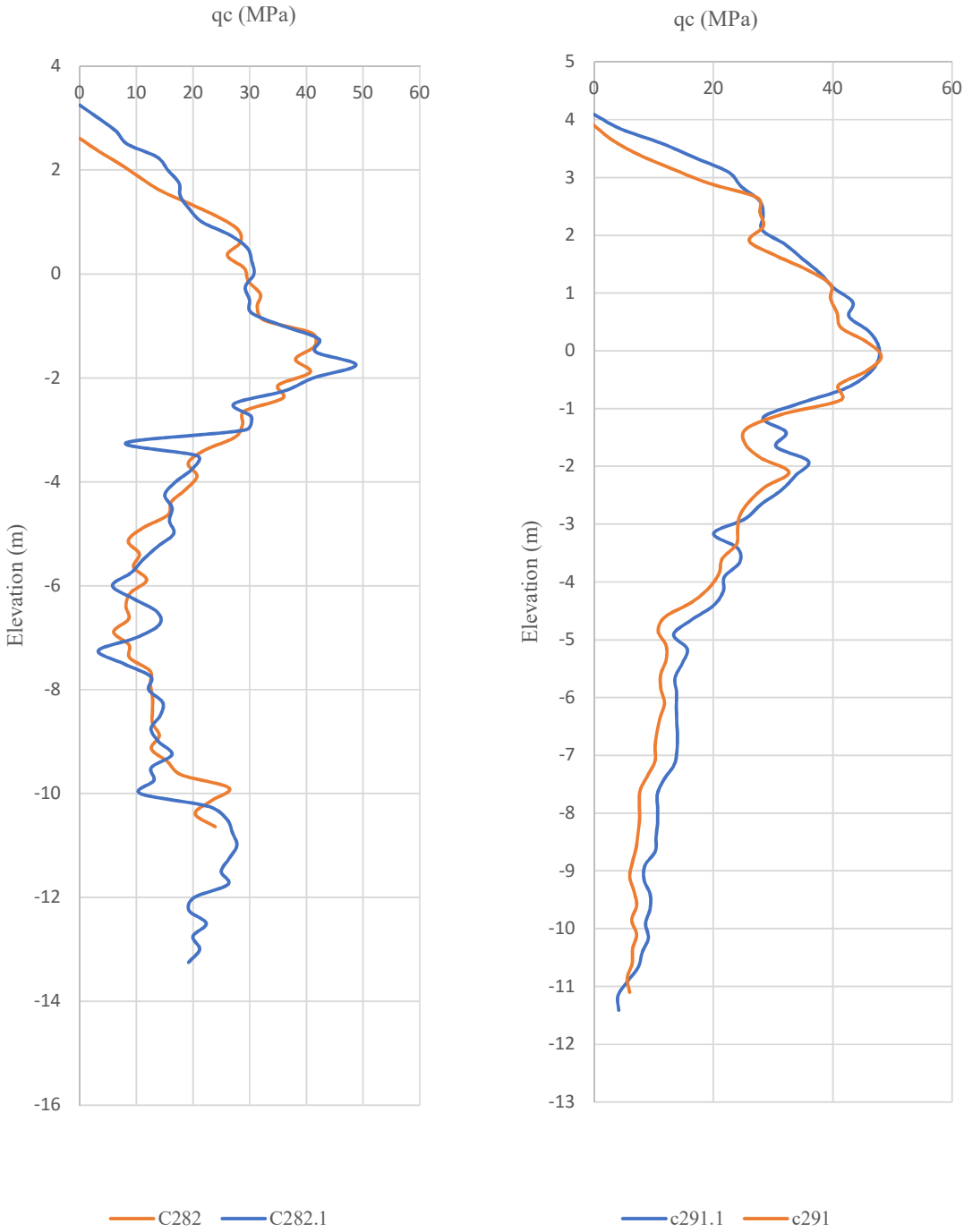

qc at age of 228 days (C282)

qc at age of 316 days (C291)

Figure A- 41: Variation of qc when compaction above 200 days

A7.2 Age effect when sand compacted by Vibro Compaction

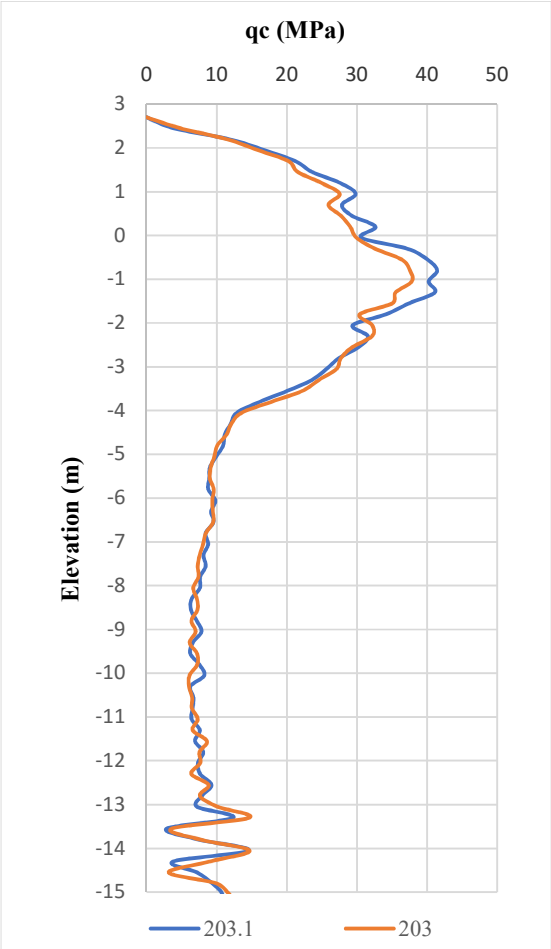

qc at age of 179 days (C203)

Figure A- 42: Variation of qc in different ages